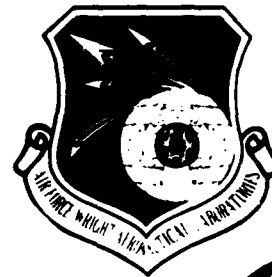


AD A093992

AFWAL-TR-80-4098



CRACK GROWTH MODELING IN AN ADVANCED POWDER METALLURGY ALLOY

(12)

Mid A. Utah
General Electric Company
Sandale, Ohio 45215

LEVEL II

DTIC
ELECTE
S JAN 22 1981 D
E

July 1980

TECHNICAL REPORT AFWAL-TR-80-4098

Final Report for Period 1 September 1977 to 1 February 1980

Approved for public release; distribution unlimited

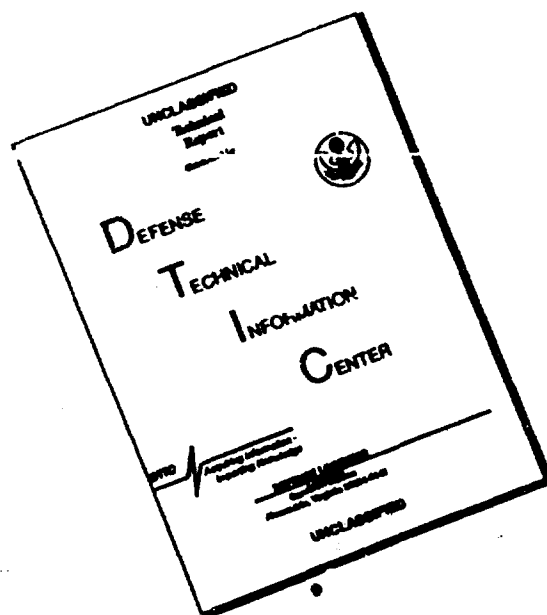
MATERIALS LABORATORY
AIR FORCE WRIGHT AERONAUTICAL LABORATORIES
AIR FORCE SYSTEMS COMMAND
WRIGHT-PATTERSON AIR FORCE BASE, OHIO 45433

148 250

80 21 022

DDC FILE COPY

DISCLAIMER NOTICE




THIS DOCUMENT IS BEST
QUALITY AVAILABLE. THE COPY
FURNISHED TO DTIC CONTAINED
A SIGNIFICANT NUMBER OF
PAGES WHICH DO NOT
REPRODUCE LEGIBLY.


NOTICE

When Government drawings, specifications, or other data are used for any purpose other than in connection with a definitely related Government procurement operation, the United States Government thereby incurs no responsibility nor any obligation whatsoever; and the fact that the government may have formulated, furnished, or in any way supplied the said drawings, specifications, or other data, is not to be regarded by implication or otherwise as in any manner licensing the holder or any other person or corporation, or conveying any rights or permission to manufacture, use, or sell any patented invention that may in any way be related thereto.

This report has been reviewed by the Office of Public Affairs (ASD/PA) and is releasable to the National Technical Information Service (NTIS). At NTIS, it will be available to the general public, including foreign nations.

This technical report has been reviewed and is approved for publication.


J.P. HENDERSON, Acting Chief
Metals Behavior Branch
Metals and Ceramics Division


DR. W.H. REIMANN, Project Engineer
Metals Behavior Branch
Metals and Ceramics Division

"If your address has changed, if you wish to be removed from our mailing list, or if the addressee is no longer employed by your organization please notify AFWAL/MLLN, W-PAFB, OH 45433 to help us maintain a current mailing list".

Copies of this report should not be returned unless return is required by security considerations, contractual obligations, or notice on a specific document.

SECURITY CLASSIFICATION OF THIS PAGE (When Data Entered)

19 REPORT DOCUMENTATION PAGE		READ INSTRUCTIONS BEFORE COMPLETING FORM
1. REPORT NUMBER AFWAL TR-80-4098	2. GOVT ACCESSION NO. AD-A093 992	3. RECIPIENT'S CATALOG NUMBER
4. TITLE (and Subtitle) Crack Growth Modeling in an Advanced Powder Metallurgy Alloy		5. TYPE OF REPORT & PERIOD COVERED Final Technical Report 1 Sep 77 - 1 Feb 80
7. AUTHOR(s) David A. Utah		6. PERFORMING ORG. REPORT NUMBER
9. PERFORMING ORGANIZATION NAME AND ADDRESS General Electric Company Evendale, Ohio		8. CONTRACT OR GRANT NUMBER(s) F33615-77-C-5082
11. CONTROLLING OFFICE NAME AND ADDRESS		10. PROGRAM ELEMENT, PROJECT, TASK AREA & WORK UNIT NUMBERS 24200105
14. MONITORING AGENCY NAME & ADDRESS (if different from Controlling Office) Dr. W. Reimann AFWAL/MLLN Wright-Patterson AFB, OH 45433		12. REPORT DATE July 1980
		13. NUMBER OF PAGES 169
		15. SECURITY CLASS. (of this Report) Unclassified
16. DISTRIBUTION STATEMENT (of this Report) Approved for public release; distribution unlimited.		15a. DECLASSIFICATION DOWNGRADING SCHEDULE
17. DISTRIBUTION STATEMENT (of the abstract entered in Block 20, if different from Report)		
18. SUPPLEMENTARY NOTES		
19. KEY WORDS (Continue on reverse side if necessary and identify by block number) Fatigue, Cyclic Crack Growth Rate, Fatigue Crack Propagation, Hold Time, Frequency, Stress Ratio, Temperature, Sigmoidal Equation, Interpolative Model.		
20. ABSTRACT (Continue on reverse side if necessary and identify by block number) An interpolative model has been developed to calculate the cyclic crack growth rate of an advanced aircraft engine disk alloy (AF115). The test variables included within the model consists of stress ratio, temperature, frequency, and hold time. The model was based on experimental results conducted within a statistically designed test program. A nonsymmetric Sigmoidal equation consisting of six independent coefficients was used to equate stress intensity range to cyclic growth rate. Two verification tests were conducted at		

DD FORM 1 JAN 73 1473

EDITION OF 1 NOV 65 IS OBSOLETE

SECURITY CLASSIFICATION OF THIS PAGE (When Data Entered)

SECURITY CLASSIFICATION OF THIS PAGE(When Data Entered)

two conditions other than those used during the development of the model to evaluate the model.

SECURITY CLASSIFICATION OF THIS PAGE(When Data Entered)

FOREWORD

This report presents the results of an investigation conducted by General Electric for Metals Behavior Branch, Metals and Ceramics Division, Air Force Materials Laboratory, Wright-Patterson Air Force Base. The work was conducted under Contract No. F33615-77-C-5082 during September 1977 and February 1980. Captain J. Hyzak was the Project Engineer reporting to Dr. W.H. Reimann. The work was conducted under supervision of H.G. Popp, Manager of Materials Behavior Engineering within the Material and Process Technology Laboratories of the Aircraft Engine Group. The final report was submitted during September, 1980.

The author wishes to express his appreciation to H.G. Popp and P. Domas for their numerous worthy suggestions during the course of the program. Appreciation is also expressed to Lynn Worpenberg for her assistance in the data analysis, and Tony Esseck and Carl Slife for conducting the experiments.

Accession For	
NTIS GRA&I	<input checked="checked" type="checkbox"/>
DTIC TAB	<input type="checkbox"/>
Unannounced	<input type="checkbox"/>
Justification	
By	
Distribution/	
Availability Codes	
Dist	Avail and/or Special
A	

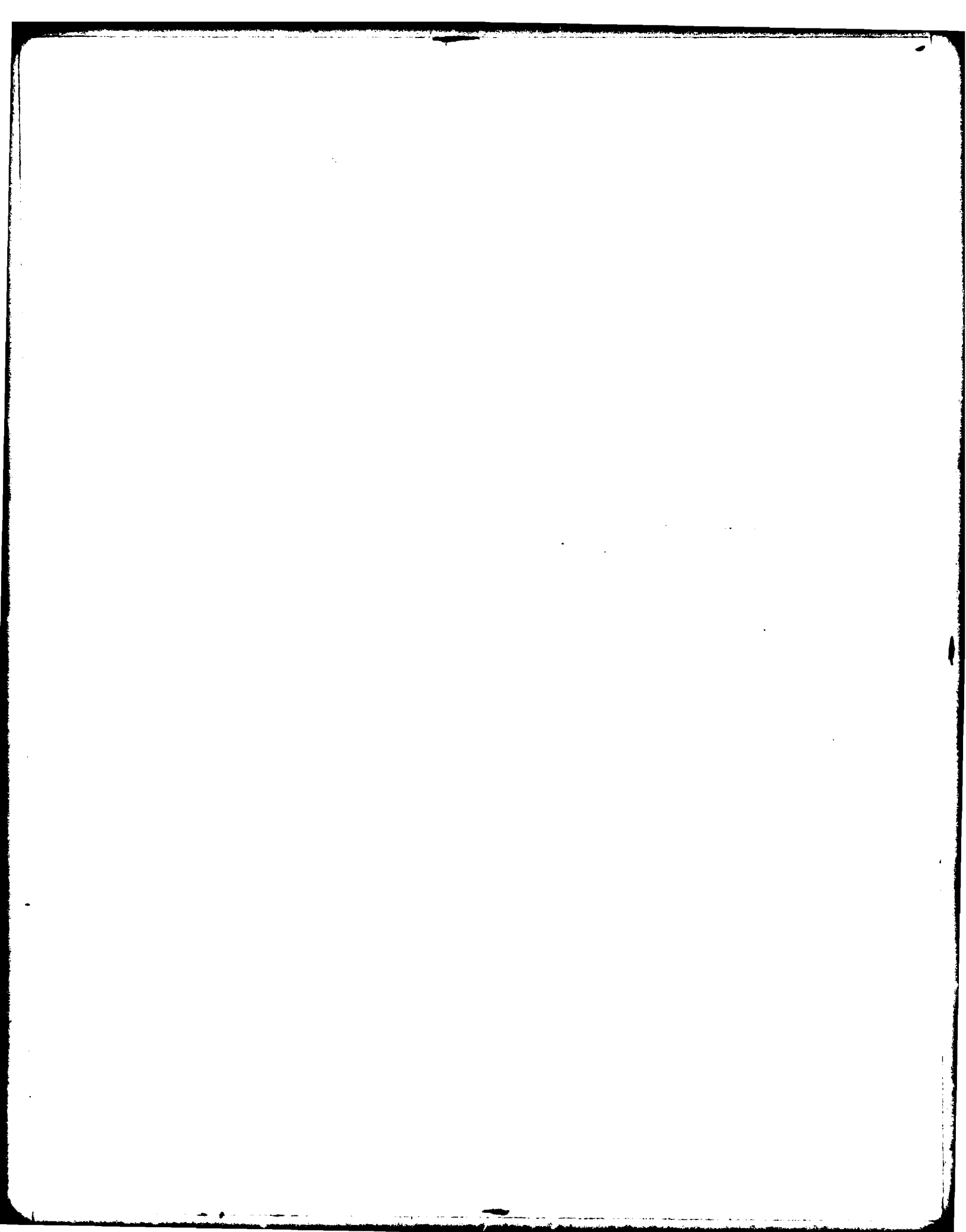


TABLE OF CONTENTS

<u>Section</u>	<u>Page</u>
I. INTRODUCTION	1
II. MATERIAL AND SPECIMEN FABRICATION	2
A. Material Processing	2
B. Specimen Fabrication	6
C. Material Characterization	6
III. EXPERIMENTAL PROGRAM	15
A. Load/Thickness Evaluation Matrix	15
B. Primary Test Matrix	15
C. Verification Tests	16
IV. EXPERIMENTAL PROCEDURES	18
A. Precracking	18
B. Test Facilities	18
C. Load Determination	22
D. Crack Growth Data Reduction	22
V. EXPERIMENTAL RESULTS	24
A. Thickness Results	24
B. Raw Experimental Data	27
C. da/dN Versus ΔK Tabulation	30
1. Frequency Effects	30
2. Hold Time Effects	30
3. Stress Ratio Effects	34
4. Temperature Effects	34
VI. INTERPOLATIVE MODEL	35
A. The Modified Sigmoidal Equation	35
B. Modeling of Experimental Conditions	38
1. Stress Intensity at Fracture, ΔK_c	38
2. The Lower Asymtote, ΔK^*	38
3. Horizontal Location of Inflection Point, ΔK_i	40
4. Vertical Location of the Inflection Point, da/dN _i	40
a. Inflection Point for Continuous Cycling Conditions, $\frac{da}{dN_i}^{CC}$	43
b. Inflection Point for Hold Time Conditions, $\frac{da}{dN_i}^{HT}$	46

TABLE OF CONTENTS (Concluded)

<u>Section</u>		<u>Page</u>
	C. Summary of Interpolative Model	52
	1. Response of Coefficients to Test Variables	52
	2. Comparison of Experimental Results to Model	62
VII	COMPUTER PROGRAMS	73
VIII	VERIFICATION OF MODEL	74
IX.	DISCUSSIONS	79
	A. Characteristics of the Interpolative Model	79
	B. Comparison to Other Studies	81
	C. Assessment of Interpolative Model	84
	D. Errors in the Modified Sigmoidal Equation	88
	1. Precracking Method Influences	88
	2. Effect of Observed Scatter at the Replica Test Condition	91
	3. Effect of Scatter in the Verification Tests	91
	E. Critical Tests for Model Application	96
	1. The Designed Matrix for This Program	96
	2. Test Requirements for Model Development of a Similar Material	98
X.	CONCLUSIONS AND RECOMMENDATIONS	101
XI.	REFERENCES	102

LIST OF ILLUSTRATIONS

<u>Figure</u>		<u>Page</u>
1.	Photomicrographs Depict the AF115 Material Micro-structure in the As-HIP Condition.	4
2.	Photomicrographs Depict the AF115 Material Micro-structure in the Fully Heat-Treated Condition.	5
3.	Location and Orientation of Compact Tension Specimens.	7
4.	Specimen Configuration for Material Qualification Experiments.	8
5.	Configuration of Compact Tension Specimen for Cyclic Crack Growth Testing.	9
6.	Tensile Properties of Heat Al339/C1003 in Comparison to Typical Properties.	12
7.	0.2% Creep Properties of Heat Al339/C1003 in Comparison to Typical Properties.	13
8.	Stress Rupture Properties of Heat Al339/C1003 in Comparison to Typical Properties.	13
9.	Low-Cycle-Fatigue Results of Heat Al339/C1003.	14
10.	Room Temperature Precracked Specimens with Subsequent Elevated Test Conditions Showing Changes in Curvature After Initiation of Testing.	19
11.	Photograph of Overall Test Set-up with MTS 5 KIP Closed-Loop Equipment and Associated Control and Monitoring Equipment.	20
12.	Photograph of Close-up View of Compact Tension Specimen in Test Fixture.	21
13.	6.35mm (0.25 inch) Thick Compact Tension Specimen Fracture Surface.	25
14.	12.5mm (0.5 inch) Thick Compact Tension Specimen Fracture Surface.	25
15.	25.4mm (1.00 inch) Thick Compact Tension Specimens Fracture Surface.	26

LIST OF ILLUSTRATIONS (Continued)

<u>Figure</u>		<u>Page</u>
16.	Cyclic Crack Growth Rate Versus Stress Intensity Factor of Three Thickness of Compact Tension Specimen with Stress Intensity Range Based on Quarter Width Curvature Corrected Crack Length.	28
17.	Cyclic Crack Growth Rate Versus Stress Intensity Factor of Three Thickness of Compact Tension Specimen with Stress Intensity Range Based on Average Surface Crack Lengths.	29
18.	Experimental Results of Crack Growth Tests Conducted at the Stress Ratio of 0.1.	31
19.	Experimental Results of Crack Growth Tests Conducted at the Stress Ratio of 0.5.	32
20..	Experimental Results of Crack Growth Tests Conducted at the Stress Ratio of 0.9.	33
21.	Illustration of Effects of the Coefficients of the Sigmoidal Equation.	36
22.	Correlation of Threshold Crack Growth and Stress Ratio (1-R) for 538, 649, and 760C (1000, 1200, and 1400F).	39
23.	Pairs of da/dN_i and ΔK_i and Associated Relationship for the Stress Ratio of 0.1 and Temperatures Between 538 and 760C (1000 and 1400F).	42
24.	Crack Growth Rate at the Inflection Point as a Function of Time per Cycle for 760C (1400F), $R = 0.5$, and No Hold Period.	44
25.	Predictions of Inflection Point (da/dN_i) Versus Stress Ratio (1-R) for Continuous Cycling Experiments.	47
26.	Hold Time Damage Factor Versus Hold Time for the Stress Ratio of 0.1 and Two Temperatures.	48
27.	Slope of the Inflection Point Versus Stress Ratio (1-R) for the Continuous Cycle Results.	51
28.	Schematic Effects of Coefficients on the Modified Sigmoidal Equation.	54
29.	Illustration of Relationship Between ΔK_i and da/dN_i at $R=0.1$ and Various Temperatures, Frequencies, and Hold Periods.	55

LIST OF ILLUSTRATIONS (Continued)

<u>Figure</u>		<u>Page</u>
30.	Illustration of Relationship Between ΔK_I and da/dN_i at $R=0.9$ and 649C (1200F).	56
31.	Illustration of Relationship Between da/dN_i and Temperature at $R=0.1$ and 0.25 Hz.	57
32.	Illustration of Relationship Between da/dN_i and Hold Time for $R=0.1$ and 0.25 Hz.	58
33.	Illustration of Relationship Between da/dN_i and Frequency at $R=0.1$ and 760C (1400F).	59
34.	Illustration of Relationship Between da/dN_i and Stress Ratio for 760C (1400F) and 0.25 Hz.	60
35.	Illustration of Relationship Between da/dN_i and Stress Ratio at 649C (1200F) and 2.5 Hz.	61
36.	Actual and Predicted Crack Growth Rate Curve for 538C (1000F), $R=0.1$ Experiments.	63
37.	Actual and Predicted Crack Growth Rate Curve for 649C (1200F), $R=0.1$ Experiments.	64
38.	Actual and Predicted Crack Growth Rate Curves for 704C (1300F), $R=0.1$ Experiments.	65
39.	Actual and Predicted Crack Growth Rate Curves for 760C (1400F), $R=0.1$ Experiments.	66
40.	Actual and Predicted Crack Growth Rate Curves for 538C (1000F), $R=0.5$ Experiments.	67
41.	Actual and Predicted Crack Growth Rate Curves for 649C (1200F), $R=0.5$ Experiments.	68
42.	Actual and Predicted Crack Growth Rate Curves for 760C (1400F), $R=0.5$ Experiments.	69
43.	Actual and Predicted Crack Growth Rate Curves for 538C (1000F), $R=0.9$ Experiments.	70
44.	Actual and Predicted Crack Growth Rate Curves for 649C (1200F), $R=0.9$ Experiments.	71

LIST OF ILLUSTRATIONS (Concluded)

<u>Figure</u>		<u>Page</u>
45.	Actual and Predicted Crack-Growth-Rate Curves for 760C (1400F), R=0.9 Experiments.	72
46.	Crack Length Versus Cycle Number of Verification Experiments.	75
47.	Predicted and Actual Crack Growth Rate for Verification Experiments.	76
48.	Results of 760C (1400F) and Stress Ratio of 0.1 Plotted as da/dt Versus ΔK Rather Than da/dN.	80
49.	Comparison of Two Cyclic Crack Growth Curves with Two Different Lower Asymtotes Compensated by the Lower Shaping Coefficient.	82
50.	Crack Length Versus Cycle Prediction Using Two Different Sets of Lower Asymtotes Compensated by the Lower Shaping Coefficient.	83
51.	Deviation in Actual and Predicted Lives Versus Four Test Variables.	86
52.	Comparison of Actual Data and Prediction Using Walker Equation for 760C (1400F) 0.25 Hz and No Hold Time.	89
53.	Comparison of Fracture Surfaces of Two Replacation Experiments.	90
54.	Correlation of S/N 4-6 Experimental Results and Predicted Curves.	92
55.	Influence of Typical Variation of Parameters Used in the Sigmodial Equation.	93
56.	Comparison of the Verification Tests Results and the Prediction with a Factor of 2.2 Increase on da/dN _i and a 10% Decrease in ΔK^* .	95
57.	Illustration of Test Matrix Used in This Program.	97

LIST OF TABLES

<u>Table</u>		<u>Page</u>
1.	Composition of AF115 Powder (A1339).	2
2.	Particle Size Distribution of AF115 Powder (A1339).	3
3.	Results of Density, Tip Response, and Oxygen Analysis of AF115 (A1339/C1003).	6
4.	Results of Qualification Test for Heat A1339/C1003 of AF115.	11
5.	Test Matrix for Experimental Program.	17
6.	Test Parameter Summary of Thickness/Load Determination Test Series.	24
7.	Slope and Intercept (at $da/dN_i = 1.0$) of Linear Relationship Between da/dN_i and ΔK_i for Various Temperatures and Stress Ratios.	41
8.	Coefficients to Determine da/dN_i for Continuous Cycling Conditions.	45
9.	Slope and Intercept (at 20 seconds) for Hold Time Damage Factor Versus Hold Period Duration for Various Temperatures, Stress Ratio and Frequencies.	50
10.	Influence of Experimental Variables on Modified Sigmoidal Equation Coefficients.	53
11.	Results of Verification Experiments.	77
12.	Predicted and Actual Lives from a Given Crack Length of Specimens Conducted in Primary Test Matrix.	85

LIST OF SYMBOLS

B	Coefficient of Sigmoidal Equation.
B'	Coefficient of Modified Sigmoidal Equation.
B ₁	Thickness of Compact Tension Specimen, mm (inch).
D	Upper Shaping Coefficient of Sigmoidal Equation.
$\frac{da}{dN}$	Crack Growth Rate, mm/cycle (inch/cycle).
$\frac{da}{dN_i}$	Crack Growth Rate at Inflection Point, mm/cycle (inch/cycle).
$\frac{da'}{dN_i}$	Slope at Inflection Point.
$\frac{da}{dN_i}^{CC}$	Crack Growth Rate at Inflection Point for Continuous Cycling Experiment, mm/cycle (inch/cycle).
$\frac{da}{dN_i}^{HT}$	Crack Growth Rate at Inflection Point for Hold Time Experiment.
HT	Length of Hold Time, Second.
ΔK	Stress Intensity Range, MPa \sqrt{m} (Ksi \sqrt{in}).
ΔK_{max}	Maximum Stress Intensity.
ΔK^*	Lower Asymtote Coefficient of Sigmoidal Equation.
ΔK_{max}^*	Lower Asymtote Coefficient at R=0.
ΔK_c	Upper Asymtote Coefficient of Sigmoidal Equation.
ΔK_{eff}	Effective Stress Intensity.
ΔK_i	Stress Intensity of Inflection Point.
P	Coefficient of Sigmoidal Equation.
ΔP	Load Range, Pounds.
Q	Lower Shaping Coefficient of Sigmoidal Equation.

LIST OF SYMBOLS (Concluded)

R	Stress Ratio, K_{min}/K_{max} .
T	Temperature, C (F).
W	Compact Tension Specimen Width, mm (inch).
a	Crack Length, mm (inch).
C, a_1 , b, d, e_1 , e_2 , f, f_1 , g, h, j, k, n, n_1 , n_2 , r, s, u, w	- Coefficients Determined by Regression Analysis.
m	Walker Equation Exponent.
σ_{ys}	Yield Strength, ksi.

SUMMARY

The cyclic crack growth behavior of an advanced aircraft engine disk alloy, AF115, has been evaluated under a wide range of test variables including stress ratio, temperature, frequency, and hold period. The test conditions were selected to be representative of advanced disk applications. An interpolative model has been developed to predict crack growth behavior within the boundaries of the test conditions evaluated. Verification tests were conducted to evaluate the accuracy of the model.

Prior to the primary test program, a thickness/load evaluation was conducted using three thicknesses of compact tension specimens. The primary test program consisted of cyclic crack growth rate experiments using compact tension specimens of a single thickness. Test temperatures ranged from 538° C (1000° F) to 760° C (1400° F) and stress ratios (R) from 0.1 to 0.9. Frequencies were varied between 0.025 Hz and 2.5 Hz with additional tensile hold periods up to five minutes. A statistically designed test program, consisting of 36 conditions, was used to systematically evaluate the test variables. Ten additional conditions were evaluated at critical locations in the matrix to enhance the test program.

The interpolative model developed utilized a modified form of the General Electric Sigmoidal equation, consisting of six independent coefficients, to equate the stress intensity range to cyclic crack growth rate. The six coefficients regulate the location and slope of the inflection point, the lower and upper asymptotes, and the low and upper shape characteristics of the crack growth curve. Relationships were made to evaluate each of the coefficients as functions of the four test variables.

At the lower temperature of 538° C (1200° F) and stress ratio of 0.1, the crack growth behavior was hold time and frequency independent. At 649° C (1200° F) and the stress ratio of 0.1, the frequency test variable was non-influential; however, hold periods of 90 seconds resulted up to a twofold increase in growth rate. At 760° C (1400° F) the frequency and hold time test variables were significant factors on crack growth behavior. At this condition a threefold difference in growth rate was observed between the fastest and slowest of the wave pattern examined. The influences of temperature, hold time, and frequency on crack growth rate behavior increased with increasing stress ratio. Depending on the other test parameters, increasing the stress ratio could either vertically increase or decrease the inflection point location of the cyclic crack growth rate versus stress intensity curve. However, there existed a saturation level in which the crack-growth rate at the inflection point would remain constant with increasing stress ratio. The Walker equation was found unsatisfactory in determining stress ratio effects.

Using test conditions other than those used during the development of the model, two verification tests were conducted at two conditions to

evaluate the model. The actual average lives of the verification tests for the two test conditions were within factors of 1.3 and 2.5 of the predicted lives. These factors were typical of the models capability of predicting the crack growth behavior of the experiments conducted to develop the model. A comparison was made with other crack-growth modeling studies. It is shown that the accuracy of the verification experiments were within the range of other elevated temperature interpolative modeling techniques. It was observed that the error in the predictive capabilities of the model increased with increasing stress ratio and remained constant for the other three test variables.

I INTRODUCTION

The concept of damage tolerant design for turbine rotor parts has become a very attractive method for cost effectiveness due to the high replacement cost of advanced engine components. Through the use of damage tolerant design concepts based on analytical fracture mechanics, the usable life of each part can potentially be extended without increasing the risk of failure. A major requirement for implementation of this concept is reliable subcritical crack growth information. At low temperatures, the crack growth behavior of engine materials is reasonably well understood. Crack propagation is not as easily defined, however, for higher temperature applications as in turbine disks where time dependent plasticity occurs. The influences of hold time at high stresses, time dependencies, and temperature and stress variations severely complicates life analysis.

The purpose of this program was to develop an improved understanding of the crack growth behavior of an advanced turbine disk material, and to develop a method for predicting a disk alloy mechanical behavior under turbine disk operating conditions. The specific objectives were to define the crack growth behavior of AF115 which is representative of an advanced powder metallurgy disk material, and to develop an interpolative model that permits accurate crack growth predictions to be made under different stress-time-temperature conditions typical of advanced turbine disk environments.

Under Phase I of the program, crack growth tests were conducted at conditions that reflect the operating conditions of an advanced family of engine designs. Variables evaluated included stress ratio, temperature, cyclic frequency, and hold time. Temperatures investigated were from 538° C (1000° F) to 760° C (1400° F), and stress ratios (R) were from 0.1 to 0.9. Frequencies between 0.025 and 2.5 Hz were examined with additional tensile hold periods up to five minutes. The stress ratio, temperature, frequency, and hold time effects were systematically investigated using a statistically designed test program. As an extension to the statistically designed program, additional tests were included to assist in the direct analysis of each of the single test variables.

A computerized interpolative program was developed in Phase II to predict cyclic crack growth behavior within the extent of the variables tested. A modified General Electric Sigmodial Equation, developed under this program, was used to describe the individual cyclic crack growth curves. The model adjusts the location and slope of the inflection point, along with the upper and lower shaping characteristics and asymptotes of the crack growth curve as a function of the test variables. A series of tests, under Phase III, was then conducted to verify the accuracy of the interpolative model.

II. MATERIAL AND SPECIMEN FABRICATION

The material selected for the investigation of cyclic crack growth behavior was AF115, a nickel-base superalloy developed by General Electric under Air Force (AFML) sponsorship⁽¹⁾. AF115 is a gamma-prime-strengthened nickel-base alloy in which titanium, aluminum, columbium, and hafnium are gamma prime formers and chromium, cobalt, molybdenum, and tungsten are strengtheners of the gamma matrix. The initial development of AF115 involved powder metallurgy HIP + forge processing. Subsequent studies included evaluation of As-HIP processing, low carbon/low hafnium modification, and effect of thermo-mechanical processing by specially controlled forging and heat treatment processes⁽²⁾. The material procured for this program was in the As-HIP condition.

A. MATERIAL PROCESSING

The AF115 powder for this program was produced by Carpenter Technology (heat number A1339) and was vacuum melted from virgin material and argon spray atomized to powder. Results of the chemical analysis of the powder are shown in Table 1 along with the minimum and maximum acceptable levels, and the aim level for each specified element in the composition. The chemical composition of the powder was well within the specified limits. Table 2 shows the particle size distribution of the powder utilized for the compact. The powder was 99.7% minus 100 mesh powder size.

Table 1. Composition of AF115 Powder (A1339).

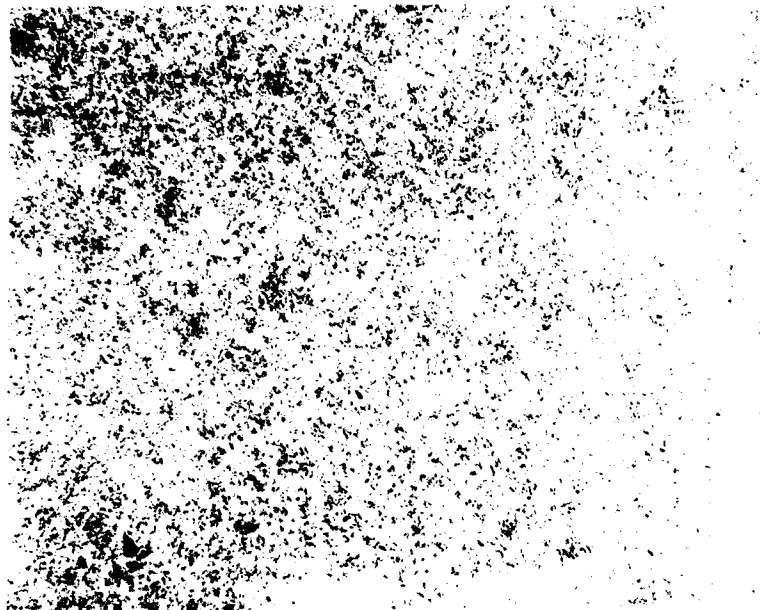
<u>Element</u>	<u>Heat A1339</u>	<u>AIM</u>	<u>Minimum</u>	<u>Maximum</u>
Carbon	0.043	0.050	0.030	0.070
Manganese	<0.01	---	---	0.15
Silicon	0.04	---	---	0.20
Sulfur	0.002	---	---	0.015
Chromium	10.68	10.7	9.95	11.45
Titanium	3.85	3.90	3.60	4.20
Aluminum	3.67	3.80	3.50	4.10
Boron	0.019	0.020	0.015	0.025
Zirconium	0.057	0.05	0.03	0.07
Iron	0.13	---	---	1.00
Cobalt	15.10	15.00	14.50	15.50
Molybdenum	2.80	2.80	2.60	3.00
Tungsten	5.67	5.90	5.60	6.20
Phosphorus	<0.005	---	---	0.015
Hafnium	0.84	0.75	0.55	0.95
Columbium	1.71	1.70	1.50	1.90
Nickel		Balance	Balance	Balance

Table 2. Particle Size Distribution
of AF115 Powder (A1339).

<u>Mesh Size</u>	<u>Weight Percent</u>
+60	0.0
-60 + 80	0.2
-80 +100	0.1
-100 +140	8.5
-140 +200	18.0
-200 +325	28.0
-325	42.5

Powder from this heat was loaded into a 203 mm (8 inch) diameter by 610 mm (24 inch) long stainless steel canister (canister number C1003) by Carpenter Technology and compacted at Industrial Materials Technology (HIP cycle number 2747) at a temperature of 1191° C (2175° F) and a pressure of 103 MPa (15 ksi) for 2 hours. The resulting compact measured 162 mm (6-3/8 inches) in diameter by 502 mm (19-3/4 inches) long. The As-HIP compact was sectioned into 14 slices, 29 mm (1-1/8 inch) to 32 mm (1-1/4 inch) thick, and heat treated. Solution treatment was performed in air at 1182° C \pm 9C (2160° F) for 4 hours followed by rapid air-cooling to room temperature. This temperature minimized thermally induced porosity (TIP) formation by assuring solution treatment below the minimum HIP temperatures. The quenching medium from the solution temperature was rapid air-cool which minimized the tendency for quench cracking. Aging was subsequently performed at 760° C (1400° F) for 16 hours followed by air cooling.

Test coupons were removed from the As-HIP compact as well as from the fully heat-treated compact for TIP, oxygen, and metallographic analysis. Table 3 lists the results of the TIP response of the test coupons after 1149° C (2100° F)/4 hours, 1177° C (2150° F)/4 hours, and 1191° C (2175° F)/4 hours exposures, and the compact after the 1182° F (2160° F)/4 hours solution heat treatment. All TIP values reported were well within the 0.5% TIP requirement. The 0.001% TIP value reported for the fully heat-treated material represents an exceptionally low TIP response. Oxygen analysis conducted on the As-HIP compact yielded acceptable values, as listed in Table 3. Shown in Figures 1 and 2 are 100X and 500X photomicrographs of etched metallographic sections of the AF115 compact in the As-HIP and full heat-treated conditions. A uniform, fully dense microstructure is evident in each of the views.

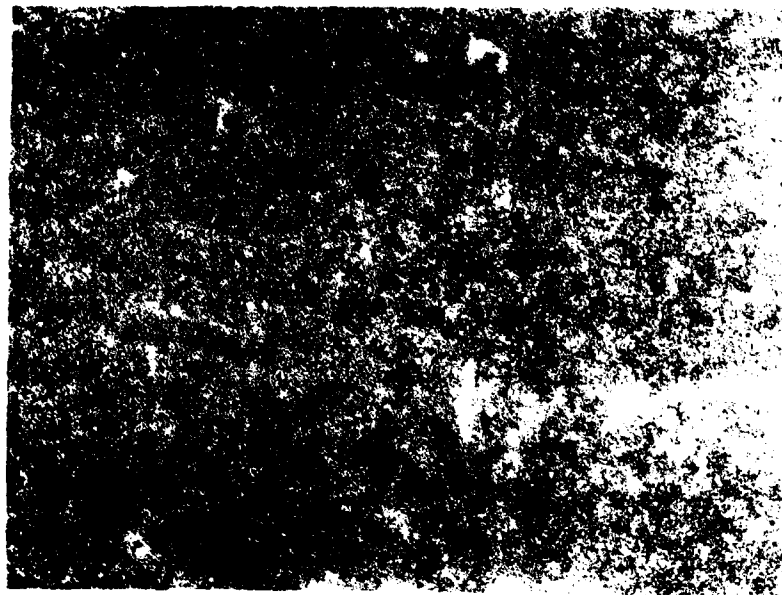


100X

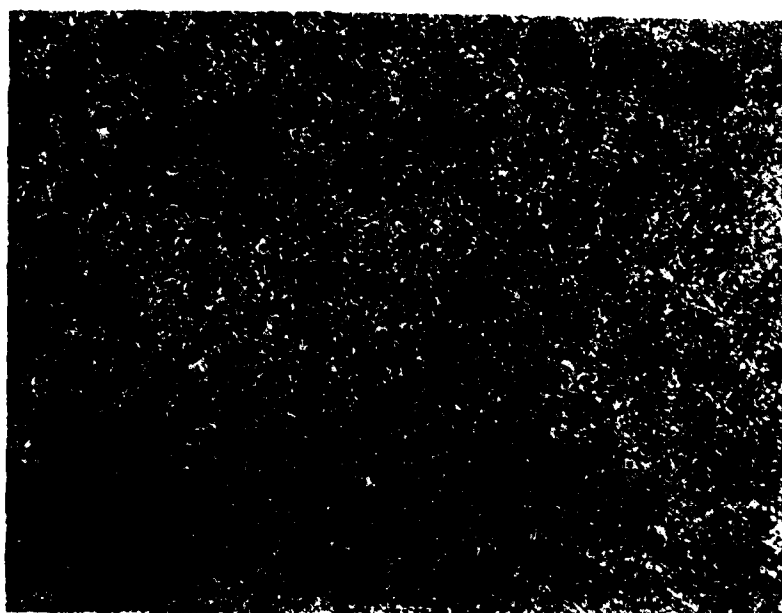


500X

Figure 1 Photomicrographs depict the AF115 Material
Microstructure in the As-HIP Condition
Etchant: 90-5-5 ($\text{HCL-HNO}_3\text{-H}_2\text{SO}_4$)



100X



500X

Figure 2 Photomicrographs depict the AF115 Material Microstructure in the fully Heat-Treated Condition

Etchant: 90-5-5 ($\text{HCL}-\text{HNO}_3-\text{H}_2\text{SO}_4$)

Table 3. Results of Density, TIP Reponse and Oxygen Analysis of AF115 (Al339/C1003).

Density, TIP Response

Density Measurements, degrees	Density		% TIP
	(gm/cm ³)	lbs/in. ³	
As-HIP (No Heat Treatment)	8.380	0.30277	---
As-HIP + 1149 C (2100 F)/4 Hours	8.369	0.30238	0.13
As-HIP + 1177 C (2150 F)/4 Hours	8.370	0.30241	0.12
As-HIP + 1191 C (2175 F)/4 Hours	8.357	0.30194	0.27
As-HIP + 1182 C (2160 F)/4 Hours, 760C (1400F)/16 Hrs.	8.378	0.30271	0.001

Oxygen Analysis

Log Corner	80 ppm O ₂
Log Center	28 ppm O ₂

B. SPECIMEN FABRICATION

Figure 3a shows the dimensions of the compact and location of the 14 slices. Slice 1 was used for the TIP and density characterization. Tensile, creep, stress rupture, and low-cycle-fatigue qualification specimens were machined from Slices 2 and 12 according to the configurations shown in Figure 4. Six compact tension specimens, two each of 6.35, 12.7, and 25.4 mm (0.25, 0.5 and 1 inch) thicknesses, were machined from Slice 6 for the thickness evaluation phase of the program (see Figure 3b). Eight 12.7 mm (0.5 inch) thick compact tension specimens were machined from Slices 4, 5, and 7 through 11; and four specimens from Slices 3 and 13 (see Figure 3c). The configuration of the machined compact tension specimens is illustrated in Figure 5. Because of the undersize diameter of the log, these specimens contained one beveled corner. It was located near one of the loading holes and had no influence on crack growth results. All compact tension specimens were identified by the slice number followed by an identification number.

C. MATERIAL CHARACTERIZATION

Tensile, creep, stress rupture, and low-cycle-fatigue (LCF) experiments were conducted to ensure the produced material was typical AF115. The results

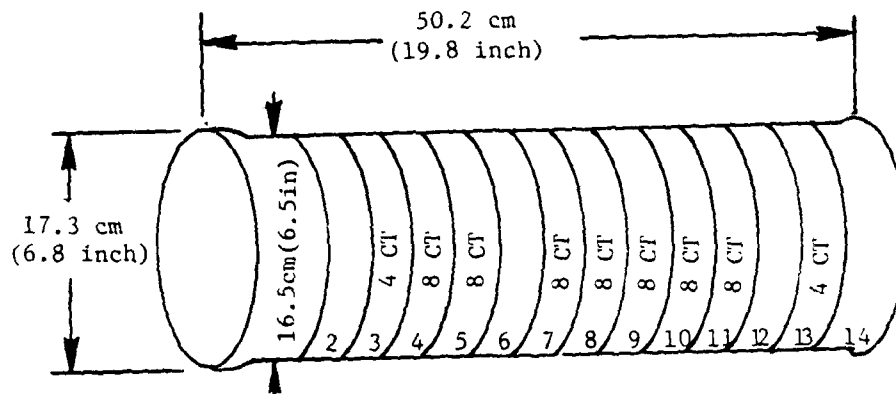


Figure 3a. Location of Slices from AF115 Material

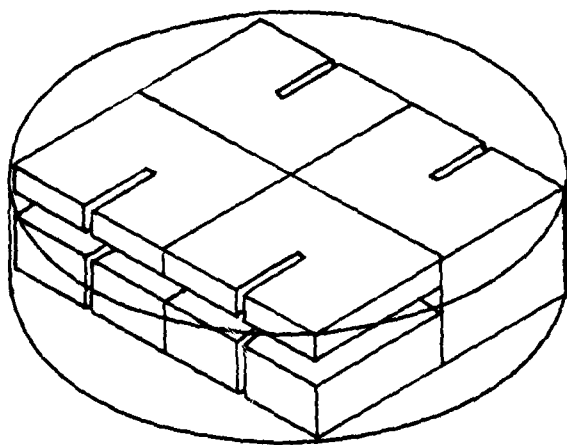


Figure 3b. Orientation of compact tension specimens for thickness evaluation.

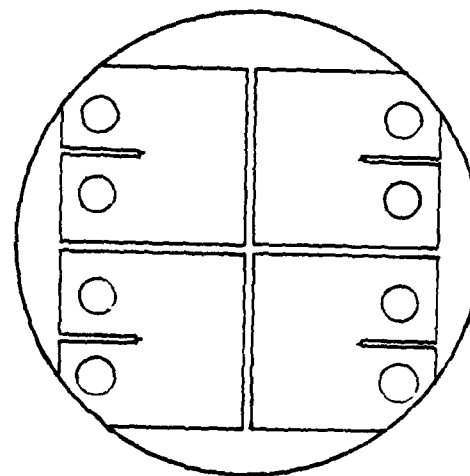
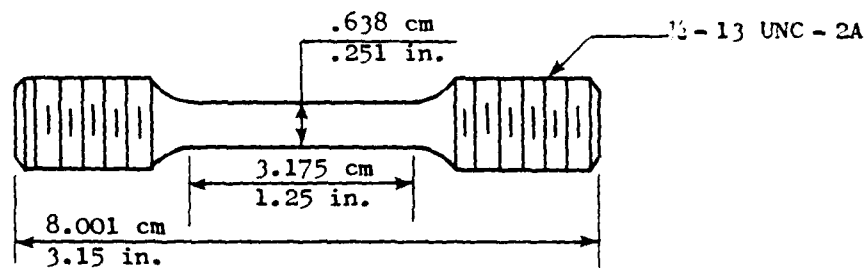
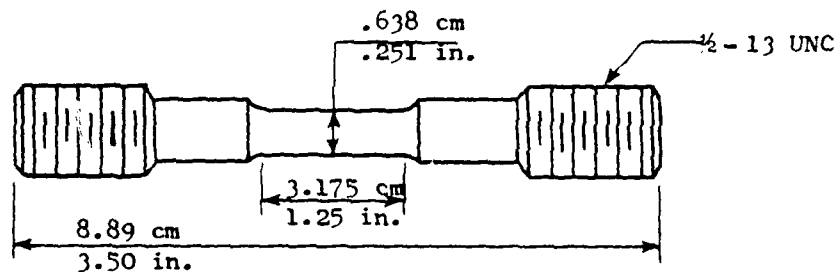


Figure 3c. Orientation of 12.2 mm (0.5 inch) compact tension specimen machined from slices.

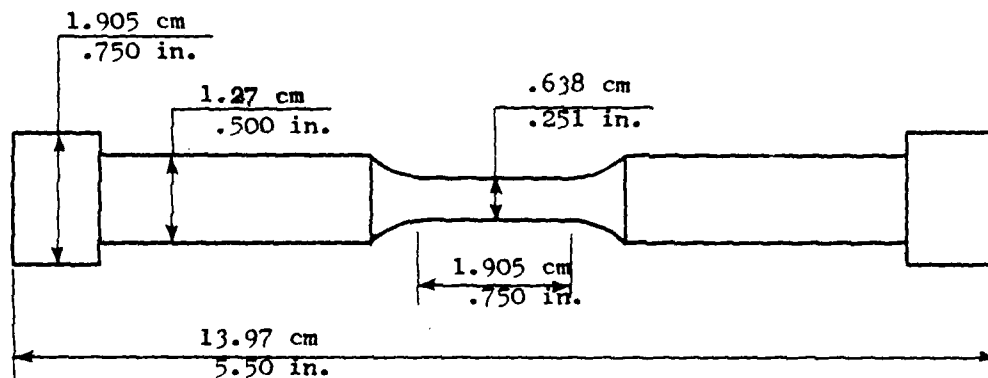
Figure 3. Location and Orientation of Compact Tension Specimens.



TENSILE SPECIMEN



CREEP & RUPTURE SPECIMEN



LOW CYCLE FATIGUE SPECIMEN

Figure 4. Specimen Configurations for Material Qualification Experiments.

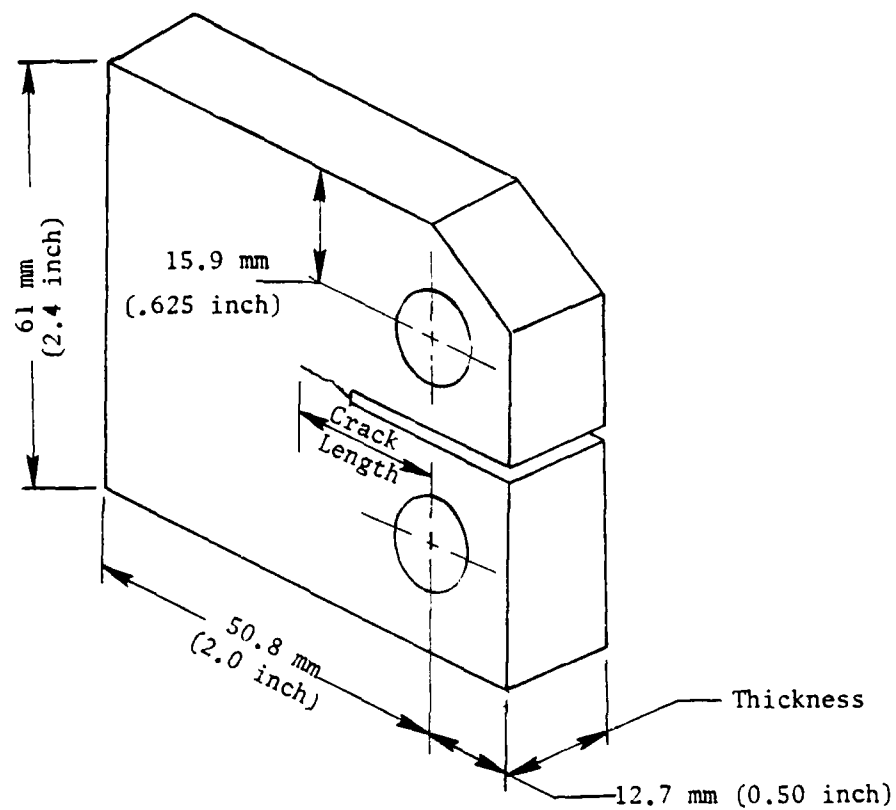


Figure 5. Configuration of Compact Tension Specimen for Cyclic Crack Growth Testing.

of the tests are reported in Table 4. Figures 6 through 8 graphically illustrate the tensile, creep, and stress rupture properties. The curves in those figures, which closely agrees with the data from this program, indicate the current expected properties of this material^(2,3). Low-cycle-fatigue experiments were tested in longitudinal strain control at 760° C (1400° F), a strain ratio (R) of zero, and test frequency of 0.33 Hz. The LCF data are well behaved in that they displayed a linear relationship when the strain ranges were plotted versus their respective fatigue lives on logarithmic coordinates (see Figures 9). The fatigue lives were compared to existing General Electric unpublished AF115 data and found above average, most likely a result of its extremely low TIP response. Based on the property levels of the qualification tests this AF115 compact was judged fully acceptable for the subsequent cyclic crack growth program.

Table 4. Results of Qualification Test for Heat of AF115 (A1339/C1003).

<u>Tensile Test Results</u>									
<u>Temperature</u>		<u>UTS</u>		<u>0.2% YS</u>		<u>0.02% YS</u>		<u>Elongation</u>	<u>RA</u>
<u>° C</u>	<u>° F</u>	<u>MPa</u>	<u>ksi</u>	<u>MPa</u>	<u>ksi</u>	<u>MPa</u>	<u>ksi</u>	<u>%</u>	<u>%</u>
23.3	74	1650.7	239.4	1133.5	164.4	1030.1	149.4	20.4	16.9
649.0	1200	1521.0	220.6	1084.6	157.3	917.7	133.1	18.3	19.1
760.0	1400	1190.1	172.6	1094.9	158.8	1062.5	154.1	8.1	8.4
760.0	1400	1200.0	174.0	1049.4	152.2	898.3	130.3	7.9	8.6

Stress Rupture Test Results

<u>Temperature</u>		<u>Stress</u>		<u>Life</u>
<u>° C</u>	<u>° F</u>	<u>MPa</u>	<u>ksi</u>	<u>Hours</u>
760	1400	689.5	100	91.4
760	1400	689.5	100	137.1

Creep Rupture Test Results

<u>Temperature</u>		<u>Stress</u>		<u>Time to 0.2%</u>
<u>° C</u>	<u>° F</u>	<u>MPa</u>	<u>ksi</u>	<u>Extension, hours</u>
760	1400	551.6	80	79.0
760	1400	551.6	80	108.0

Low-Cycle-Fatigue Test Results

760° C (1400° F), Longitudinal Strain Control, $A_e = 1$

<u>Total Strain</u>	<u>Fatigue Life,</u>
<u>Percent</u>	<u>Cycles</u>
1.1	1,502
0.9	2,239
0.9	3,042
0.7	24,560
0.55	77,371
0.55	91,547

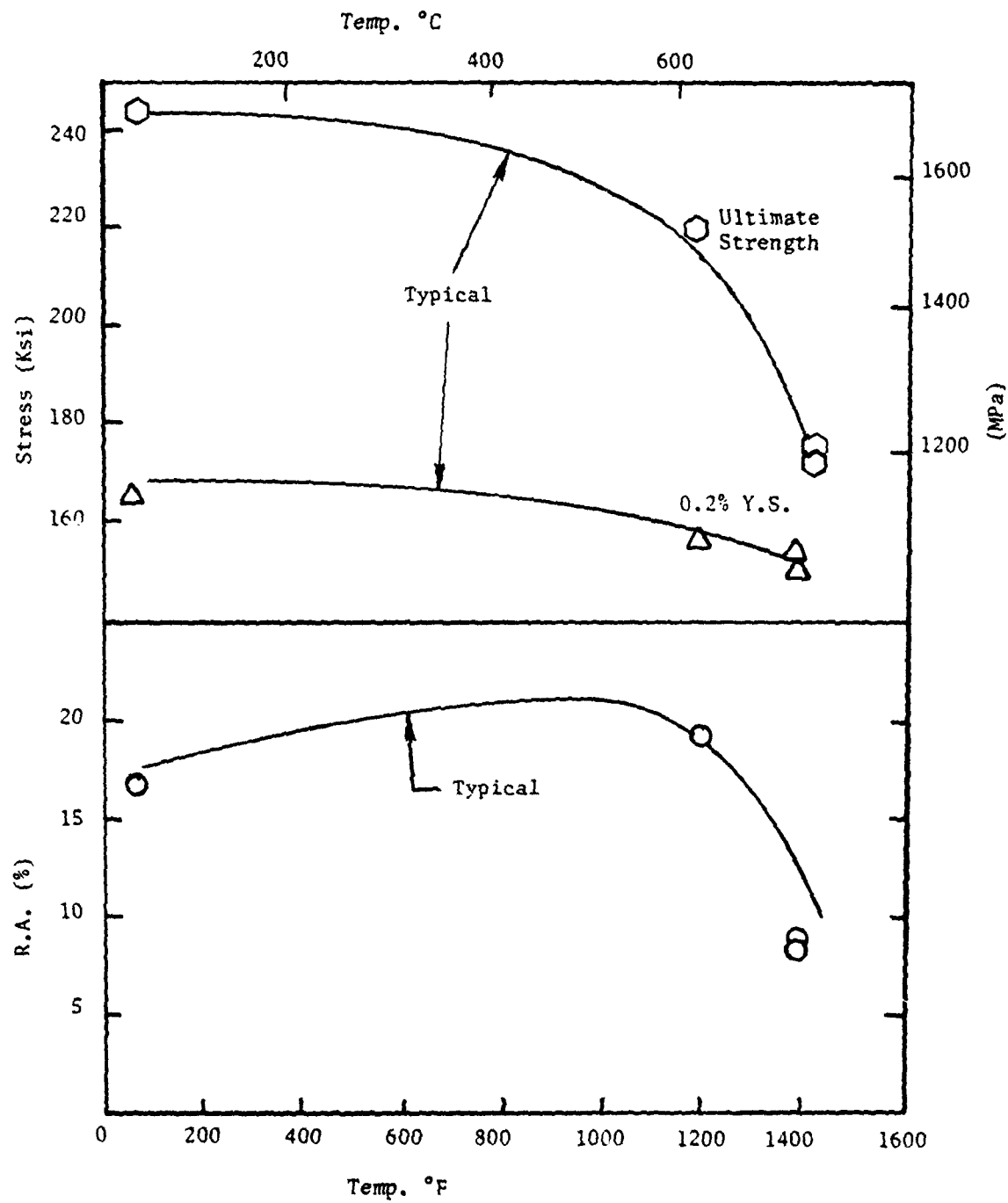


Figure 6. Tensile Properties of Heat A1339/C1003 in Comparison to Typical Properties

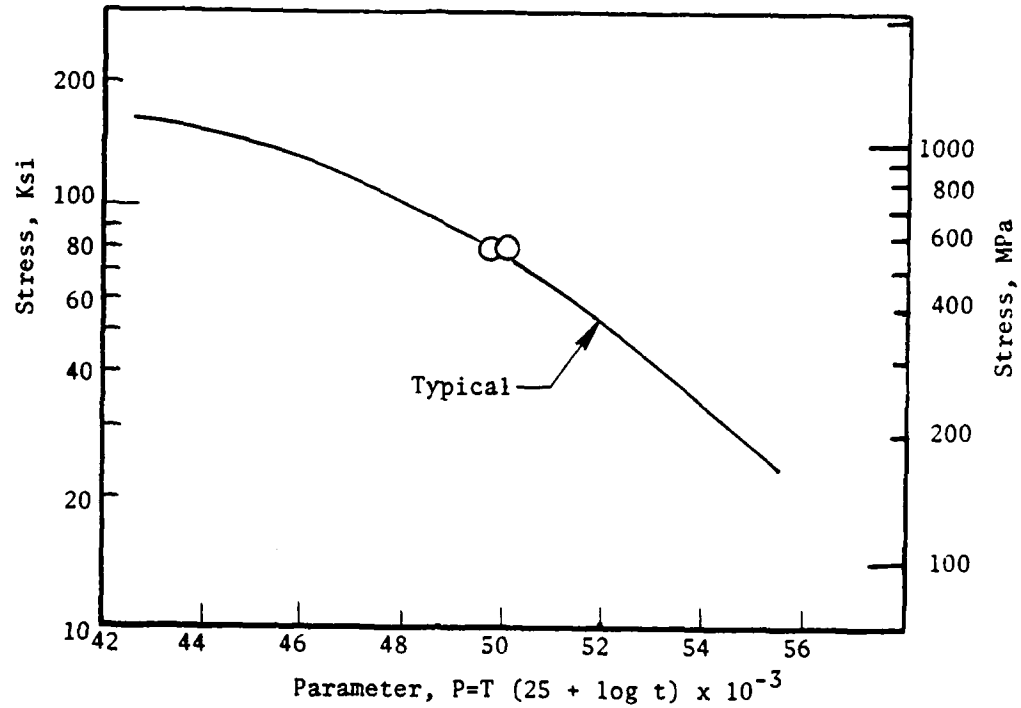


Figure 7. 0.2% Creep Properties of Heat Al339/C1003 in Comparison to Typical Properties

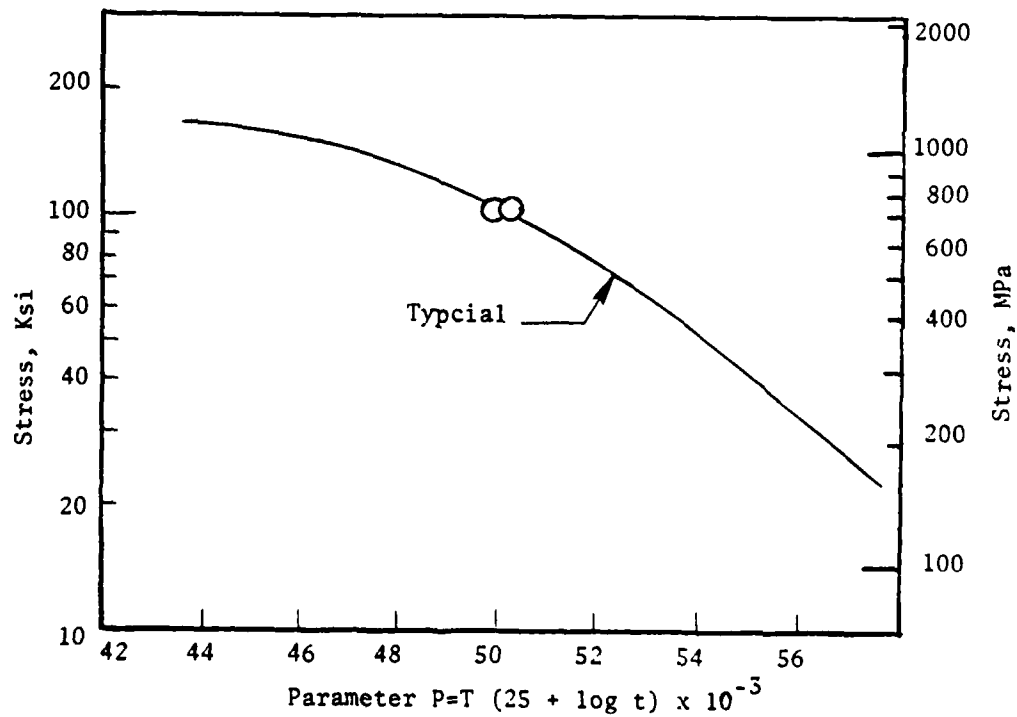


Figure 8. Stress Rupture Properties of Heat Al339/C1003 in Comparison to Typical Properties.

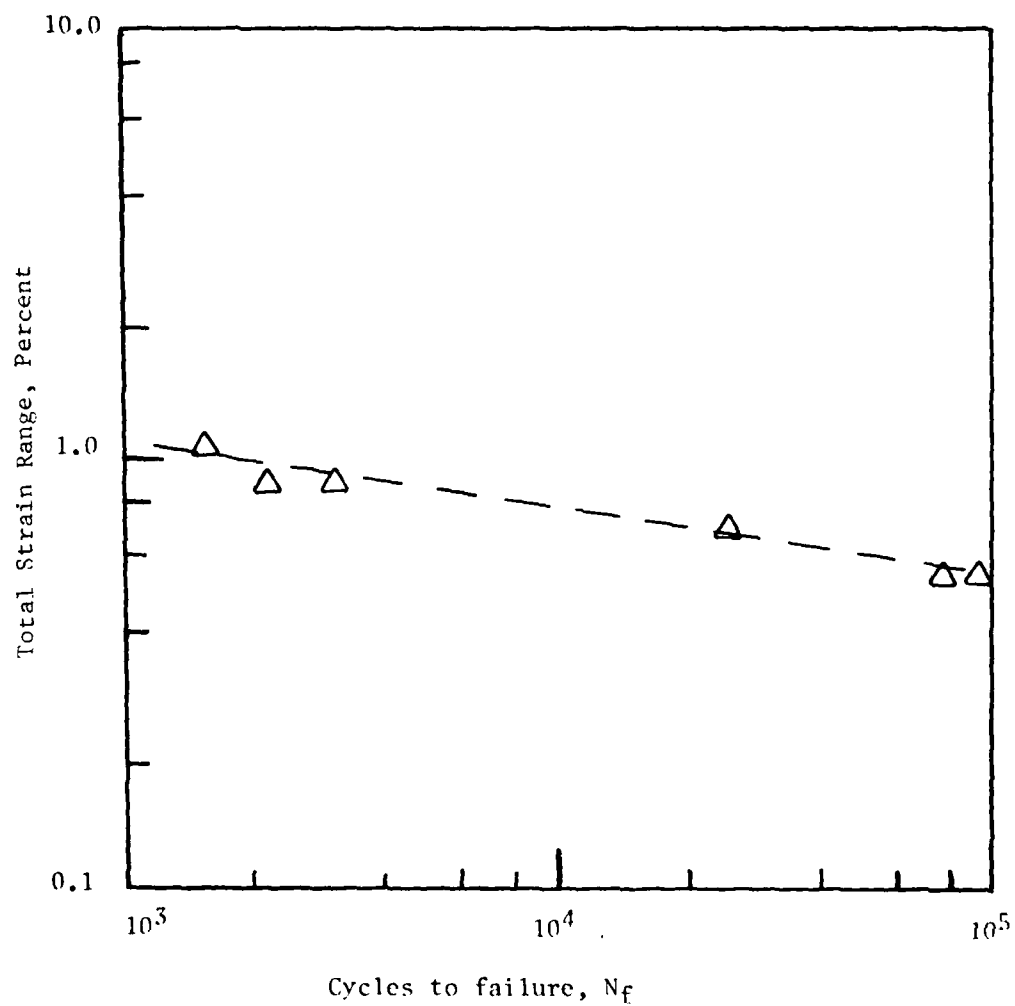


Figure 9. Low-Cycle-Fatigue Results of Heat A1339/C1003.

III. EXPERIMENTAL PROGRAM

The experimental program was separated in three phases. Initially six experiments were conducted to determine the specimen thickness effect on crack growth behavior and the loads to be used for the primary test program. Secondly, the primary test program was conducted using a uniform test specimen of thickness determined from the results of the initial phase. After the interpolative model was completed four verification experiments were conducted to evaluate the success of the model. Each of these phases will be discussed within the following subsections.

A. LOAD/THICKNESS EVALUATION MATRIX

As the initial test series, 6 compact tension specimens were tested at 760° C (1400° F), a stress ratio of 0.025, and frequency of 0.33 Hz to determine for the primary test program the minimum thickness of test specimen that provides essential plane strain crack growth data. Two load ranges, 7399 Newtons (1650 lb) and 8896 Newtons (2000 lb), were utilized. The load ranges were calculated to result in applied net section stresses of 40% and 60% of the 760° C (1400° F) yield strength (0.2%) of this AF115 material based on a total crack length of 20.3 mm (0.8 inch). The specimens were precracked to a crack length consistent with the requirement to initiate testing at 16.47 MPa \sqrt{m} (15 ksi $\sqrt{in.}$). Two specimens of three thicknesses; namely, 25.4 mm (1.00 inch), 12.7 mm (0.50 inch), and 6.35 mm (0.25 inch) were tested.

B. PRIMARY TEST MATRIX

The objective of the primary test matrix was to conduct a sufficient number of experiments at various conditions so that the crack growth characteristics of AF115 could be accurately evaluated within the range of the test conditions. For test efficiency, a statistically partial factorial box design experimental program was selected - specifically the hypercuboctahedron box design. The test conditions were tailored so that the data were gathered at critical levels of each variable to satisfy the subsequent Analysis of Variation (ANOVA).

This technique allowed the influences of each of the variables to be determined independently of the other variables, as well as the possible interactions between these variables. Thus, it was possible to test only selected conditions without sacrificing significant confidence in the interpolative model. In certain areas, such as high temperatures and long hold periods, it was expected that the effects would be more complex than could be fully determined by this statistical design. Therefore, to improve predictions in such areas, additional experiments were added. The designed matrix is shown in

Table 5. The A's and B's indicate the tests in the primary matrix divided into two orthogonal blocks and which of the two test equipment systems was to be used for that test. The X's indicate the extra tests added to the hyper-cuboctahedron box design. At the center of the matrix, four tests at a single condition were concentrated to determine a measure of variability in the data.

The stress ratios evaluated were 0.1, 0.5, and 0.9. These essentially covered the entire range possible in the cyclic loading of the compact tension specimen and were also considered adequate for most turbine disk design conditions where stress is primarily due to centrifugal loading. Three levels of cyclic frequency (0.025, 0.25, and 2.5 Hz) were selected for coverage. Test temperatures ranged from 538° to 760° C (1000° to 1400° F). Below 538° C (1000° F) hold time and frequency effects should not occur while 760° C (1400° F) is the upper limit for usage of AF115. Hold times up to 300 seconds were evaluated which was considered adequate to assess the importance of most turbine disk hold times.

C. VERIFICATION TESTS

Two verification experiments were conducted at two conditions selected by the Materials Laboratory (AFWAL) after the completion of the development of the interpolative model. Those conditions are outlined below:

Test Condition 1 593° C (1100° F), R = 0.3, 0.1 Hz, no hold time

Test Condition 2 704° C (1300° F), R = 0.6, 0.1 Hz, 30 sec hold

Table 5. Expanded Test Matrix.

Frequency, Hz	g Ratio	704° C (1300° F)				538° C (1000° F)				649° C (1200° F)				760° C (1400° F)			
		Hold Time, sec				Hold Time, sec				Hold Time, sec				Hold Time, Sec			
		0	9	90	300	0	9	90	300	0	9	90	300	0	9	90	300
0.025	0.1						A			A	B				B		
(1.5 CPM)	0.5						A	B							B	A	
	0.9						B				B	B				A	
0.25	0.1	X		X			A	X	B	X		X	X	B		A	X
(15 CPM)	0.5												AA				X
													BB				
	0.9						B	A						A	B		
2.5	0.1							B			B	A			X	A	
(150 CPM)	0.5						B	A							A	B	
	0.9						A				A	B				B	

NOTES:

A's and B's indicate the tests in the primary balanced matrix are divided into two orthogonal blocks (A and B) of 18 tests each for a total of 36 tests.

X's indicate the extra tests (10) in the expanded matrix for a total of 46 tests.

IV. EXPERIMENTAL PROCEDURES

All cyclic crack growth experiments were conducted at General Electric, Aircraft Engine Group (AEG), in two servo-controlled, electrohydraulic test systems operated in closed-loop control. Details on precracking, load determinations, heating, and crack measuring will be discussed within this section.

A. PRECRACKING

The compact tension specimens were EDM notched followed by precracking at either room or elevated temperature. Initially, the specimens were precracked at room temperature at 30 Hz with cyclic loads being stepped down in 10% increments as a function of precrack length. The final precrack length and applied loads produced a stress intensity range less than or equal to the initial stress intensity of the subsequent elevated temperature cyclic crack growth tests. The specimens were reversed within the test system, if required, to maintain reasonably even surface crack lengths. Approximately half of the specimens were precracked in this fashion. During early stage of testing it appeared that the precracking was interfering with the normal crack growth behavior since the curvature of the crack would rapidly change shortly after initiation of crack extension as noted in Figure 10. The surface measurements of S/N 4-8 satisfies the ASTM E647⁽⁴⁾ requirements which recommends that the variation in the two measured crack lengths be less than 0.025 times the width or 0.25 times the thickness, whichever is greater. As noted in Figure 10 the precracking process was, however, clearly influential during the early segment of crack growth. Other specimens, such as S/N 5-3, did not satisfy the ASTM requirements but the crack front became uniform during early crack growth. After these observations, precracking was conducted at elevated temperature within the system used for testing so that the final precracking was done at the test condition loads. Even then a few of the specimens produced uneven crack fronts. Specimen bending, other than that expected, was thoroughly examined prior to the test program. The affect that precracking had on growth rate will be discussed in a later section. The method of precracking used on each specimen and final crack measurements are listed on both surfaces within the experimental data.

B. TEST FACILITIES

Figure 11 depicts a view of one of two cyclic crack growth test facilities. It consists of a MTS 22.2 kN (5000 lb) closed-loop, electrohydraulic, servo-controlled, low-cycle-fatigue machine and associated control and monitoring equipment. The second facility consists of a 44.4 kN (10,000 lb) Pagasus system. In Figure 12, a close-up view of a compact tension specimen installed in the load train is provided. Specimen heating was provided by a specially designed split shell three zone resistance furnace equipped with quartz viewing windows. Conventional 20X traveling microscopes were used to monitor

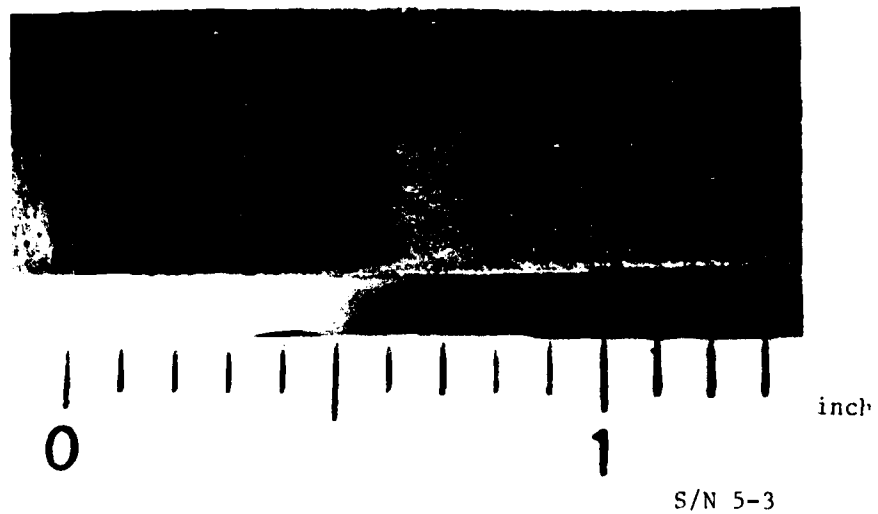
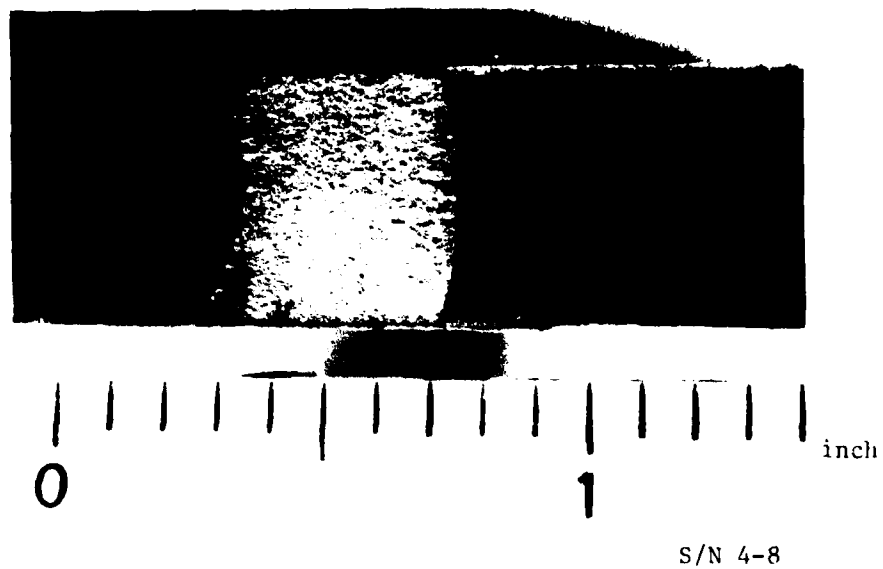


Figure 10. Room Temperature Precracked Specimens with Subsequent Elevated Test Conditions Showing Changes in Curvature After Initiation of Testing



Figure 11. Photograph of overall test set-up with MTS 5 KIP closed-loop equipment and associated control and monitoring equipment.

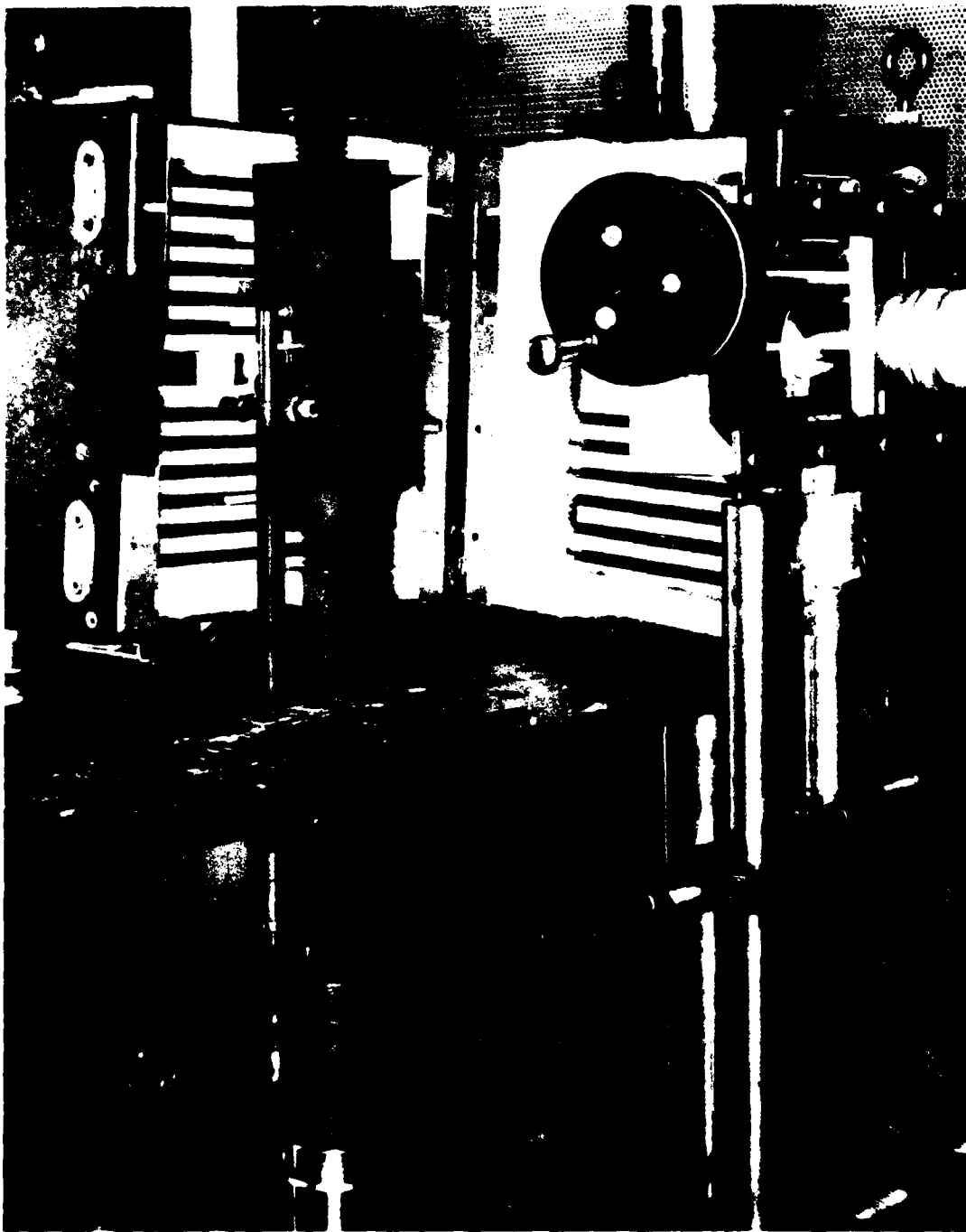


Figure 12. Photograph of close-up view of compact tension specimen in test fixture.

crack growth along both the front and back surfaces of the specimens. In each view of Figures 11 and 12, the split-shell resistance furnace and traveling microscope are shown.

Since transient growth rates can result from interruption of long durations the experiments were generally conducted continuously until failure. If significant growth of the crack was expected prior to the next schedule recording, the test was stopped and the static tensile load reduced to approximately 445 N (100 lb) and temperature reduced to 427° C (800° F). As will be noticed in the presentation of the data, some fluctuations occurred within the cyclic crack growth versus stress intensity results, and were probably a response to test interruptions. Because of the durations of these tests, these interruptions were unavoidable.

C. LOAD DETERMINATION

Based on the load/thickness evaluation, maximum loads were selected as 8.07, 9.35, and 13.99 kN (1815, 2102, 3145 lb) for the stress ratios of 0.1, 0.5, and 0.9, respectively. With a crack length of 16.5 mm (0.65 inch), these loads produced effective 16.47 MPa \sqrt{m} (15 ksi $\sqrt{in.}$) stress intensity range based on the Walker expression:

$$\Delta K_{eff} = \Delta K_{max} (1-R)^m \quad (1)$$

with the exponent (m) of 0.25. After a few experiments it became obvious that the higher temperature experiments with hold periods produced an insufficient range of crack growth rate while at lower temperature the duration of the tests became impractically long. Therefore, for the lower temperature experiments the procedure of successively increasing the load or crack length was implemented to produce various segments of the crack growth rate versus stress intensity curve. For the higher temperature experiments, the loads had to be decreased for the room temperature precracked specimens to produce a suitable amount of crack growth. The elevated temperature precracking of the specimens was conducted by initiating the crack from the EDM slot at loads above the test conditions and successively decreasing the loads. Reasonable growth rates were maintained during this elevated temperature precracking until the loads given above were achieved. The loads at which tests were conducted are summarized with the data.

D. CRACK GROWTH DATA REDUCTION

At the conclusion of each test, the raw crack length versus accumulative cycle data were reduced to cyclic crack growth rate (da/dN) by use of the seven-point sliding polynomial technique recommended by ASTM⁽⁴⁾. The crack lengths were adjusted for curvature by the ASTM recommended quarter width average crack length and maximum crack length technique⁽⁵⁾. In a few cases, insufficient crack length measurements were taken to produce a reasonable crack

growth rate versus stress intensity curve, especially since the seven-point sliding polynomial technique does not calculate crack growth rates for the first three and last three crack length measurements. In those cases, the crack length versus cycle number curve was visually estimated through the collected data points and additional points extracted from that curve. The stress intensity range value associated with the mid crack length of each set of consecutive seven points determined by:

$$\Delta K = \left(\frac{\Delta P}{B_1 \sqrt{W}} \right) \left(\frac{2 + \frac{a}{W}}{\left[1 - \frac{a}{W} \right]} \right)^{3/2} \left(0.886 + 4.64 \left(\frac{a}{W} \right) - 13.32 \left(\frac{a}{W} \right)^2 + 14.72 \left(\frac{a}{W} \right)^2 - 5.62 \left(\frac{a}{W} \right)^3 \right) \quad (2)$$

Thus pairs of da/dN and ΔK values were available for evaluation.

V. EXPERIMENTAL RESULTS

Pairs of crack length (from each side of the compact tension specimen) and cycle number were recorded from each of the crack growth tests. Those pairs were reduced into cyclic crack growth rate versus stress intensity data. The results of the experiments are summarized within the following subsections.

A. THICKNESS RESULTS

Six compact tension specimens, two each of three thicknesses, were tested to evaluate the thickness effect of the compact specimen geometry on crack growth behavior. Table 6 list the pertinent test parameters for these six tests. Specimen 6-3 failed during the high-cycle-fatigue, room temperature precracking as a result of an equipment malfunction and was not repeated. Figures 13, 14, and 15 show the fracture surfaces of the five tested specimens.

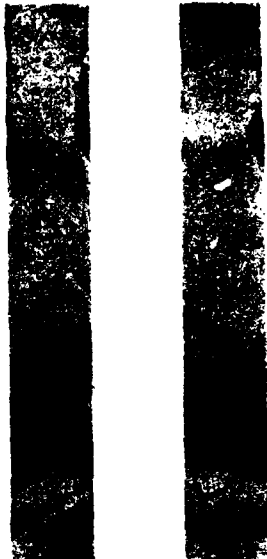
Table 6. Test Parameter Summary of Thickness/Load Determination Test Series.

Specimen S/N	Thickness,		Precrack*		Load Range		Precrack Temperature,	
	mm	inches	mm	inches	Newton's	lb	° C	° F
1-3	25.40	1.0	19.1	0.75	14,678	3300	R.T.	R.T.
2-3	25.40	1.0	14.5	0.57	17,792	4000	760	1400
3-3	12.70	0.50	15.2	0.60	8,896	2000	760	1400
4-4	12.70	0.50	21.3	0.84	7,339	1650	R.T.	R.T.
5-3	6.35	0.25	19.6	0.77	3,336	750	R.T.	R.T.
6-3	6.35	0.25	---	---	---	---	760	1400

*Precrack dimension tabulated is referenced from the center of the specimen pin hole.

Test Parameters: 760° C (1400° F) R = 0.025, 0.33 Hz

Bottom Half Top Half

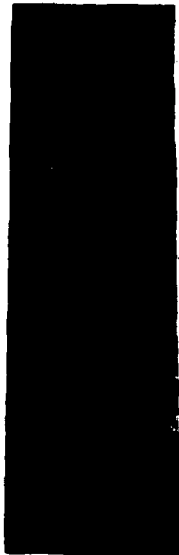


S/N 5-3 2X

Figure 13. 6.35 mm (0.25 inch) Thick Compact Tension Specimen Fracture Surface

Bottom Half

Top Half



S/N 3-3

2X

Bottom Half

Top Half



S/N 4-3

2X

Figure 14. 12.5 (0.5 inch) Thick Compact Tension Specimen Fracture Surface

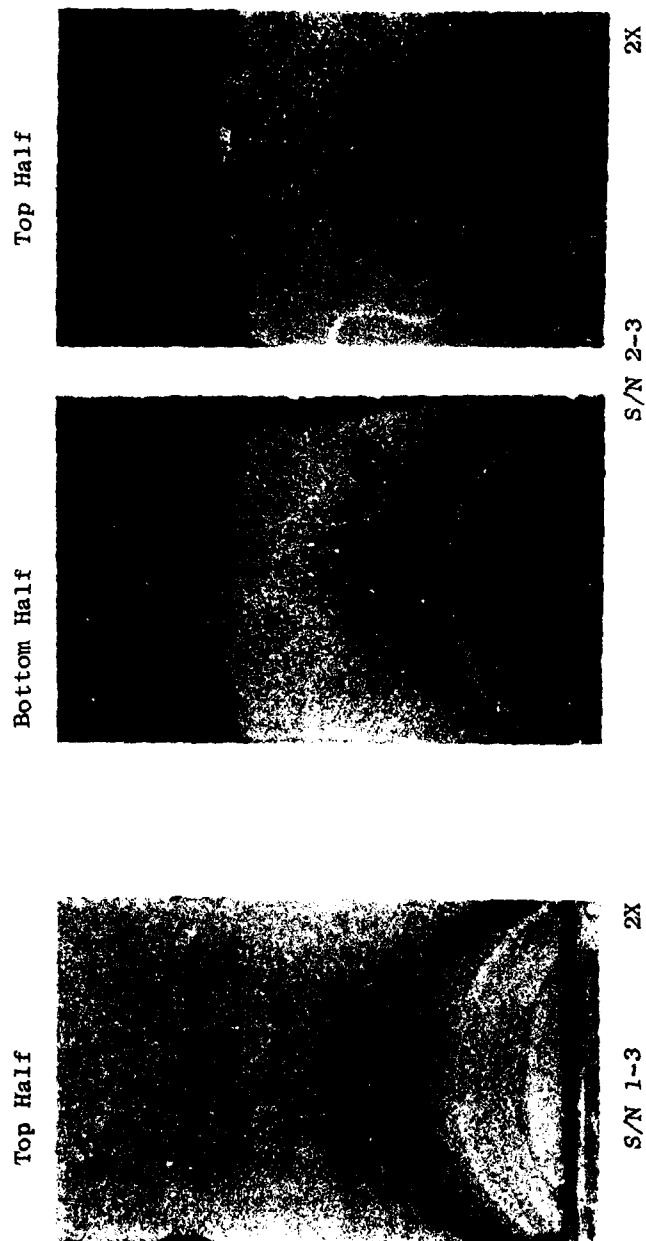


Figure 15 25.4mm (1 inch) Thick Compact Tension Specimens Fracture Surface

As shown in Figure 15, an extensive and variable crack front curvature resulted from the 25.4 mm (1 inch) thick specimens experiment. Figure 13 exhibits photographs of 6.4 mm (0.25 inch) specimen. This specimen fracture showed minimal curvature resulting from the actual cyclic crack growth test, but the precrack grew significantly deeper on one of the specimen's surface. This specimen was reversed in the test machine load train repeatedly during precracking to minimize this tendency; however, the uneven precrack persisted. The 6.4 mm (0.25 inch) thick specimen, being somewhat more flexible, is considered more sensitive to load train alignment. Figures 16 and 17 graphically show the da/dN versus ΔK values of the five experiments. Presented in Figure 16 are the data after incorporation of the ASTM 3 point crack front curvature correction. The data appears to form a single population independent of specimen thickness or applied load level. The 6.4 mm (0.25 inch) thick specimen appears to demonstrate a lower threshold stress intensity compared to the 25.4 mm (1 inch) thick specimen. This difference may be a result from the significant curvature noted in the thicker specimens. The data with the curvature correction clearly populates a single curve in the mid and upper crack growth rate regions indicating an insensitivity to the loads and thickness examined. Figure 17 shows the results with the stress intensity range based on the average surface crack length measurements. Use of the surface measurement clearly differentiates the 25.4 mm (1 inch) thick specimen data from the 12.7 and 6.35 mm (0.5 and 0.25 inch) thick specimen data.

Based on the results from the test series discussed above, the 12.7 mm (0.5 inch) thick specimen and the lower range (equivalent to 40% of the 0.2% yield strength) were selected as conditions for the primary test matrix program. The 12.7 mm (0.5 inch) thick specimen was selected to avoid the crack front curvature problems associated with the 25.4 mm (1 inch) thick specimen and the flexibility problems (uneven crack growth) associated with the 6.35 mm (0.25 inch) specimen. The lower load range was used based on the preferred use of a longer precrack specimen. The longer precrack was preferred to avoid potential shadowing affects associated with the EDM precrack notch.

B. RAW EXPERIMENTAL DATA

Pairs of measured crack length and accumulated cycle are tabulated within Appendix A for all experiments conducted within the primary test program. Included are the precracking conditions and test loads for each test. When the ASTM E647 recommendation that the uncracked ligament of the compact tension specimen be less than $(4/\pi)(K_{max}/\sigma_{ys})^2$ was exceeded, it is noted in Appendix A. This recommendation limits the specimen to be predominately elastic. While such situations did occasionally exist, this restriction was ignored during the development of the interpolative model. Techniques such as nonlinear fracture mechanics would be required to alleviate this concern which was outside the scope of this program.

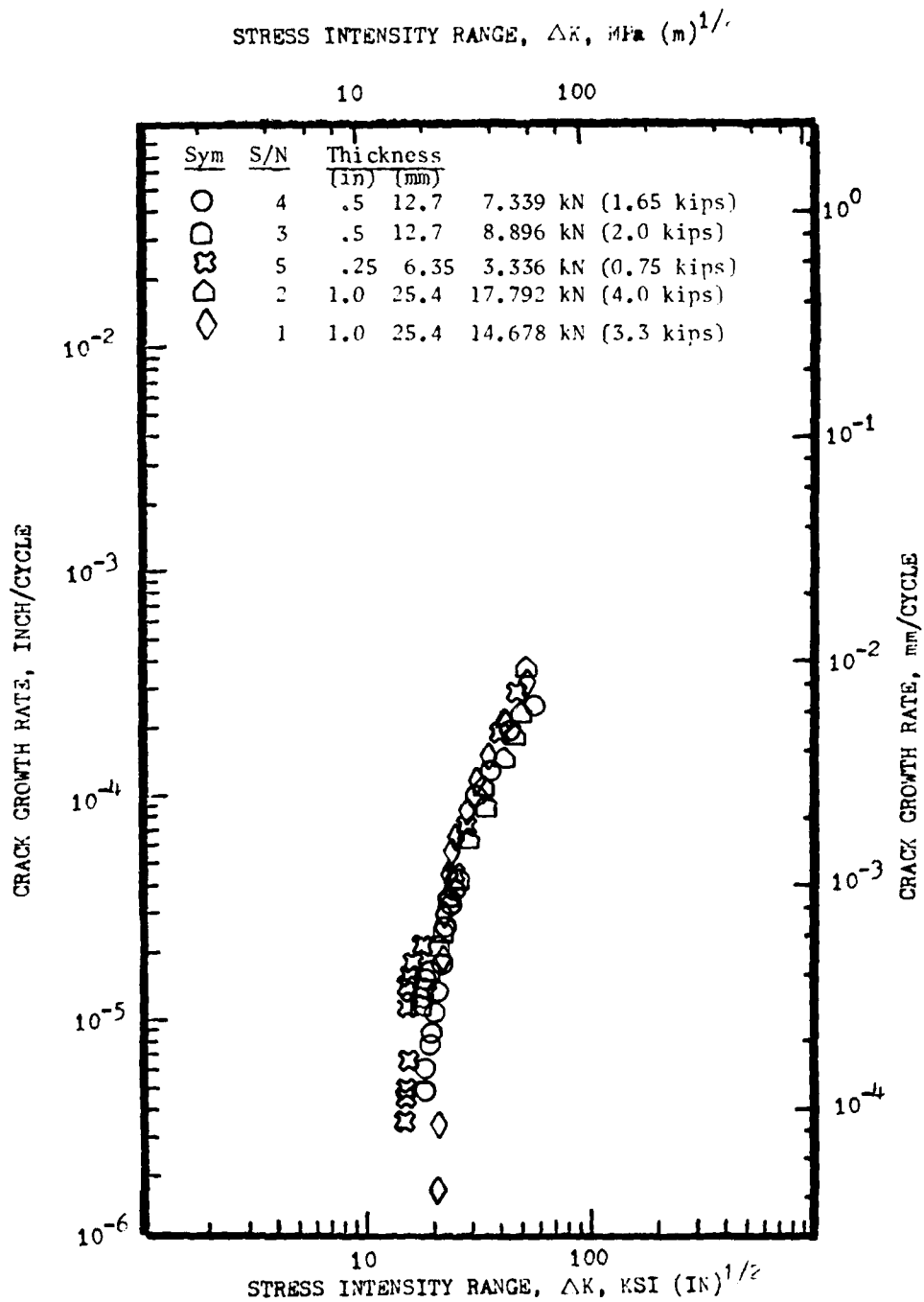


Figure 16. Cyclic Crack Growth Rate Versus Stress Intensity Factor of Three Thickness of Compact Tension Specimen with Stress Intensity Range Based on Average Surface Crack Lengths.

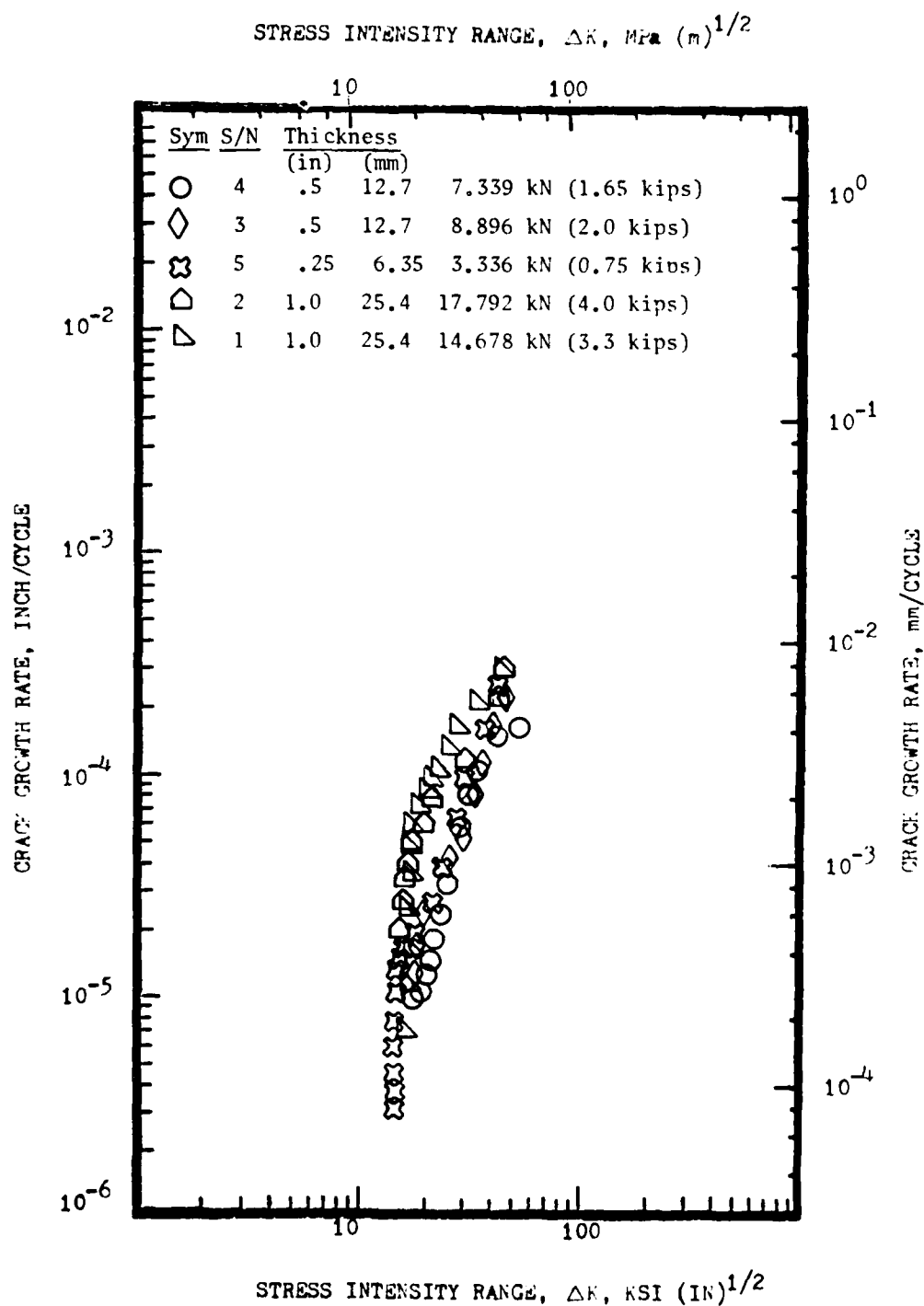


Figure 17. Cyclic Crack Growth Rate Versus Stress Intensity Factor of Three Thickness of Compact Tension Specimen with Stress Intensity Range Based on Average Surface Crack Lengths.

C. da/dN Versus ΔK Tabulation

The reduced cyclic crack growth rate versus stress intensity factor for each of the conducted tests are tabulated in Appendix B. The procedures used to derive these values were discussed earlier (Section 4.4). If the cyclic crack growth rate data was determined from an estimated crack length versus cycle number curve due to insufficient data being collected, it is noted in Appendix B. Plots of da/dN versus ΔK are present in Figures 18 through 20. The following observations for each of the test variables were made from these plots.

1. Frequency Effects

The following observations have been made with regard to frequency effects as indicated in Figures 18 through 20.

- At 538° C (1000° F) and 649° C (1200° F) and the stress ratio of 0.1 the frequency effect was negligible; however, at higher stress ratios an effect was observed. For example, at 649° C (1200° F) and stress ratio of 0.9 there existed up to a 2 decade difference in growth rate between the slowest and fastest continuous cycling experimental results.
- At 760° C (1400° F) and stress ratio of 0.1 (Figure 18d), a factor of three increase was observed between 2.5 Hz and 0.25 Hz experimental results. At the stress ratio of 0.5 an order of magnitude was observed for the same change in frequency (Figure 19c). With hold periods less variation in growth rate existed between frequencies.
- When approaching the lower and upper asymptotes the frequency of the experiments became insignificant.

2. Hold Time Effects

The following observations have been made with regard to hold time effects.

- At 538° C (1000° F) hold time was noninfluential at the stress ratio of 0.1 and had only a slight effect at $R = 0.9$ (Figures 18a and 20).
- At 649° C (1200° F) and a stress ratio of 0.1, a 90 second hold period increased the growth rate up to a factor of 20 for all three frequencies (Figure 18b). At the stress ratio of 0.9 and 2.5 Hz a 2-1/2 order of magnitude increase in growth rate was observed when a 90 second hold period was added (Figure 20b).
- At 760° C (1400° F) and stress ratio of 0.1 the difference between the fastest cycle (2.5 Hz) and slowest cycle (0.25 Hz + 300 second hold) produced a 3 decade increase in growth rate (Figure 18d). A two order of magnitude increase was observed between the 0.25 Hz ($R = 0.1$) condition and that with a 90 second hold period.

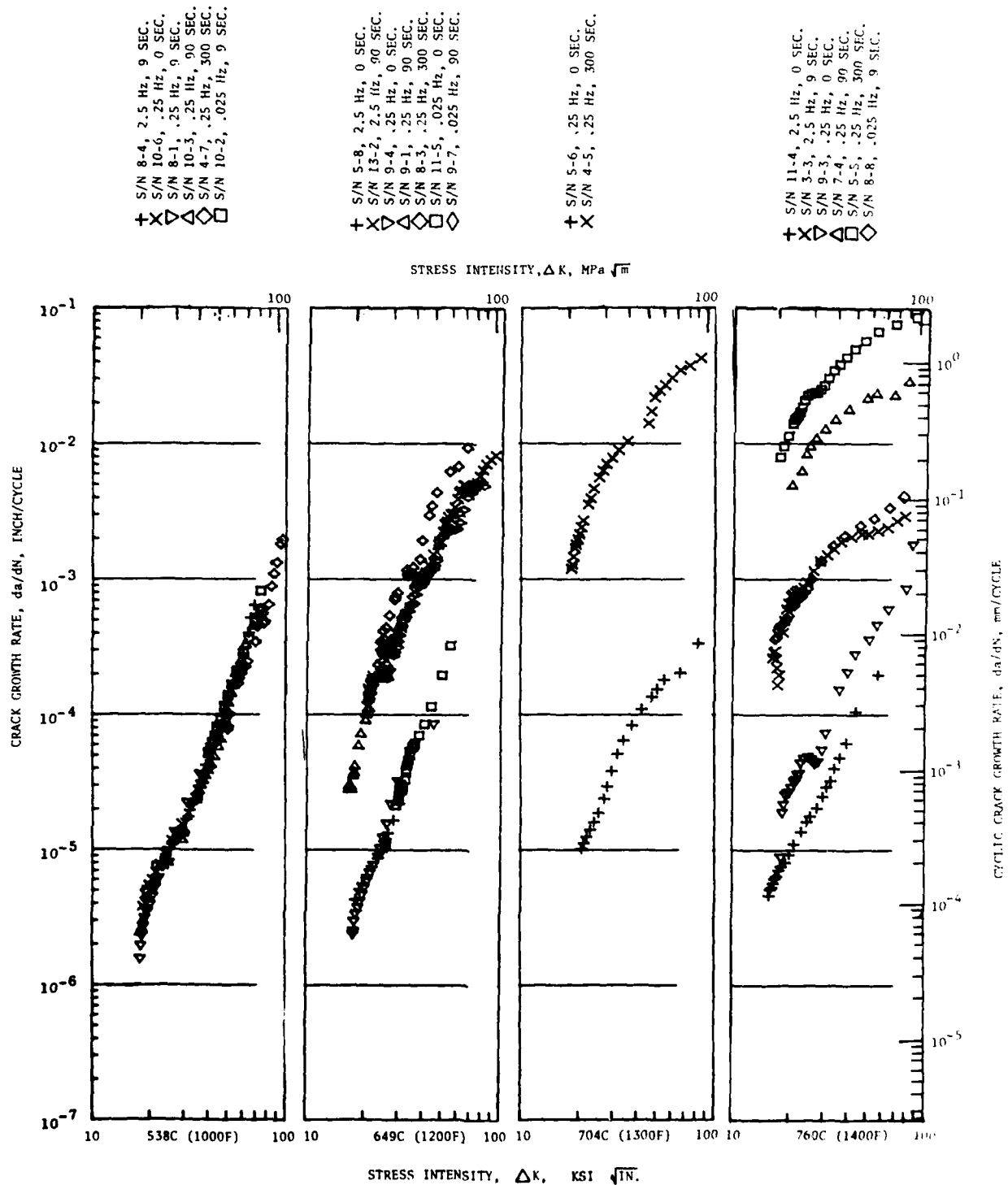


Figure 18. Experimental Results of Crack Growth Tests Conducted at the Stress Ratio of 0.1.

+ S/N 5-7, 2.5 Hz, 0 SEC.
 x S/N 4-3, 2.5 Hz, 90 SEC.
 v S/N 5-3, .025 Hz, 0 SEC.
 Δ S/N 8-7, .025 Hz, 90 SEC.

+ S/N 11-7, .25 Hz, 9 SEC.
 x S/N 11-1, .25 Hz, 9 SEC.
 v S/N 8-5, .25 Hz, 9 SEC.
 Δ S/N 4-6, .25 Hz, 9 SEC.

+ S/N 9-8, 2.5 Hz, 0 SEC.
 x S/N 7-8, 2.5 Hz, 90 SEC.
 v S/N 3-1, .25 Hz, 0 SEC.
 Δ S/N 4-1, .025 Hz, 0 SEC.
 ◇ S/N 4-2, .025 Hz, 90 SEC.

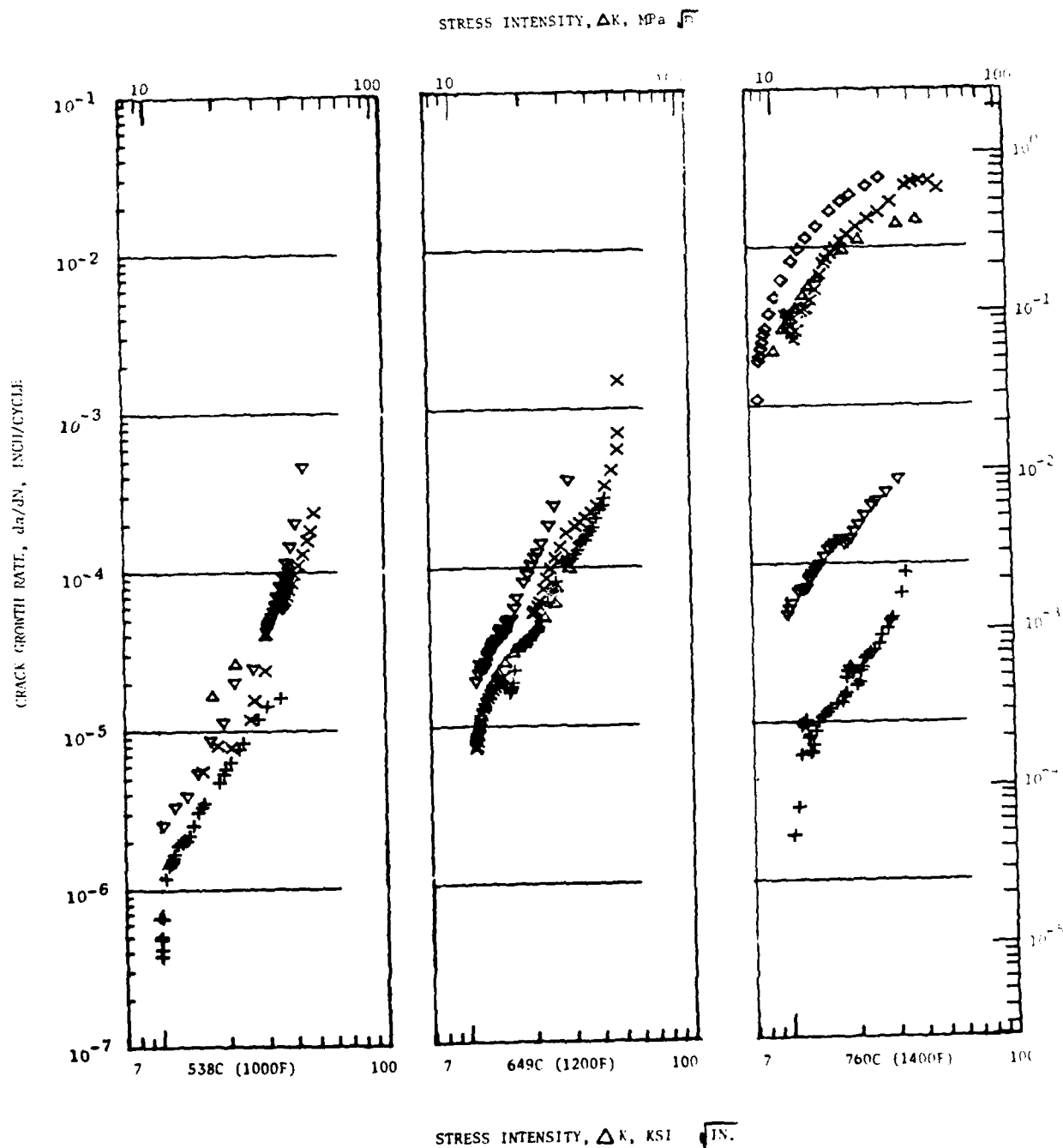


Figure 19. Experimental Results of Crack Growth Tests Conducted at the Stress Ratio of 0.5.

+ S/N 11-2, 2.5 Hz, 9 SEC.
 X S/N 4-8, .25 Hz, 0 SEC.
 ▽ S/N 10-1, .25 Hz, 90 SEC.
 △ S/N 5-1, 2.5 Hz, 9 SEC.

+ S/N 11-6, 2.5 Hz, 0 SEC.
 X S/N 8-6, 2.5 Hz, 90 SEC.
 ▽ S/N 10-5, .025 Hz, 0 SEC.
 △ S/N 3-4, .025 Hz, 90 SEC.

+ S/N 5-2, 2.5 Hz, 9 SEC.
 X S/N 4-4, .25 Hz, 0 SEC.
 ▽ S/N 10-7, .25 Hz, 90 SEC.
 △ S/N 11-8, .025 Hz, 9 SEC.

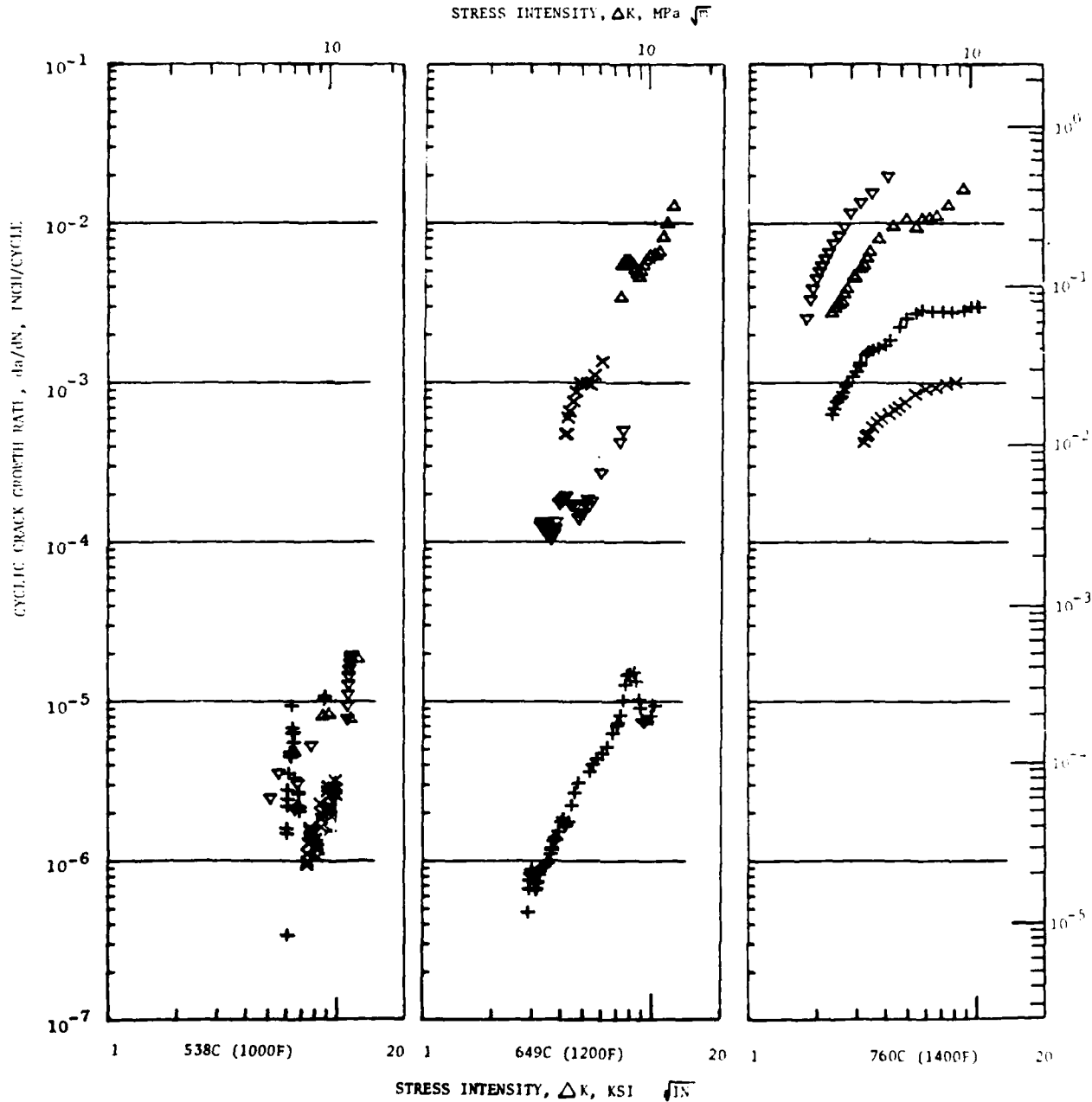


Figure 20. Experimental Results of Crack Growth Tests Conducted at the Stress Ratio of 0.9.

- The influences of hold time, when present, decreased when approaching the lower and upper asymptotes.

3. Stress Ratio Effects

Increasing stress ratio would either increase, decrease, or not change the vertical location of the inflection point of the crack growth curve. The direction depended on the other test condition. The range between ΔK^* and ΔK_C decreased with the combination of increasing stress ratio and decreasing temperature.

4. Temperature Effects

Temperature had the following effects on crack growth behavior.

- At a stress ratio of 0.1 without hold period, approximately 1/2 an order of magnitude variation in growth rate was observed between the 538° C (1000° F) and 760° C (1400° F) experimental results (0.25 Hz). When a 300 second hold period was included, a three decade increase in growth rate was observed between the two temperatures. As would be expected, as temperature increased the influences of hold time and frequency increased.

VI. INTERPOLATIVE MODEL

The interpolative model was developed using modified form of the General Electric Sigmoidal Equation to relate cyclic growth rate to stress intensity range for conditions within the limits of the test variables investigated. The modified equation contains six independent coefficients that are expressible as the slope and location of the inflection point, the lower and upper asymptotes, and the lower and upper shaping characteristics of the cyclic crack growth rate versus stress intensity curve. As will be shown, each of these parameters are relatable to the four test variables; namely, temperature, stress ratio, frequency, and hold time.

A. THE MODIFIED SIGMOIDAL EQUATION

In the late sixties, a six parameter sigmoidal equation was developed by General Electric which had the flexibility of corresponding to the complete range of traditional, nonsymmetric cyclic crack rate versus stress intensity data^(b).

That sigmoidal equation is:

$$\frac{da}{dN} = e^B \left(\frac{\Delta K}{\Delta K^*} \right)^P \left(\ln \frac{\Delta K}{\Delta K^*} \right)^Q \left(\ln \frac{\Delta K_c}{\Delta K} \right)^D \quad (3)$$

In logarithmic form:

$$\ln (da/dN) = B + P (\ln \Delta K - \ln \Delta K^*) + Q \ln (\ln \Delta K - \ln \Delta K^*) + D \ln (\ln \Delta K_c - \ln \Delta K) \quad (4)$$

Figure 21 illustrates the manner in which the coefficients of Equation 3 interact. The lower and upper asymptotes are expressed by ΔK^* and ΔK_c , respectively. The coefficients Q and D are shaping coefficients that control the lower and upper sections of the sigmoidal curve (see Figure 21a). Decreasing absolute values of the D or Q exponents results in a sharper transition at the appropriate end of the curve. The coefficient P adds to the sigmoidal equation a control of rotation at the inflection point of the crack growth curve. The coefficient B consists of a vertical movement of the curve. The location of the inflection point in the vertical direction is controlled by the combination of B, P, and ΔK^* (see Figure 21b). That interaction makes it nearly impossible to express the coefficients of the Sigmoidal Equation as a function of the test variables.

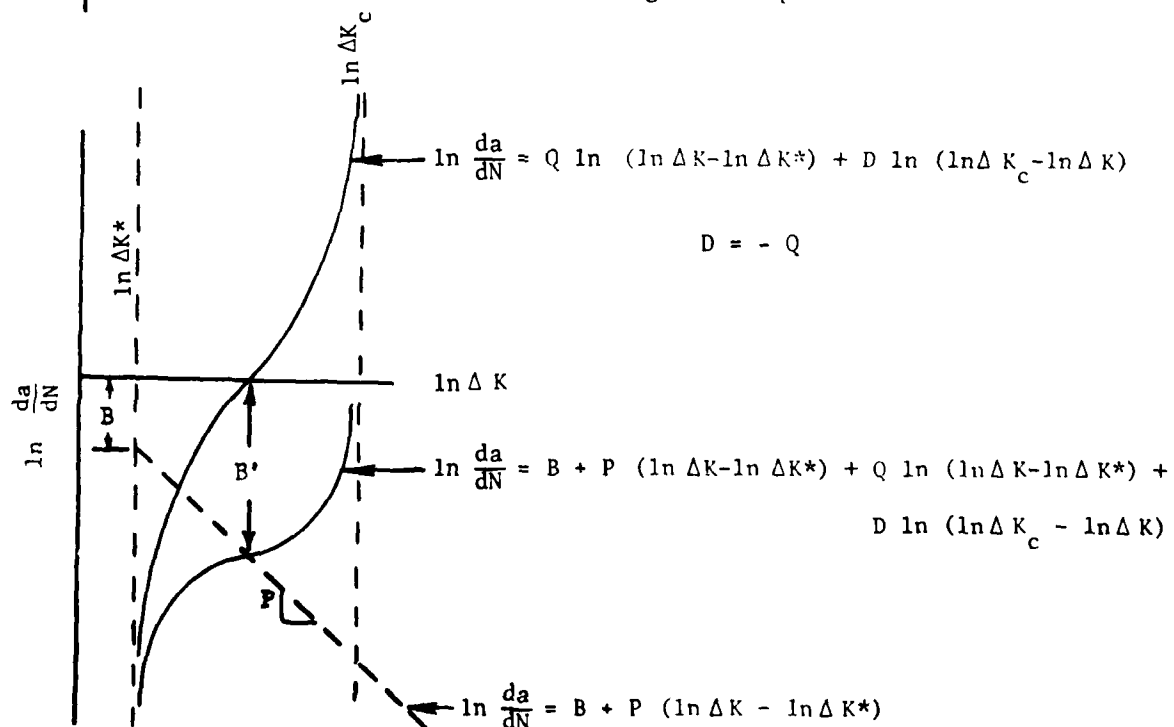
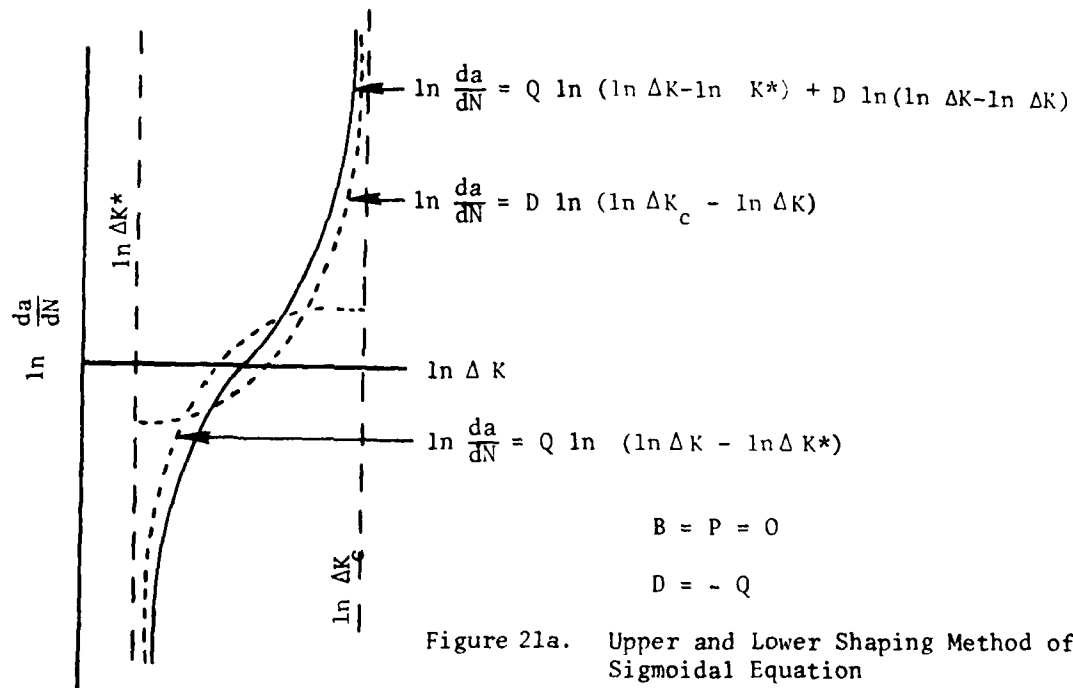


FIGURE 21b.

LOCATION AND ROTATION OF THE INFLECTION POINT BY THE SIGMOIDAL EQUATION

Figure 21. Illustration of Affects of the Coefficients of the Sigmoidal Equation.

To simplify Equation 3 so that the individual coefficients could be related to the test variables in a straight-forward manner, the equation was modified to:

$$\frac{da}{dN} = e^{B'} \left(\frac{\Delta K}{\Delta K_i} \right)^P \left(\ln \frac{\Delta K}{\Delta K^*} \right)^Q \left(\ln \frac{\Delta K_c}{\Delta K} \right)^D \quad (5)$$

The revised coefficient B' is simply the natural logarithmic magnitude of the vertical displacement of the inflection point of the symmetric crack growth rate versus stress intensity curve from the crack growth rate of unity. (see Figure 21b). The second term in Equation 5 contains ΔK_i , the location of the inflection point on the horizontal axis, rather than ΔK^* as in Equation 3. However, ΔK_i can be calculated from four of the other coefficients by:

$$\Delta K_i = \exp \left[\frac{\sqrt{Q} (\ln \Delta K_c) + \sqrt{-D} (\ln \Delta K^*)}{\sqrt{Q} + \sqrt{-D}} \right] \quad (6)$$

Further modifications permits the sigmoidal equation to be described by the vertical location of inflection point (da/dN_i), the horizontal location of inflection point (ΔK_i), the slope at the inflection point (da/dN_i'), the upper and lower shaping coefficients (D and Q), and the upper and lower asymptotes (ΔK_c and ΔK^*):

$$\frac{da}{dN} = \left(\frac{da}{dN_i} \right) \left(\frac{\Delta K}{\Delta K_i} \right)^{\left(\frac{da'}{dN_i} - \frac{Q}{\ln (\Delta K_i / \Delta K^*)} + \frac{D}{\ln (\Delta K_c / \Delta K_i)} \right)} \left(\frac{\ln (\Delta K / \Delta K^*)}{\ln (\Delta K_i / \Delta K^*)} \right)^Q \left(\frac{\ln (\Delta K_c / \Delta K)}{\ln (\Delta K_c / \Delta K_i)} \right)^D \quad (7)$$

Expressions were generated to relate ΔK_i , da/dN_i , da/dN_i' , ΔK_c , ΔK^* , and Q to the four test variables. The coefficients in Equation 5 are obtained by the following expressions.

$$D = - \left(\frac{\sqrt{Q} \ln (\Delta K_i / \Delta K_c)}{\ln (\Delta K_i / \Delta K^*)} \right)^2 \quad (8)$$

$$B' = \ln \left(\frac{da}{da_i} \right) - Q \ln \left[\ln (\Delta K_i / \Delta K^*) \right] - D \ln \left[\ln (\Delta K_c / \Delta K_i) \right], \quad (9)$$

and

$$P = \frac{da'}{dN_i} - Q / \ln (\Delta K_i / \Delta K^*) + D / \ln (\Delta K_c / \Delta K_i) \quad (10)$$

The relationship between the coefficients in Equation 7 and the four test variables will be given in the following subsections.

B. MODELING OF EXPERIMENTAL CONDITIONS

The slope and location of the inflection point, asymptotes, and shaping coefficients were equated to temperature, stress ratio, frequency, and hold time. Some of the coefficients required interaction with only one or two of the four test variables. Others, such as for the inflection point were found more complex and related to all four test variables. In many situations during the development of this model the coefficients governing the crack growth curve were estimated since tests were not conducted at all possible combinations of the four test variables. As permitted by the use of the hyper-cuboctahedron test program, the estimations were achieved by considering the surrounding test results in which only one test variable was different from that being examined. Details of each of the derived relationships are given below.

1. Stress Intensity At Fracture, ΔK_C

The final crack length was measured from each of the failed specimen and the stress intensity range calculated based on that crack length and applied loads of the test. A correlation of the final stress intensity range to frequency, hold period, or temperature was not present. There was, as would be expected, a dependency on stress ratio, such that:

$$\Delta K_C = \Delta K_{\max} (1-R) \quad (11)$$

The value of ΔK_{\max} was calculated to be 111 MPa \sqrt{m} 122 ksi $\sqrt{in.}$

2. The Lower Asymtote, ΔK^*

The lower asymptote ΔK^* , was estimated from each set of da/dN versus ΔK data. It was found relatable to stress ratio and temperature and independent of frequency and hold periods. For the stress ratio of 0.1 and temperatures between 538° and 760° C (1000° to 1400° F), ΔK^* was estimated as 10.98 MPa \sqrt{m} (10 ksi $\sqrt{in.}$). When plotted versus 1-R on logarithmic coordinates, as suggested by Klasnel and Lukas⁽⁷⁾ for the threshold, linear relationships were observed for each temperature (see Figure 22), so that:

$$\Delta K^* = \Delta K_{\max}^* (1-R)^n \quad (12)$$

For each temperature, ΔK_{\max}^* is the intercept at the stress ratio of zero, and n the slope. They were related to temperature by:

$$n \text{ or } \Delta K_{\max}^* = a_1 + b (T-1000)^d, \quad (13)$$

where a_1 , b , and d are coefficients determined by simple regression analysis.

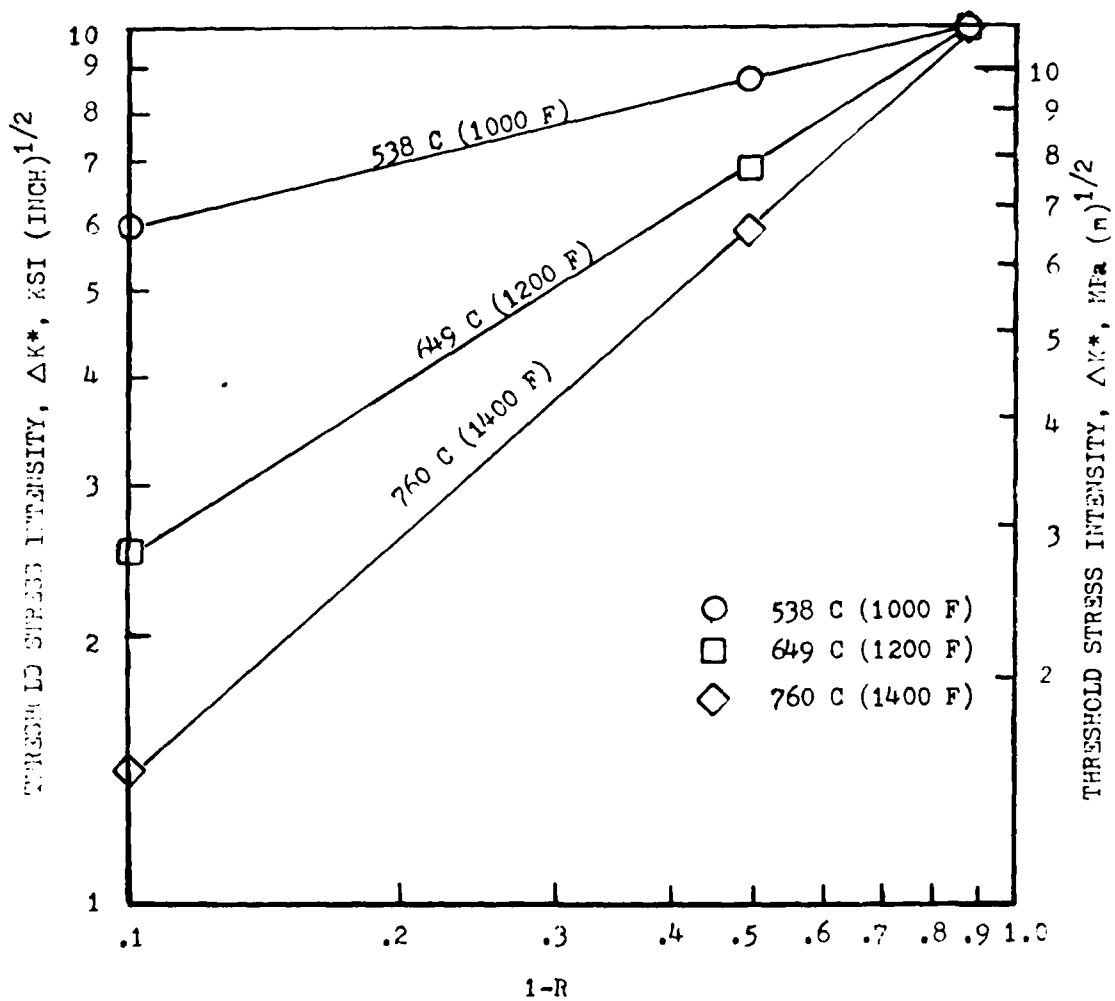


Figure 22. Correlation of Threshold Crack Growth and Stress Ratio (1-R) for 538, 649, and 760 C (1000, 1200, and 1400 F).

3. Horizontal Location Of Inflection Point, ΔK_i

The cyclic crack growth rate and stress intensity range at the inflection point (da/dN_i , ΔK_i) were determined for each set of experimental data by either multiple regression analysis or simple visual inspection. In examination of the da/dN_i and ΔK_i pairs on logarithmic coordinates, linear relationships were observed for each combination of temperature and stress ratio, so that:

$$\Delta K_i = f(da/dN_i, R, T) \quad (14)$$

Since such a linear relationship between ΔK_i and da/dN_i exist, then:

$$\Delta K_i = C (da/dN_i)^{n_1} \quad (15)$$

where for each combination for temperature and stress ratio, C represents the intercept of the relationship at da/dN_i of unity, and n_1 the slope between the relationship of da/dN_i and ΔK_i . Table 7 summarizes these constants. Figure 23 presents all pairs of da/dN_i and ΔK_i at the stress ratio of 0.1. Note that at this stress ratio, temperature was noninfluential on the relationship. The intercepts were related to stress ratios by the expression:

$$C = C_{@ 0.1} + e(1-R)^f \quad (16)$$

where e and f were related to temperature using the form of Equation 13. The slope n_1 , was set equal to 0.13 for stress ratios up to and including 0.5. For higher stress ratios the following relationship was used -

$$n_1 = e_1 \left(\log \frac{0.5}{(1-R)} \right)^{f_1} \quad (17)$$

4. Vertical Location Of The Inflection Point, da/dN_i

The vertical distance of the inflection point from the crack growth rate of unity, da/dN_i , was found to be influenced by temperature, frequency, hold time, and stress ratio:

Table 7. Slope and Intercept ($da/dN = 1.0$) of Linear Relationship Between da/dN_i and ΔK_i for Various Temperatures and Stress Ratios.

Temperature	Stress Ratios	Slope	Intercept, ksi $\sqrt{\text{in.}}$
538° C (1000° F)	0.1	.13	120.5
	0.5	.13	77.27
	0.9	.00	8.00
649° C (1200° F)	0.1	.13	120.5
	0.5	.13	77.27
	0.9	.04	8.69
760° C (1400° F)	0.1	.13	120.5
	0.5	.13	77.27
	0.9	.13	16.37

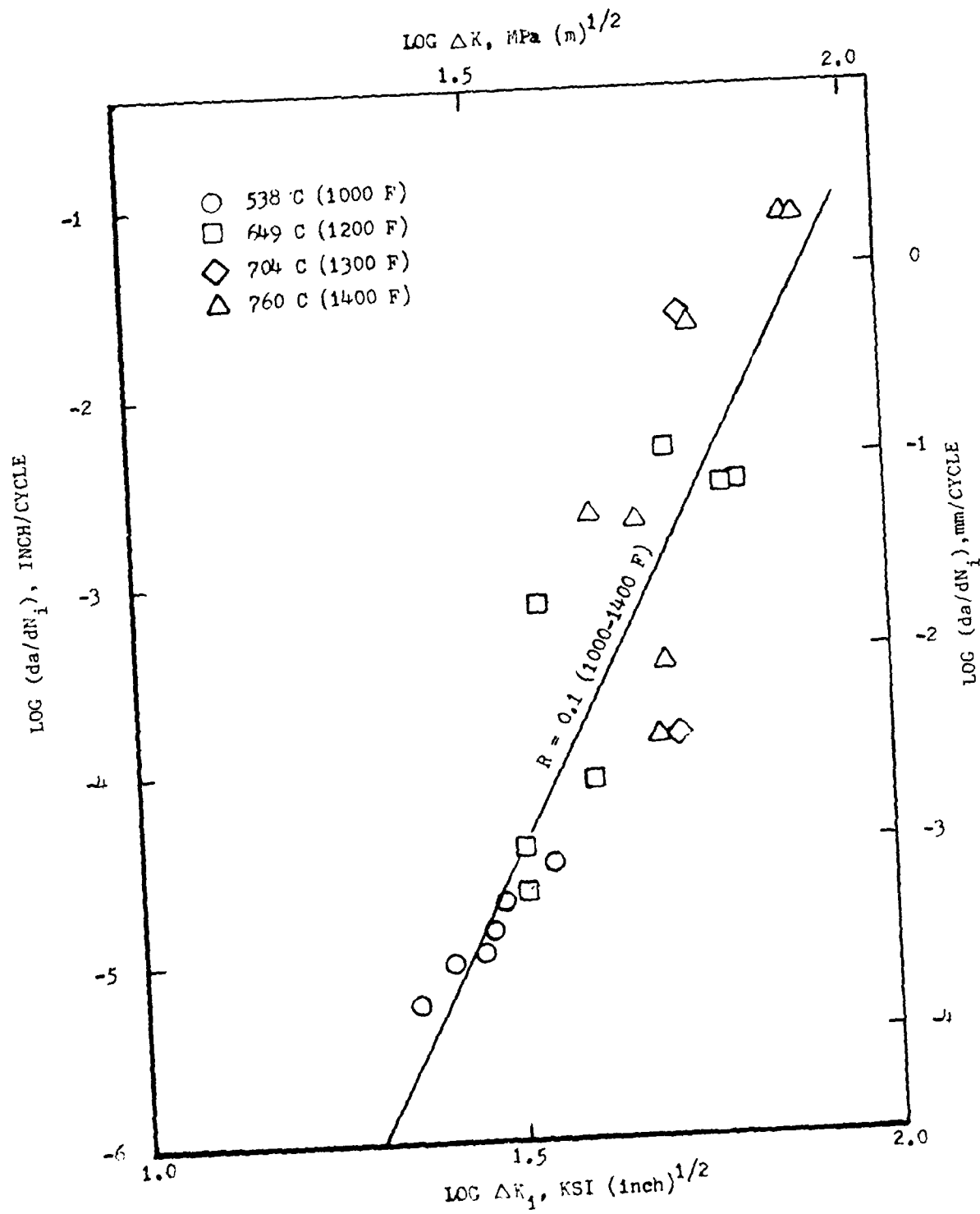


Figure 23. Pairs of da/dN_i and ΔK_i and Associated Relationship for the Stress Ratio of 0.1 and Temperatures Between 538 and 760 °C (1000 and 1400 °F).

$$\frac{da}{dN_i} = f(T, v, HT, R) \quad (18)$$

The inflection point for each of hold time conditions, da/dN_i^{HT} , was found calculable by adding a hold time damage onto the location of the inflection point of the cycling portion of the wave pattern, da/dN_i^{CC} , such that:

$$\log \frac{da^{HT}}{dN_i} = \log \left(\frac{da^{HT}}{dN_i} \bigg/ \frac{da^{CC}}{dN_i} \right) + \log \left(\frac{da^{CC}}{dN_i} \right) \quad (19)$$

The second term on the right side in Equation 19 was related to temperature, frequency, and stress ratio:

$$\frac{da^{CC}}{dN_i} = f(v, T, R) \quad (20)$$

and will be discussed first.

a. Inflection Point For Continuous Cycling Conditions, $\frac{da^{CC}}{dN_i}$

For each stress ratio and temperature combination, da/dN_i from the continuous cycling experiments were plotted on logarithmic coordinates versus the time per cycle. A near linear relationship existed at 760° C (1400° F) and stress ratio of 0.5 (see Figure 24). This was the only condition that three frequencies were examined and a variation in crack growth behavior was observed.

To model this behavior:

$$\text{Log} \left(\frac{da^{CC}}{dN_i} \right) = f \left(\log \frac{2.5}{v} \right)^h + j \quad (21)$$

was used, where g, h, and j are coefficients related to temperature and stress ratio. Without the exponent h, a linear relationship is described by the expression. The exponent adds curvature to the relationship that was required to describe the 760° C (1400° F) and stress ratio of 0.9 condition where blunting of the crack-tip reduced the rate of damage at 0.025 Hz. The values of g, h, and j are presented in Table 8. They were related to temperature by Equation 13.

The stress ratio was introduced into the evaluation by calculating a linear relationship for da/dN_i versus $\log(1-R)$ between the stress ratio of

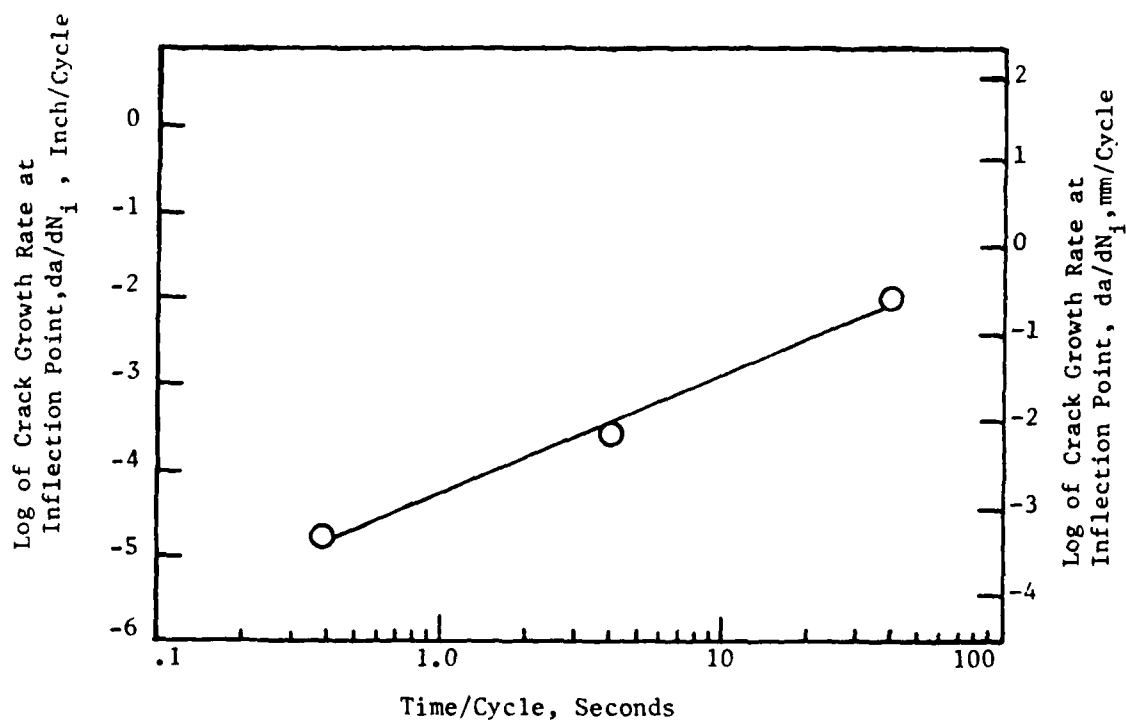


Figure 24. Crack Growth Rate at the Inflection Point as a Function of Time Per Cycle for 760C (1400F) $R=0.5$ and No Hold Period

Table 8. Coefficients to Determine da/dN_i
For Continuous Cycling Conditions.

Temperature	Stress Ratios	g	h	j
538° C (1000° F)	0.1	0.0	1.00	-4.88
	0.5	0.2	1.00	-5.55
	0.9	0.5	0.99	-6.20
649° C (1200° F)	0.1	0.0	1.00	-4.52
	0.5	0.75	1.00	-5.00
	0.9	0.95	1.03	-5.51
760° C (1400° F)	0.1	0.86	1.08	-4.52
	0.5	1.29	1.14	-4.77
	0.9	1.72	0.72	-4.77

0.1 and 0.5 and extending it until a saturation point (no change in da/dN_i with decreasing $1-R$) is achieved. That is, no change in da/dN_i is allowed to exceed that for da/dN_i at $R = 0.9$. This can be expressed by:

$$\text{Log } \frac{da}{dN_i} = \left[\frac{\text{Log } \frac{da}{dN_i}^{R=0.1} / \frac{da}{dN_i}^{R=0.5}}{(\text{Log } 0.9 - \text{Log } 0.5)} \right] \text{Log } (0.9/R) + \left[\text{Log } \frac{da}{dN_i}^R @ 0.1 \right] \quad (22)$$

The value of da/dN_i is, however, limited to the value of da/dN_i calculated at the stress ratio of 0.9. This bi-linear effect has been observed by others⁽⁸⁾ in which a lower saturation condition was observed for the coefficient governing Region I crack growth and an upper saturation for the coefficient controlling Region II crack growth. In considering the location of da/dN_i when temperature, frequency, and hold periods are added to the effect of stress ratio this assumption appears valid. The predicted relationship between da/dN_i and $(1-R)$ for continuous cycling condition are presented in Figure 25.

b. Inflection Point For Hold Time Conditions, $\frac{da}{dN_i}^{HT}$

The first term on the right side of Equation 19, the hold time damage factor, was determined to be influenced by temperature, stress ratio, frequency, and hold time:

$$\frac{da}{dN_i}^{HT} / \frac{da}{dN_i}^{CC} = f(T, R, \nu, HT) \quad (23)$$

When this damage hold time factor was plotted versus the duration of the hold period on logarithmic coordinates, a linear relationship was observed. Figure 26 present the damage factors for the stress ratio of 0.1. Assuming a linear relationship between the damage factor and hold period, then:

$$\text{log } \left[\frac{da}{dN_i}^{HT} / \frac{da}{dN_i}^{CC} \right] = k + e_2 \left(\text{log } \frac{HT}{20} \right) \quad (24)$$

where for each combination of temperature, frequency and stress ratio k and e_2 are the intercept (at 20 seconds) and slope, respectively. It will suffice to say that stress ratio was manipulated in the same fashion as the non-hold-time conditions. Therefore, the only discussion will be to be relate k and e_2 to temperature and frequency.

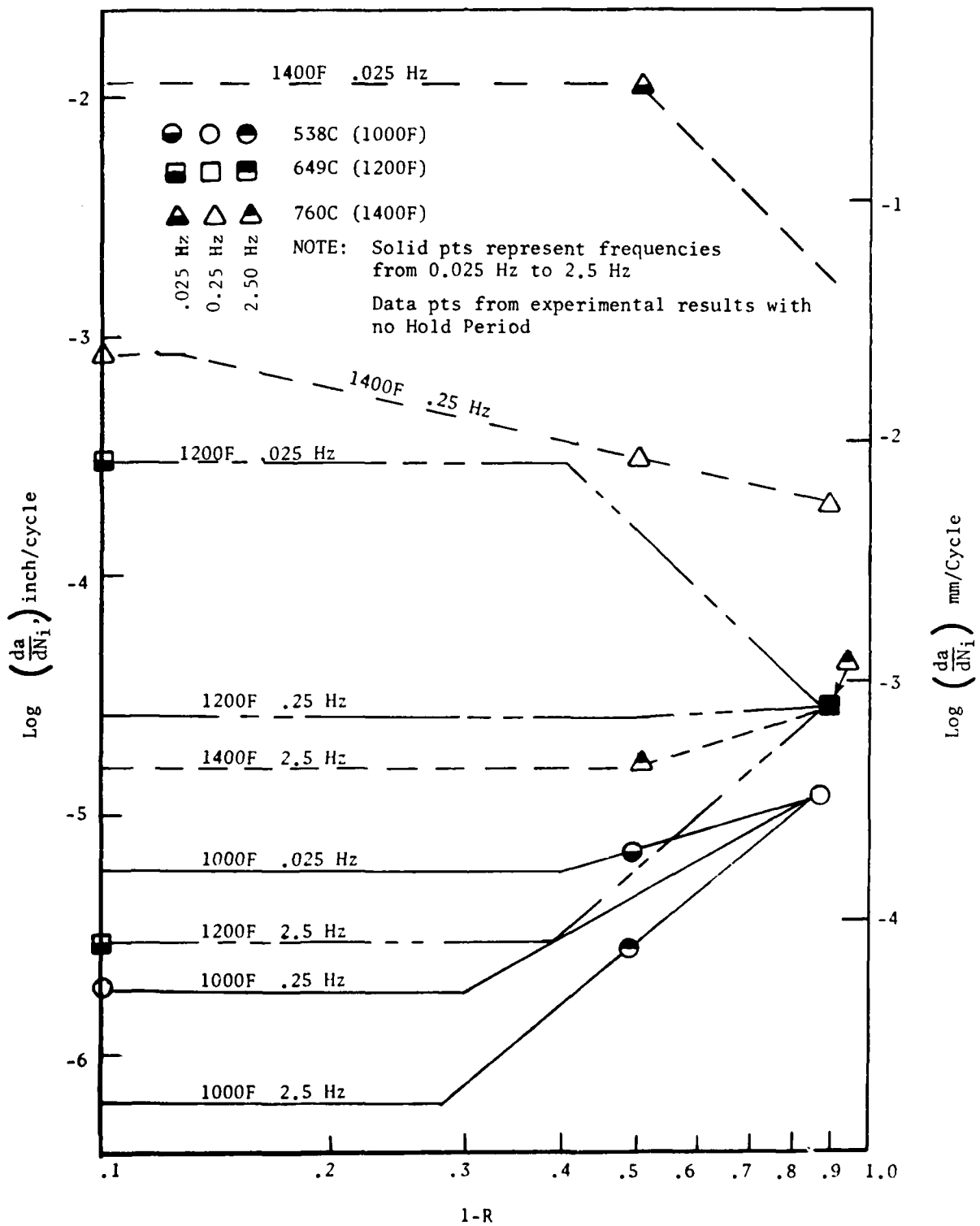


FIGURE 25 Predictions of Inflection Point (da/dN_i) Versus stress Ratio (1-R) for Continuous Cycling Equipment

Top 1/2 filled = 2.5 Hz
 Bottom 1/2 filled = .025 Hz
 Empty = 0.25 Hz
 Solid = .025 to 2.5 Hz

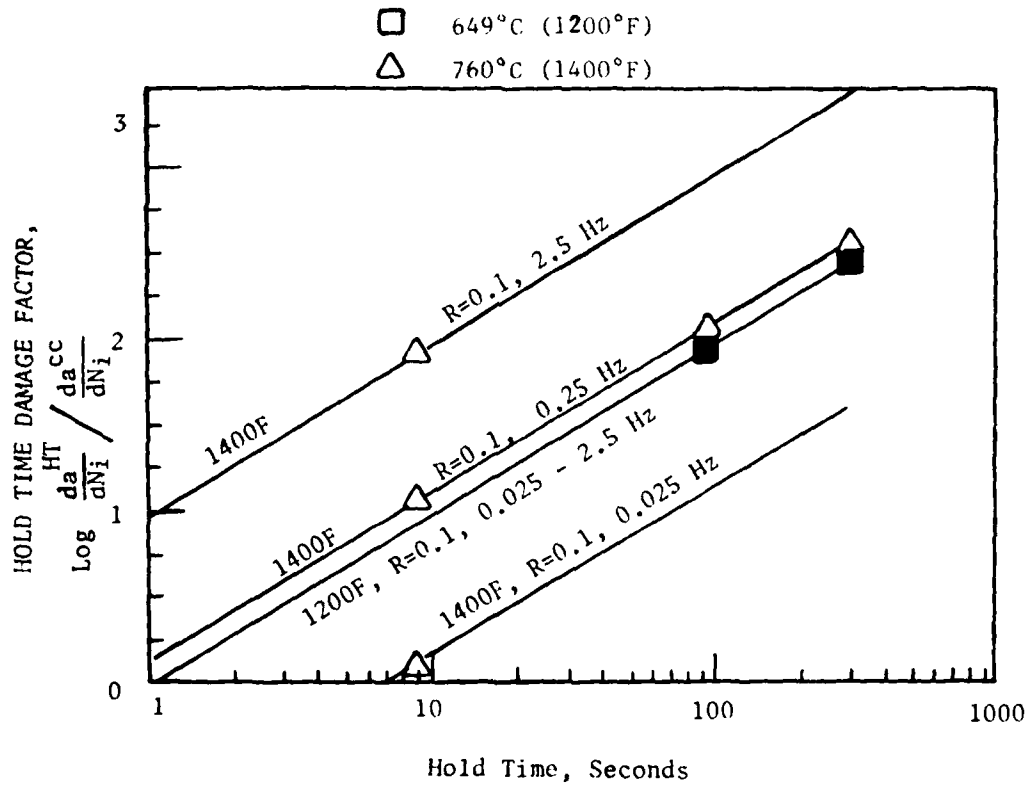


FIGURE 26. Hold Time Damage Factor Versus Hold Time for the Stress Ratio of 0.1 and Two Temperatures

The slope and intercepts for the frequency of 0.25 Hz were related to temperature by the simple power expression:

$$k \text{ or } e_2 = r (T-1000)^s, \quad (25)$$

where r and s were evaluated by simple regression analysis. For each temperature, the coefficients in Equation 25 were related to frequency by:

$$r \text{ or } s = u \left(\log \frac{\nu}{.025} \right)^{w-1}, \quad (26)$$

where, once again, u and w are determined by simple regression analysis. Tabulations of the slopes and intercepts for each combination of temperature and stress ratio are presented in Table 9.

5. Slope Of Inflection Point, da/dN_i'

The slope of the inflection point (da/dN_i') was modeled in the same manner as the location of the vertical location of the inflection point. For each stress ration, da/dN_i' is calculated by Equation 19 through 21 and 23 through 26, substituting da/dN_i' for da/dN_i and using the appropriate coefficients. Each of the three stress ratios were evaluated separately and a bi-linear assumption used as discussed in the last section. Figure 27 show the prediction of da/dN_i' versus $1-R$ on logarithmic coordinates by the model for the three frequencies without hold period. The data points indicate the calculated value of da/dN_i' from the tests conducted.

6. The Lower Shaping Coefficients, Q

The lower shaping coefficient was related to the test variables rather than the upper shaping coefficient. This seems appropriate as the majority of the life of a sample is consumed in the low growth regime where the variables have a chance to influence growth. To determine Q the relationships between the coefficients (da/dN_i , ΔK^* , da/dN_i' , ΔK_c , and ΔK_i) and test variables were implemented into Equation 7 along with Equation 8 and an analysis performed on each set of experimental crack growth data. For the 760° C (1400° F) at stress ratio from 0.1 to 0.9, and for the stress ratios of 0.9 at 649° C (1200° F) the coefficient Q was found nearly equal to 3.0. At other conditions Q was relatable to stress ratio by:

$$Q = n_2 (1-R)^{-.57} \quad (29)$$

Where n_2 was related to temperature using simple regression analysis based on Equation 13.

Table 9. Slope and Intercept (at 20 Seconds) for Hold Time Damage Factor Versus Hold Period Duration for Various Temperatures, Stress and Ratio and Frequencies.

Temperature	Stress Rates	Slope			Intercept		
		0.025 Hz	0.25 Hz	2.5 Hz	0.025 Hz	0.25 Hz	2.5 Hz
538° C (1000° F)	0.1	0.0	0.0	0.0	0.0	0.0	0.0
	0.5	0.0	0.55	0.64	0.0	0.0	0.0
	0.9	0.0	0.64	0.84	0.20	0.15	0.47
649° C (1200° F)	0.1	1.00	1.00	1.00	1.30	1.30	1.30
	0.5	0.88	1.36	1.45	0.62	0.87	1.06
	0.9	0.82	1.36	1.50	0.55	0.87	1.67
760° C (1400° F)	0.1	1.0	1.0	1.0	0.46	1.41	2.28
	0.5	0.66	0.93	0.99	0.10	1.31	2.55
	0.9	0.54	0.90	0.99	0.25	0.94	2.65

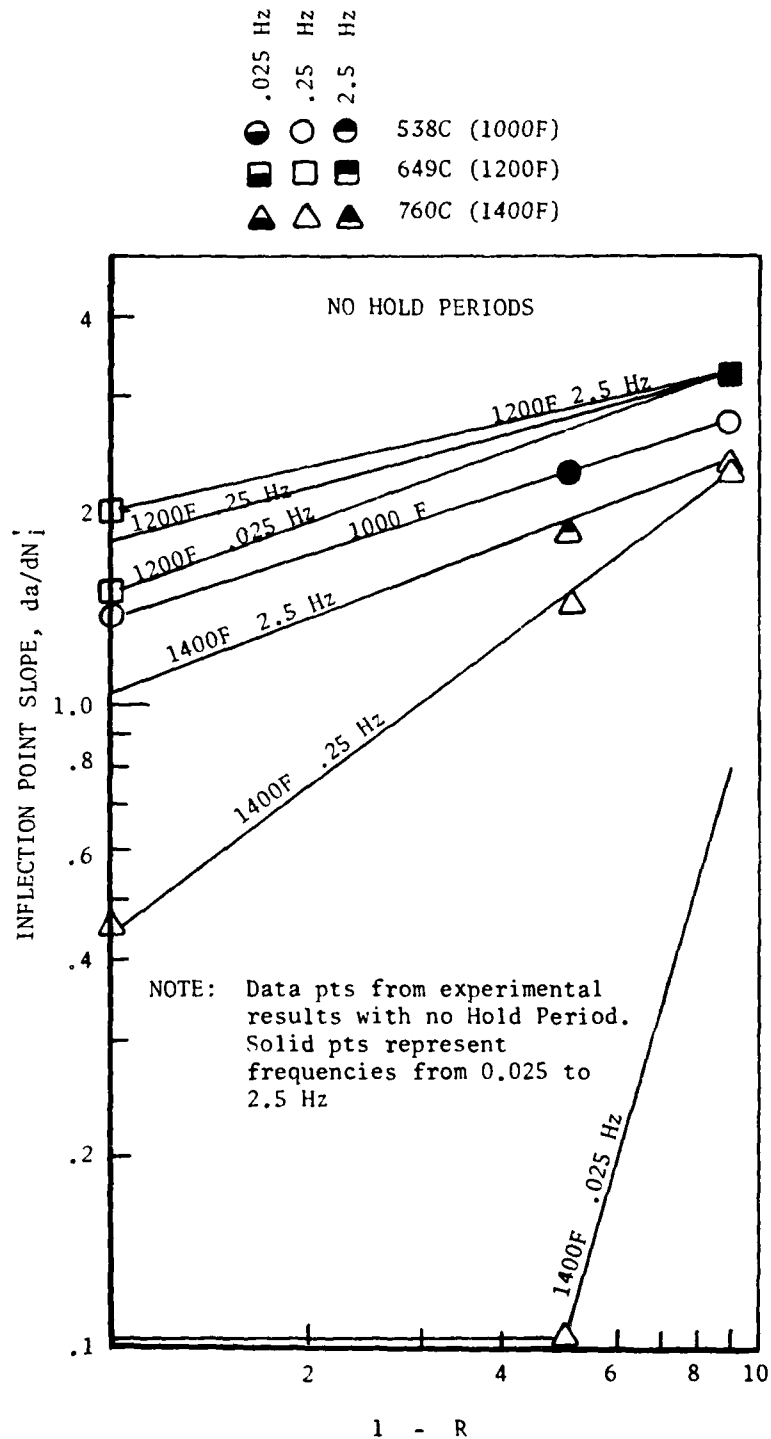


Figure 27. Slope of the Inflection Point Versus Stress Ratio (1-R) for Continuous Cycle Results

C. SUMMARY OF INTERPOLATIVE MODEL

During the primary test program observations were made on the response of the crack growth behavior of AF115 to the four test variables as discussed in an earlier section. The interpolative model was developed to satisfy these observations which will be briefly summarized within the following paragraph.

1. Response Of Coefficients To Test Variables

A summary of the coefficients influenced by the four test variables are indicated in Table 10. Figure 28 indicate the possible movement of the sigmoidal cyclic crack growth curve relative to increasing values of the test variables as outlined below.

- ΔK_C decreased with increasing stress ratio; independently of the temperature, frequency or hold time.
- ΔK^* decreased with decreasing stress ratio. At $R = 0.1$, ΔK^* was temperature insensitive, however, for higher stress ratios, ΔK^* was lower for higher temperatures as shown in Figure 22.
- The location of ΔK_i was proportionally related, on logarithmic coordinates, to da/dN_i . At the stress ratio 0.1, the relationship between the two was insensitive to temperature as noted from predictions made by the model shown in Figure 23. At higher stress ratios, the slope between the da/dN_i and ΔK_i relationship increased with decreasing temperature (compare linear lines in Figures 29 and 30).
- The location of the inflection point on the crack growth axis, da/dN_i , increased with increasing temperature (Figure 31) and hold period (Figure 32), and decreasing frequency (Figure 33). With respect to stress ratio it either increased (Figure 34) or decreased (Figure 35), depending on the other test condition. When plotted versus $(1-R)$ on logarithmic coordinates, a saturation point existed for a given set of conditions that da/dN_i did not surpass (Figure 25).
- The slope of the inflection point was predictable in the same manner as its vertical location. It decreased with increasing hold period and temperature and increased with increasing frequency as also indicated in Figures 31 through 33.
- The lower shaping coefficient was constant for all 760° C (1400° F) conditions and 648° C (1200° F) and stress ratio below 0.5. At other conditions a sharper transition existed at growth rates approaching the lower asymptote.

Table 10. Influence of Experimental Variables on
Modified Sigmoidal Equation Coefficients.

	Temperature	Frequency	Hold-Time	Stress Ratio
ΔK^*				X
ΔK_c	X			X
ΔK_i	X	X	X	X
da/dN_i	X	X	X	X
da/dN_i	X	X	X	X
Q	X			X

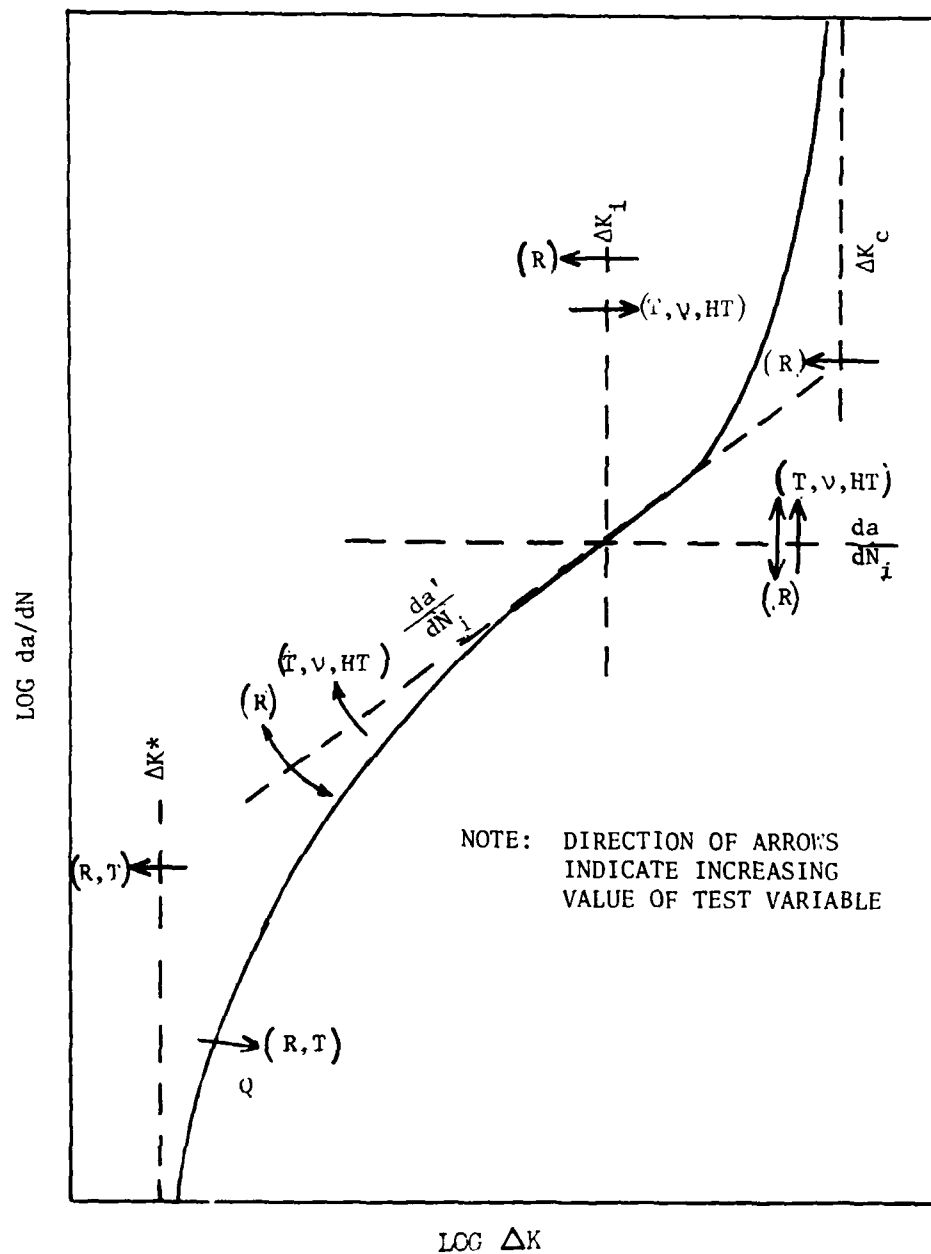


Figure 28. Schematic Effects of Model Coefficients on the Modified Sigmoidal Equation.

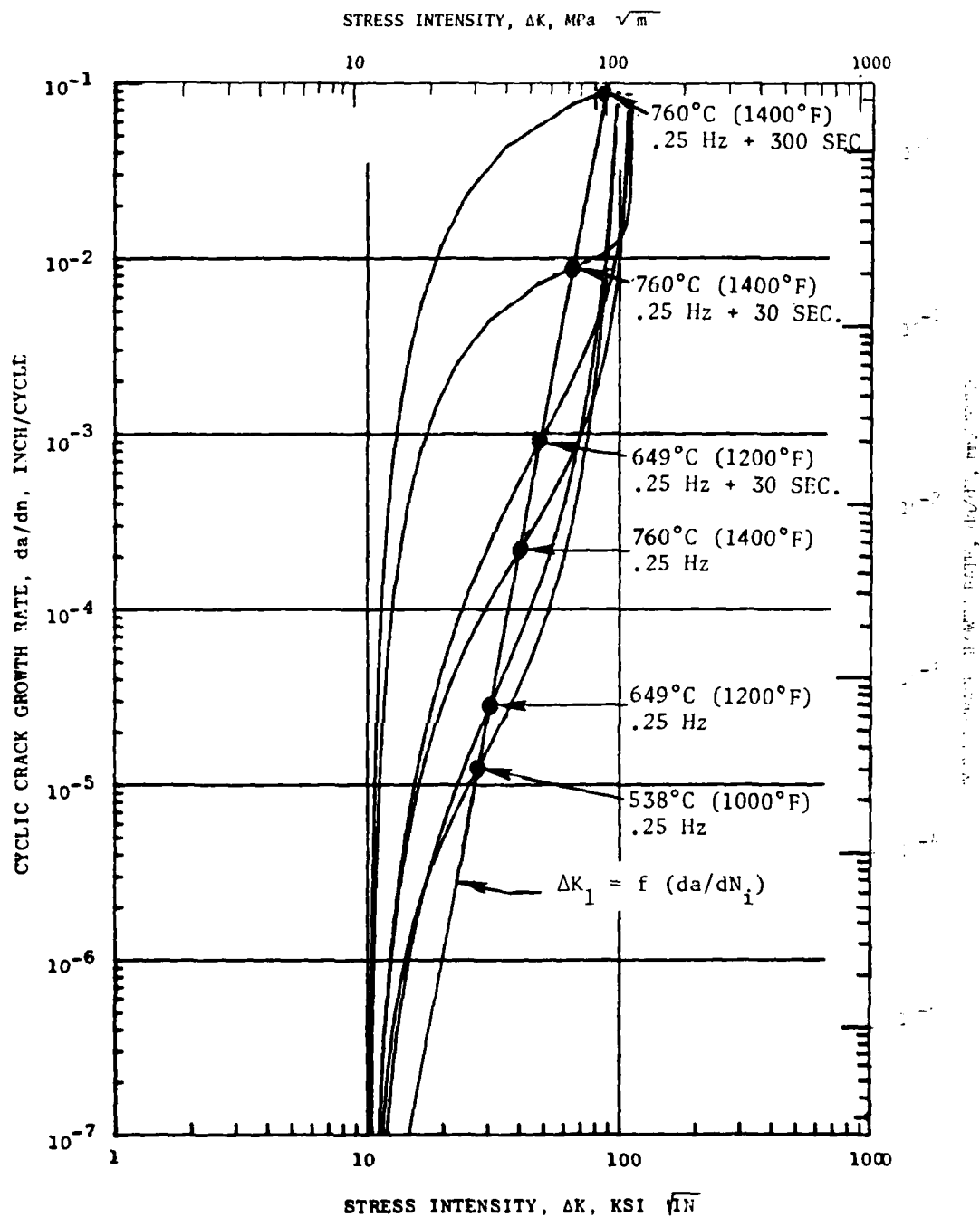


Figure 29. Illustration of Relationship Between ΔK_I and da/dN_I at $R = 0.1$ and Various Temperatures, Frequencies, and Hold Periods.

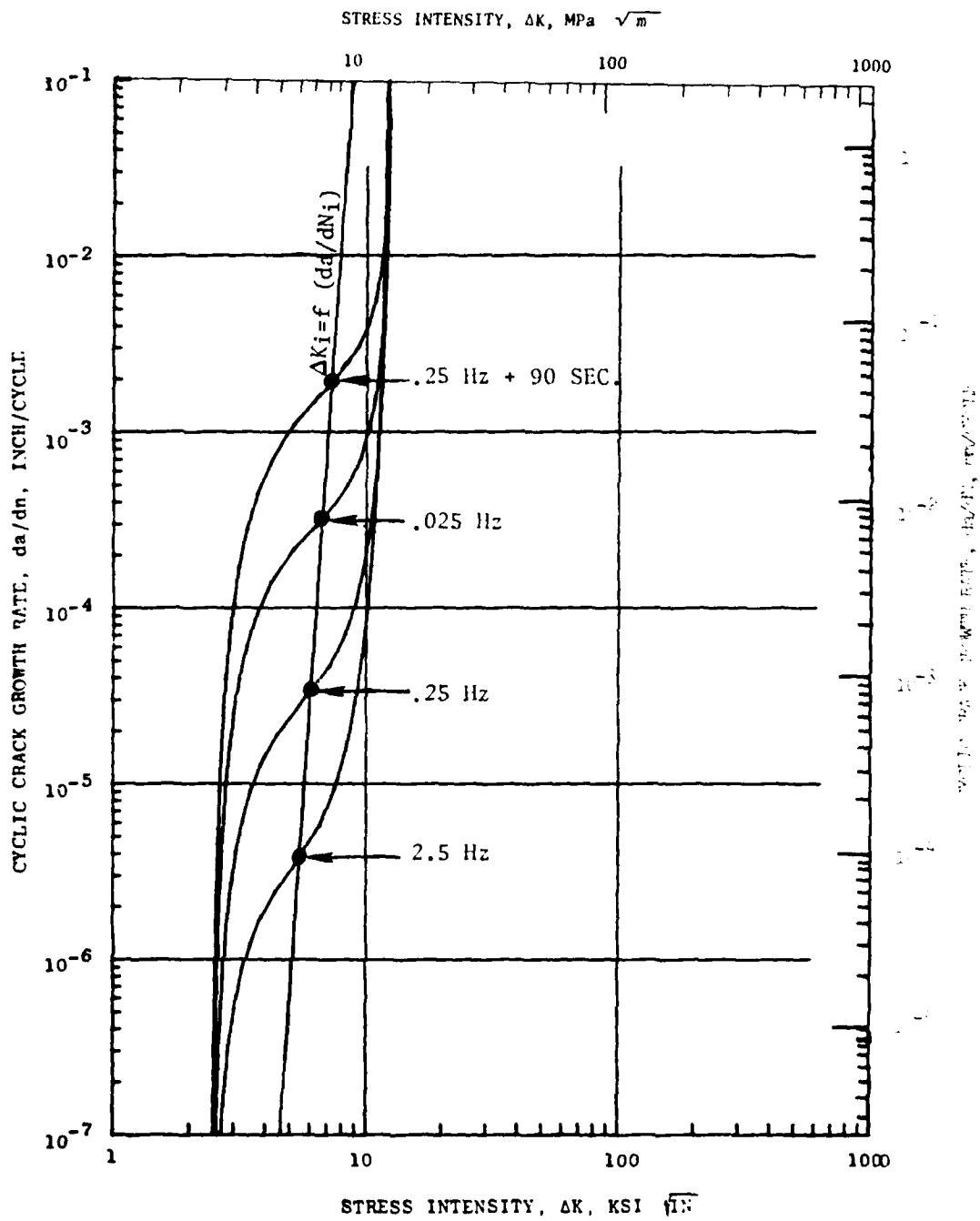


Figure 30. Illustration of Relationship Between ΔK_i and da/dN_i at $R = 0.9$ and 649°C (1200°F)

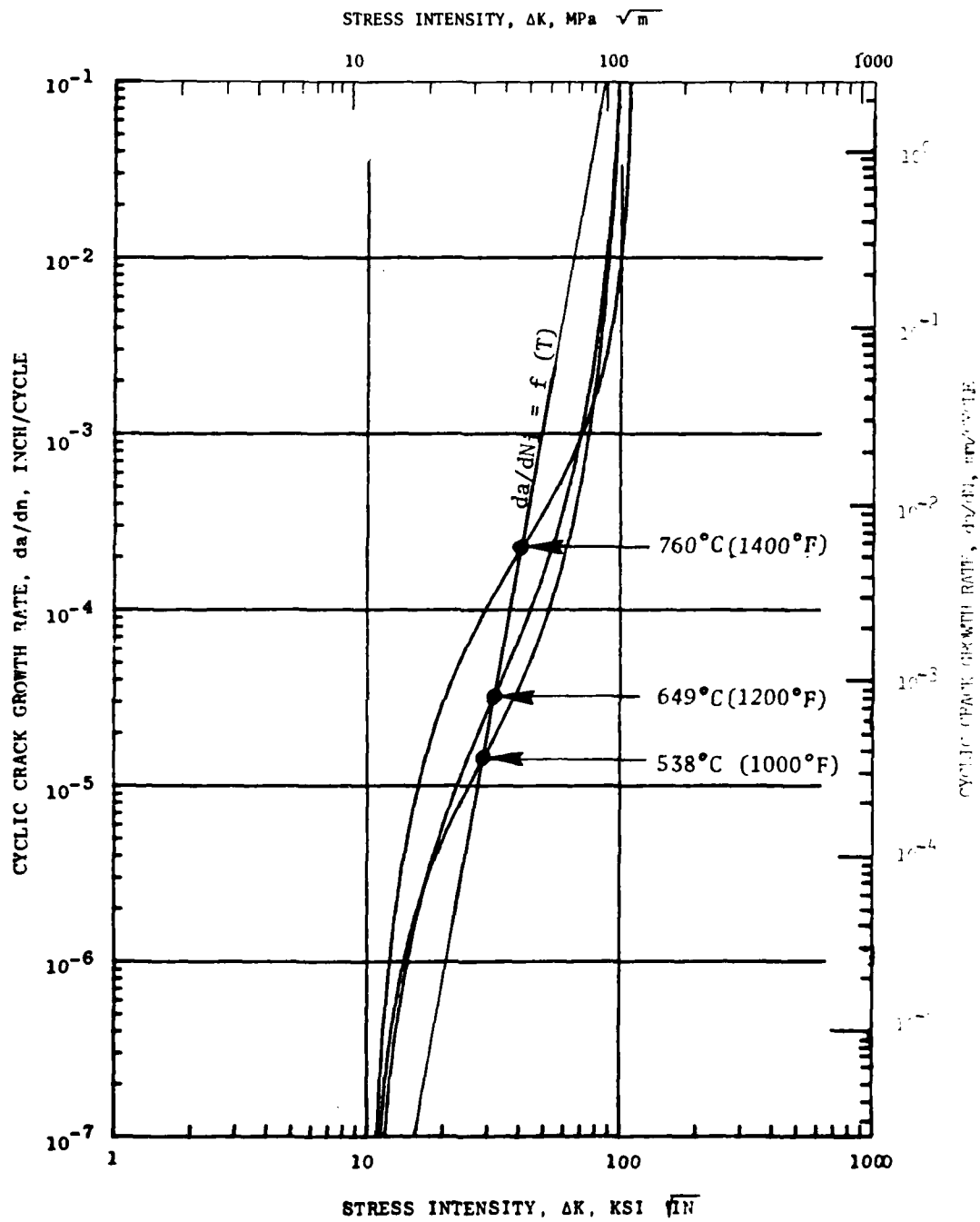


Figure 31. Illustration of Relationship Between da/dN_i and Temperature at $R = 0.1$ and 0.25 Hz.

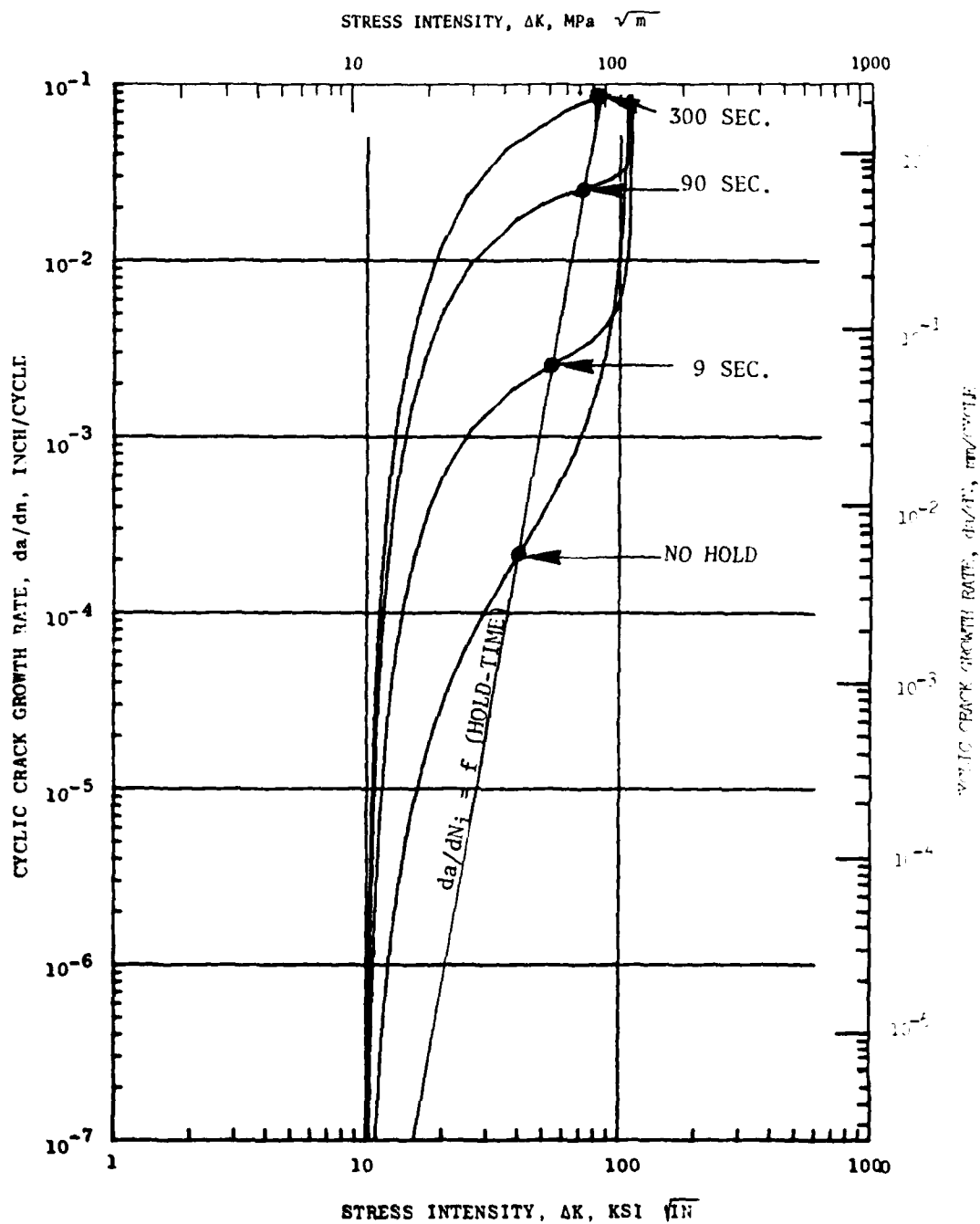


Figure 32. Illustration of Relationship Between da/dN_i and Hold Time for $R = 0.1$ and 0.25 Hz.

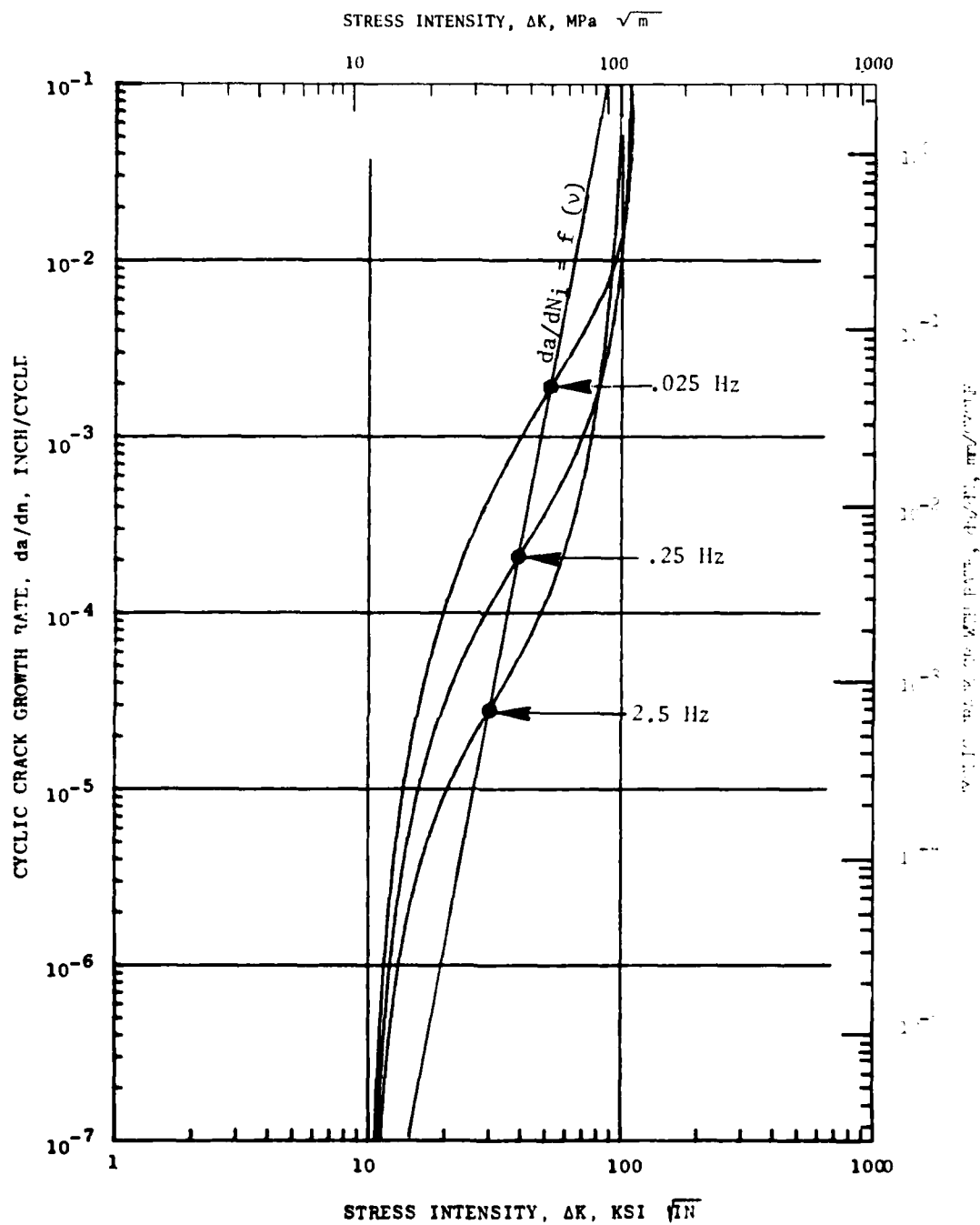


Figure 33. Illustration of Relationship Between da/dN and frequency at $R = 0.1$ and 760°C (1400°F).

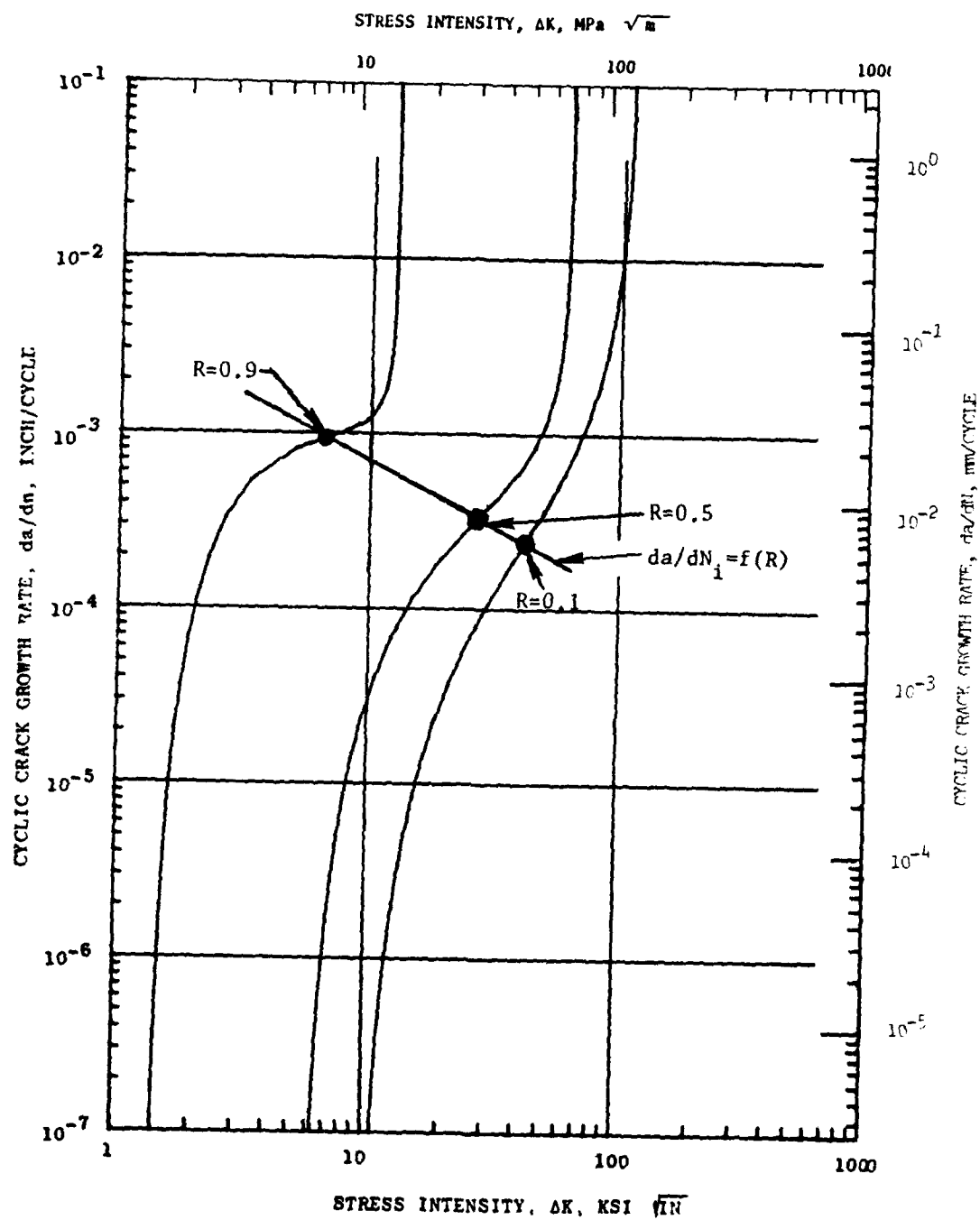


Figure 34. Illustration of Relationship Between da/dN_1 and Stress Ratio for 760°C (1400°F) and 0.25 Hz .

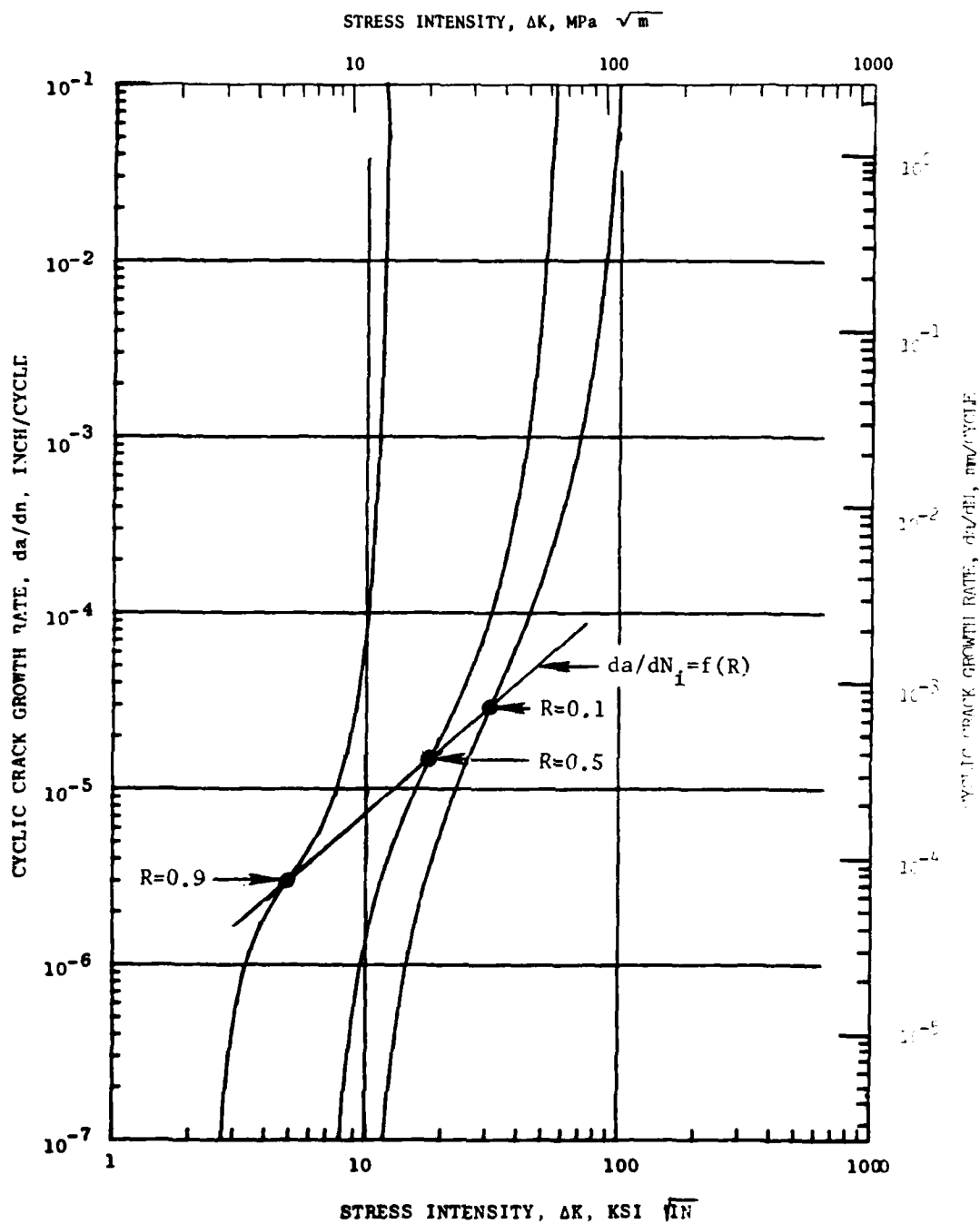


Figure 35. Illustration of Relationship Between da/dN_1 and Stress Ratio at 649°C (1200°F) and 2.5Hz .

2. Comparison of Experimental Results To Model

Figures 36 through 45 show the predicted cyclic crack growth curves from the model versus the associated data from the experimental program. Within the mid-region of crack growth, the data were predicted by the model within a factor of two. At growth rates approaching the asymptotes, the stress intensity calculated from the experimental results were within 15% of the predicted values. However, as will be shown, the worse prediction of the model in calculating the life of the experiments conducted to generate the model was a factor of 5.5 with the overall predictability of the model being much better.

SYMBOL	SPECIMEN	FREQUENCY	HOLD TIME
△	S/N 10-2	.025	9
□	S/N 10-6	.25	0
◇	S/N 8-1	.25	9
○	S/N 8-4	2.5	9
+	S/N 10-3	.25	90
+	S/N 4-7	2.5	300

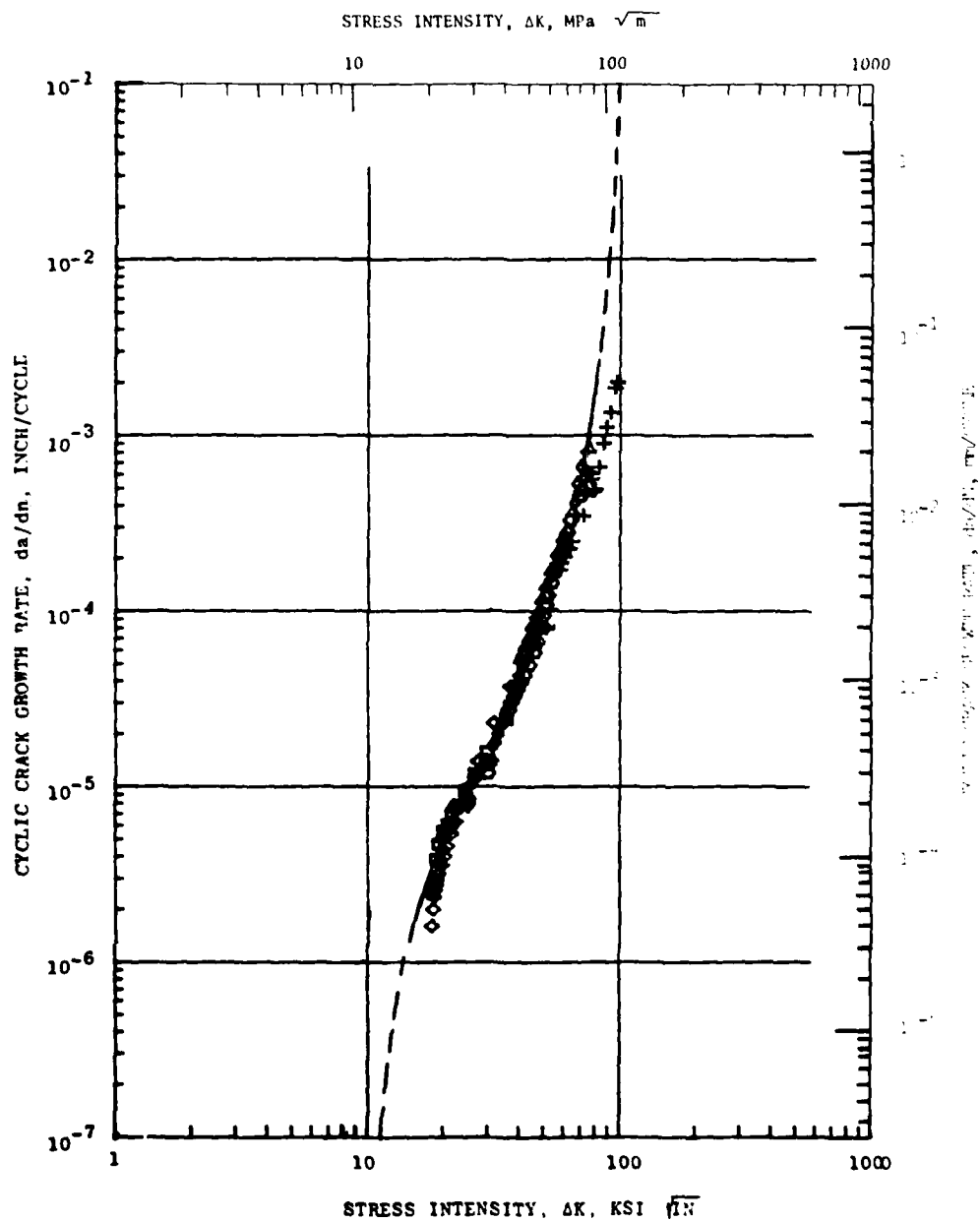


Figure 36. Actual and Predicted Crack Growth Rate Curve for 538°C (1000°F), R=0.1 Experiments.

SYMBOL	SPECIMEN	FREQUENCY	HOLD TIME
X	S/N 9-4	.25	0
+	S/N 11-5	.025	0
▽	S/N 5-8	2.5	0
◇	S/N 13-2	2.5	90
□	S/N 9-1	.25	90
◇	S/N 9-7	.025	90
◇	S/N 8-3	.25	300

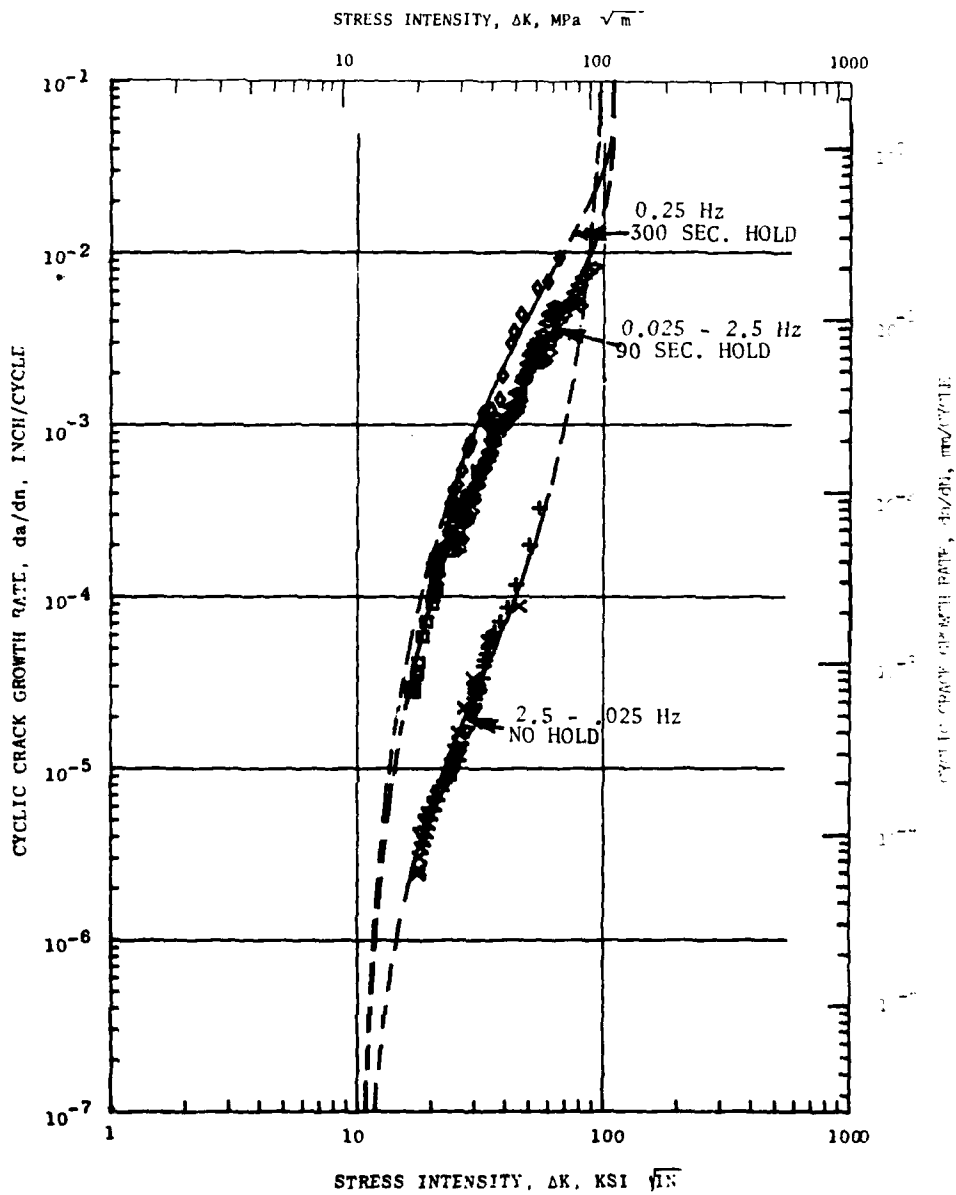


Figure 37. Actual and Predicted Crack Growth Rate Curves for 649°C (1200°F), R= 0.1 Experiments.

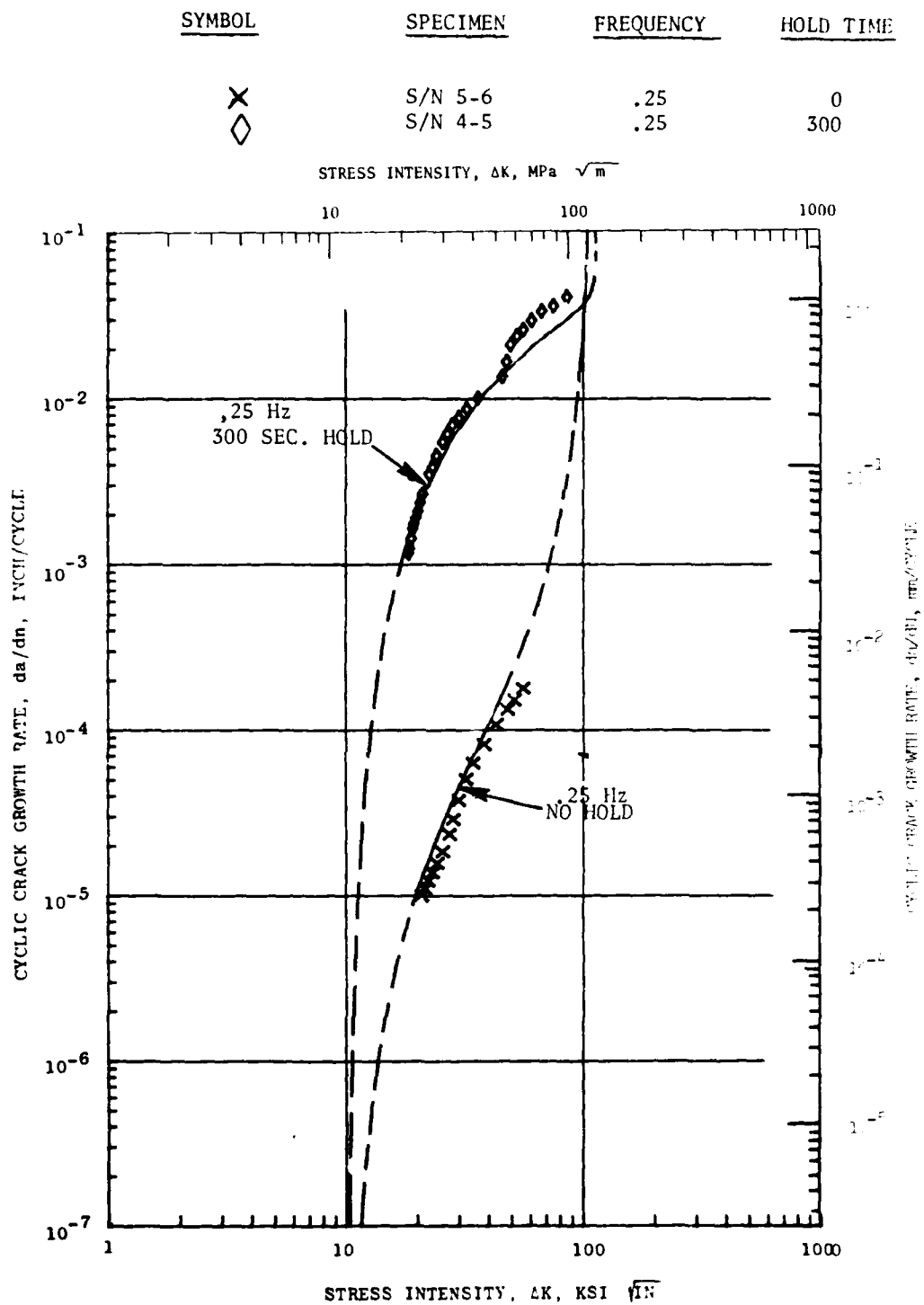


Figure 38. Actual and Predicted Crack Growth Rate Curves for 704°C (1300°F), R=0.1, 0.25 Hz Experiments.

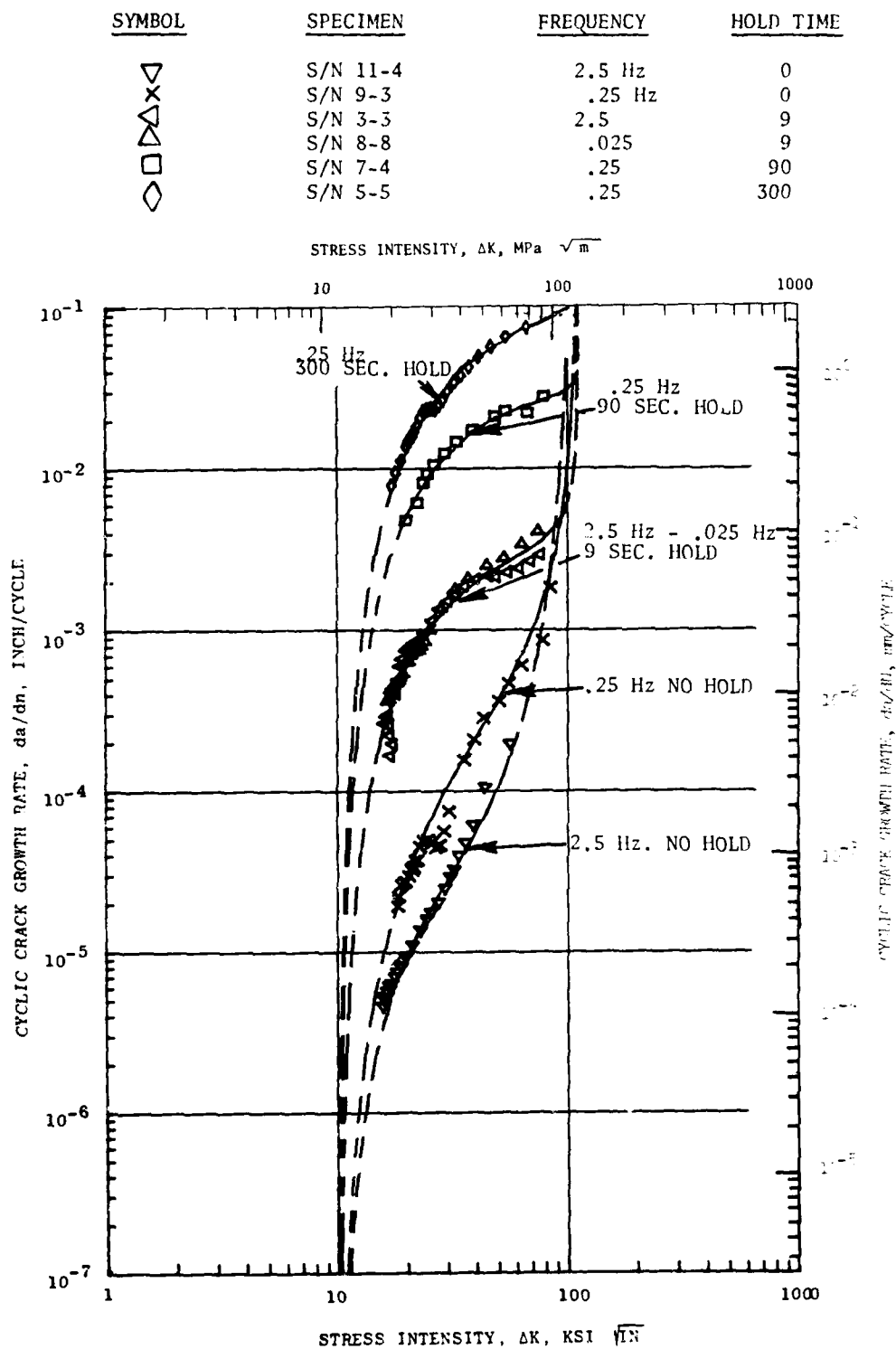


Figure 39. Actual and Predicted Crack Growth Rate Curves, for 760°C (1400°F), R=0.1 Experiments

SYMBOL	SPECIMEN	FREQUENCY	HOLD TIME
▽	S/N 5-7	2.5	0
◇	S/N 4-3	2.5	90
+	S/N 5-3	.025	0
◇	S/N 8-7	.025	90

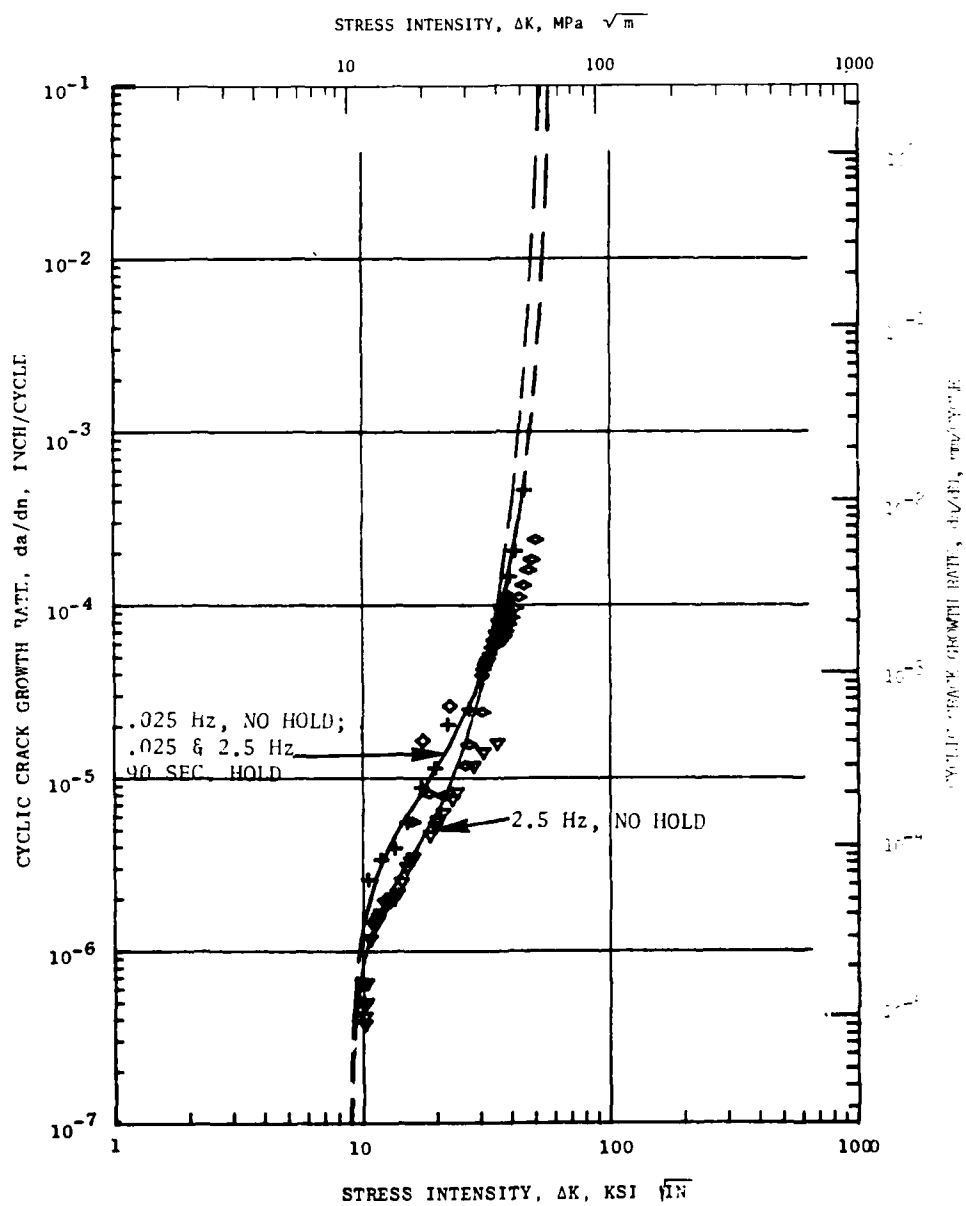


Figure 40. Actual and Predicted Crack Growth Rate Curves for 538°C (1000°F), R= 0.5 Experiments.

SYMBOL	SPECIMEN	FREQUENCY	HOLD TIME
x	S/N 8-5	.25	9
Δ	S/N 11-7	.25	9
▽	S/N 11-1	.25	9
+	S/N 4-6	.25	9

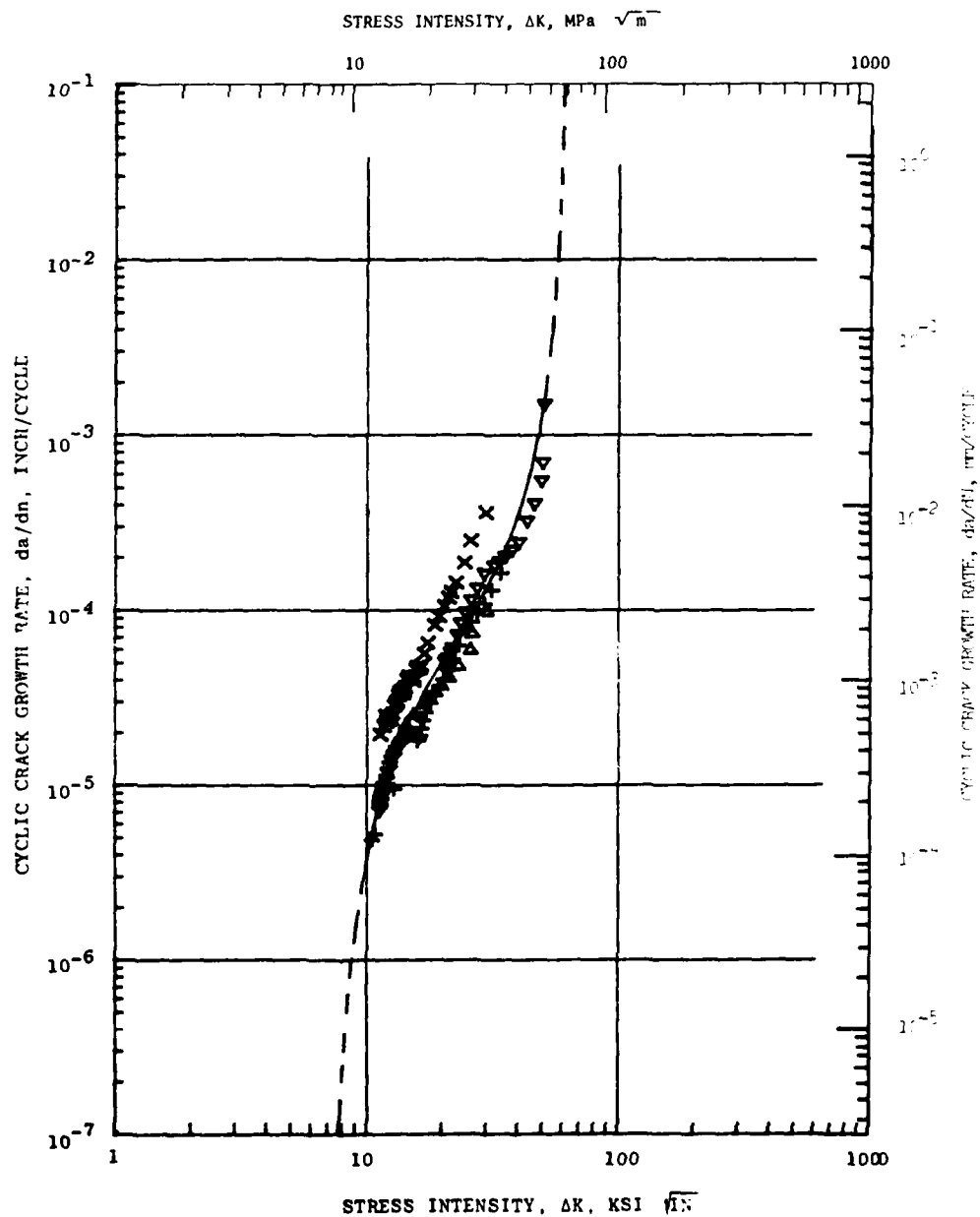


Figure 41. Actual and Predicted Crack Growth Rate Curves for 649°C (1200°F), $R \approx 0.5$, .25 Hz, 9 Second Hold Experiments.

SYMBOL	SPECIMEN	FREQUENCY	HOLD TIME
▽	S/N 9-8	2.5	0
×	S/N 3-1	.25	0
+	S/N 4-1	.025	0
◇	S/N 7-8	2.5	90
◇	S/N 4-2	.025	90

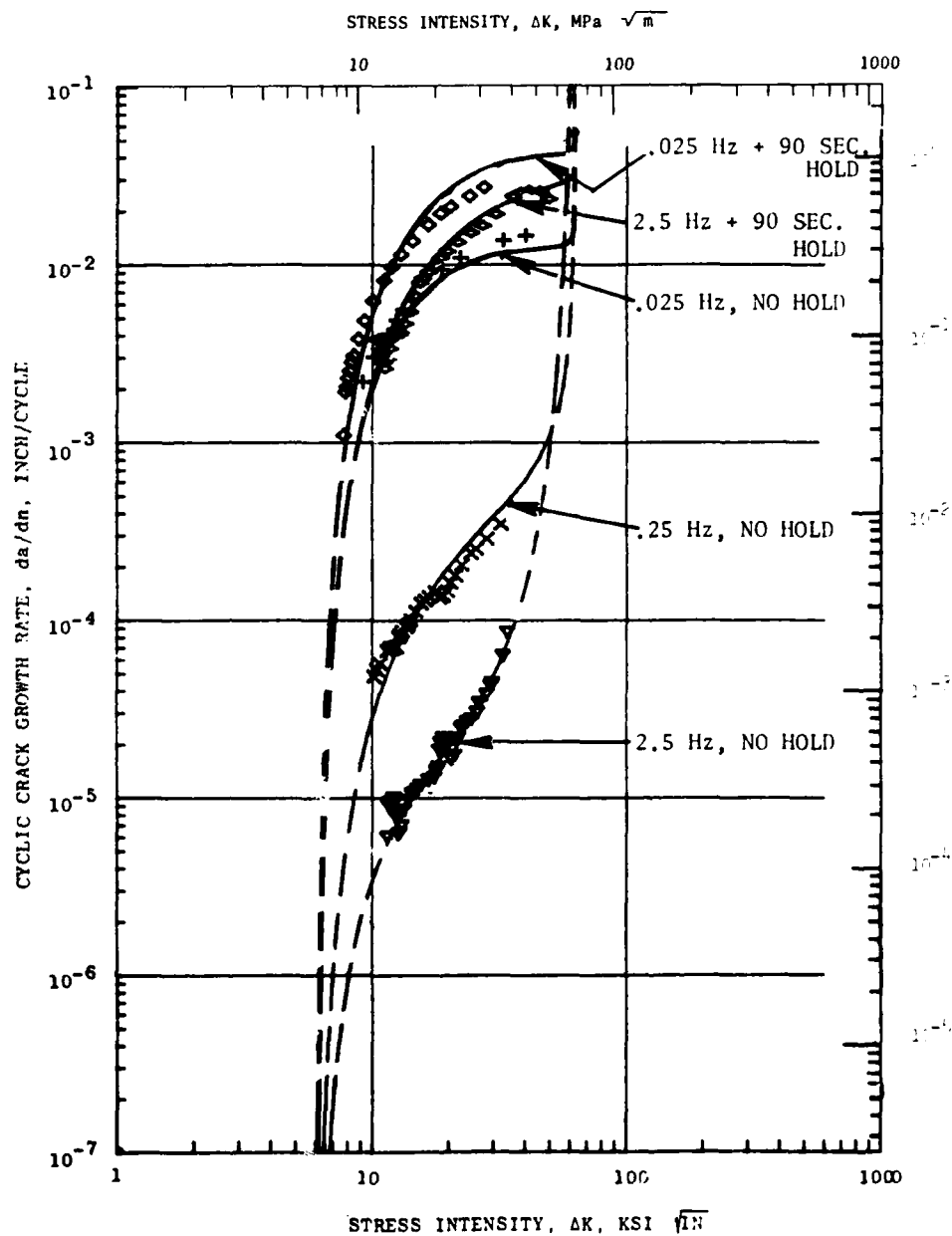


Figure 42. Actual and Predicted Crack Growth Rate Curves for 760°C (1400°F), R=0.5 Experiments.

SYMBOL	SPECIMEN	FREQUENCY	HOLD TIME
X	S/N 4-8	.25	0
△	S/N 11-2	2.5	9
△	S/N 5-1	.025	9
□	S/N 10-1	.25	90

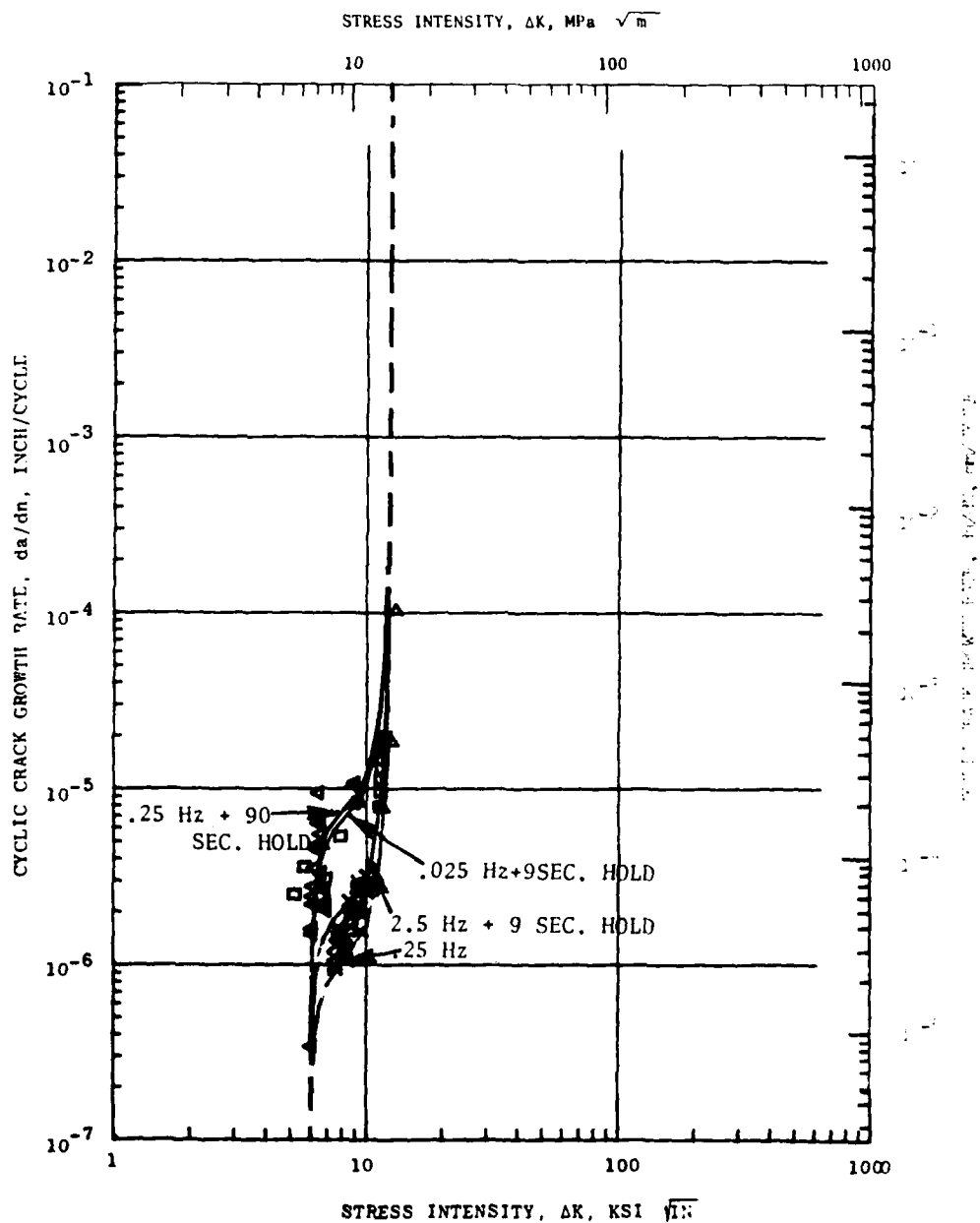


Figure 43. Actual and Predicted Crack Growth Rate Curves for 538°C (1000°F), R= 0.9 Experiments.

SYMBOL	SPECIMEN	FREQUENCY	HOLD TIME
▽	S/N 11-6	2.5	0
+	S/N 10-5	.025	0
◇	S/N 8-6	2.5	90
◇	S/N 3-4	.025	90

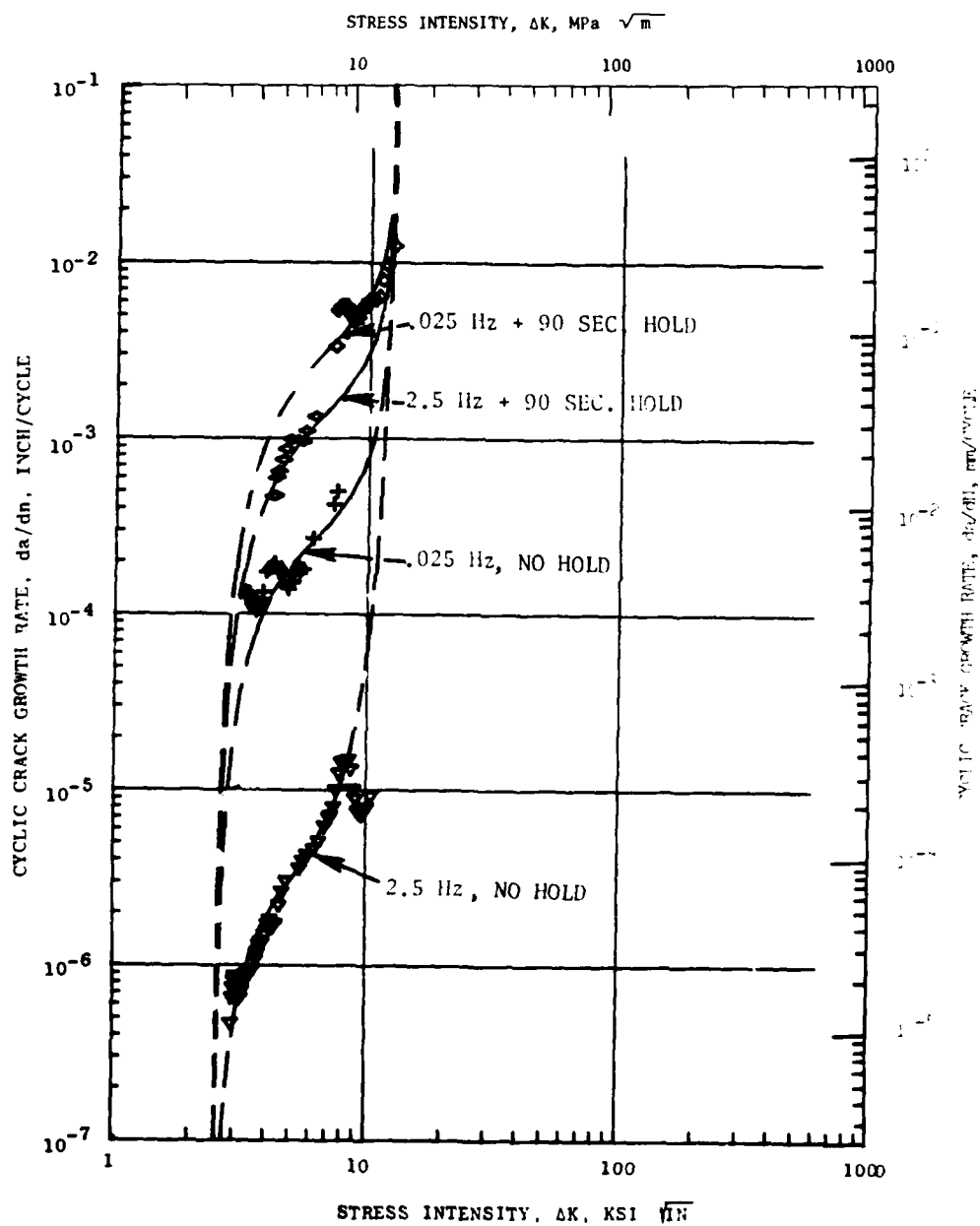


Figure 44. Actual and Predicted Crack Growth Rate Curves for 649°C (1200°F), R=0.9 Experiments.

SYMBOL	SPECIMEN	FREQUENCY	HOLD TIME
X	S/N 4-4	.25	0
Δ	S/N 5-2	2.5	9
Δ	S/N 11-8	.025	9
□	S/N 10-7	.25	90

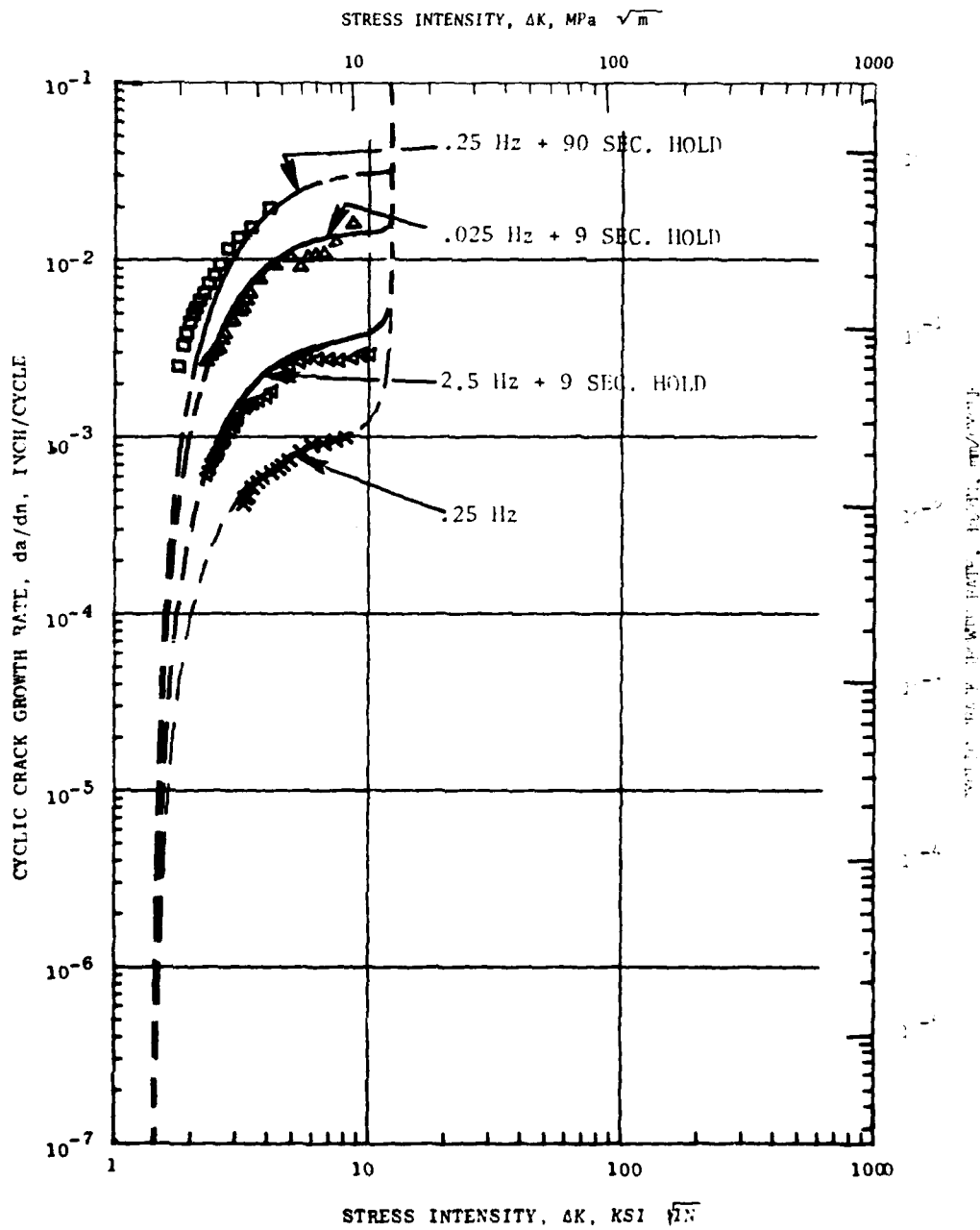


Figure 45. Actual and Predicted Crack Growth Rate Curves for 760°C (1400°F), R=0.9 Experiments.

VII. COMPUTER PROGRAMS

A computer program was written that is capable of determining the crack growth rate behavior of AF115 for conditions within the range studied. Those conditions are listed below:

Temperature	538° - 760° C (1000°-1400° F)
Stress Ratio	0.1 - 0.9
Frequency	0.025 - 2.5 Hz
Tensile Hold Time	0 - 300 Seconds

The software was written in ANSI Standard FORTRAN and was demonstrated on the CDC 6600 computer system at WPAFB under NOS/BE operating system. Because of the manner that this model was developed, the program is not capable of extrapolations outside of the conditions listed above. A listing of the program is given in Appendix C. The input for the program consists of temperature (F), stress ratio (R), time for cycling portion of wave pattern (seconds), and length of hold period (seconds). The inputs are separated by commas. As output, the coefficients of the modified Sigmoidal Equation (Equation 5) are given. The crack length versus cycle number for a specific specimen geometry and load conditions can be determined by any appropriate iteration routine. An example along with the instructions is given in Appendix C.

VIII. VERIFICATION OF MODEL

Four verification experiments were conducted to determine the accuracy of the interpolative model. Test conditions were selected by the Air Force after the completion of the model. They were:

Tests 1 - 2: 537° C (1000° F), R = 0.3, 0.1 Hz

Tests 3 - 4: 704° C (1300° F), R = 0.6, 0.1 Hz, 30 second hold

Results of the experiments were graphically present in form of a crack length versus cycle number in Figure 46, and da/dN versus ΔK in Figure 47. Included are the predicted curves as calculated by the model. Tabulation of the data are given in Table 11. The average fatigue life of two verification tests conducted at 593° C (1100° F) was within 30% of the prediction by the model. The 704° C (1300° F) experiments were less accurately predicted; however, the average of the two tests were still within a factor of 2-1/2 on total life. The extent of the accuracy of the model due to typical scatter in crack growth testing will be reviewed in the next section.

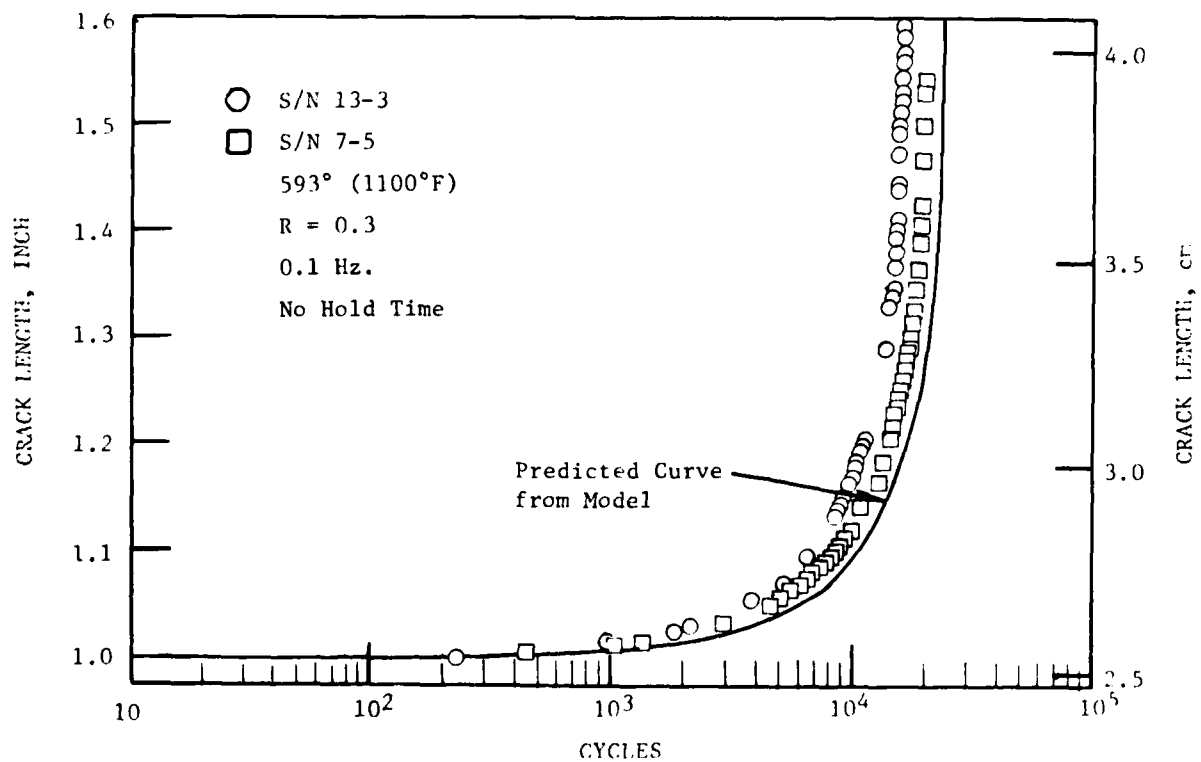
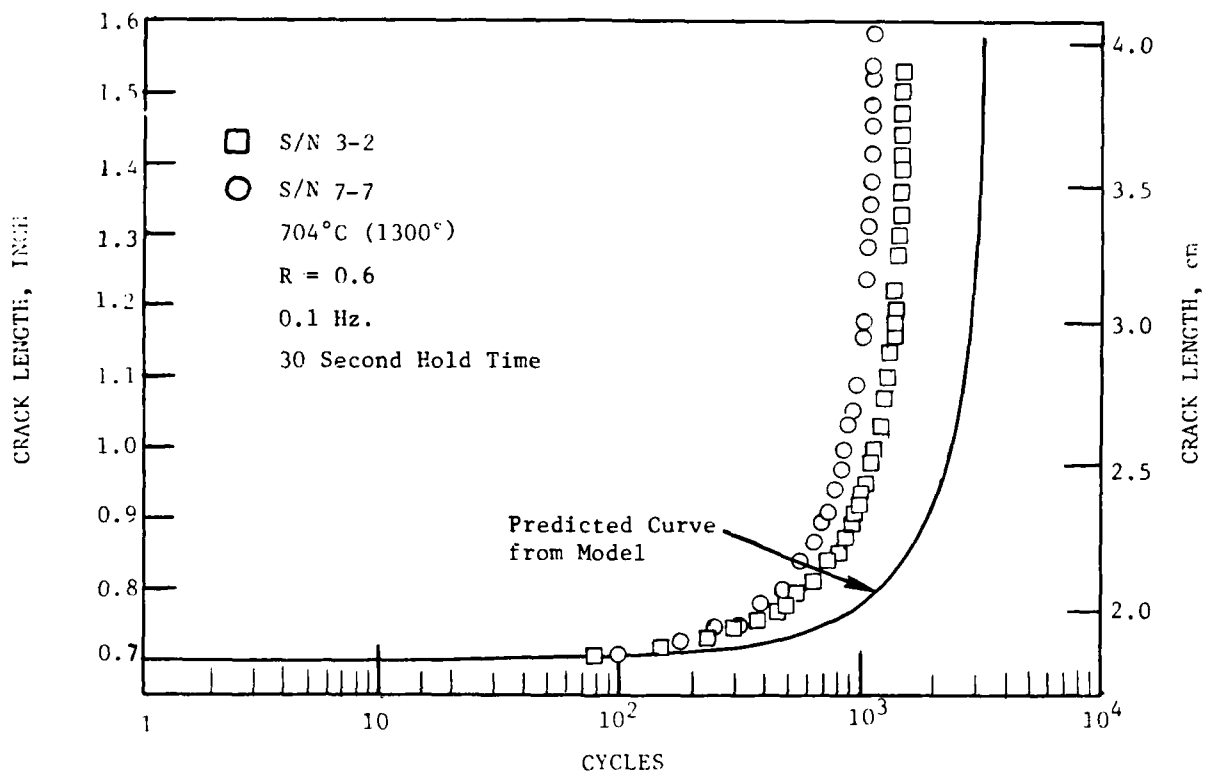


Figure 46. Crack Length Versus Cycle Number of Verification Experiments.

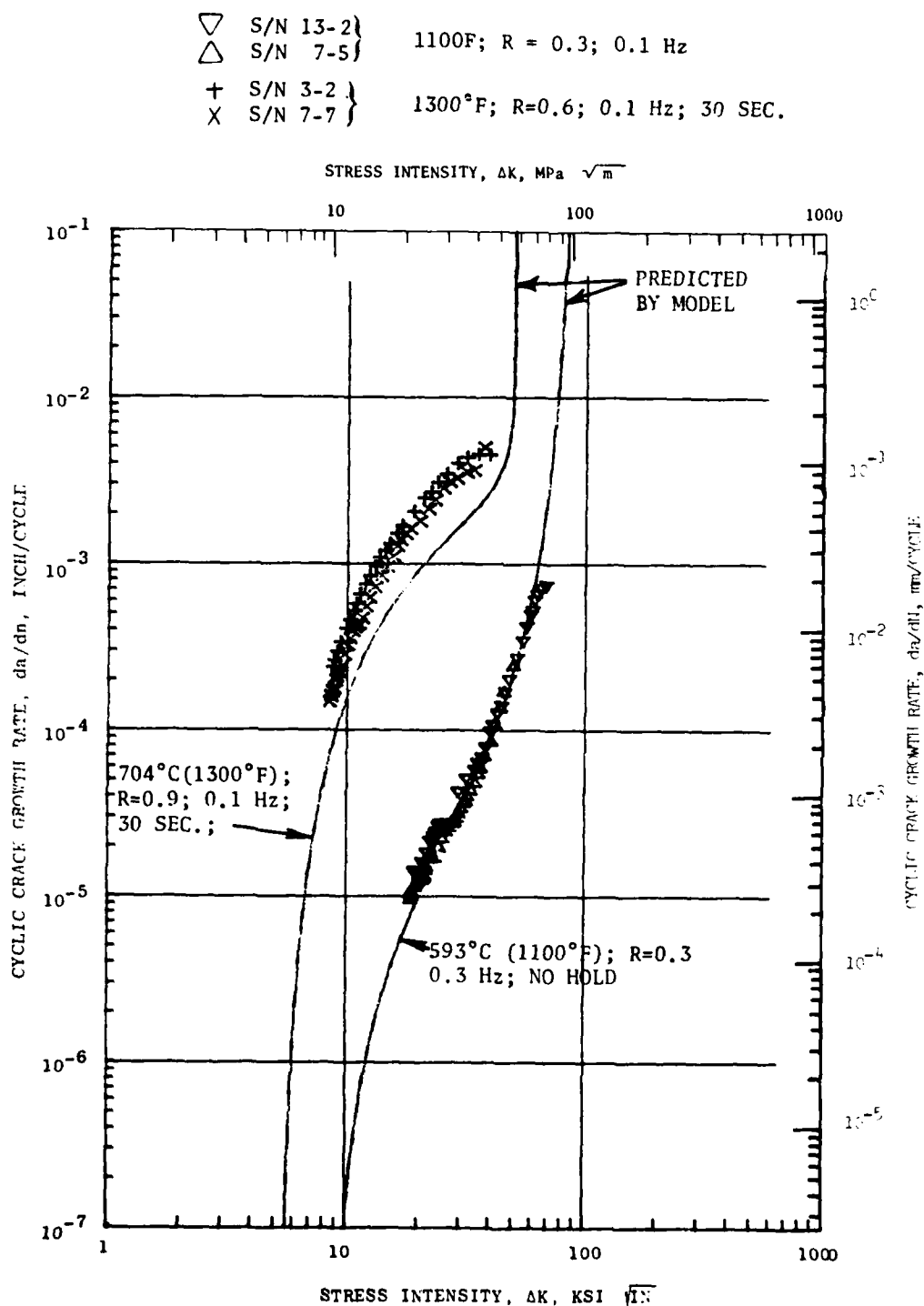


Figure 47. Predicted and Actual Crack Growth Rate for Verification Experiments.

Table 11. Results of Verification Experiments.

SEVEN POINT INCREMENTAL POLYNOMIAL METHOD FOR DETERMINING DA/DN

SPEC NO. 3-2 NO. POINTS= 32
SPECIMEN: CT R= .5 IN. W= 2 IN.
PAIN 1.33 KIPS PMA= 2.22 KIPS R= .599991 TEST FREQ.= .1 HZ
TEMP.= 1300 F ENVIRONMENT= AIR

OBS NO.	CYCLES	A	DELK	DA/DN
1	0	.700		
2	100	.716		
3	161	.732		
4	254	.751	8.56	2.330e-04
5	308	.758	8.70	2.566e-04
6	386	.783	8.95	2.899e-04
7	469	.804	9.24	3.315e-04
8	577	.846	9.75	4.014e-04
9	640	.871	10.10	4.531e-04
10	696	.899	10.48	5.135e-04
11	734	.917	10.76	5.673e-04
12	776	.942	11.15	6.456e-04
13	824	.974	11.69	7.380e-04
14	856	1.001	12.17	8.387e-04
15	899	1.038	12.88	9.453e-04
16	924	1.059	13.38	1.072e-03
17	954	1.094	14.15	1.180e-03
18	975	1.117	14.77	1.300e-03
19	1002	1.140	15.80	1.491e-03
20	1022	1.182	16.70	1.659e-03
21	1053	1.239	18.65	2.027e-03
22	1075	1.284	20.55	2.439e-03
23	1087	1.317	22.05	2.661e-03
24	1097	1.345	23.48	3.032e-03
25	1108	1.377	25.58	3.401e-03
26	1119	1.412	26.31	3.923e-03
27	1127	1.453	31.04	4.273e-03
28	1135	1.483	34.67	4.458e-03
29	1142	1.521	38.67	4.442e-03
30	1147	1.542		
31	1153	1.547		
32	1157	1.583		

SEVEN POINT INCREMENTAL POLYNOMIAL METHOD FOR DETERMINING DA/DN

SPEC NO. S/N 7-7 NO. POINTS= 40
SPECIMEN: CT R= .5 IN. W= 2 IN.
PAIN 1.333 KIPS PMA= 2.222 KIPS R= .59991 TEST FREQ.= .1 HZ
TEMP.= 1300 F ENVIRONMENT= AIR

OBS NO.	CYCLES	A (KIPS)	DELK	DA/DN
1	0	.700		
2	80	.712		
3	149	.725		
4	232	.738	8.43	1.649e-04
5	306	.750	8.57	1.681e-04
6	381	.761	8.71	1.761e-04
7	455	.776	8.86	1.946e-04
8	499	.783	8.95	2.079e-04
9	560	.796	9.12	2.222e-04
10	635	.815	9.33	2.402e-04
11	736	.843	9.65	2.804e-04
12	808	.856	9.92	3.191e-04
13	859	.875	10.15	3.490e-04
14	915	.899	10.43	3.868e-04
15	952	.913	10.67	4.056e-04
16	986	.926	10.89	4.166e-04
17	1019	.940	11.09	4.264e-04
18	1059	.958	11.37	4.606e-04
19	1115	.983	11.83	5.397e-04
20	1156	1.005	12.25	6.120e-04
21	1205	1.037	12.88	7.084e-04
22	1253	1.075	13.67	8.230e-04
23	1291	1.107	14.46	9.358e-04
24	1325	1.137	15.34	1.083e-03
25	1345	1.161	15.96	1.249e-03
26	1358	1.178	16.44	1.364e-03
27	1375	1.202	17.28	1.476e-03
28	1390	1.226	18.09	1.587e-03
29	1417	1.274	19.86	1.773e-03
30	1437	1.302	21.53	2.100e-03
31	1449	1.331	22.83	2.364e-03
32	1463	1.362	24.76	2.787e-03
33	1471	1.393	26.35	3.045e-03
34	1479	1.415	28.22	3.190e-03
35	1489	1.447	31.06	3.484e-03
36	1496	1.475	33.31	3.598e-03
37	1505	1.503	36.83	4.919e-03
38	1511	1.532		
39	1517	1.554		
40	1522	1.623		

Table 11. Results of Verification Experiments (Concluded).

SEVEN POINT INCREMENTAL POLYNOMIAL METHOD FOR DETERMINING DA/DN

SPEC NO. S/N 7-5 NO. POINTS= 46
SPECIMEN: CT D= .5 IN. U= 2 IN.
PAIN .579 KIPS PMAX= 1.93 KIPS R= .3 TEST FREQ.= .1 HZ
TEMP.= 1100 F ENVIRONMENT=AIR

OBS NO.	CYCLES	A	DELK	DA/DN
1	0	1.001		
2	447	1.005		
3	1032	1.011		
4	1306	1.014	18.86	1.036e-05
5	2904	1.031	19.37	1.118e-05
6	4614	1.050	20.01	1.189e-05
7	5109	1.058	20.20	1.231e-05
8	5654	1.064	20.43	1.308e-05
9	6104	1.069	20.44	1.267e-05
10	6414	1.074	20.77	1.232e-05
11	6852	1.080	20.96	1.248e-05
12	7347	1.085	21.18	1.271e-05
13	7736	1.089	21.34	1.310e-05
14	8192	1.094	21.56	1.414e-05
15	8451	1.100	21.71	1.472e-05
16	8872	1.104	21.94	1.685e-05
17	9338	1.114	22.29	1.684e-05
18	9765	1.120	22.57	1.683e-05
19	9987	1.130	22.70	1.670e-05
20	10991	1.141	23.35	1.669e-05
21	12298	1.144	24.34	1.917e-05
22	13320	1.183	25.28	2.179e-05
23	14219	1.204	26.35	2.401e-05
24	14714	1.218	27.00	2.550e-05
25	15144	1.228	27.63	2.707e-05
26	15429	1.233	28.04	2.719e-05
27	15639	1.242	28.41	2.740e-05
28	15929	1.252	28.87	2.903e-05
29	16284	1.260	29.51	3.086e-05
30	16659	1.270	30.26	3.323e-05
31	17044	1.287	31.21	3.578e-05
32	17201	1.292	31.59	3.661e-05
33	17409	1.299	32.13	3.913e-05
34	17815	1.315	33.25	4.258e-05
35	18128	1.327	34.40	4.727e-05
36	18393	1.343	35.49	5.351e-05
37	18568	1.352	36.31	5.796e-05
38	18857	1.366	37.92	6.822e-05
39	19154	1.389	39.97	8.340e-05
40	19334	1.403	41.64	1.059e-04
41	19491	1.421	43.60	1.338e-04
42	19606	1.433	45.25	1.668e-04
43	19773	1.444	49.42	2.398e-04
44	19922	1.496		
45	19987	1.528		
46	20004	1.539		

SEVEN POINT INCREMENTAL POLYNOMIAL METHOD FOR DETERMINING DA/DN

SPEC NO. 13-3 NO. POINTS= 46
SPECIMEN: CT D= .5 IN. U= 2 IN.
PAIN .56 KIPS PMAX= 1.93 KIPS R= .3005181 TEST FREQ.= .1 HZ
TEMP.= 1100 F ENVIRONMENT=AIR

OBS NO.	CYCLES	A	DELK	DA/DN
1	0	1.000		
2	230	1.000		
3	965	1.017		
4	1881	1.026	19.25	1.435e-05
5	2187	1.029	19.35	1.413e-05
6	3800	1.056	19.99	1.386e-05
7	5298	1.070	20.72	1.613e-05
8	6768	1.096	21.62	1.853e-05
9	7928	1.121	22.43	2.160e-05
10	8627	1.136	23.09	2.166e-05
11	8850	1.140	23.31	2.307e-05
12	9174	1.146	23.62	2.415e-05
13	9344	1.152	23.79	2.455e-05
14	9710	1.163	24.22	2.679e-05
15	10042	1.170	24.66	2.746e-05
16	10330	1.179	25.02	2.743e-05
17	10645	1.187	25.45	2.533e-05
18	10846	1.193	25.64	2.682e-05
19	11173	1.202	26.09	2.741e-05
20	11444	1.205	26.45	2.752e-05
21	12885	1.259	29.30	4.292e-05
22	13630	1.290	31.62	5.133e-05
23	14280	1.330	34.35	5.787e-05
24	14502	1.341	35.43	6.481e-05
25	14640	1.350	36.24	6.250e-05
26	14770	1.358	36.93	6.940e-05
27	14920	1.369	37.92	7.970e-05
28	15130	1.381	39.72	9.865e-05
29	15160	1.393	40.03	9.869e-05
30	15240	1.399	40.88	1.077e-04
31	15360	1.412	42.42	1.268e-04
32	15470	1.424	44.06	1.410e-04
33	15560	1.438	45.74	1.699e-04
34	15640	1.454	47.40	2.043e-04
35	15750	1.473	51.28	2.737e-04
36	15810	1.492	54.04	3.463e-04
37	15840	1.505	55.87	4.249e-04
38	15870	1.517	58.39	4.930e-04
39	15881	1.522	59.44	5.200e-04
40	15893	1.531	60.67	5.992e-04
41	15905	1.537	62.22	6.570e-04
42	15917	1.543	64.15	7.061e-04
43	15935	1.560	67.32	7.462e-04
44	15947	1.569		
45	15965	1.582		
46	15980	1.594		

IX. DISCUSSIONS

A. CHARACTERISTICS OF THE INTERPOLATIVE MODEL

The following characteristics of the interpolative model developed within this program were considered significant features required by the model.

- Non-symmetric cyclic crack growth rate versus stress intensity curves were generated by the model. In many of the experimental results, such as S/N 5-5 in Figure 18, nonsymmetric characteristics of crack growth curves were observed. No physical reasoning was known for suspecting crack growth behavior of a sample to be symmetric about some point, even though a number of models by other authors contain this characteristic.
- The model distinguished a difference between various wave patterns of equal duration. For example, the growth behavior of a slow cycle with short hold period was predicted differently than a fast cycle with long hold period of equal time. This approach varied from others (9, 10) where the use of total time per cycle, regardless of the frequency or hold period, was used to correlate the data. As noted in Figure 48, the use of crack growth rate per unit time (da/dt) significantly reduced the range of variation in the experimental results in comparison to crack growth per cycle (compare the variation in growth rate between the experimental results shown in Figures 48 and 18d). Even though the variation was reduced on the da/dt plot, an order of magnitude variation in crack growth behavior still existed. This amount of variation, as will be shown later, was unacceptable for low stress ratio conditions. The model was developed by separating the cycle into two phases, the cycling portion and a hold time portion. By this method it contains the necessary ingredients to predict crack growth behavior of difficult wave patterns such as fast cycles with short hold periods.
- The model was developed so that each of the coefficients in the modified sigmoidal equation (Equation 5) were independent and related to the test variables. Three of the coefficients were acquired from the inflection point region, an area generally well defined. Two of the coefficients are the asymptotes. The upper asymptotes were easily estimated (see Section VI B.1). In the past the lower asymptotes have been considered to have significant impact on life predictions. As will be shown in the next paragraph, a wide range of variation in the lower asymptote can be compensated by the lower shaping coefficient, Q . The lower shaping coefficient was the final coefficient evaluated, and calculated by performing a simple regression analysis that produced the optimum correlation to the data after the relationships of the test variables to the other coefficients were known and implemented into the analyses.

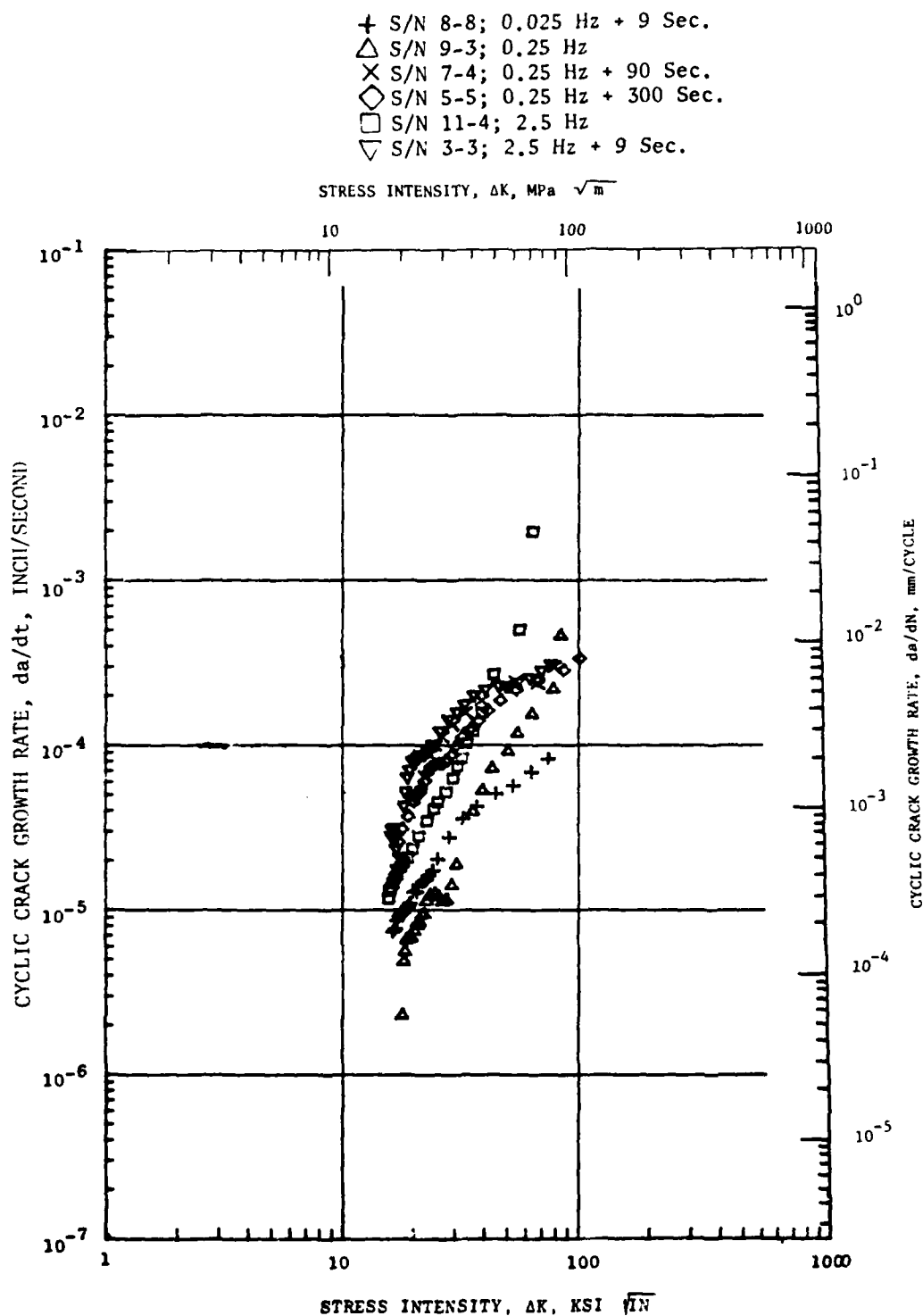


Figure 48. Results of 760°C (1400°F) and Stress Ratio of 0.1
Plotted as da/dt Versus ΔK Rather than da/dN .

- The crack growth curves were asymptotic. It is easily understood that such a behavior was expected when approaching the unstable crack growth regime. At the lower end, the modified sigmoidal equation had the flexibility of adjusting the lower shaping coefficient Q , to account for the selection of the lower asymptote. As shown in Figure 49 two cyclic crack growth curves are present, one with a lower asymptote of $10.98 \text{ MPa } \sqrt{\text{m}}$ ($10 \text{ Ksi } \sqrt{\text{in.}}$) and the other at $9.33 \text{ MPa } \sqrt{\text{m}}$ ($8.5 \text{ Ksi } \sqrt{\text{in.}}$). In regions above $2.5 \times 10^{-5} \text{ mm/cycle}$ ($10^{-6} \text{ inch/cycle}$), no significant variation between the curves was present. Nor was there any difference indicated in the life prediction using the two coefficients as shown in Figure 50. Recall that the selection of ΔK^* was based on high frequency, no hold time experimental results that produced growth rates in the 10^{-6} mm/cycle ($10^{-7} \text{ inch/cycle}$) regime. In most turbine applications it is expected that life analysis would be initiated within this region, partially a result of the current capabilities of the reliable crack detection technique.

B. COMPARISON TO OTHER STUDIES

In order to accurately access the results of the interpolative model, the capabilities of other predictive techniques and confidence within crack growth data will be reviewed. Numerous studies have been conducted to describe crack growth behavior of various materials at room temperatures. The effects of stress ratio has been an ingredient of many of these studies. Of course, the influences of hold time and frequency are of little importance at room temperatures. At elevated temperature where time-dependent damage can occur, some attempts have been made to describe a material's capability to resist fatigue crack propagation (9-17). A few observations from these studies are listed below.

1. In a study⁽¹⁸⁾ which included 68 crack propagation tests conducted at room temperature under constant-amplitude loading and a single set of conditions, the raw crack length versus cycle measurements varied by 30% on the cycle coordinate. A factor of two in crack growth rate at equivalent stress intensity values was constantly observed in the da/dN versus ΔK when the seven point incremental polynomial method was used to calculate da/dN .
2. In another study by Hudak⁽¹⁸⁾ which included the development of the three component interpolative model for room temperature condition and stress ratios from 0.1 to 0.8, a 45% error was calculated when the model was used to predict the life of one of the experiments used in the development of the model. Only eight of the 66 experiments used to develop the model were evaluated by the model.
3. A 2 to 1 intralaboratory (within the same lab) variability in crack growth rate measurements was typically observed in an ASTM round-robin program⁽¹⁹⁾ on crack growth variability. The overall

$$\Delta K_c = 110. \text{ Ksi} \sqrt{\text{in}}$$

$$\frac{da'}{dN_1} = 1.0$$

$$\Delta K_i = 36.4 \text{ Ksi} \sqrt{\text{in}}$$

$$\frac{da}{dN_1} = 1 \times 10^{-4} \text{ inch/cycle}$$

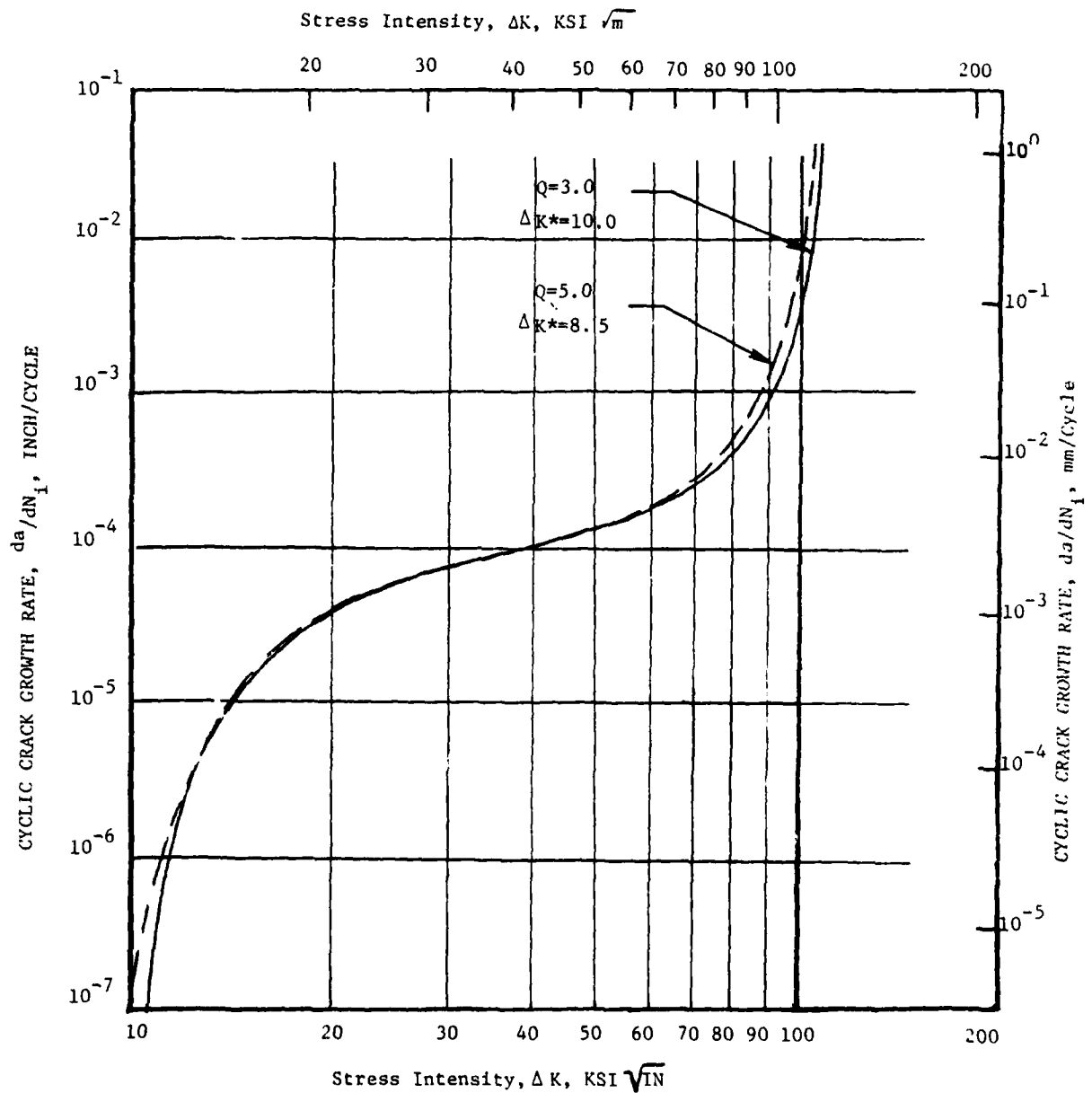


Figure 49. Comparison of Two Cyclic Crack Growth Curves with Two Different Lower Asymptotes Compensated by the Lower Shaping Coefficient

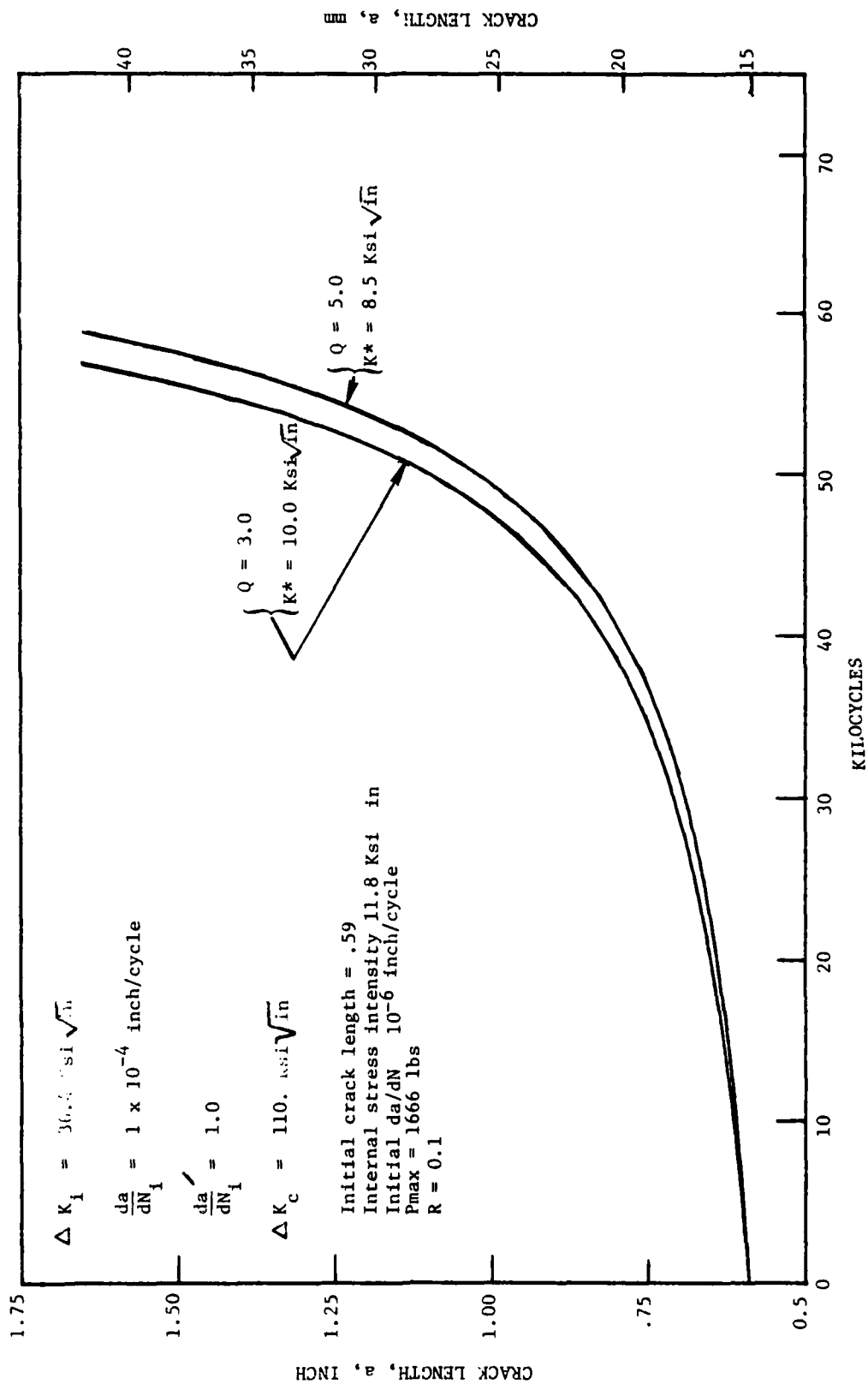


Figure 50. Crack Length Versus Cycle Prediction Using Two Different Sets of Coefficients

interlaboratory variability was approximately a factor of three. Fifteen laboratories participated within this program and all tests were conducted at one condition (room temperature, 5 Hz, $R = 0.1$). It was concluded by the authors that the state-of-the-art (1975) variability under optimum room temperature testing conditions was about 2 to 1 on da/dN at a given ΔK level for a single homogeneous material.

4. The best simple correlation of hold time and stress ratio ($R = 0.05$ through 0.8) effects on Inconel 718 at 650°C (1200°F) was by the maximum stress intensity value on a da/dt basis⁽¹⁰⁾. This method, however, produced a factor of $4\text{--}1/2$ on crack growth rate at moderate growth rates with larger variations at low and high growth rates. In another study⁽²⁰⁾ on the same material, a factor of two was observed in the crack growth rate 427°C (800°F) for three stress ratios ($R = 0.05, 0.333, \text{ and } 0.5$) when the Walker expression was used to correlate the data. The highest measured growth rate in this study was only 5×10^{-5} inch/cycle since the specimens were not cycled to failure.
5. In reviewing the variation of creep crack growth rate experiments, it was noted⁽²¹⁾ that crack growth rates at a given value of ΔK is about a factor of thirty. A much less variation, a factor of four, was noticed in the work done in another study⁽²²⁾ on Inconel 718.

Based on these room-temperature studies, the interpolative model was expected to have a minimum error possibility of a factor of two. The elevated temperature environment could possibly increase this factor. Furthermore, based on typical creep crack growth data, the error probably would increase with increasing stress ratio.

C. ASSESSMENT OF INTERPOLATIVE MODEL

In order to assess the reliability of the interpolative model, a measure of variation was achieved by predicting the life of experimental conditions used to generate the model and comparing those results of the experimental data. For each test conducted in the primary test program, the test conditions were entered into the interpolative model and the coefficients of the modified sigmoidal equation calculated. An integration of the equation with the coefficients was then conducted for each condition by the Gauss Quadrature technique, resulting in predictions of crack length and cycles number. For any experiment that the da/dN versus ΔK curve was determined by successively increasing the crack length or loads, only the final segment was analyzed. Tabulated in Table 12 are comparisons between the predicted and actual number of cycles to failure. Also included are the ratios between the two lives. With the exception of two specimens (S/N 11-2 and 10-7), the predicted lives were within a factor of three of actual life, with 93 percent of those within a factor of two. Shown in Figure 51 are plots of the logarithm of the ratio

Table 12. Predicted and Actual Lives from a Given Crack Length of Specimens Conducted in Primary Test Matrix.

Specimen Number	R	RT	v	HT	Predicted Life	Actual ^(a) Life	Ratio of Predicted Versus Actual	Initial Crack Length For Prediction
8-4	0.1	1000	2.5	9	53,000	52,429	1.011	0.875
10-6			0.25	0	70,500	74,877	0.942	0.819
8-1				9	79,100	107,345	0.737	0.795
10-3				90	7,200	6,725	1.071	1.021
4-7				300	770 ^(c)	1,031	0.747	1.404
10-2			0.025	9	3,400	2,883	1.200	0.923
5-8		1200	2.5	0	73,800	74,512	0.990	0.776
13-2				90	1,820	1,561	1.166	0.790
9-4			0.25	0	65,300	59,334	1.101	0.772
9-1				90	5,050	5,479	0.922	0.745
8-3				300	750	1,341	0.559	0.937
11-5			0.025	0	8,960	7,837	1.143	0.899
9-7				90	1,080	1,217	0.887	0.883
5-6		1300	0.25	0	24,450	25,450	1.000	0.798
4-5				300	180	188	0.957	0.839
11-4		1400	2.5	0	78,600	55,200	1.424	0.720
3-3				9	1,060	1,270	0.835	0.738
9-3			0.25	0	11,700	12,723	0.920	0.824
7-4				90	82	78	1.051	0.833
5-5				300	54	53	1.019	0.710
8-8			0.025	9	1,010	964	1.048	0.777
5-7		1000	2.5	0	241,800	305,450	0.792	0.813
4-3				90	1,380	3,058	0.457	1.015
5-3			0.025	0	3,720	3,535	1.052	0.983
8-7				90	b			
11-7		1200	0.25	9	7,110	9,906	0.718	1.044
11-1					3,140	3,088	1.017	1.189
8-5					29,100	13,512	2.154	0.787
4-6					27,700	28,156	0.984	0.792
9-8		1400	2.5	0	6,360	10,604	1.667	0.810
7-8				90	123	140	0.879	0.714
3-1			0.25	0	10,900	8,350	1.305	0.677
4-1			0.025	0	307	237	1.295	0.856
4-2				90	130	101	1.287	0.795
11-2	0.9	1000	2.5	9	92,000	16,997	5.413	1.142
4-8			0.25	0	84,000	112,400	0.747	1.038
10-1				90	1,260	3,416	0.369	1.228
5-1			2.5	9		c		
11-6		1200	2.5	0	470,000	421,282	1.116	0.765
8-6				90	640	530	1.20	0.863
10-5			0.025	0	4,700	3,413	1.377	0.775
3-4				90	350	508	0.689	0.799
5-2		1400	2.5	9	400	526	0.775	0.815
4-4			0.25	0	965	1,050	0.916	0.815
10-7				90	520	129	4.031	0.804
11-8			0.025	9	112	168	0.667	0.764

(a) Life of Final Segment of Test Without Load Increases or Crack Extensions

(b) Equipment Malfunction

(c) Specimen Failed During Crack Extension

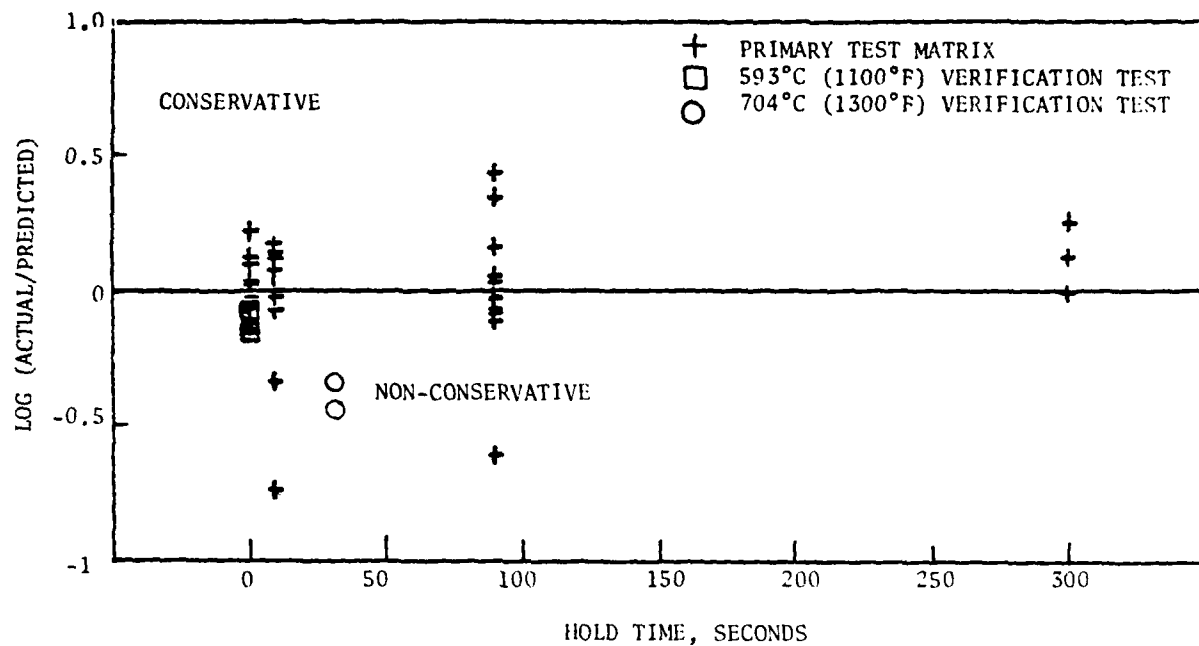


Figure 51a. Deviation Versus Hold Time

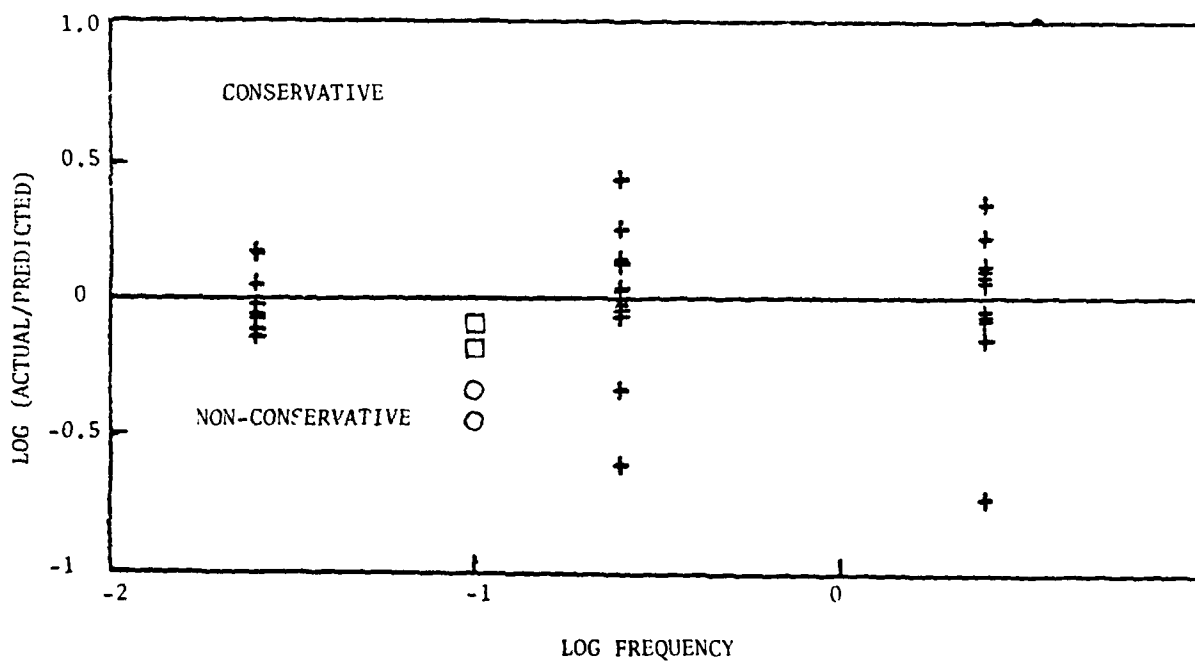


Figure 51b. Deviation Versus Frequency

Figure 51. Deviation in Actual and Predicted Lives Versus Four Test Variables

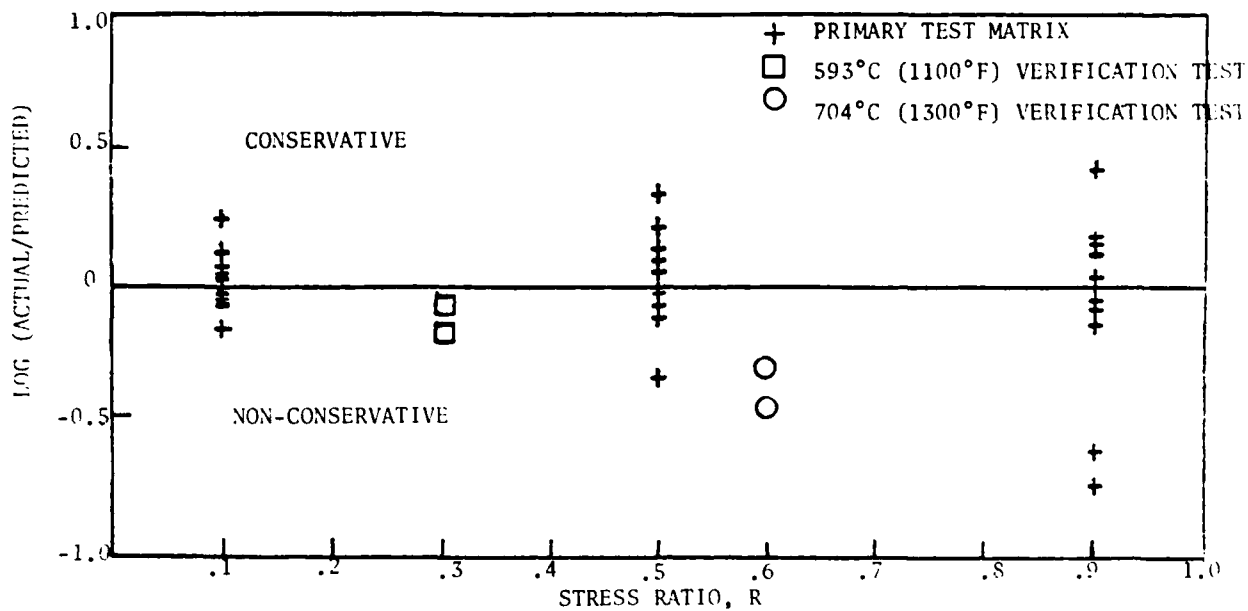


Figure 51c. Deviation Versus Stress Ratio

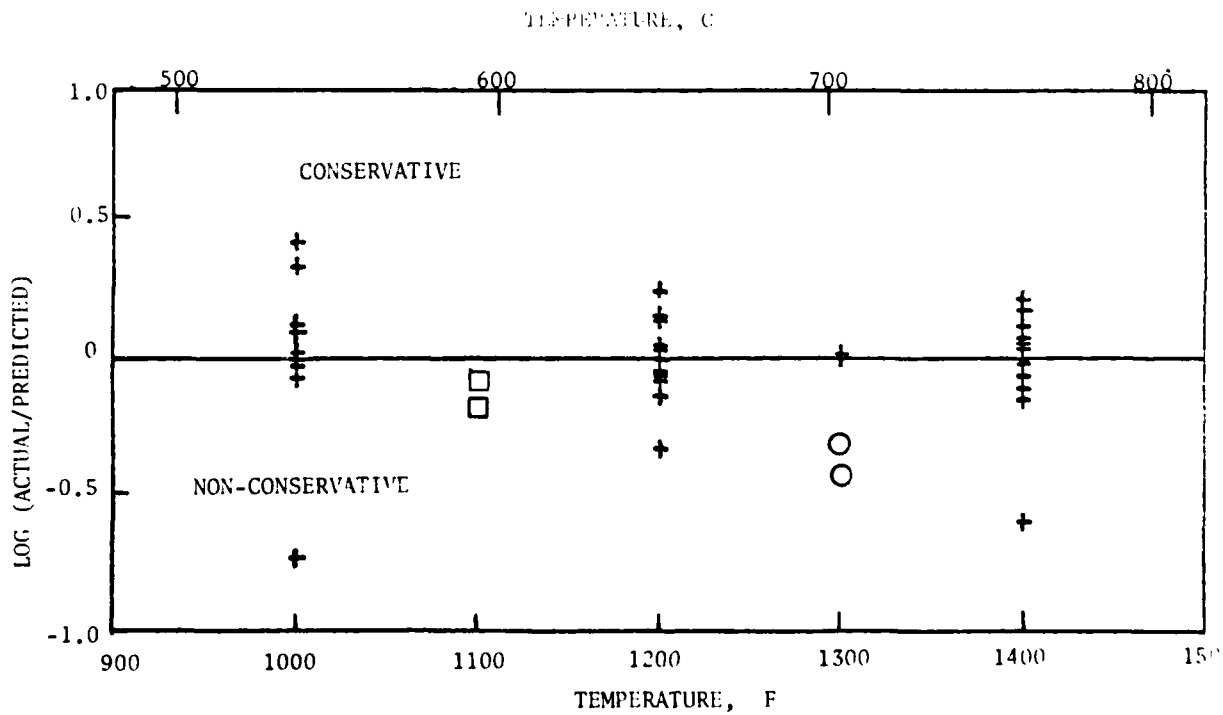


Figure 51d. Deviation Versus Temperature

Figure 51. Continue

of the actual and predicted lives versus each of the four test variable. As noted, the predictions of the primary matrix experiments were evenly scattered from the ideal prediction line. The verification test predictions were non-conservative but within the range of deviation of the primary matrix predictions. It is obvious that the deviation was proportionally related to stress ratio which can be explained by the increase in scatter in creep crack growth experimental results in comparison to cyclic crack growth experiments. While the modeling of the stress ratio effects on the inflection point was somewhat complex and requires a minimum of three levels of stress ratio, the use of the Walker Expression (Eq. 1) was found considerably less accurate as indicated in Figure 52. The deviation of temperature and hold time were generally uniform. It appeared that the deviation increased with increasing frequency; however, this is believed to be attributed to the fewer tests conducted at slow frequencies.

D. ERRORS IN THE MODIFIED SIGMOIDAL EQUATION

1. Precracking Method Influences

As with any model of this nature, the typical scatter of the experiments will produce different impacts on the life predicting success of the model. In the construction of the primary test matrix, four replica experiments were placed at the center of the hypercuboctahedron box design. The results of the four replica tests, conducted at 649° C (1200° F), $R = 0.5$, 0.25 Hz and 9 second hold period, are present in the plot of da/dN versus ΔK in Figure 41. As noted, a factor of three differences in growth rate was determined from the experimental results which might be considered high, based on other studies. If the one set of data was eliminated (Specimen 8-5), the scatter in the growth rate was reduced to less than factor of two. In examination of the four experimental results, it was noted that specimen 8-5 was the only specimen of the four which was prepacked at room temperature. Shown in Figure 53 are photographs of the fracture surfaces for specimen 8-5 along with that of specimen 11-1, also tested at the same conditions. Note that the crack front of specimen 8-5 was initially uneven and, in fact, remained uneven throughout the test. The difference between the two surface crack lengths was 0.090 inch at the start of the experiment and finished at 0.066 inch. This was not uncommon for many of the room temperature precracked specimens. Additionally, many of the room temperature precrack specimens had considerable curvature at initiation of the elevated temperature tests which rapidly decreased after little growth (see Figure 10). It is believed that there was an influence on the da/dN versus ΔK results when the surface crack measurements were uneven or if significant change in the crack front occurred shortly after the initiation of the test. The exact influence that these observations had on the growth rate behavior or calculation are not understood by the author.

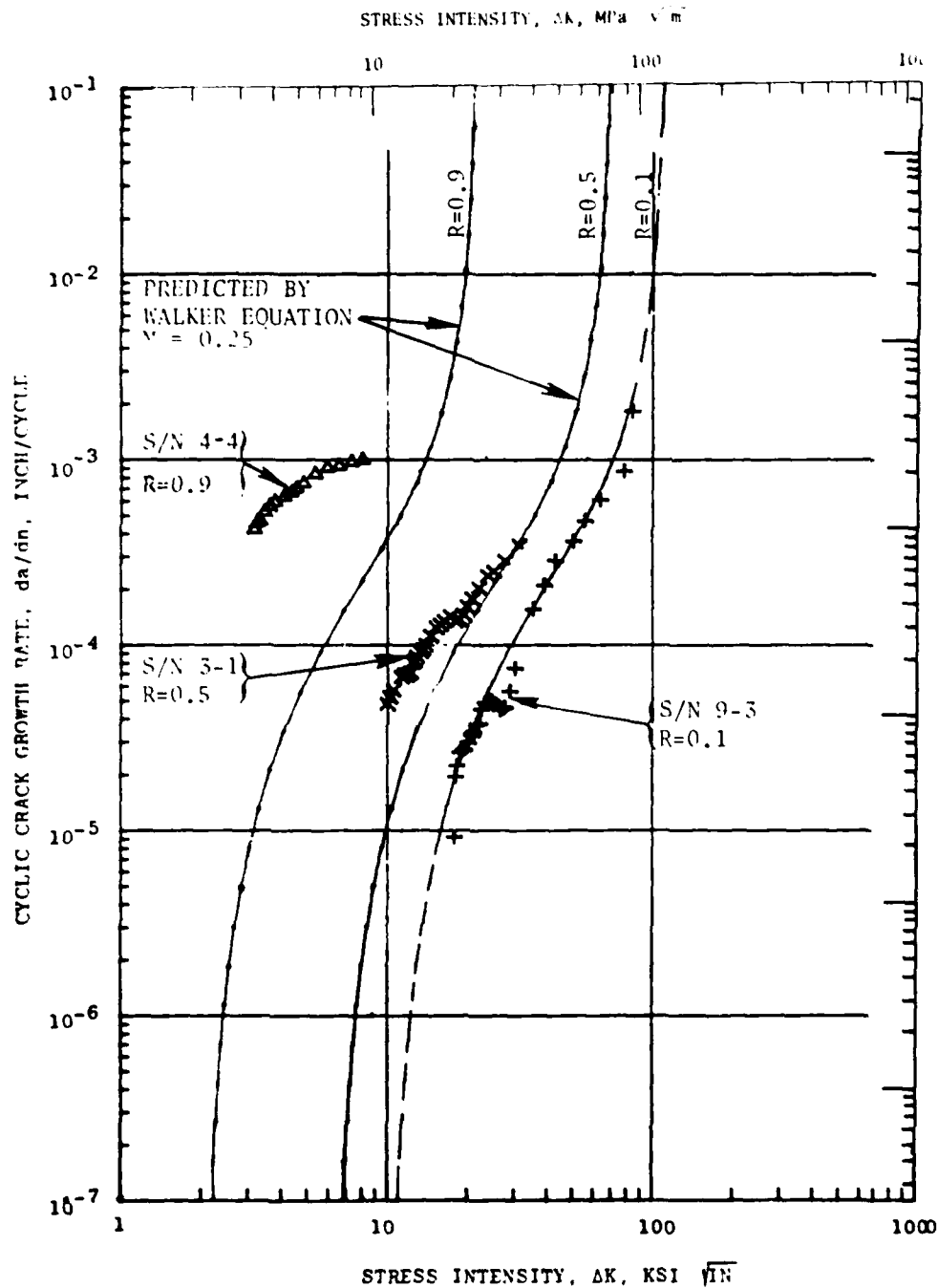


Figure 52. Comparison of Actual Data and Prediction Using Walker Equation for 760°C (1400F), 0.25 Hz and No Hold-Time.

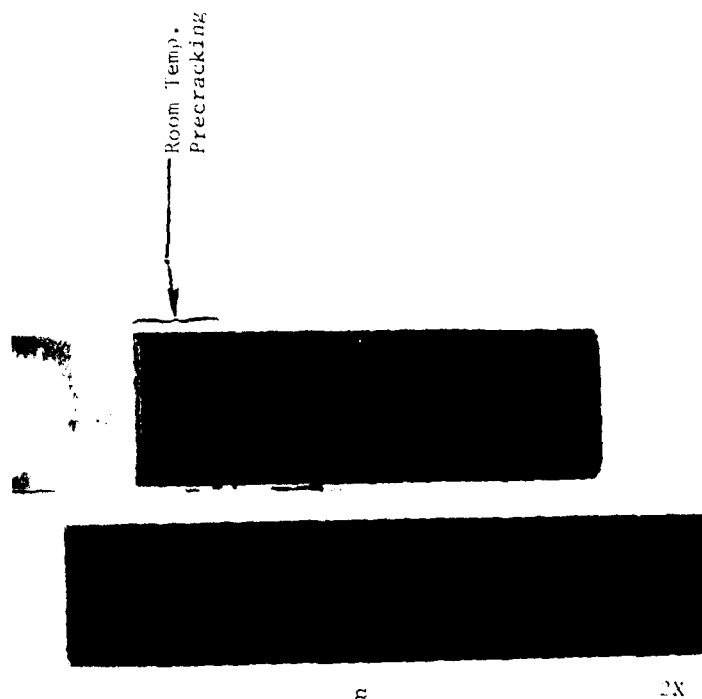


Figure 53a. Room Temp. Precracked Specimen S/N 8-5

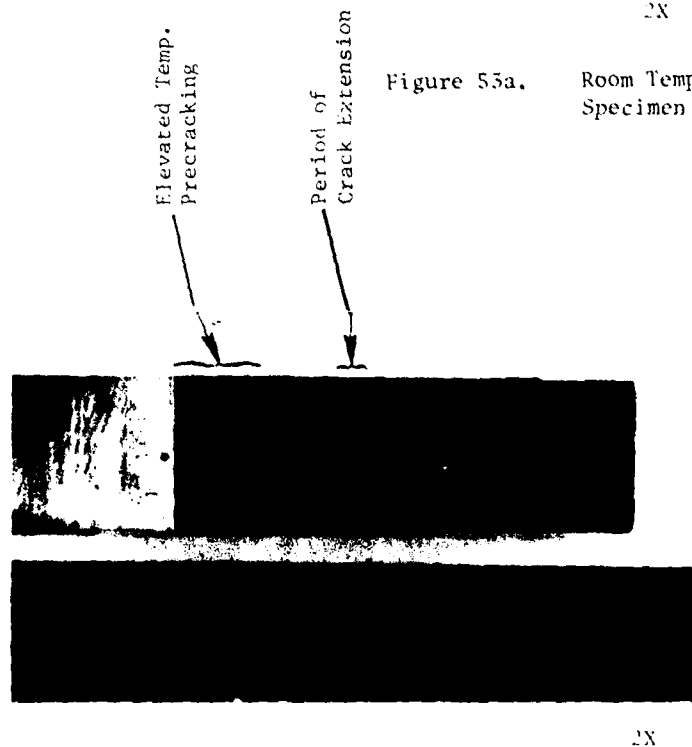


Figure 53b. Elevated Temp. Precrack Specimen S/N 11-1

Figure 53. Comparison of Fracture Surfaces of Room and Elevated Temperature Precracked Specimens

2. Effect of Observed Scatter at the Replica Test Condition

The variation in crack growth behavior in the results of the replication experiments, along with observations from other studies was applied to each of the coefficients of the interpolative model to establish the least overall possible error within the model. Of the four replication experiments, Specimen 4-6 produced an extremely good correlation by the "best fit" model as indicated in Figure 54. Its initial crack length and test loads were selected to study the effect of the observed scatter in the data. The value of da/dN at the inflection point was varied so that a factor of two existed. The stress intensity at the inflection point was varied by a total factor of 1.25. The slope of the inflection point, asymptotes, and upper shaping coefficients were varied by $\pm 10\%$. Each of the values were separately fixed within the interpolative model and the coefficients of the modified sigmoidal equation determined. In Figure 55, the effect that these changes had on the crack growth calculation are graphical presented. The location of the inflection point appears to have the largest impact on life and can easily be determined. The lower asymptote has somewhat less impact. Less than a factor of two change in life was noted due to a change of any one of the coefficients within the limits set above (Figure 55A through 55c). When the modifications were combined to form a worse case condition, the influence was approximately a factor of three (see Figure 55D).

3. Effect of Scatter in the Verification Tests

Since the interpolative model was accurate only within an average factor of 2-1/2 for the 704° C (1300° F), $R = 0.6$, and 0.1 Hz with a 30 second hold verification test condition, the source of error of this test condition was examined. In the comparison of the crack growth data versus the prediction (Figure 47), it was obvious that the predicted location of the da/dN at the inflection point was at least a factor of two lower than the data. Furthermore, the lower asymptote appears somewhat incorrect in the prediction. If the inflection point was increased by a factor of 2.25 and the ΔK^* decreased by 10%, the verification test condition would have been accurately predicted (see Figure 56). Errors by the model in determining the coefficients of the verification condition were close to what was considered typical variation in crack-growth data.

In consideration of the test conducted within the primary test matrix with conditions close to surrounding the verification test condition, it was noted that experimental data was scarce. For example, the only 649° C (1200° F) tests conducted at the stress ratio of 0.5 were the four replica test at a single condition (0.25 Hz plus 9 second hold period) which produced a calculated inflection point at 1.8×10^{-3} mm/cycle (7×10^{-5} inch/cycle). At 760° C (1400° F) and stress ratio of 0.5, the nearest experimental results were from tests conducted at 0.025 and 2.5 Hz without hold periods, with resulting inflection points

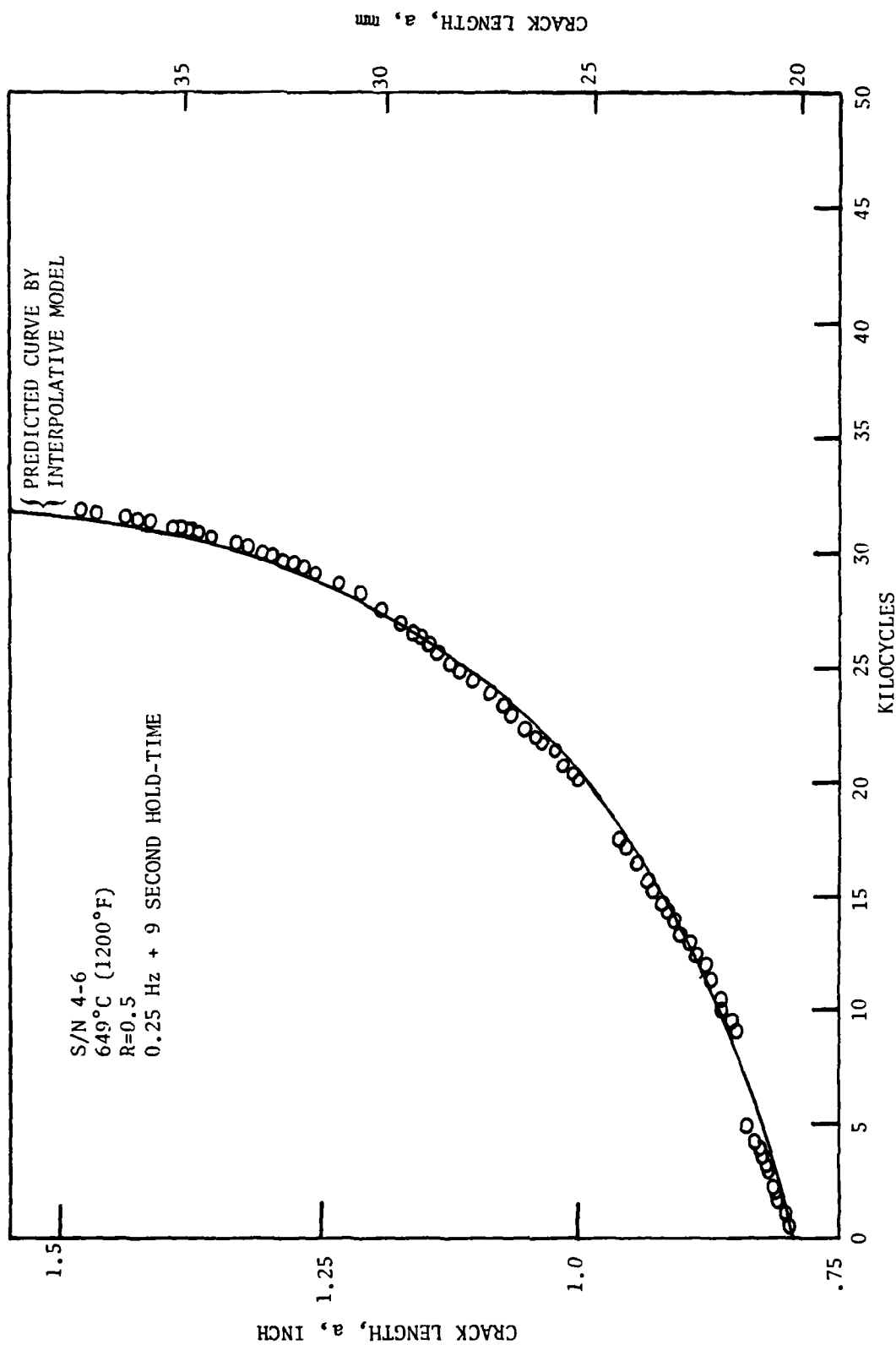


Figure 54 Correlation of S/N 4-6 Experimental Results and Predicted Curves

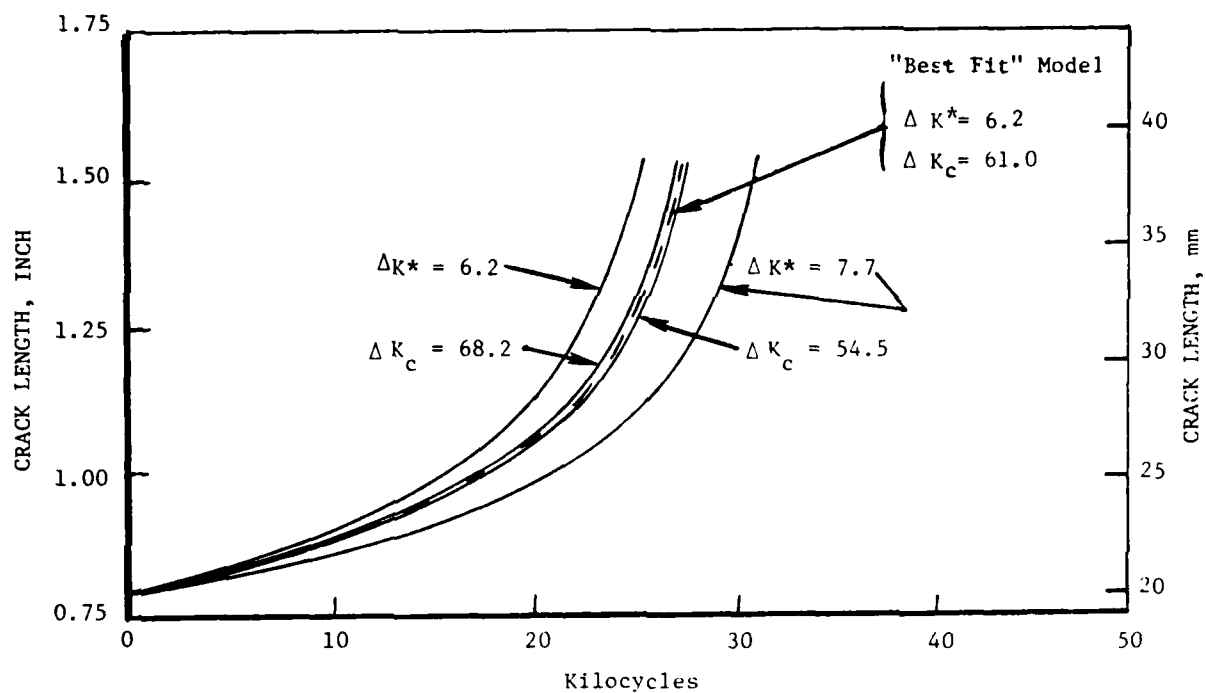


Figure 55a. Variation of Asymptotes, ΔK_c and ΔK^*

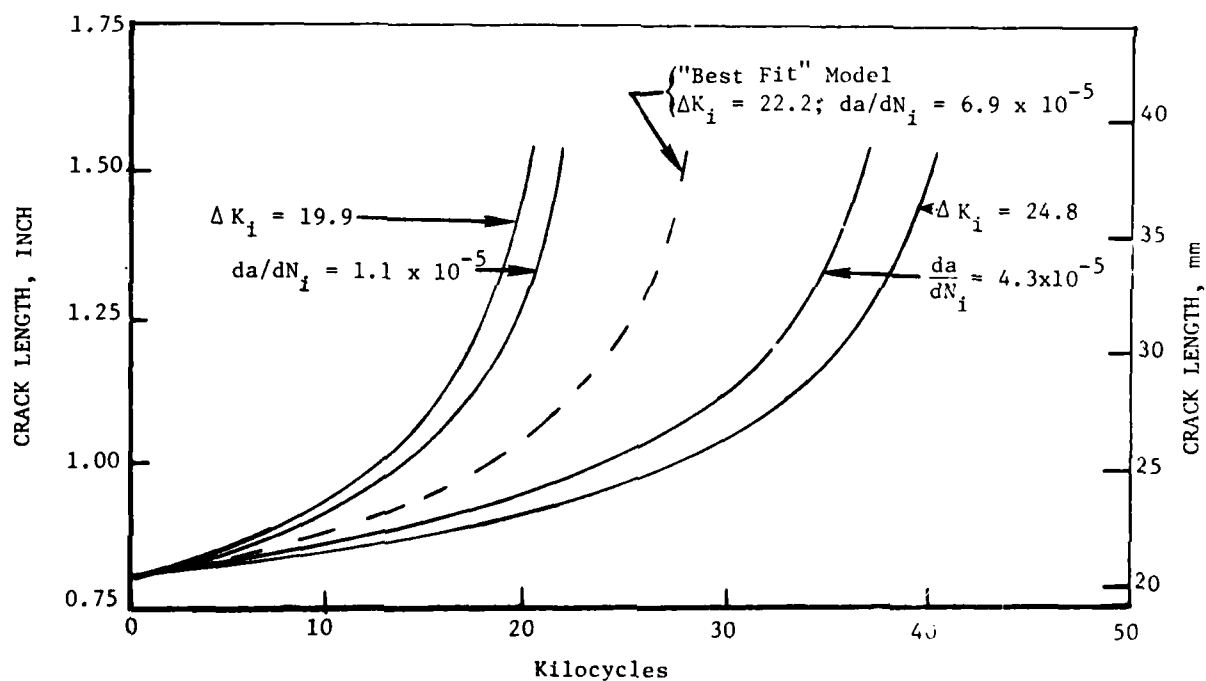


Figure 55b. Variation of Location of Inflection Point, da/dN_i and ΔK_i

Figure 55. Influence of Typical Variation of Parameters Used In The Sigmodial Equation

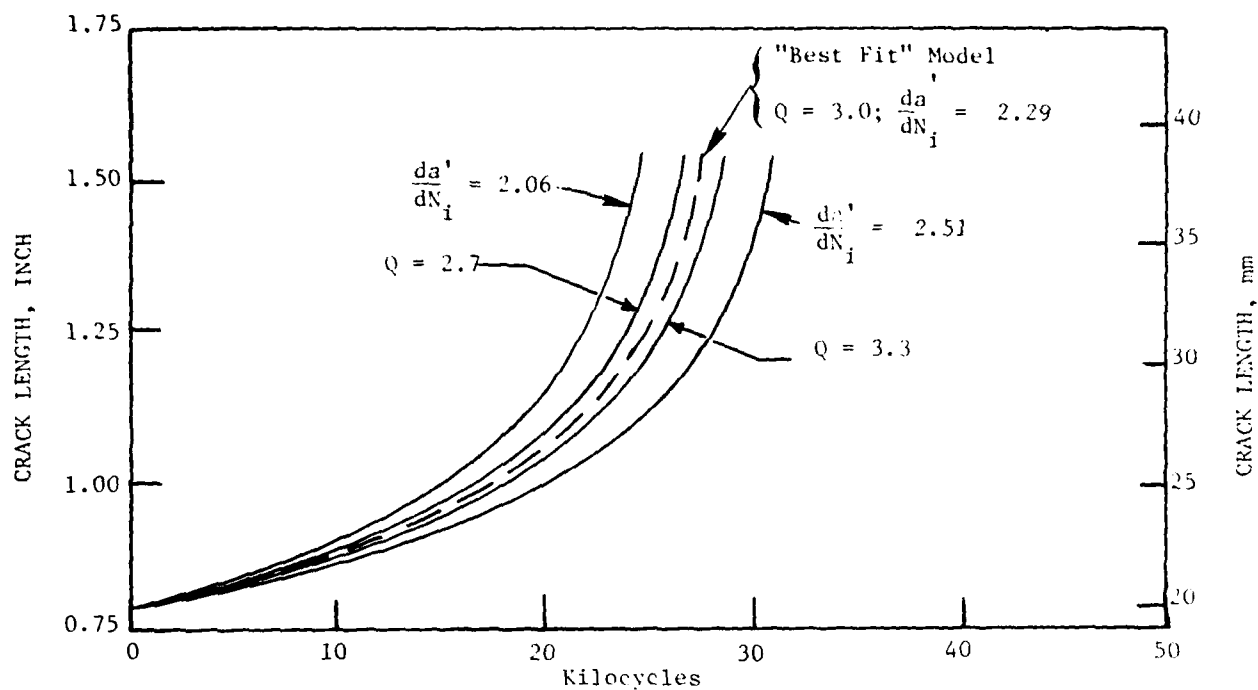


Figure 55c. Influence of Typical Variation of Parameters Used In The Sigmodal Equation

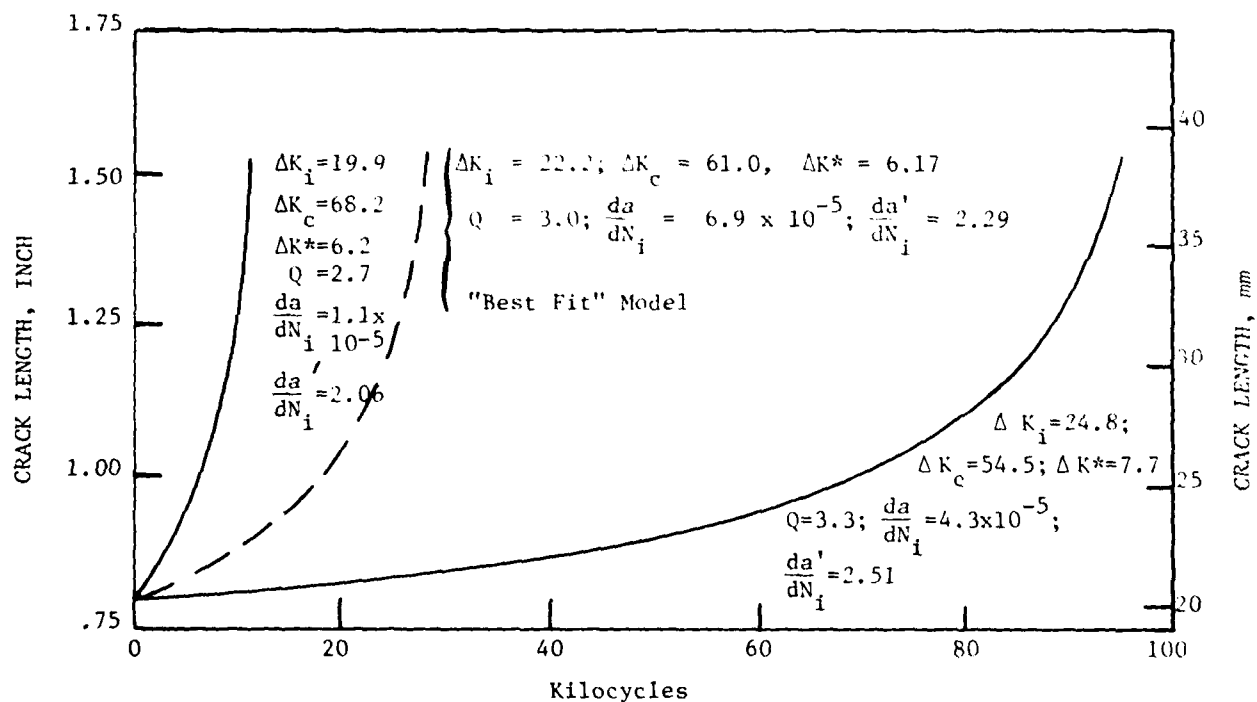


Figure 55d. Combination of all Parameters

Figure 55. Continued

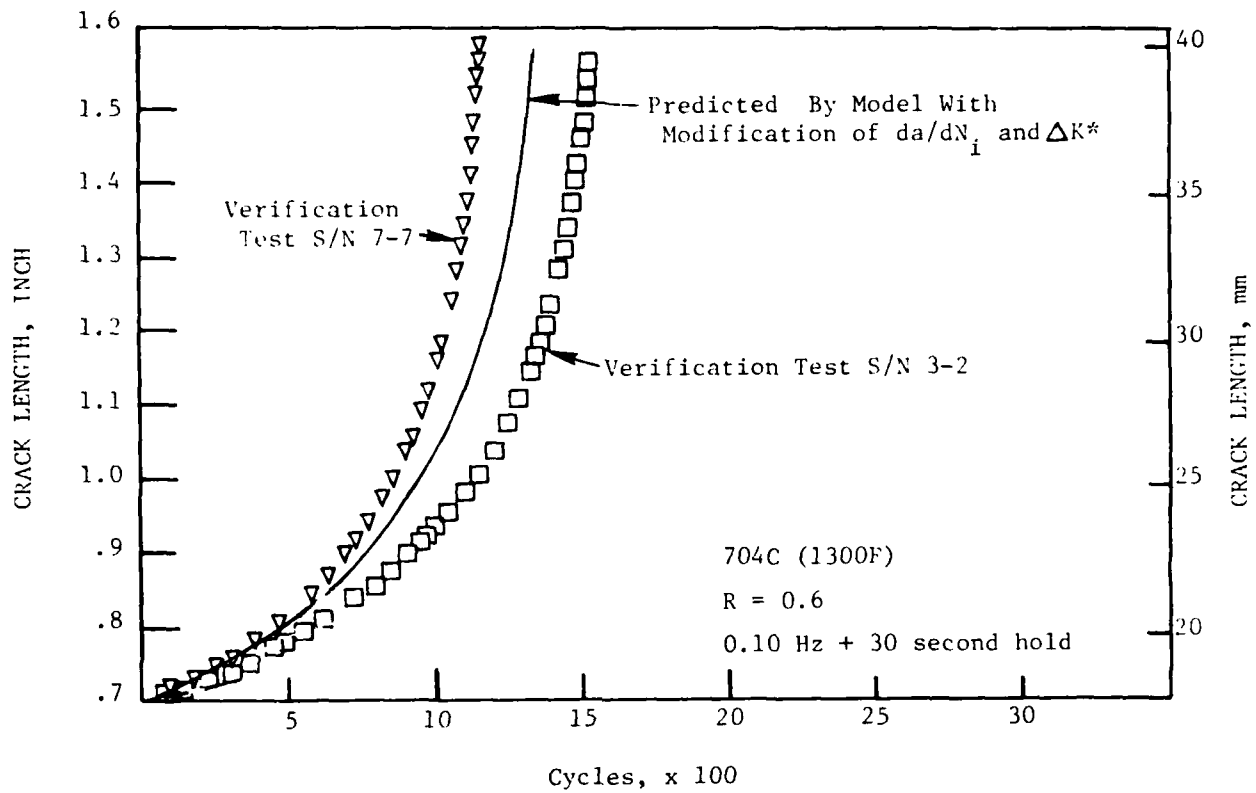


Figure 56. Comparison of the Verification Tests Results and the Prediction with a Factor of 2.2 Increase on da/dN_i and a 10% Decrease in ΔK^*

of 3.0×10^{-1} mm/cycle (1.2×10^{-2} inch/cycle) and 7.6×10^{-3} mm/cycle (3.0×10^{-4} inch/cycle). Thus, the nearest relative conditions to this verification test were at temperatures of $\pm 38^\circ \text{C}$ (100°F), a slightly lower stress ratio, and most importantly, resulting growth-rates at the inflection point of almost an order of magnitude difference. As would be expected, some inaccuracies exist within the modeling. In retrospection of the primary test matrix, some comments appear worthy.

E. CRITICAL TESTS FOR MODEL APPLICATIONS

Prior to discussing the required amount of data required to apply the interpolative model for another material, the test matrix used to develop this model will be reviewed.

1. The Designed Matrix for This Program

Tests conducted to develop the interpolative model were based on the "4-factor hypercuboctahedron" test matrix design, with ten additional test conducted to enhance the matrix. Figure 57 illustrates the designed matrix. Each circle in the figure represents a single test, except for the solid point at the center which represents the four replication experiments. The five X's in the figure indicate the conditions where the extra tests were added to enhance the matrix. The other five additional tests are listed.

The hypercuboctahedron designed matrix populates the majority of the experiments at the extremities of each test variables. When a model is already known, this type of design permits a more uniform confidence in the predictions as a function of the test variable. If the test conditions had been evenly distributed within each test variable, then the best confidence in a prediction would be expected at the center with less confidence at the extremities. It should be noted that the basic hypercuboctahedron test matrix does not include three levels of any single test variables to be examined while the other variables are held constant. Therefore, ten tests were added to the hypercuboctahedron test matrix to supplement the test program. Four of the ten tests were conducted at conditions which results were redundant of the results collected from the hypercuboctahedron matrix program. For examples, specimens 4-7 and 8-1 were conducted at 538°C (1000°F) and stress ratio of 0.1, a condition where crack growth was known, from the other data, to be time and cyclic independent (see Figure 19a). The other two tests, specimens 9-4 and 9-1, were conducted at the mid-frequency level (0.25 Hz) at 648°C (1200°F) and a stress ratio of 0.1. The two outer frequency level experiments from the hypercuboctahedron designed matrix produced essentially identical crack growth curves. Since specimens 9-1 and 9-4 showed that there was no in crack growth between the high and low frequencies, as would be expected, no new information was added by the test at 0.25 Hz. While temperature and long hold time effects were well defined for the stress ratio of 0.1 and frequency of 0.25 Hz

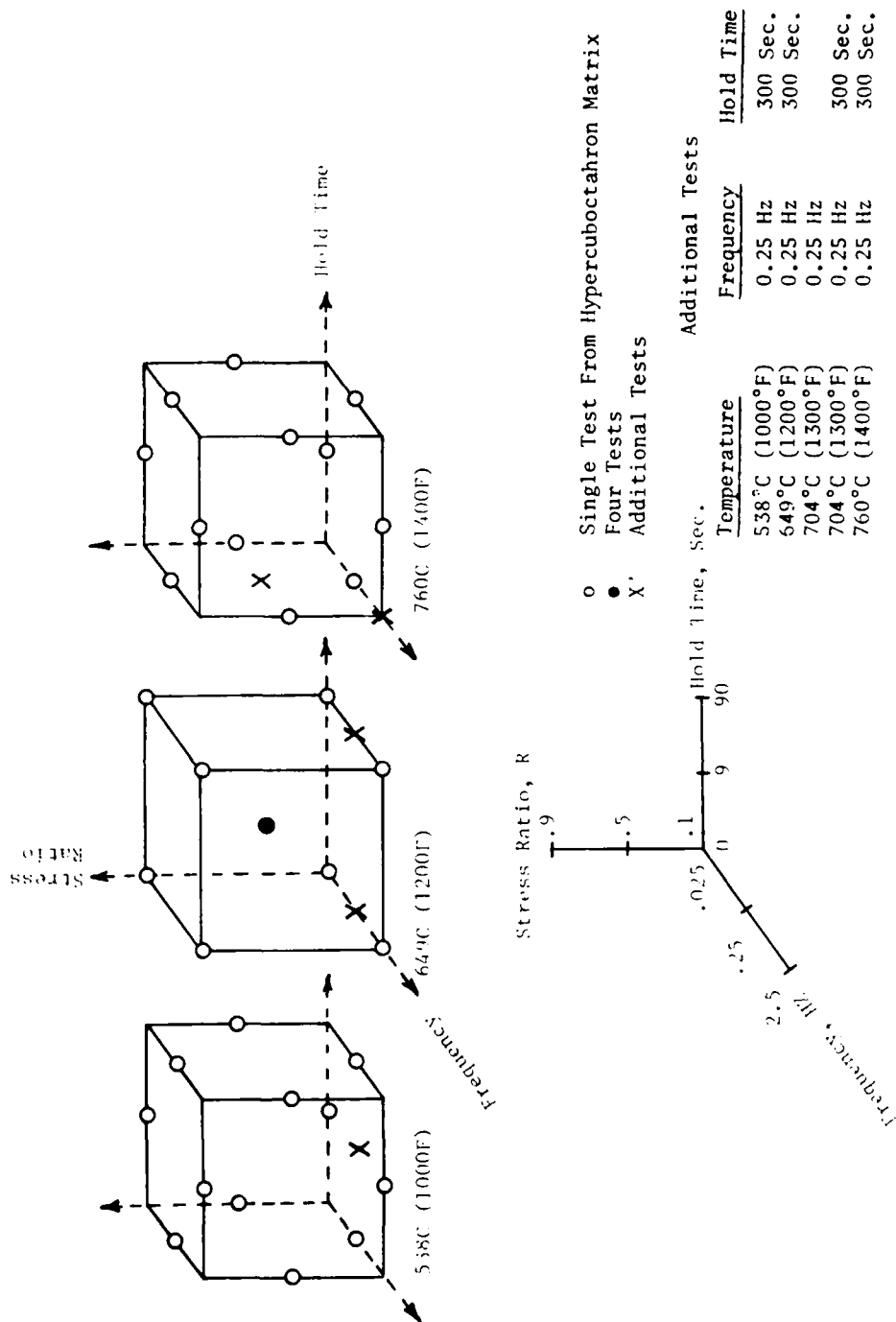


Figure 57. Illustration of Test Matrix Used In This Program

by four of the remaining six additional tests conducted to enhance the program, there was only a single set of conditions [760° C (1400° F), $R = 0.5$] in which three levels of frequency were examined. At this condition, a significant frequency effect was present. There was no single condition where three levels of hold time were conducted except at 538° C (1000° F) where hold time did not have an influence on crack growth behavior.

During the development of the model, because of voids in the matrix, approximations of crack growth behavior were required. At some conditions the approximations were obvious. For example the 9 second hold time, 760° C (1400° F), and 0.25 Hz point in Figure 26 was derived from the 2.5 and 0.025 Hz with 9 second hold period experimental results which produced essentially identical crack growth characteristics (see S/N 3-3 and 8-8 in Figure 18). Other conditions, especially at the center of the matrix, the approximations were more difficult and required consideration of two or more test variables. In hindsight, the approximations could have been simplified by a better selection of the ten extra test conditions.

2. Test Requirements for Model Development of a Similar Material

During the model development, a few observations were made and assumed valid. These observations, as listed below, will be considered applicable in establishing the recommendations for applying the interpolative model to similar materials.

1. The vertical location and slope of the inflection point was linearly related (logarithmic coordinates) to the length of hold time (see Figure 26).
2. The vertical location and slope of the inflection point for continuous cycling conditions was linearly related to frequency (see Figure 24) except for high stress ratio and temperature situations when blunting slowed down the crack growth.
3. For each temperature and stress ratio combination, the horizontal position of the inflection point was linearly related to its vertical position (Figure 23).
4. The vertical location and slope of the inflection point was related to $1-R$; however, for a given temperature and wave pattern, the location and slope will not exceed a saturation level (Figure 25 and 27).
5. The upper asymptote was related only to stress ratio (Equation 11).
6. The lower asymptote was related by the expression suggested by Klesnil and Lukas' (7). The constants were, however, a function of temperature (Figure 22).

The following minimal tests were required, using these assumptions, to apply the model to a similar material without the necessity of estimating crack growth behavior through the interactions between test variables, as required in this program. To determine the coefficients for the linear relationships (Equation 21) between the vertical location and slope of the inflection point, and the frequency for the continuous cycling conditions (as in Figure 24), two tests are required for each stress ratio and temperature combination. Considering three levels of stress ratio and temperature, this would require 18 tests. To evaluate the hold time damage factor as discussed in Section VI, B.4.6, the vertical location and slope of the inflection point are assumed linearly related to the length of hold time. Thus, two experiments are required to determine the relationship (Equations 24-26). Since these relationships will vary for each temperature, frequency, and stress ratio, a total of fifty-four tests are required when three levels of each variable are examined. For best results, conditions should be selected so that the tests produce both a large and small magnitude of hold time damage. By collecting the information for these two relationships, the other relationships between the test variables and coefficients are easily attainable. Thus, 72 tests are recommended.

If the tests were conducted in a systematic fashion, the number of tests could be reduced as results were accumulated. For example, in the case of AF 115 at the stress ratio of 0.1, there was not a frequency or hold time effect at 538° C (1000° F), or a frequency effect at 649° F (1200° F). In considering this, only three tests would be required at 538° C (1000° F), two frequencies and one hold time, rather than eight tests recommended above. At 649° C (1200° F), the number of tests could be reduced by three by examining only two frequencies and three hold periods.

Additional reduction in testing might be possible if additional assumptions are made. For example, at stress ratio of 0.1, the slope between the hold time damage factor and hold time might be constant as suggested in Figure 26. Another assumption might be that if the cyclic frequency could be considered insignificant for long hold time conditions, then only one frequency would be required with a long hold period. Near the creep regime, the data might be well correlated by da/dt rather than da/dN , thus reducing the number of test in the area. Each of these areas need further exploration to determine if and when these observations are valid.

Testing costs and time to acquire this information could be greatly reduced by the method proposed by Gangloff (24) in which the entire range of stress intensity normally found in compact tension specimens is acquired much faster in cylindrical bars with EDM notches. As an example, the efficiency of this approach can be made using the coefficients of the modified sigmoidal equation generated in this program for 649° C (1200° F), $R = 0.1$, 0125 Hz. With an initial crack growth rate of 1×10^5 mm/cycle (4×10^{-7} inch/cycle), the testing time in this surface flawed tensile bar would be reduced from 11 days down to 27 hours. Furthermore, material requirements can be reduced since the specimen material required for surface flawed tensile specimen is considerably less than the compact tension.

The purpose of this program was to develop an improved understanding of crack growth behavior of AF115 and to develop a method for predicting its behavior under turbine operating conditions. The quantity of data generated in this program were by no means sufficient for design purposes, especially since only a single heat of material was examined. Four heats of material might be considered the minimum acceptable quantity to be investigated before the retirement-for-cause concept could be considered for life management of AF115 or any other turbine disk material. Consideration must be given to the number of tests per independent variable. The manner in which the data are analyzed must be considered since it has been shown (18) to significantly impact the statistical confidence of the predicted properties. For example, the incremented sliding polynomial technique (as used in this program) produced different scatter than the Secant method which calculates the slope between each set of adjoining crack length versus cycles pairs. Surprisingly, the modified Secand method was found to introduce the least amount of variations into the growth rate data, even over more complex techniques. This method averages two adjacent crack growth rates, calculated by the Secant method, so that the growth rate data coincide with the original crack length versus cycle data.

X. CONCLUSIONS AND RECOMMENDATIONS

An interpolative model has been developed to determine crack growth behavior of AF115 under a wide range of test conditions typical of disk operating conditions. The following conclusion and recommendations are made from the observations generated during in the development of the model and verification of it.

1. The range of the test variable examined had a significant influence on crack growth behavior of AF115.
2. Linear-elastic-fracture mechanics can be used to predict crack growth behavior of a single geometry and limited load levels however, this has not been verified for other geometries.
3. The modified sigmoidal equation and its coefficients is capable of predicting the typical, non-symenetric crack growth rate curve for various test conditions by equating the coefficients to the test variables.
4. The scatter associated with cyclic crack growth rate testing is a factor of three or more at a stress ratio of 0.5, possible due to the use of the room-temperature precracking techniques for many of the experiments conducted within this program. It is recommended that future elevated temperatures crack growth rate testing be conducted with precracking conducted at elevated temperature with final conditions being at actual test conditions.
5. The possibility of error associated with the interplative model increases with increasing stress ratio. It is recommended that a statistical evaluation of the range of scatter of typical crack growth rate experimental results be evaluated.

REFERENCES

1. Bartos, J.L., "Development of a Very High Strength Disk Alloy for 1400⁰F Service", AFML-TR-74-187, General Electric Company, December, 1974.
2. Carlosn, D.M., "Advanced Superalloy Dual - Property Turbine Disk", Quarterly Reports 1 - 4, Contract Number F33615-77-C-5253
3. Redden, T.K. and Duvelius, L.T., "Mechanical Properties of As-Hip and Thermo-Mechanically Processed AF115 Alloy", TM79-351, General Electric Company, August, 1979.
4. Annual Book of ASTM Standards, Part 10 E467
5. Ibid, E399
6. Knaus, W.L., "A New Crack Growth Correlation", TM70-813, General Electric Company, October, 1970.
7. Klesnel, M. and Lukas, P., "Effect of Stress Cycle Asymmetry on Fatigue Crack Growth", Material Science Engineering, 1972, pp. 231-240.
8. Saxena, A., Hudak, S.J. and Jouris, J.M., "A three Component Model for Representing Wide Range Fatigue Crack Growth", Engineering Fracture Mechanics, Volume 12, pp. 103-115, 1979.
9. Wallace, R.M., Annes, C.G., and Sims, D.L., "Application of Fracture Mechanics of Elevated Temperature", AFML-TR-76-176, April, 1977.
10. Shahinian, P. and Sadananda, K. "Effects of Stress Ratio and Hold-Time on Fatigue Crack Growth in Alloy 718", Trans. ASME, Volume 101, July, 1979, pp. 224-230.
11. Shahani, V. and Popp, H.G., "Evaluation of Cyclic Behavior of Aircraft Turbine Disk Alloys", NASA-CR-159433, June, 1978.
12. Coles, A., Johnson, R.E., and Popp, H.G., "Utility of Surface-Flawed Tensile Bars in Cyclic Life Studies", Journal of Engineering Materials and Technology, Volume 98, pp. 305-315, October, 1976.
13. Clavel, M. and Pinlau, A., "Frequency and Wave-Form Effects on the Fatigue Crack Growth Behavior of Alloy 718 at 298K and 823K", Metallurgical Transaction, Volume 9A, pp. 471-480, April, 1978.

REFERENCES

14. Popp, H.G. and Coles, A., "Subcritical Crack Growth Criteria for Inconel 718 at Elevated Temperature", AFFDL-TR-70-144, Proceedings of the Air Force Conference on Fatigue and Fracture on Aircraft Structure and Materials, pp. 71-85, September, 1970.
15. Shahinian, P. and Sadananda, K., "Crack Growth Behavior Under Creep-Fatigue Conditions in Alloy 718", MPC-3, ASME, pp. 365-390.
16. Shahinian, P., "Fatigue Crack-Growth Characteristics of High-Temperature Alloys", Metals Technology, pp. 372-380, November, 1978.
17. Sadananda, K. and Shahinian, P., "A Fracture Mechanics Approach to High Temperature Fatigue Crack Growth in Udimet 700", Engineering Fracture Mechanics, Volume 11, pp. 73-86, 1979.
18. Verkler, D.A., Hillberry, B.M. and Goel, P.K. "The Statistical Nature of Fatigue Crack Propagation", Trans of ASME, Volume 101, pp. 148-153, April, 1979.
19. Clark, W.G. and Hudak, S.J., "Variability in Fatigue Crack Growth Rate Testing", Journal of Testing and Evaluation, JTEVA, Volume 3, No. 6, pp. 454-476, 1975.
20. Melk, W.J. and James, L.A., "The Fatigue-Crack Propagation Response of Two Nickel-Base Alloys in a Liquid Sodium Environment", Journal of Engineering Materials and Testing, Volume 101, pp. 205-213, July, 1979.
21. Landers, J.D. and Begley, "A Fracture Mechanics Approach to Creep Crack Growth", Mechanics of Crack Growth, ASTM STP 520, American Society for Testing and Materials, pp. 128-148, 1976.
22. Sadananda, K. and Shahinian P, "Creep Crack Growth in Alloy 718", Metallurgical Transaction, Volume 8A, pp. 439-449, March, 1977.
23. Hudak, et al, "Development of Standard Methods of Testing and Analysis Fatigue Crack Growth Rate Data", AFML-TR-78-40, May, 1978.
24. Gangloff, R.P. "Electric Potential Monitoring of Fatigue Crack Formation and Growth from Small Defects", General Electric Company, 79CRD267, January, 1980.

APPENDIX A

SPECIMEN NO. 3-1		SPECIMEN NO. 4-1		SPECIMEN NO. 4-5		SPECIMEN NO. 4-8	
DELK	DADN	DELK	DADN	DELK	DADN	DELK	DADN
9.94	0.4720000E-04	8.94	0.2130000E-02	18.08	0.1170000E-02	7.44	0.1080000E-02
10.17	0.5150000E-04	9.88	0.2940000E-02	18.24	0.1250000E-02	7.46	0.9690000E-06
10.47	0.5610000E-04	10.38	0.3290000E-02	18.52	0.1430000E-02	7.48	0.9200000E-06
11.22	0.6670000E-04	10.73	0.3500000E-02	18.83	0.1650000E-02	7.56	0.1260000E-05
11.53	0.6860000E-04	11.28	0.3960000E-02	19.07	0.1760000E-02	7.71	0.1580000E-05
11.72	0.6740000E-04	12.17	0.4760000E-02	19.47	0.1920000E-02	7.73	0.1520000E-05
11.99	0.6910000E-04	12.96	0.5450000E-02	19.80	0.2100000E-02	7.77	0.1400000E-05
12.20	0.6960000E-04	14.00	0.6160000E-02	20.25	0.2360000E-02	7.78	0.1400000E-05
12.46	0.7880000E-04	18.30	0.9140000E-02	20.76	0.2650000E-02	7.80	0.1300000E-05
12.63	0.8110000E-04	21.61	0.1070000E-01	21.97	0.3490000E-02	7.82	0.1480000E-05
12.86	0.8490000E-04	31.97	0.1340000E-01	22.72	0.3860000E-02	7.98	0.1450000E-05
13.34	0.9000000E-04	39.11	0.1430000E-01	23.60	0.4550000E-02	8.14	0.1340000E-05
13.59	0.9330000E-04			25.12	0.5480000E-02	8.22	0.1150000E-05
13.87	0.9840000E-04	SPECIMEN NO. 4-2		26.29	0.6150000E-02	8.26	0.1030000E-05
14.49	0.1100000E-03	DELK	DADN	27.52	0.6900000E-02	8.33	0.1150000E-05
15.21	0.1220000E-03			29.41	0.7660000E-02	8.53	0.2240000E-05
15.80	0.1270000E-03	7.56	0.1070000E-02	31.76	0.8720000E-02	8.61	0.1590000E-05
16.35	0.1330000E-03	7.65	0.1870000E-02	35.36	0.1010000E-01	8.64	0.1790000E-05
17.27	0.1410000E-03	7.75	0.2000000E-02	44.95	0.1370000E-01	8.68	0.1920000E-05
17.94	0.1320000E-03	7.85	0.2240000E-02	46.68	0.1680000E-01	8.93	0.2040000E-05
18.60	0.1350000E-03	7.98	0.2460000E-02	48.45	0.2130000E-01	9.19	0.2670000E-05
19.30	0.1430000E-03	8.12	0.2740000E-02	51.44	0.2400000E-01	9.23	0.2880000E-05
19.86	0.1590000E-03	8.27	0.2980000E-02	54.80	0.2630000E-01	9.29	0.2170000E-05
20.76	0.1750000E-03	8.64	0.3700000E-02			9.32	0.2170000E-05
22.01	0.2010000E-03	9.13	0.4690000E-02			9.36	0.2030000E-05
23.89	0.2340000E-03	9.64	0.6040000E-02	SPECIMEN NO. 4-6		9.39	0.2110000E-05
25.05	0.2470000E-03	10.90	0.7940000E-02	DELK	DADN	9.44	0.2050000E-05
27.57	0.2810000E-03	11.64	0.9410000E-02			9.46	0.1520000E-05
31.35	0.3400000E-03	12.66	0.1100000E-01			9.58	0.1850000E-05
		14.08	0.1320000E-01			9.72	0.2590000E-05
SPECIMEN NO. 3-3		16.24	0.1630000E-01			9.78	0.2740000E-05
DELK	DADN	18.13	0.1880000E-01	7.30	0.1000000E-06	9.84	0.2820000E-05
15.93	0.2680000E-03	19.85	0.2060000E-01	11.06	0.8290000E-05	9.92	0.3140000E-05
16.14	0.2870000E-03	23.45	0.2370000E-01	11.18	0.8800000E-05	9.99	0.2540000E-05
16.42	0.2920000E-03	26.74	0.2640000E-01	11.32	0.9240000E-05	10.05	0.2540000E-05
16.68	0.2540000E-03			11.46	0.9760000E-05	10.11	0.2770000E-05
16.75	0.2190000E-03	SPECIMEN NO. 4-3		11.78	0.1130000E-04		
16.89	0.1640000E-03	DELK	DADN	12.17	0.1310000E-04	SPECIMEN NO. 5-1	
17.26	0.1940000E-03			12.65	0.1550000E-04	DELK	DADN
17.97	0.3980000E-03	8.00	0.1000000E-06	13.25	0.1830000E-04		
18.21	0.4870000E-03	15.39	0.3550000E-05	14.04	0.2150000E-04	4.62	0.4680000E-05
18.61	0.5910000E-03	18.17	0.8060000E-05	15.08	0.2490000E-04	8.73	0.7890000E-05
19.05	0.6350000E-03	20.92	0.7800000E-05	16.45	0.2860000E-04	9.31	0.8110000E-05
19.64	0.7390000E-03	25.56	0.1170000E-04	17.30	0.3070000E-04	11.59	0.7580000E-05
20.09	0.7550000E-03	26.51	0.1550000E-04	18.29	0.3330000E-04	12.50	0.1800000E-04
20.67	0.7790000E-03	29.81	0.2390000E-04	19.45	0.3630000E-04	12.90	0.1000000E-03
21.16	0.8120000E-03	33.98	0.5800000E-04	20.91	0.4040000E-04		
21.97	0.8170000E-03	34.61	0.5940000E-04	22.78	0.4730000E-04		
22.84	0.8560000E-03	35.27	0.6170000E-04	25.40	0.5830000E-04		
23.81	0.9350000E-03	35.99	0.6390000E-04	25.79	0.7240000E-04		
25.62	0.1130000E-02	36.74	0.6610000E-04	29.51	0.9700000E-04		
27.63	0.1330000E-02	37.58	0.7020000E-04			SPECIMEN NO. 5-2	
30.13	0.1480000E-02	38.47	0.7680000E-04	SPECIMEN NO. 4-7		DELK	DADN
32.51	0.1640000E-02	39.52	0.8430000E-04	DELK	DADN	2.30	0.6070000E-03
35.44	0.1850000E-02	40.71	0.9550000E-04			2.35	0.6610000E-03
39.75	0.2020000E-02	42.19	0.1100000E-03	26.39	0.1120000E-04	2.41	0.7310000E-03
45.14	0.2120000E-02	44.05	0.1290000E-03	28.47	0.1240000E-04	2.48	0.7680000E-03
48.70	0.2110000E-02	46.41	0.1580000E-03	40.82	0.4080000E-04	2.53	0.7900000E-03
54.76	0.2240000E-02	47.86	0.1820000E-03	51.28	0.7830000E-04	2.57	0.8380000E-03
61.53	0.2360000E-02	49.69	0.2370000E-03	51.63	0.8220000E-04	2.64	0.9190000E-03
68.89	0.2440000E-02			52.37	0.1020000E-03	2.70	0.9640000E-03
75.46	0.2880000E-02			57.63	0.1710000E-03	2.85	0.1050000E-02
				58.16	0.1870000E-03	2.95	0.1130000E-02
SPECIMEN NO. 3-4		DELK	DADN	59.84	0.2020000E-03	3.06	0.1280000E-02
DELK	DADN	3.17	0.4090000E-03	61.66	0.2240000E-03	3.05	0.1230000E-02
7.12	0.3290000E-02	3.23	0.4450000E-03	62.79	0.2250000E-03	3.24	0.1440000E-02
7.22	0.3260000E-02	3.31	0.4540000E-03	64.26	0.2470000E-03	3.32	0.1500000E-02
7.40	0.3540000E-02	3.45	0.5080000E-03	70.95	0.3460000E-03	3.48	0.1530000E-02
7.59	0.3580000E-02	3.61	0.5460000E-03	72.24	0.4540000E-03	3.67	0.1580000E-02
7.79	0.3540000E-02	3.78	0.5800000E-03	73.05	0.5460000E-03	3.94	0.1660000E-02
8.01	0.5320000E-02	4.08	0.6170000E-03	73.78	0.6090000E-03	4.14	0.1790000E-02
8.22	0.4910000E-02	4.34	0.6510000E-03	74.85	0.6040000E-03	4.56	0.2160000E-02
8.41	0.4440000E-02	4.53	0.6830000E-03	75.91	0.6040000E-03	4.87	0.2430000E-02
8.57	0.4390000E-02	4.81	0.7260000E-03	76.76	0.5610000E-03	5.35	0.2610000E-02
8.74	0.4790000E-02	5.32	0.8160000E-03	78.03	0.4740000E-03	5.68	0.2750000E-02
8.96	0.5210000E-02	5.91	0.8840000E-03	78.12	0.4910000E-03	6.29	0.2710000E-02
9.25	0.5600000E-02	6.55	0.9030000E-03	82.06	0.6540000E-03	7.00	0.2700000E-02
9.55	0.5990000E-02	7.30	0.9460000E-03	85.02	0.8990000E-03	7.66	0.2670000E-02
10.20	0.6040000E-02	8.02	0.9760000E-03	87.48	0.1100000E-02	8.64	0.2740000E-02
10.54	0.6340000E-02			90.72	0.1330000E-02	9.34	0.2890000E-02
10.89	0.7820000E-02			94.61	0.1830000E-02	10.12	0.2880000E-02
11.31	0.9540000E-02			96.62	0.1980000E-02		
12.08	0.1220000E-01						

* CRACK LENGTH VS. CYCLE NUMBER CURVES WERE ESTIMATED THROUGH THE EXISTING DATA POINTS AND ADDITIONAL POINTS EXTRACTED FROM THAT CURVE.

SPECIMEN NO. 5-3 *

DELK	DADN
10.33	0.2570000E-05
11.67	0.3360000E-05
13.24	0.3910000E-05
14.89	0.5500000E-05
16.97	0.8800000E-05
19.32	0.1140000E-04
21.70	0.2040000E-04
26.42	0.2500000E-04
30.20	0.4270000E-04
30.63	0.4540000E-04
31.09	0.4770000E-04
31.58	0.4950000E-04
32.10	0.5250000E-04
32.64	0.5700000E-04
33.26	0.6290000E-04
34.00	0.7070000E-04
34.85	0.8210000E-04
35.91	0.9550000E-04
37.16	0.1150000E-03
38.72	0.1460000E-03
40.89	0.2050000E-03
44.36	0.4600000E-03

SPECIMEN NO. 5-5

DELK	DADN
17.06	0.7710000E-02
17.83	0.9250000E-02
18.83	0.1100000E-01
19.74	0.1350000E-01
20.13	0.1450000E-01
20.57	0.1500000E-01
21.07	0.1550000E-01
21.51	0.1650000E-01
22.07	0.1800000E-01
22.70	0.2020000E-01
23.47	0.2200000E-01
24.45	0.2270000E-01
25.45	0.2300000E-01
26.40	0.2280000E-01
27.42	0.2420000E-01
28.55	0.2590000E-01
29.98	0.2950000E-01
31.95	0.3350000E-01
34.30	0.3710000E-01
37.20	0.4180000E-01
40.88	0.4820000E-01
46.20	0.5540000E-01
53.83	0.6480000E-01
66.68	0.7350000E-01
85.68	0.8500000E-01

SPECIMEN NO. 5-6

DELK	DADN
21.16	0.1100000E-04
21.88	0.1230000E-04
22.76	0.1380000E-04
23.80	0.1570000E-04
25.10	0.1840000E-04
26.79	0.2350000E-04
27.87	0.2890000E-04
29.34	0.3760000E-04
31.50	0.5040000E-04
33.82	0.6310000E-04
37.37	0.8200000E-04
42.13	0.1080000E-03
47.10	0.1330000E-03
50.33	0.1520000E-03
54.71	0.1790000E-03
66.06	0.2000000E-03
81.40	0.3300000E-03

SPECIMEN NO. 5-7

DELK	DADN
9.89	0.6530000E-04
10.01	0.4820000E-04
10.06	0.3750000E-04
10.06	0.4150000E-04
10.12	0.5090000E-04
10.21	0.6510000E-04
10.57	0.1170000E-03
10.93	0.1400000E-03
11.13	0.1450000E-03
11.34	0.1500000E-03
11.43	0.1560000E-03
11.58	0.1660000E-03
12.00	0.1900000E-03
12.48	0.1970000E-03
12.62	0.1940000E-03
12.84	0.2040000E-03
13.17	0.2010000E-03
13.53	0.2170000E-03
14.06	0.2520000E-03
14.84	0.3050000E-03
15.39	0.3300000E-03
15.74	0.3490000E-03
18.45	0.4710000E-03
19.38	0.5320000E-03
19.72	0.5720000E-03
20.76	0.6320000E-03
22.55	0.7600000E-03
23.64	0.8330000E-03
27.63	0.1180000E-02
30.26	0.1420000E-02
34.48	0.1590000E-02

SPECIMEN NO. 5-8

DELK	DADN
18.04	0.4220000E-05
18.92	0.5020000E-05
19.52	0.5550000E-05
20.68	0.6420000E-05
21.89	0.7430000E-05
23.58	0.8600000E-05
24.45	0.9590000E-05
24.91	0.1080000E-04
25.38	0.1150000E-04
25.85	0.1190000E-04
26.48	0.1320000E-04
28.07	0.1640000E-04
30.09	0.2160000E-04
43.90	0.4500000E-04

SPECIMEN NO. 7-4

DELK	DADN
19.65	0.4700000E-02
22.09	0.6000000E-02
23.34	0.8000000E-02
24.46	0.9140000E-02
26.26	0.1040000E-01
28.97	0.1220000E-01
32.72	0.1440000E-01
38.45	0.1710000E-01
47.89	0.2070000E-01
53.39	0.2240000E-01
66.41	0.2180000E-01
78.18	0.2750000E-01

SPECIMEN NO. 7-8

DELK	DADN
10.19	0.3650000E-02
10.37	0.3740000E-02
10.57	0.3740000E-02
10.77	0.3130000E-02
10.87	0.2770000E-02
10.97	0.2540000E-02
11.32	0.2840000E-02
11.55	0.3290000E-02
12.03	0.3820000E-02
12.44	0.3950000E-02
12.73	0.4030000E-02
13.18	0.4530000E-02
13.81	0.5280000E-02
14.50	0.6520000E-02
15.12	0.7710000E-02
15.52	0.8190000E-02
16.27	0.8840000E-02
17.23	0.9540000E-02
18.13	0.1060000E-01
19.29	0.1160000E-01
21.21	0.1300000E-01
23.85	0.1470000E-01
26.56	0.1610000E-01
29.92	0.1870000E-01
34.96	0.2360000E-01
37.33	0.2490000E-01
40.30	0.2550000E-01
44.50	0.2530000E-01
48.41	0.2280000E-01

SPECIMEN NO. 8-1 *

DELK	DADN
18.02	0.1590000E-05
18.24	0.1980000E-05
18.51	0.2340000E-05
18.83	0.2740000E-05
19.23	0.3160000E-05
19.69	0.3510000E-05
20.20	0.3980000E-05
20.81	0.4560000E-05
21.55	0.5310000E-05
22.46	0.6260000E-05
23.62	0.7620000E-05
25.16	0.9910000E-05
27.43	0.1380000E-04
31.61	0.2280000E-04
36.84	0.3700000E-04
45.38	0.6490000E-04

SPECIMEN NO. 8-3

DELK	DADN
20.52	0.1220000E-03
20.88	0.1300000E-03
21.30	0.1430000E-03
21.78	0.1640000E-03
22.37	0.1890000E-03
23.05	0.2310000E-03
23.96	0.2970000E-03
24.53	0.3560000E-03
25.27	0.4340000E-03
25.79	0.5320000E-03
26.37	0.4090000E-03
26.32	0.5320000E-03
27.80	0.6990000E-03
28.14	0.7270000E-03
28.85	0.7860000E-03
32.20	0.1150000E-02
32.60	0.1040000E-02
32.60	0.1080000E-02
34.70	0.1200000E-02
37.60	0.1380000E-02
38.48	0.1900000E-02
41.72	0.2910000E-02
42.93	0.3410000E-02
45.64	0.4280000E-02
53.22	0.6110000E-02
58.87	0.6670000E-02
65.60	0.9140000E-02

SPECIMEN NO. 8-4

DELK	DADN
19.32	0.3790000E-05
19.47	0.3830000E-05
19.59	0.3760000E-05
19.68	0.4200000E-05
19.81	0.4410000E-05
20.14	0.5170000E-05
20.31	0.5250000E-05
20.69	0.5460000E-05
21.91	0.6350000E-05
23.45	0.7620000E-05
24.54	0.8490000E-05
24.67	0.9180000E-05
24.99	0.7830000E-05
25.14	0.8270000E-05
25.21	0.7730000E-05
25.50	0.8490000E-05
26.73	0.1120000E-04
26.98	0.1130000E-04
27.35	0.1180000E-04
27.78	0.1220000E-04
28.27	0.1270000E-04
29.10	0.1380000E-04
31.22	0.1690000E-04
32.07	0.1770000E-04
32.64	0.1970000E-04
33.51	0.2170000E-04
34.09	0.2250000E-04
35.21	0.2580000E-04
36.32	0.2950000E-04
37.30	0.3230000E-04
38.05	0.3620000E-04
39.58	0.4270000E-04
40.95	0.4870000E-04
43.99	0.6140000E-04
45.20	0.7050000E-04
45.49	0.7420000E-04
46.86	0.8250000E-04
48.20	0.9800000E-04
50.51	0.1220000E-03
53.53	0.1600000E-03
55.39	0.1770000E-03
56.48	0.1940000E-03
59.36	0.2270000E-03
61.58	0.2830000E-03
65.38	0.4050000E-03
67.10	0.5220000E-03
69.61	0.6480000E-03

* CRACK LENGTH VS. CYCLE NUMBER CURVES WERE ESTIMATED THROUGH THE EXISTING DATA POINTS AND ADDITIONAL POINTS EXTRACTED FROM THAT CURVE.

SPECIMEN NO. 8-5		SPECIMEN NO. 8-8		SPECIMEN NO. 9-4		SPECIMEN NO. 9-8	
DELK	DADN	DELK	DADN	DELK	DADN	DELK	DADN
7.50	0.1000000E-05	16.27	0.3550000E-03	17.61	0.2380000E-05	10.35	0.1890000E-05
11.11	0.1940000E-04	16.64	0.3480000E-03	17.75	0.2510000E-05	10.90	0.2840000E-05
11.49	0.2170000E-04	16.91	0.4150000E-03	17.89	0.2980000E-05	11.25	0.4100000E-05
11.67	0.2490000E-04	17.22	0.4390000E-03	18.21	0.3380000E-05	11.33	0.9230000E-05
11.79	0.2380000E-04	17.47	0.4520000E-03	18.57	0.3740000E-05	11.53	0.9570000E-05
11.92	0.2340000E-04	17.96	0.4640000E-03	18.96	0.4140000E-05	11.89	0.1010000E-04
12.09	0.2460000E-04	18.34	0.4810000E-03	19.42	0.4660000E-05	11.93	0.9390000E-05
12.29	0.2370000E-04	18.71	0.5020000E-03	19.96	0.5250000E-05	12.22	0.7810000E-05
12.45	0.2560000E-04	19.13	0.5280000E-03	20.59	0.5960000E-05	12.31	0.8040000E-05
12.63	0.2830000E-04	19.74	0.6150000E-03	21.37	0.6800000E-05	12.43	0.6290000E-05
12.75	0.2840000E-04	20.36	0.6240000E-03	22.31	0.7760000E-05	12.58	0.6400000E-05
12.89	0.2950000E-04	20.91	0.6790000E-03	23.47	0.8950000E-05	12.78	0.7060000E-05
13.00	0.3010000E-04	21.63	0.7140000E-03	24.15	0.1030000E-04	13.10	0.8660000E-05
13.17	0.3230000E-04	22.45	0.7360000E-03	24.95	0.1240000E-04	13.53	0.9810000E-05
13.29	0.3370000E-04	23.02	0.7830000E-03	25.88	0.1570000E-04	14.04	0.1060000E-04
13.47	0.3420000E-04	23.81	0.8350000E-03	27.24	0.2190000E-04	14.35	0.1080000E-04
13.58	0.3430000E-04	25.04	0.9810000E-03	29.57	0.3250000E-04	14.81	0.1130000E-04
13.65	0.3430000E-04	27.98	0.1330000E-02	34.06	0.5410000E-04	15.22	0.1190000E-04
13.75	0.3310000E-04	32.10	0.1730000E-02	45.27	0.8540000E-04	16.34	0.1270000E-04
13.86	0.3450000E-04	36.67	0.2040000E-02			17.23	0.1310000E-04
13.96	0.3600000E-04	44.39	0.2440000E-02			17.53	0.1430000E-04
14.15	0.4000000E-04	52.35	0.2740000E-02			17.87	0.1500000E-04
14.41	0.4160000E-04	62.70	0.3300000E-02			17.99	0.1870000E-04
14.71	0.4070000E-04	72.93	0.3990000E-02			18.26	0.2060000E-04
14.90	0.4010000E-04					18.63	0.2200000E-04
15.13	0.3920000E-04					18.96	0.2130000E-04
15.18	0.4120000E-04					19.32	0.1990000E-04
15.39	0.4550000E-04					19.97	0.1480000E-04
15.55	0.4700000E-04					20.09	0.1670000E-04
15.76	0.4440000E-04					20.74	0.1740000E-04
15.96	0.4620000E-04					20.98	0.2080000E-04
16.16	0.4780000E-04					21.40	0.2190000E-04
16.66	0.5620000E-04					21.96	0.2480000E-04
17.15	0.6460000E-04					22.38	0.2550000E-04
18.32	0.8160000E-04					23.21	0.2700000E-04
19.10	0.9140000E-04					24.18	0.2790000E-04
19.84	0.1050000E-03					25.39	0.3050000E-04
20.68	0.1170000E-03					25.81	0.3450000E-04
21.12	0.1260000E-03					27.56	0.3840000E-04
22.14	0.1430000E-03					28.58	0.4300000E-04
22.88	0.1860000E-03					28.97	0.4470000E-04
25.32	0.2480000E-03					31.95	0.6350000E-04
29.17	0.3570000E-03					33.23	0.8580000E-04
SPECIMEN NO. 8-6		SPECIMEN NO. 9-1		SPECIMEN NO. 9-7		SPECIMEN NO. 10-1	
DELK	DADN	DELK	DADN	DELK	DADN	DELK	DADN
4.00	0.3800000E-03	16.44	0.2740000E-04	25.24	0.2060000E-03	7.44	0.1080000E-05
4.09	0.4580000E-03	16.49	0.2920000E-04	25.49	0.1890000E-03	7.46	0.9690000E-06
4.16	0.4630000E-03	16.85	0.2870000E-04	25.69	0.2020000E-03	7.48	0.9200000E-06
4.20	0.5850000E-03	16.98	0.2730000E-04	25.89	0.1810000E-03	7.56	0.1260000E-05
4.27	0.6380000E-03	17.40	0.3450000E-04	26.51	0.2120000E-03	7.71	0.1580000E-05
4.45	0.7390000E-03	17.48	0.3630000E-04	27.88	0.2680000E-03	7.73	0.1520000E-05
4.56	0.8490000E-03	17.64	0.4050000E-04	28.15	0.2860000E-03	7.77	0.1400000E-05
4.78	0.9650000E-03	18.41	0.5730000E-04	29.52	0.3100000E-03	7.78	0.1400000E-05
5.12	0.9560000E-03	19.00	0.7020000E-04	29.20	0.3080000E-03	7.80	0.1300000E-05
5.31	0.9350000E-03	20.05	0.8890000E-04	30.01	0.4300000E-03	7.82	0.1480000E-05
5.51	0.1080000E-02	20.25	0.9840000E-04	30.47	0.4460000E-03	7.98	0.1450000E-05
5.95	0.1310000E-02	20.62	0.1080000E-03	30.99	0.4860000E-03	8.14	0.1340000E-05
		20.94	0.1090000E-03	31.58	0.5190000E-03	8.20	0.1150000E-05
		23.71	0.1800000E-03	32.36	0.5650000E-03	8.22	0.1230000E-05
		25.70	0.2330000E-03	33.74	0.6210000E-03	8.26	0.1030000E-05
		26.88	0.2720000E-03	34.82	0.6560000E-03	8.33	0.1150000E-05
		27.87	0.3640000E-03	35.78	0.7610000E-03	8.53	0.2240000E-05
		30.63	0.5330000E-03	37.37	0.8610000E-03	8.61	0.1590000E-05
		35.42	0.9020000E-03	38.65	0.9400000E-03	8.64	0.1790000E-05
		45.74	0.1470000E-02	39.83	0.1000000E-02	8.68	0.1920000E-05
SPECIMEN NO. 9-3		SPECIMEN NO. 9-3		SPECIMEN NO. 9-3		SPECIMEN NO. 9-3	
DELK	DADN	DELK	DADN	DELK	DADN	DELK	DADN
18.02	0.1906000E-04	18.02	0.1906000E-04	47.39	0.1740000E-02	9.19	0.2670000E-05
18.22	0.2190000E-04	18.22	0.2190000E-04	48.82	0.2000000E-02	9.23	0.2880000E-05
18.48	0.2580000E-04	18.48	0.2580000E-04	50.38	0.2130000E-02	9.29	0.2170000E-05
19.20	0.2670000E-04	19.20	0.2670000E-04	52.59	0.2270000E-02	9.32	0.2170000E-05
19.48	0.2690000E-04	19.48	0.2690000E-04	54.71	0.2280000E-02	9.36	0.2030000E-05
20.08	0.2930000E-04	20.08	0.2930000E-04	56.21	0.2260000E-02	9.39	0.2110000E-05
20.65	0.3230000E-04	20.65	0.3230000E-04	57.80	0.2310000E-02	9.44	0.2050000E-05
20.81	0.3180000E-04	20.81	0.3180000E-04	60.19	0.2580000E-02	9.46	0.1520000E-05
21.14	0.3330000E-04	21.14	0.3330000E-04	62.84	0.3220000E-02	9.58	0.1850000E-05
21.54	0.3450000E-04	21.54	0.3450000E-04	65.77	0.3940000E-02	9.72	0.2590000E-05
22.03	0.3700000E-04	22.03	0.3700000E-04	68.82	0.4290000E-02	9.78	0.2740000E-05
22.42	0.4440000E-04	22.42	0.4440000E-04	71.73	0.4850000E-02	9.84	0.2820000E-05
23.27	0.4810000E-04	23.27	0.4810000E-04	74.12	0.5030000E-02	9.92	0.3140000E-05
24.44	0.4940000E-04	24.44	0.4940000E-04	77.72	0.5110000E-02	9.99	0.2540000E-05
25.29	0.4730000E-04	25.29	0.4730000E-04	80.29	0.4820000E-02	10.05	0.2540000E-05
26.37	0.4390000E-04	26.37	0.4390000E-04			10.11	0.2770000E-05
27.01	0.4490000E-04	27.01	0.4490000E-04				
27.57	0.4530000E-04	27.57	0.4530000E-04				
28.77	0.5530000E-04	28.77	0.5530000E-04				
30.10	0.7370000E-04	30.10	0.7370000E-04				
35.28	0.1540000E-03	35.28	0.1540000E-03				
38.78	0.2070000E-03	38.78	0.2070000E-03				
42.67	0.2810000E-03	42.67	0.2810000E-03				
49.95	0.3590000E-03	49.95	0.3590000E-03				
54.80	0.4610000E-03	54.80	0.4610000E-03				
62.80	0.6000000E-03	62.80	0.6000000E-03				
77.10	0.8540000E-03	77.10	0.8540000E-03				
83.10	0.1800000E-02	83.10	0.1800000E-02				

* CRACK LENGTH VS. CYCLE NUMBER CURVES WERE ESTIMATED THROUGH THE EXISTING DATA POINTS AND ADDITIONAL POINTS EXTRACTED FROM THAT CURVE.

BLK	DADN
19.52	0.5000000E-05
21.89	0.7400000E-05
35.59	0.2500000E-04
40.57	0.5300000E-04
41.50	0.5718000E-04
42.55	0.6250000E-04
43.75	0.6840000E-04
45.14	0.8130000E-04
46.89	0.9530000E-04
49.12	0.1160000E-03
50.98	0.1390000E-03
53.42	0.1680000E-03
56.65	0.2120000E-03
61.43	0.2870000E-03
64.93	0.3620000E-03
70.08	0.4930000E-03
74.73	0.8270000E-03

DELK	DADN
3.22	0.1250000E-03
3.24	0.1310000E-03
3.29	0.1290000E-03
3.33	0.1390000E-03
3.36	0.1210000E-03
3.40	0.1220000E-03
3.41	0.1110000E-03
3.47	0.1070000E-03
3.51	0.1148000E-03
3.54	0.1090000E-03
3.56	0.1030000E-03
3.62	0.1090000E-03
3.67	0.1100000E-03
3.71	0.1130000E-03
3.76	0.1200000E-03
3.78	0.1320000E-03
3.87	0.1720000E-03
3.88	0.7500000E-03

DELK	DADM
11.06	0.7180000E-05
11.12	0.7380000E-05
11.17	0.7400000E-05
11.28	0.7990000E-05
11.41	0.8780000E-05
11.55	0.9820000E-05
11.71	0.1090000E-04
11.90	0.1260000E-04
12.11	0.1300000E-04
12.34	0.1400000E-04
12.59	0.1500000E-04
12.88	0.1590000E-04
13.19	0.1690000E-04
13.52	0.1770000E-04
13.90	0.1850000E-04
14.09	0.1900000E-04
14.30	0.1930000E-04
14.52	0.1950000E-04

BEK	BAW
15.48	0.4583000E-05
15.65	0.5110000E-05
15.94	0.5270000E-05
16.22	0.5690000E-05
16.33	0.6140000E-05
16.90	0.6380000E-05
17.43	0.7070000E-05
17.90	0.7540000E-05
18.69	0.8060000E-05
19.63	0.9240000E-05
20.81	0.1100000E-04
22.66	0.1360000E-04
24.13	0.1610000E-04
25.13	0.1720000E-04
27.18	0.2030000E-04
29.08	0.2470000E-04
30.51	0.2910000E-04
31.87	0.3240000E-04
33.37	0.3990000E-04
35.57	0.4770000E-04
38.56	0.6150000E-04
43.16	0.1050000E-03
55.62	0.1960000E-03

DELK	DADN
18.06	0.2426000E-05
18.45	0.2580000E-05
18.80	0.2937000E-05
21.35	0.4000000E-05
25.02	0.8000000E-05
29.86	0.1180000E-04
30.21	0.1320000E-04
30.60	0.1390000E-04
34.20	0.2720000E-04
37.08	0.3000000E-04
38.06	0.3240000E-04
39.16	0.3530000E-04
40.42	0.3860000E-04
41.88	0.4290000E-04
43.62	0.4890000E-04
45.79	0.5770000E-04
47.12	0.6580000E-04
48.78	0.7930000E-04
49.53	0.9220000E-04
50.46	0.1080000E-03
51.62	0.1220000E-03
53.03	0.1440000E-03
54.79	0.1690000E-03
56.93	0.2040000E-03
59.72	0.2480000E-03
63.17	0.3270000E-03
68.70	0.4480000E-03

DELK	DADM
18.64	0.3820000E-05
19.23	0.4680000E-05
20.01	0.5510000E-05
20.83	0.6040000E-05
21.80	0.6820000E-05
22.99	0.7790000E-05
24.43	0.9360000E-05
26.50	0.1170000E-04
29.61	0.1560000E-04
35.48	0.2400000E-04

DELK	DADN
1.76	0.2460000E-02
1.84	0.3240000E-02
1.89	0.3780000E-02
1.95	0.4370000E-02
2.01	0.4850000E-02
2.07	0.5270000E-02
2.14	0.5810000E-02
2.22	0.6390000E-02
2.32	0.7240000E-02
2.44	0.8090000E-02
2.58	0.9260000E-02
2.75	0.1130000E-01
3.04	0.1310000E-01
3.41	0.1500000E-01
4.01	0.1920000E-01

DELK	DAIN
25.75	0.1080000E-04
28.98	0.2120000E-04
29.60	0.2290000E-04
29.85	0.2480000E-04
30.13	0.2660000E-04
30.34	0.2820000E-04
30.60	0.2930000E-04
30.72	0.3000000E-04
31.07	0.2710000E-04
31.26	0.2810000E-04
32.27	0.3250000E-04
32.53	0.3850000E-04
32.96	0.4178000E-04
33.51	0.4540000E-04
34.16	0.4930000E-04
35.01	0.5710000E-04
35.34	0.5740000E-04
35.66	0.5790000E-04
36.07	0.6070000E-04
38.01	0.7000000E-04
40.55	0.8440000E-04
43.97	0.1140000E-03
49.64	0.1940000E-03
54.82	0.3210000E-03

DELK	DADM
6.07	0.3330000E-04
6.07	0.1450000E-05
6.07	0.1360000E-05
6.10	0.2140000E-05
6.11	0.2380000E-05
6.13	0.2720000E-05
6.18	0.3440000E-05
6.20	0.4420000E-05
6.32	0.4490000E-05
6.35	0.4380000E-05
6.38	0.4630000E-05
6.39	0.6190000E-05
6.41	0.6480000E-05
6.39	0.9200000E-05
6.51	0.6270000E-05
6.53	0.5400000E-05
6.57	0.3240000E-05
6.59	0.2060000E-05
6.73	0.2170000E-05
6.85	0.2450000E-05
6.86	0.2580000E-05
6.88	0.2000000E-05
6.89	0.2140000E-05
6.90	0.2800000E-05
6.91	0.2120000E-05
8.86	0.1007000E-04
8.93	0.1056000E-04

APPENDIX B

PRECRACKING CONDITIONS
 SPEC NO. 3-3
 INIT. TEMP.= 70 F INIT. LOAD= 0 LBS INIT. STRESS RATIO= .03
 FINAL TEMP.= 70 F FINAL LOAD= 0 LBS FINAL STRESS RATIO= .03
 NO. OF INCREMENTS 0
 FINAL SIZE LT. SIDE= .101 RT. SIDE= .015

NO. POINTS= 25
 PMIN .053 KIPS PHAX= 2.053 KIPS R= .0258159
 TEMP.= 1400 F ENVIRONMENT=AIR
 SPECIMEN:CT B= .4985 IN. W= 2

OBS NO.	CYCLES	A (MEAS.)	REMARKS
1	50	.599	
2	100	.600	
3	200	.601	
4	400	.604	
5	1000	.610	
6	2000	.621	
7	3000	.633	
8	4000	.645	
9	5000	.659	
10	6000	.673	
11	8000	.703	
12	10000	.734	
13	12000	.767	
14	14000	.809	
15	16000	.859	
16	18000	.919	
17	20000	.986	
18	22000	1.067	
19	23000	1.133	
20	23500	1.182	
21	24000	1.249	
22	24300	1.302	
23	24500	1.359	
24	24700	1.424	
25	24797	1.475	

PRECRACKING CONDITIONS
 SPEC NO. 4-2
 INIT. TEMP.= 1200 F INIT. LOAD= 1800 LBS INIT. STRESS RATIO= .5
 FINAL TEMP.= 1200 F FINAL LOAD= 4000 LBS FINAL STRESS RATIO= .5
 NO. OF INCREMENTS 5
 FINAL SIZE LT. SIDE= .216 RT. SIDE= .225

NO. POINTS= 21
 PMIN .75 KIPS PHAX= 1.5 KIPS R= .5
 TEMP.= 1400 F ENVIRONMENT=AIR
 SPECIMEN:CT B= .502 IN. W= 2.002

OBS NO.	CYCLES	A (MEAS.)	REMARKS
1	0	.739	
2	23	.763	
3	43	.801	
4	50	.821	
5	55	.837	
6	59	.839	
7	66	.865	
8	71	.884	
9	77	.909	
10	83	.947	
11	86	.983	
12	89	1.004	
13	94	1.047	
14	98	1.088	
15	104	1.138	
16	108	1.175	
17	111	1.229	
18	115	1.321	
19	118	1.364	
20	121	1.450	

PRECRACKING CONDITIONS
 SPEC NO. 4-1
 INIT. TEMP.= 70 F INIT. LOAD= 0 LBS INIT. STRESS RATIO= .5
 FINAL TEMP.= 70 F FINAL LOAD= 0 LBS FINAL STRESS RATIO= .5
 NO. OF INCREMENTS 0
 FINAL SIZE LT. SIDE= .259 RT. SIDE= .244

NO. POINTS= 18
 PMIN .7 KIPS PHAX= 1.4 KIPS R= .5
 TEMP.= 1400 F ENVIRONMENT=AIR
 SPECIMEN:CT B= .494 IN. W= 2.002

OBS NO.	CYCLES	A (MEAS.)	REMARKS
1	0	.817	
2	82	.854	
3	99	.880	
4	113	.906	
5	140	.982	
6	150	1.006	
7	156	1.018	
8	165	1.063	
9	175	1.100	
10	182	1.133	
11	190	1.179	
12	207	1.292	
13	214	1.163	
14	225	1.487	
15	229	1.354	
16	231	1.382	
17	234	1.420	
18	237	1.670	exceeds ASTM crack length requirement

PRECRACKING CONDITIONS

SPEC NO. 4-3
INIT. TEMP. = 70 F INIT. LOAD = 0 LBS INIT. STRESS RATIO = .5
FINAL TEMP. = 70 F FINAL LOAD = 0 LBS FINAL STRESS RATIO = .5
NO. OF INCREMENTS 0
FINAL SIZE LT. SIDE = .272 RT. SIDE = .194

NO. POINTS = 30
PMIN 1.5 KIPS PMAX = 3 KIPS R = .5
TEMP. = 1000 F ENVIRONMENT = AIR
SPECIMEN:CT B = .496 IN. U = 2

OBS NO.	CYCLES	A (REAS.)	REMARKS
1	0	.782	
2	50	.782	
3	500	.782	
4	1470	.785	
5	3131	.794	
6	4405	.806	
7	4458	.804	
8	4705	.808	
9	4787	.808	
10	5145	.808	
11	5407	.808	
12	5514	.813	
13	5609	.815	
14	5754	.816	
15	5820	.817	
16	6128	.817	
17	6346	.817	
18	6456	.819	
19	6560	.819	
20	6676	.823	
21	6751	.823	
22	8050	.827	
23	8285	.827	
24	8356	.828	
25	8617	.831	
26	8645	.831	
27	8984	.832	
28	9187	.832	
29	9335	.834	
30	9369	.834	

NO. POINTS = 17
PMIN 1.65 KIPS PMAX = 3.3 KIPS R = .5
TEMP. = 1000 F ENVIRONMENT = AIR
SPECIMEN:CT B = .496 IN. U = 2

OBS NO.	CYCLES	A (REAS.)	REMARKS
1	0	.834	
2	8	.835	
3	43	.836	
4	133	.837	
5	192	.837	
6	220	.837	
7	255	.837	
8	894	.840	
9	1080	.842	
10	1130	.842	
11	1866	.849	
12	1957	.851	
13	2131	.853	
14	2483	.853	
15	2760	.853	
16	2875	.857	
17	2918	.857	

NO. POINTS = 17
PMIN 1.815 KIPS PMAX = 3.63 KIPS R = .5
TEMP. = 1000 F ENVIRONMENT = AIR
SPECIMEN:CT B = .496 IN. U = 2

OBS NO.	CYCLES	A (REAS.)	REMARKS
1	0	.858	
2	31	.858	
3	48	.861	
4	134	.861	
5	160	.861	
6	214	.862	
7	563	.863	
8	701	.863	
9	847	.866	
10	917	.866	
11	989	.868	
12	1096	.869	
13	1146	.869	
14	2417	.875	
15	2545	.878	
16	2630	.879	
17	2770	.880	

NO. POINTS= 12
 PMIN 1.997 KIPS PMAX= 3.993 KIPS R= .5001252

TEMP.= 1000 F ENVIRONMENT=AIR
 SPECIMEN:CT B= .496 IN. U= 2

OBS NO.	CYCLES	A (REAS.)	REMARKS
1	0	.080	
2	4	.080	
3	48	.081	
4	214	.082	
5	292	.083	
6	405	.084	
7	442	.087	
8	708	.088	
9	876	.089	
10	977	.090	
11	1105	.093	
12	1227	.093	

NO. POINTS= 19
 PMIN 2.197 KIPS PMAX= 4.392 KIPS R= .5002277

TEMP.= 1000 F ENVIRONMENT=AIR
 SPECIMEN:CT B= .496 IN. U= 2

OBS NO.	CYCLES	A (REAS.)	REMARKS
1	0	.959	
2	25	.963	
3	314	.963	
4	354	.963	
5	390	.963	
6	438	.966	
7	494	.969	
8	536	.972	
9	620	.973	
10	782	.975	
11	849	.977	
12	931	.981	
13	1268	.984	
14	1441	.990	
15	1509	.993	
16	1607	.993	
17	1778	.996	
18	1830	.998	
19	1851	1.001	

NO. POINTS= 18
 PMIN 2.197 KIPS PMAX= 4.392 KIPS R= .5002277

TEMP.= 1000 F ENVIRONMENT=AIR
 SPECIMEN:CT B= .496 IN. U= 2

OBS NO.	CYCLES	A (REAS.)	REMARKS
1	0	.095	
2	4	.095	
3	80	.096	
4	232	.096	
5	432	.096	
6	657	.092	
7	733	.094	
8	831	.094	
9	877	.095	
10	963	.095	
11	1355	.099	
12	1422	.090	
13	1448	.091	
14	1478	.091	
15	1522	.092	
16	1562	.094	
17	1693	.098	
18	1807	.090	

NO. POINTS= 32
 PMIN 2.417 KIPS PMAX= 4.831 KIPS R= .5003105

TEMP.= 1000 F ENVIRONMENT=AIR
 SPECIMEN:CT B= .496 IN. U= 2

OBS NO.	CYCLES	A (REAS.)	REMARKS
1	0	1.001	
2	14	1.004	
3	67	1.005	
4	130	1.007	
5	186	1.008	
6	241	1.009	
7	482	1.013	
8	587	1.017	
9	787	1.029	
10	1238	1.057	
11	1291	1.063	
12	1329	1.067	
13	1383	1.068	
14	1431	1.070	
15	1463	1.072	
16	1511	1.073	
17	1654	1.078	
18	2194	1.113	
19	2250	1.116	
20	2306	1.124	
21	2337	1.131	
22	2372	1.138	
23	2408	1.139	
24	2440	1.143	
25	2583	1.147	
26	2731	1.179	
27	2819	1.191	
28	2864	1.197	
29	2928	1.211	
30	2991	1.225	
31	3012	1.240	
32	3052	1.250	

PRECRACKING CONDITIONS

SPEC NO. 4-7
INIT. TEMP. = 1000 F INIT. LOAD = 3400 LBS INIT. STRESS RATIO = .1
FINAL TEMP. = 1000 F FINAL LOAD = 1815 LBS FINAL STRESS RATIO = .1
NO. OF INCREMENTS 7
FINAL SIZE LT. SIDE = .3219 RT. SIDE = .2213

NO. POINTS = 14
PMIN .182 KIPS PMAX = 1.815 KIPS R = .1002755 TEST FREQ. = .25 HZ
TEMP. = 1000 F ENVIRONMENT = AIR
SPECIMEN: CT D = .5293 IN. W = 2.013

OBS NO. CYCLES A (REAS.) REMARKS

1	0	.951
2	31	.952
3	105	.953
4	225	.955
5	398	.955
6	499	.958
7	551	.957
8	582	.956
9	655	.956
10	933	.956
11	1204	.961
12	1372	.961
13	1416	.962
14	1451	.968

NO. POINTS = 31
PMIN .182 KIPS PMAX = 1.815 KIPS R = .1002755 TEST FREQ. = .25 HZ
TEMP. = 1000 F ENVIRONMENT = AIR
SPECIMEN: CT D = .5293 IN. W = 2.013

OBS NO. CYCLES A (REAS.) REMARKS

1	0	1.381
2	67	1.386
3	101	1.392
4	134	1.392
5	274	1.397
6	318	1.402
7	353	1.408
8	409	1.411
9	676	1.441
10	697	1.451
11	746	1.459
12	792	1.466
13	821	1.474
14	852	1.481
15	959	1.510
16	974	1.516
17	981	1.519
18	987	1.523
19	993	1.527
20	999	1.531
21	1005	1.536
22	1017	1.541
23	1072	1.544
24	1046	1.551
25	1060	1.564
26	1070	1.572
27	1076	1.578
28	1084	1.590
29	1087	1.597
30	1090	1.603
31	1094	1.613

exceeds ASTM crack length requirement

PRECRACKING CONDITIONS

SPEC NO. 4-6
INIT. TEMP. = 70 F INIT. LOAD = 0 LBS INIT. STRESS RATIO = .9
FINAL TEMP. = 70 F FINAL LOAD = 0 LBS FINAL STRESS RATIO = .9
NO. OF INCREMENTS 0
FINAL SIZE LT. SIDE = .246 RT. SIDE = .215

NO. POINTS = 93
PMIN 4.142 KIPS PMAX = 4.602 KIPS R = .9000435 TEST FREQ. = .25 HZ
TEMP. = 100 F ENVIRONMENT = AI
SPECIMEN: CT D = .495 IN. W = 2.001

OBS NO. CYCLES A (REAS.) REMARKS

OBS NO.	CYCLES	A (REAS.)	REMARKS
1	193903	1.038	VARIOUS LOAD CHANGES
2	195053	1.038	PMAX = 4.536 KIPS PMIN = 5.062 KIPS
3	195903	1.040	
4	196953	1.042	
5	198253	1.043	
6	200177	1.044	
7	206189	1.051	
8	214103	1.063	
9	215453	1.066	
10	217043	1.067	
11	217853	1.068	
12	218903	1.070	
13	220233	1.072	
14	228141	1.083	
15	236203	1.096	
16	239553	1.100	
17	241053	1.102	
18	244241	1.105	
19	249633	1.109	
20	258903	1.121	
21	260941	1.125	
22	262343	1.131	
23	263703	1.137	
24	272265	1.145	
25	279553	1.165	
26	280553	1.167	
27	281653	1.169	
28	282333	1.170	
29	283478	1.174	
30	284353	1.175	
31	285393	1.178	
32	286403	1.178	
33	291024	1.187	
34	294689	1.189	
35	295933	1.197	
36	297103	1.200	
37	298113	1.203	
38	299613	1.207	
39	300953	1.210	
40	302103	1.212	
41	303278	1.216	
42	304878	1.220	
43			

PRECRACKING CONDITIONS

SPEC NO. 5-1
INIT. TEMP.= 1000 F INIT. LOAD= 6000 LBS INIT. STRESS RATIO= .9
FINAL TEMP.= 1000 F FINAL LOAD= 5790 LBS FINAL STRESS RATIO= .9
NO. OF INCREMENTS 11
FINAL SIZE LT. SIDE= .199 RT. SIDE= .241

NO. POINTS= 30
PMIN 7.079 KIPS PHAX= 7.965 KIPS R= .8887633
TEMP.= 1000 F ENVIRONMENT=AIR
SPECIMEN:CT B= .498 IN. U= 2.005

OBS NO.	CYCLES	A(MEAS.)	REMARKS
1	0	.816	
2	81	.816	
3	718	.814	
4	925	.819	
5	1007	.822	
6	1239	.822	
7	1425	.821	
8	1910	.823	
9	2729	.826	
10	2838	.826	
11	2918	.826	
12	3036	.828	
13	3126	.828	
14	3228	.828	
15	3340	.836	
16	3781	.840	
17	4391	.843	
18	4510	.843	
19	4741	.847	
20	4861	.850	
21	5027	.856	
22	5170	.860	
23	5436	.863	
24	5565	.866	
25	6183	.865	
26	6853	.866	
27	7000	.866	
28	7191	.866	
29	7550	.868	
30	7924	.867	

NO. POINTS= 16
PMIN 7.15 KIPS PHAX= 7.844 KIPS R= .9115247
TEMP.= 1000 F ENVIRONMENT=AIR
SPECIMEN:CT B= .498 IN. U= 2.005

OBS NO.	CYCLES	A(MEAS.)	REMARKS
1	0	.874	
2	115	.874	
3	266	.875	
4	354	.877	
5	416	.877	
6	574	.882	
7	693	.884	
8	2484	.893	
9	3401	.902	
10	3504	.904	
11	3588	.905	
12	3713	.905	
13	3824	.905	
14	3899	.905	
15	4376	.904	
16	4776	.906	

NO. POINTS= 16
PMIN 7.15 KIPS PHAX= 7.944 KIPS R= .9000503
TEMP.= 1000 F ENVIRONMENT=AIR
SPECIMEN:CT B= .498 IN. U= 2.005

OBS NO.	CYCLES	A(MEAS.)	REMARKS
1	0	1.010	
2	147	1.011	
3	239	1.011	
4	1430	1.020	
5	1605	1.020	
6	3080	1.025	
7	4358	1.038	
8	4569	1.038	
9	4777	1.038	
10	4961	1.039	
11	5279	1.040	
12	5610	1.042	
13	5990	1.047	
14	6134	1.047	
15	6384	1.049	
16	6680	1.052	

PRECRACKING CONDITIONS

SPEC NO. 5-2
INIT. TEMP.= 1345 F INIT. LOAD= 5000 LBS INIT. STRESS RATIO= .5
FINAL TEMP.= 1379 F FINAL LOAD= 2500 LBS FINAL STRESS RATIO= .9
NO. OF INCREMENTS 19
FINAL SIZE LT. SIDE= .2693 RT. SIDE= .2229

NO. POINTS= 34
PHIN 1.71 KIPS PHAX= 1.9 KIPS R= .9
TEMP.= 1400 F ENVIRONMENT=AIR
SPECIMEN:CT B= .499 IN. U= 2.009

OBS NO. CYCLES A(MEAS.) REMARKS

1	0	.892
2	12	.894
3	25	.906
4	37	.920
5	82	.936
6	109	.960
7	132	.973
8	148	.984
9	163	1.001
10	183	1.015
11	198	1.028
12	231	1.067
13	250	1.081
14	269	1.105
15	269	1.105
16	293	1.136
17	303	1.156
18	318	1.177
19	336	1.204
20	360	1.248
21	374	1.261
22	398	1.304
23	411	1.339
24	426	1.372
25	434	1.403
26	447	1.438
27	460	1.469
28	472	1.510
29	486	1.535
30	494	1.560
31	502	1.588
32	512	1.614
33	521	1.647
34	526	1.655

PRECRACKING CONDITIONS

SPEC NO. 5-3
INIT. TEMP.= 70 F INIT. LOAD= 0 LBS INIT. STRESS RATIO= .5
FINAL TEMP.= 70 F FINAL LOAD= 0 LBS FINAL STRESS RATIO= .5
NO. OF INCREMENTS 0
FINAL SIZE LT. SIDE= .245 RT. SIDE= .201

NO. POINTS= 43
PHIN 1.5 KIPS PHAX= 3.001 KIPS R= .4998334
TEMP.= 1000 F ENVIRONMENT=AIR
SPECIMEN:CT B= .5 IN. U= 2.001

OBS NO. CYCLES A(MEAS.) REMARKS

OBS NO.	CYCLES	A(MEAS.)	REMARKS
1	0	.857	VARIOUS LOAD CHANGES
2	394	.840	
3	1395	.870	
4	2135	.875	
5	2170	.876	PHAX= 3.301 KIPS PHIN= 1.650 KIPS
6	2327	.878	
7	2715	.883	
8	3825	.896	
9	4269	.901	
10	4337	.902	PHAX= 3.602 KIPS PHIN= 1.815 KIPS
11	4410	.903	
12	4515	.906	
13	4623	.908	
14	4945	.914	
15	5111	.918	
16	5160	.920	
17	5299	.922	
18	6037	.933	PHAX= 3.926 KIPS PHIN= 1.997 KIPS
19	6995	.957	
20	7085	.960	
21	7197	.963	
22	7307	.966	
23	7453	.970	
24	8065	.981	
25	8320	.989	PHAX= 4.358 KIPS PHIN= 2.194 KIPS
26	9187	1.027	
27	9304	1.036	
28	9433	1.042	
29	9515	1.047	
30	9599	1.052	
31	9730	1.059	
32	9858	1.065	
33	10424	1.101	
34	10576	1.115	
35	10677	1.125	
36	10842	1.142	
37	10934	1.153	
38	11441	1.227	
39	11533	1.250	
40	11582	1.270	
41	11624	1.284	
42	11663	1.304	
43	11700	1.334	

PRECRACKING CONDITIONS
 SPEC. NO. S-3
 INIT. TEMP. = 70 F INIT. LOAD = 0 LBS INIT. STRESS RATIO = .03
 FINAL TEMP. = 70 F FINAL LOAD = 0 LBS FINAL STRESS RATIO = .03
 NO. OF INCREMENTS 0
 FINAL SIZE LT. SIDE = .101 RT. SIDE = .015

NO. POINTS = 25
 PMIN .03 KIPS PMAX = .77 KIPS R = .025974
 TEMP. = 1400 F ENVIRONMENT = AIR
 SPECIMEN: CT R = .249 IN. W = 2

DIS NO.	CYCLES	A (MEAS.)	REMARKS
1	100	.772	
2	1000	.773	
3	1300	.773	
4	1600	.774	
5	1850	.775	
6	2000	.776	
7	2500	.778	
8	3000	.782	
9	4000	.792	
10	5000	.806	
11	6000	.822	
12	8000	.858	
13	10000	.898	
14	12000	.938	
15	14000	.982	
16	16000	1.026	
17	18000	1.074	
18	20000	1.130	
19	22000	1.190	
20	23000	1.252	
21	24000	1.398	
22	24100	1.438	
23	24200	1.474	
24	24300	1.492	
25	24422	1.562	

PRECRACKING CONDITIONS
 SPEC NO. 7-4
 INIT. TEMP. = 70 F INIT. LOAD = 0 LBS INIT. STRESS RATIO = .1
 FINAL TEMP. = 70 F FINAL LOAD = 0 LBS FINAL STRESS RATIO = .1
 NO. OF INCREMENTS 0
 FINAL SIZE LT. SIDE = .24 RT. SIDE = .245

NO. POINTS = 14
 PMIN .145 KIPS PMAK = 1.815 KIPS R = .0909091
 TEMP. = 1400 F ENVIRONMENT = AIR
 SPECIMEN: CT B = .498 IN. W = 2

OBS NO. CYCLES AREA(S) REMARKS

1	0	.833
2	30	.974
3	34	.998
4	40	1.046
5	45	1.092
6	50	1.146
7	55	1.214
8	60	1.286
9	65	1.374
10	67	1.424
11	70	1.490
12	72	1.545
13	74	1.577

exceeds ASTM crack length requirement

PRECRACKING CONDITIONS
 SPEC NO. 8-1
 INIT. TEMP. = 70 F INIT. LOAD = 0 LBS INIT. STRESS RATIO = .1
 FINAL TEMP. = 70 F FINAL LOAD = 0 LBS FINAL STRESS RATIO = .1
 NO. OF INCREMENTS 0
 FINAL SIZE LT. SIDE = .26 RT. SIDE = .23

NO. POINTS = 27
 PMIN .165 KIPS PMAK = 1.815 KIPS R = .0909091
 TEMP. = 1000 F ENVIRONMENT = AIR
 SPECIMEN: CT B = .503 IN. W = 2

OBS NO. CYCLES AREA(S) REMARKS

1	0	.795
2	233	.795
3	4292	.801
4	5817	.803
5	11007	.806
6	13327	.806
7	17710	.811
8	31181	.821
9	33173	.826
10	37913	.837
11	40040	.842
12	44615	.853
13	47214	.859
14	51346	.871
15	53522	.876
16	58080	.892
17	60585	.901
18	64705	.915
19	66840	.926
20	72444	.949
21	78257	.979
22	80690	.995
23	84950	1.023
24	87430	1.043
25	91610	1.078
26	98408	1.150
27	101026	1.195

PRECRACKING CONDITIONS
 SPEC NO. B-3
 INIT. TEMP. = 1200 F INIT. LOAD = 3400 LBS INIT. STRESS RATIO = .1
 FINAL TEMP. = 1200 F FINAL LOAD = 1900 LBS FINAL STRESS RATIO = .1
 NO. OF INCREMENTS 10
 FINAL SIZE LT. SIDE = .226 RT. SIDE = .172

NO. POINTS = 36
 PMIN .182 KIPS PMAX = 1.815 KIPS R = .1002755
 TEMP. = 1200 F ENVIRONMENT = AIR
 SPECIMEN: CT B = .4998 IN. W = 2.004

OBS NO.	CYCLES	A (INCHES)	REMARKS
1	0	.937	
2	28	.937	
3	101	.945	
4	197	.942	
5	239	.945	
6	243	.946	
7	309	.976	
8	346	.983	
9	386	.985	
10	486	1.007	
11	593	1.007	
12	661	1.008	
13	786	1.012	
14	830	1.012	
15	872	1.030	
16	920	1.045	
17	937	1.057	
18	1060	1.104	
19	1114	1.135	
20	1124	1.142	
21	1144	1.154	
22	1207	1.213	
23	1212	1.216	
24	1212	1.222	
25	1236	1.250	
26	1271	1.284	
27	1279	1.301	
28	1296	1.309	
29	1302	1.347	
30	1309	1.383	
31	1320	1.422	
32	1326	1.453	
33	1331	1.498	
34	1335	1.547	
35	1340	1.544	
36	1341	1.631	exceeds ASTM crack length requirement

PRECRACKING CONDITIONS
 SPEC NO. B-4
 INIT. TEMP. = 1000 F INIT. LOAD = 3400 LBS INIT. STRESS RATIO = .1
 FINAL TEMP. = 1000 F FINAL LOAD = 1815 LBS FINAL STRESS RATIO = .1
 NO. OF INCREMENTS 8
 FINAL SIZE LT. SIDE = .3242 RT. SIDE = .233

NO. POINTS = 56
 PMIN .182 KIPS PMAX = 1.815 KIPS R = .1002755
 TEMP. = 1000 F ENVIRONMENT = AIR
 SPECIMEN: CT B = .495 IN. W = 2.001

OBS NO.	CYCLES	A (INCHES)	REMARKS
1	0	.875	
2	1871	.881	
3	2898	.882	
4	3742	.886	
5	4155	.896	
6	7519	.902	
7	8703	.903	
8	9841	.911	
9	10481	.913	
10	13050	.921	
11	14115	.935	
12	14683	.935	
13	16685	.944	
14	23392	.984	
15	29961	1.024	
16	33433	1.055	
17	3391	1.060	
18	34738	1.065	
19	35234	1.072	
20	35468	1.076	
21	36315	1.078	
22	39133	1.104	
23	39569	1.112	
24	40248	1.119	
25	41000	1.128	
26	41785	1.138	
27	43011	1.154	
28	45510	1.191	
29	46307	1.204	
30	46805	1.214	
31	47481	1.228	
32	47848	1.233	
33	48530	1.253	
34	49080	1.267	
35	49470	1.275	
36	49786	1.290	
37	50242	1.305	
38	50565	1.317	
39	51140	1.350	
40	51310	1.360	
41	51347	1.364	
42	51515	1.374	
43	51649	1.388	
44	51815	1.403	
45	51974	1.423	
46	52052	1.439	
47	52090	1.443	
48	52173	1.463	
49	52230	1.471	
50	52291	1.498	
51	52314	1.499	
52	52338	1.514	
53	52363	1.532	
54	52377	1.538	
55	52391	1.553	
56	52412	1.578	exceeds ASTM crack length requirement

PRECRACKING CONDITIONS

SPEC NO. 8-7
INIT. TEMP.= 70 F INIT. LOAD= 0 LBS INIT. STRESS RATIO= .5
FINAL TEMP.= 70 F FINAL LOAD= 0 LBS FINAL STRESS RATIO= .5
NO. OF INCREMENTS 0
FINAL SIZE LT. SIDE= .249 RT. SIDE= .136

NO. POINTS= 11
PHIN 1.310 KIPS PHAX= 2.636 KIPS R= .5
TEMP.= 1000 F ENVIRONMENT=AIR
SPECIMEN:CT B= .4945 IN. U= 2

OBS NO.	CYCLES	A(NEAS.)	REMARKS
1	0	.770	
2	7	.770	
3	31	.779	
4	505	.786	
5	625	.786	
6	699	.786	
7	730	.788	
8	816	.789	
9	870	.790	
10	971	.790	
11	1246	.791	

NO. POINTS= 13
PHIN 1.753 KIPS PHAX= 3.507 KIPS R= .4998574

TEMP.= 1000 F ENVIRONMENT=AIR
SPECIMEN:CT B= .4945 IN. U= 2

OBS NO.	CYCLES	A(NEAS.)	REMARKS
1	0	.817	
2	40	.817	
3	335	.823	
4	420	.823	
5	484	.823	
6	538	.825	
7	673	.830	
8	746	.830	
9	1434	.847	
10	1624	.853	
11	1684	.854	
12	1728	.856	
13	1784	.858	

NO. POINTS= 20
PHIN 1.095 KIPS PHAX= 3.858 KIPS R= .4911871

TEMP.= 1000 F ENVIRONMENT=AIR
SPECIMEN:CT B= .4945 IN. U= 2

OBS NO.	CYCLES	A(NEAS.)	REMARKS
1	0	.860	
2	46	.860	
3	78	.860	
4	137	.861	
5	187	.862	
6	327	.864	
7	523	.870	
8	569	.872	
9	613	.873	
10	680	.875	
11	738	.875	
12	972	.881	
13	1206	.883	
14	1325	.888	
15	1360	.890	
16	1372	.891	
17	1464	.895	
18	1512	.895	
19	2149	.898	
20	2287	.902	

NO. POINTS= 19
PHIN 2.085 KIPS PHAX= 4.244 KIPS R= .4912818

TEMP.= 1000 F ENVIRONMENT=AIR
SPECIMEN:CT B= .4945 IN. U= 2

OBS NO.	CYCLES	A(NEAS.)	REMARKS
1	0	.906	
2	4	.906	
3	51	.909	
4	102	.911	
5	365	.918	
6	478	.924	
7	603	.928	
8	672	.929	
9	758	.934	
10	812	.937	
11	1159	.939	
12	1311	.943	
13	1387	.952	
14	1463	.956	
15	1506	.957	
16	1594	.962	
17	1742	.967	
18	1817	.970	
19	2048	.974	

NO. POINTS= 16
PHIN 2.294 KIPS PHAX= 4.668 KIPS R= .491431
TEMP.= 1000 F ENVIRONMENT=AIR
SPECIMEN:CT B= .4945 IN. U= 2

OBS NO.	CYCLES	A(NEAS.)	REMARKS
1	0	.993	
2	28	.996	
3	76	.997	
4	120	.998	
5	158	.997	
6	533	1.014	
7	598	1.026	
8	674	1.031	
9	766	1.035	
10	833	1.041	
11	1048	1.059	
12	1151	1.065	
13	1274	1.077	
14	1340	1.083	
15	1446	1.098	

PRECRACKING CONDITIONS
 SPEC NO. 9-1
 INIT. TEMP. = 70 F INIT. LOAD = 0 LBS INIT. STRESS RATIO = .1
 FINAL TEMP. = 70 F FINAL LOAD = 0 LBS FINAL STRESS RATIO = .1
 NO. OF INCREMENTS 0
 FINAL SIZE LT. SIDE = .257 RT. SIDE = .133

NO. POINTS = 22
 PMIN .165 KIPS PHAX = 1.815 KIPS R = .0909091
 TEMP. = 1200 F ENVIRONMENT = AIR
 SPECIMEN:CT B = .4995 IN. U = 2

OBS NO.	CYCLES	A (MEAS.)	REMARKS
1	0	.745	invalid precrack
2	7	.745	
3	443	.750	
4	561	.762	
5	703	.763	
6	799	.769	
7	939	.769	
8	1363	.784	
9	1581	.788	
10	2272	.807	
11	2406	.811	
12	2600	.817	
13	3274	.850	
14	3644	.872	
15	4126	.907	
16	4209	.918	
17	4341	.931	
18	4453	.943	
19	5048	1.020	
20	5297	1.069	
21	5401	1.094	
22	5967	1.114	

PRECRACKING CONDITIONS
 SPEC NO. 9-4
 INIT. TEMP. = 70 F INIT. LOAD = 0 LBS INIT. STRESS RATIO = .1
 FINAL TEMP. = 70 F FINAL LOAD = 0 LBS FINAL STRESS RATIO = .1
 NO. OF INCREMENTS 0
 FINAL SIZE LT. SIDE = .229 RT. SIDE = .214

NO. POINTS = 23
 PMIN .165 KIPS PHAX = 1.815 KIPS R = .0909091
 TEMP. = 1200 F ENVIRONMENT = AIR
 SPECIMEN:CT B = .499 IN. U = 2

OBS NO.	CYCLES	A (MEAS.)	REMARKS
1	0	.771	
2	411	.778	
3	1080	.781	
4	1485	.785	
5	2090	.785	
6	2450	.785	
7	3562	.787	
8	4190	.787	
9	4625	.791	
10	5510	.793	
11	6146	.796	
12	43800	.966	
13	46275	.983	
14	49080	1.005	
15	50330	1.010	
16	51390	1.030	
17	52270	1.042	
18	53754	1.061	
19	55403	1.085	
20	56530	1.105	
21	57400	1.125	
22	58516	1.149	
23	59334	1.172	

PRECRACKING CONDITIONS
 SPEC NO. 9-3
 INIT. TEMP. = 70 F INIT. LOAD = 0 LBS INIT. STRESS RATIO = .1
 FINAL TEMP. = 70 F FINAL LOAD = 0 LBS FINAL STRESS RATIO = .1
 NO. OF INCREMENTS 0
 FINAL SIZE LT. SIDE = .242 RT. SIDE = .245

NO. POINTS = 32
 PMIN .165 KIPS PHAX = 1.815 KIPS R = .0909091
 TEMP. = 1400 F ENVIRONMENT = AIR
 SPECIMEN:CT B = .4985 IN. U = 2

OBS NO.	CYCLES	A (MEAS.)	REMARKS
1	0	.823	
2	1005	.827	
3	1340	.830	
4	2064	.836	
5	2405	.855	
6	3116	.868	
7	3766	.887	
8	4225	.899	
9	4961	.921	
10	5630	.932	
11	5790	.949	
12	6124	.956	
13	6467	.968	
14	6930	.980	
15	7276	.997	
16	7701	1.014	
17	8250	1.043	
18	8647	1.082	
19	9190	1.092	
20	9582	1.106	
21	9937	1.121	
22	10390	1.142	
23	10853	1.173	
24	11393	1.212	
25	11721	1.233	
26	12000	1.283	
27	12200	1.333	
28	12400	1.388	
29	12500	1.423	
30	12600	1.483	
31	12700	1.523	
32	12723	1.566	

PRECRACKING CONDITIONS
 SPEC NO. 9-7
 INIT. TEMP.= 1100 F INIT. LOAD= 4000 LBS INIT. STRESS RATIO= .1
 FINAL TEMP.= 1100 F FINAL LOAD= 1815 LBS FINAL STRESS RATIO= .1
 NO. OF INCREMENTS 14
 FINAL SIZE LT. SIDE= .231 RT. SIDE= .262

NO. POINTS= 48
 PMIN .22 KIPS PMAX= 2.197 KIPS R= .1001366
 TEMP.= 1200 F ENVIRONMENT=AIR
 SPECIMEN:CT B= .499 IN. W= 1.997

OBS NO. CYCLES A(MEAS.) REMARKS

1	0	.883	
2	247	.928	
3	308	.938	
4	369	.953	
5	399	.958	
6	432	.965	
7	461	.971	
8	540	.982	
9	676	1.019	
10	698	1.024	
11	772	1.045	
12	797	1.052	
13	822	1.064	
14	843	1.069	
15	864	1.084	
16	887	1.095	
17	912	1.105	
18	954	1.131	
19	980	1.150	
20	1002	1.162	
21	1032	1.186	
22	1052	1.198	
23	1067	1.224	
24	1082	1.233	
25	1091	1.242	
26	1105	1.259	
27	1114	1.270	
28	1119	1.277	
29	1126	1.284	
30	1138	1.297	
31	1143	1.311	
32	1151	1.328	
33	1158	1.344	
34	1165	1.361	
35	1170	1.369	
36	1175	1.381	
37	1182	1.398	
38	1188	1.412	
39	1193	1.426	
40	1197	1.444	
41	1200	1.462	
42	1202	1.471	
43	1205	1.480	
44	1207	1.498	
45	1209	1.504	
46	1212	1.521	
47	1215	1.531	
48	1217	1.541	exceeds ASTM crack length requirement

PRECRACKING CONDITIONS
 SPEC NO. 9-8
 INIT. TEMP.= 70 F INIT. LOAD= 0 LBS INIT. STRESS RATIO= .5
 FINAL TEMP.= 70 F FINAL LOAD= 0 LBS FINAL STRESS RATIO= .5
 NO. OF INCREMENTS 0
 FINAL SIZE LT. SIDE= .125 RT. SIDE= .275

NO. POINTS= 49
 PMIN .952 KIPS PMAX= 1.9 KIPS R= .5010526
 TEMP.= 1400 F ENVIRONMENT=AIR
 SPECIMEN:CT B= .5 IN. W= 1.993

OBS NO. CYCLES A(MEAS.) REMARKS

1	0	.802	invalid precrack
2	874	.810	
3	7525	.821	
4	9347	.828	
5	10890	.852	
6	11519	.892	
7	11605	.909	
8	11734	.919	
9	11936	.932	
10	11958	.945	
11	12118	.956	
12	12188	.965	
13	12299	.971	
14	12469	.973	
15	12610	.988	
16	12804	1.000	
17	12999	1.026	
18	13233	1.045	
19	13345	1.059	
20	13539	1.078	
21	13671	1.097	
22	13993	1.130	
23	14210	1.170	
24	14279	1.172	
25	14338	1.176	
26	14382	1.186	
27	14415	1.194	
28	14453	1.204	
29	14496	1.213	
30	14538	1.222	
31	14628	1.235	
32	14649	1.245	
33	14745	1.253	
34	14784	1.262	
35	14826	1.270	
36	14869	1.281	
37	14901	1.292	
38	14945	1.307	
39	15029	1.323	
40	15101	1.341	
41	15124	1.356	
42	15193	1.372	
43	15228	1.387	
44	15243	1.404	
45	15313	1.426	
46	15339	1.447	
47	15365	1.466	
48	15393	1.495	
49	15417	1.539	

PRECRACKING CONDITIONS

SPEC NO. 10-2
INIT. TEMP.= 1000 F INIT. LOAD= 4000 LBS INIT. STRESS RATIO= .1
FINAL TEMP.= 1000 F FINAL LOAD= 2129 LBS FINAL STRESS RATIO= .1
NO. OF INCREMENTS 7
FINAL SIZE LT. SIDE= .142 RT. SIDE= .213

NO. POINTS= 27
PMIN .386 KIPS PMAX= 3.864 KIPS R= .0998963
TEMP.= 1000 F ENVIRONMENT=AIR
SPECIMEN:CT B= .502 IN. U= 2.0067

NO. POINTS= 16
PMIN .24 KIPS PMAX= 2.4 KIPS R= .1
TEMP.= 1000 F ENVIRONMENT=AIR
SPECIMEN:CT B= .502 IN. U= 2.0067

OBS NO.	CYCLES	A (MEAS.)	REMARKS
1	0	.679	
2	838	.683	
3	1038	.683	
4	1426	.684	
5	1681	.687	
6	2006	.688	
7	3273	.692	
8	4473	.693	
9	4834	.695	
10	5036	.696	
11	6351	.702	
12	6511	.703	
13	6766	.705	
14	7055	.705	
15	7173	.705	
16	7257	.705	

NO. POINTS= 14
PMIN .264 KIPS PMAX= 2.64 KIPS R= .1
TEMP.= 1000 F ENVIRONMENT=AIR
SPECIMEN:CT B= .502 IN. U= 2.0067

OBS NO.	CYCLES	A (MEAS.)	REMARKS
1	0	.705	
2	862	.709	
3	970	.711	
4	1099	.712	
5	1389	.715	
6	1484	.717	
7	1589	.718	
8	1898	.718	
9	1982	.720	
10	2776	.724	
11	2934	.727	
12	3209	.729	
13	3323	.729	
14	3469	.729	

NO. POINTS= 17
PMIN .35138 KIPS PMAX= 3.5138 KIPS R= .1
TEMP.= 1000 F ENVIRONMENT=AIR
SPECIMEN:CT B= .502 IN. U= 2.0067

OBS NO.	CYCLES	A (MEAS.)	REMARKS
1	0	.747	
2	697	.766	
3	905	.773	
4	971	.774	
5	1309	.780	
6	1465	.781	
7	1558	.784	
8	1725	.787	
9	4315	.852	
10	4376	.854	
11	4470	.854	
12	4543	.860	
13	4674	.863	
14	4740	.866	
15	4811	.866	
16	5013	.874	
17	5439	.885	

OBS NO.	CYCLES	A (MEAS.)	REMARKS
1	0	.885	
2	472	.922	
3	863	.925	
4	1001	.931	
5	1077	.933	
6	1148	.941	
7	1403	.961	
8	1680	.980	
9	1840	.992	
10	2514	1.060	
11	2625	1.064	
12	2646	1.073	
13	2745	1.085	
14	2799	1.094	
15	2835	1.104	
16	2877	1.107	
17	2945	1.116	
18	3003	1.132	
19	3046	1.143	
20	3084	1.150	
21	3207	1.177	
22	3252	1.184	
23	3419	1.247	
24	3454	1.272	
25	3498	1.294	
26	3540	1.337	
27	3555	1.379	

PRECRACKING CONDITIONS

SPEC NO. 10-3
INIT. TEMP.= 70 F INIT. LOAD= 0 LBS INIT. STRESS RATIO= .1
FINAL TEMP.= 70 F FINAL LOAD= 0 LBS FINAL STRESS RATIO= .1
NO. OF INCREMENTS 0
FINAL SIZE LT. SIDE= .242 RT. SIDE= .259

NO. POINTS= 27
PMIN .165 KIPS PMAX= 1.051 KIPS R= .089141
TEMP.= 1000 F ENVIRONMENT=AIR
SPECIMEN:CT B= .498 IN. W= 2

OBS NO. CYCLES A(NEAS.) REMARKS

1	0	.026
2	250	.027
3	2658	.028
4	4509	.034
5	5434	.036
6	6345	.037
7	7227	.040
8	8343	.041
9	10027	.046
10	10948	.050
11	11881	.052
12	13134	.054
13	13710	.056
14	15274	.061
15	16788	.063
16	18044	.069
17	18959	.071
18	20462	.073
19	21219	.076
20	21720	.079
21	22033	.081
22	22903	.082
23	23760	.084
24	24681	.087
25	25604	.090
26	26979	.095
27	27681	.097

NO. POINTS= 6
PMIN .182 KIPS PMAX= 1.997 KIPS R= .0911367
TEMP.= 1000 F ENVIRONMENT=AIR
SPECIMEN:CT B= .498 IN. W= 2

OBS NO. CYCLES A(NEAS.) REMARKS

1	0	.900
2	781	.902
3	1852	.903
4	1629	.907
5	2538	.912
6	3092	.912

NO. POINTS= 9
PMIN .2 KIPS PMAX= 2.197 KIPS R= .0910332
TEMP.= 1000 F ENVIRONMENT=AIR
SPECIMEN:CT B= .498 IN. W= 2

OBS NO. CYCLES A(NEAS.) REMARKS

1	0	.915
2	427	.919
3	1284	.923
4	3148	.939
5	4111	.949
6	4309	.949
7	5018	.953
8	5914	.963
9	6323	.965

NO. POINTS= 8
PMIN .22 KIPS PMAX= 2.417 KIPS R= .0910219
TEMP.= 1000 F ENVIRONMENT=AIR
SPECIMEN:CT B= .498 IN. W= 2

OBS NO. CYCLES A(NEAS.) REMARKS

1	0	.968
2	287	.971
3	890	.978
4	1228	.982
5	1669	.987
6	2634	1.000
7	3073	1.007
8	3562	1.013

NO. POINTS= 9
PMIN .242 KIPS PMAX= 2.659 KIPS R= .0910117
TEMP.= 1000 F ENVIRONMENT=AIR
SPECIMEN:CT B= .498 IN. W= 2

OBS NO. CYCLES A(NEAS.) REMARKS

1	0	1.017
2	368	1.021
3	917	1.031
4	1362	1.039
5	1830	1.052
6	2313	1.063
7	3624	1.107
8	5431	1.184
9	6352	1.257

PRECRACKING CONDITIONS
 SPEC NO. 10-5
 INIT. TEMP.= 1100 F INIT. LOAD= 4900 LBS INIT. STRESS RATIO= .9
 FINAL TEMP.= 1100 F FINAL LOAD= 3700 LBS FINAL STRESS RATIO= .9
 NO. OF INCREMENTS 6
 FINAL SIZE LT. SIDE= .2291 RT. SIDE= .1939

NO. POINTS= 42
 PMIN 2.831 KIPS PMAX= 3.145 KIPS R= .900159
 TEMP.= 1200 F ENVIRONMENT=AIR
 SPECIMEN:CT B= .499 IN. W= 2.014

OBS NO.	CYCLES	A(MEAS.)	REMARKS
1	0	.775	
2	31	.775	
3	154	.785	
4	221	.790	
5	344	.801	
6	391	.811	
7	465	.819	
8	515	.829	
9	592	.839	
10	662	.843	
11	692	.846	
12	793	.861	
13	863	.870	
14	922	.873	
15	978	.877	
16	1094	.893	
17	1176	.900	
18	1243	.912	
19	1331	.917	
20	1373	.922	
21	1493	.937	
22	1571	.953	
23	1644	.975	
24	1724	.990	
25	1900	1.012	
26	2014	1.036	
27	2098	1.050	
28	2195	1.064	
29	2244	1.076	
30	2311	1.081	
31	2376	1.085	
32	2428	1.097	
33	2484	1.112	
34	2561	1.120	
35	2636	1.133	
36	2728	1.152	
37	2967	1.193	
38	3247	1.283	
39	3276	1.297	
40	3327	1.326	
41	3359	1.340	
42	3413	1.382	

PRECRACKING CONDITIONS
 SPEC NO. 10-6
 INIT. TEMP.= 70 F INIT. LOAD= 0 LBS INIT. STRESS RATIO= .1
 FINAL TEMP.= 70 F FINAL LOAD= 0 LBS FINAL STRESS RATIO= .1
 NO. OF INCREMENTS 0
 FINAL SIZE LT. SIDE= .237 RT. SIDE= .255

NO. POINTS= 7
 PMIN .165 KIPS PMAX= 1.015 KIPS R= .0909091
 TEMP.= 1000 F ENVIRONMENT=AIR
 SPECIMEN:CT B= .4965 IN. W= 2

OBS NO.	CYCLES	A(MEAS.)	REMARKS
1	0	.796	
2	4470	.752	
3	16152	.822	
4	38580	.915	
5	49140	.978	
6	60870	1.078	
7	67972	1.165	

PRECRACKING CONDITIONS
 SPEC NO. 10-7
 INIT. TEMP.= 70 F INIT. LOAD= 0 LBS INIT. STRESS RATIO= .9
 FINAL TEMP.= 70 F FINAL LOAD= 0 LBS FINAL STRESS RATIO= .9
 NO. OF INCREMENTS 0
 FINAL SIZE LT. SIDE= .254 RT. SIDE= .247

NO. POINTS= 25
 PMIN 1.386 KIPS PMAX= 1.54 KIPS R= .9 TEST FREQ.= .25 HZ
 TEMP.= 1400 F ENVIRONMENT=AIR
 SPECIMEN:CT B= .496 IN. W= 2.0045

OBS NO.	CYCLES	A(MEAS.)	REMARKS
1	0	.799	
2	7	.807	
3	18	.826	
4	24	.832	
5	29	.839	
6	35	.848	
7	41	.865	
8	47	.880	
9	58	.895	
10	64	.929	
11	70	.949	
12	74	.969	
13	78	.986	
14	82	1.007	
15	86	1.034	
16	90	1.063	
17	94	1.087	
18	98	1.121	
19	102	1.162	
20	106	1.204	
21	110	1.266	
22	115	1.361	
23	120	1.433	
24	125	1.544	

PRECRACKING CONDITIONS
 SPEC NO. 11-1
 INIT. TEMP. = 1200 F INIT. LOAD = 5000 LBS INIT. STRESS RATIO = .5
 FINAL TEMP. = 1200 F FINAL LOAD = 2102 LBS FINAL STRESS RATIO = .5
 NO. OF INCREMENTS 15
 FINAL SIZE LT. SIDE = .225 RT. SIDE = .253

NO. POINTS = 48
 PMIN 1.051 KIPS PHAX = 2.102 KIPS R = .5
 TEMP. = 1200 F ENVIRONMENT = AIR
 SPECIMEN: CT B = .4997 IN. U = 2

OBS NO.	CYCLES	A (MEAS.)	REMARKS
1	0	.810	
2	300	.812	
3	800	.816	
4	2800	.835	
5	4287	.842	
6	4997	.847	
7	5547	.853	
8	6088	.856	
9	6594	.862	
10	14042	1.004	
11	16631	1.014	
12	17221	1.020	
13	17681	1.035	
14	17884	1.037	
15	18144	1.040	
16	18400	1.049	
17	18678	1.056	
18	30040	1.122	*EXTENDING CRACK INCREASE TO 150 CPM
19	38022	1.189	
20	38152	1.196	
21	38284	1.204	
22	38518	1.212	
23	38678	1.220	
24	38774	1.226	
25	39133	1.243	
26	39302	1.255	
27	39459	1.266	
28	39694	1.287	
29	39796	1.294	
30	39870	1.304	
31	39950	1.313	
32	40050	1.325	
33	40184	1.333	
34	40209	1.350	
35	40214	1.361	
36	40389	1.375	
37	40432	1.383	
38	40482	1.391	
39	40570	1.406	
40	40693	1.429	
41	40780	1.449	
42	40820	1.460	
43	40870	1.472	
44	40916	1.483	
45	40967	1.502	
46	41008	1.516	
47	41046	1.535	
48	41107	1.559	exceeds ASTM crack length requirement

PRECRACKING CONDITIONS
 SPEC NO. 11-2
 INIT. TEMP. = 1000 F INIT. LOAD = 5000 LBS INIT. STRESS RATIO = .5
 FINAL TEMP. = 1000 F FINAL LOAD = 4700 LBS FINAL STRESS RATIO = .9
 NO. OF INCREMENTS 1
 FINAL SIZE LT. SIDE = .208 RT. SIDE = .1925

NO. POINTS = 36
 PMIN 4.5 KIPS PHAX = 5 KIPS R = .9
 TEMP. = 1000 F ENVIRONMENT = AIR
 SPECIMEN: CT B = .499 IN. U = 1.992

OBS NO.	CYCLES	A (MEAS.)	REMARKS
1	0	.905	
2	916	.905	
3	2752	.907	
4	3339	.907	
5	9400	.916	
6	15663	.917	
7	16220	.918	
8	16627	.919	
9	17034	.919	
10	18029	.919	
11	18463	.921	
12	19198	.924	
13	19902	.926	
14	21794	.931	
15	25119	.945	
16	25298	.947	
17	26326	.950	
18	26803	.952	
19	27121	.954	
20	27544	.955	
21	27855	.957	
22	28728	.966	
23	29320	.973	
24	30627	.974	
25	31154	.976	
26	38712	.989	
27	43335	1.000	
28	44020	1.002	
29	44454	1.003	
30	45108	1.004	
31	45692	1.005	
32	46100	1.006	
33	46843	1.008	
34	47689	1.009	
35	48471	1.012	
36	48967	1.012	

NO. POINTS = 14
 PMIN 4.5 KIPS PHAX = 5 KIPS R = .9
 TEMP. = 1000 F ENVIRONMENT = AIR
 SPECIMEN: CT B = .499 IN. U = 1.992

OBS NO.	CYCLES	A (MEAS.)	REMARKS
1	0	1.057	
2	10850	1.061	
3	15750	1.064	
4	27600	1.063	
5	43400	1.072	
6	57800	1.078	
7	70582	1.083	
8	78951	1.087	
9	87946	1.091	
10	94619	1.095	
11	99642	1.097	
12	102961	1.099	
13	132300	1.118	
14	143948	1.122	

NO. POINTS = 12
 PMIN 4.5 KIPS PHAX = 5 KIPS R = .9
 TEMP. = 1000 F ENVIRONMENT = AIR
 SPECIMEN: CT B = .499 IN. U = 1.992

OBS NO.	CYCLES	A (MEAS.)	REMARKS
1	0	1.122	
2	193	1.122	
3	476	1.122	
4	809	1.122	
5	1353	1.123	
6	1836	1.126	
7	2372	1.131	
8	8154	1.151	
9	8601	1.154	
10	14903	1.275	
11	16181	1.284	

PRECRACKING CONDITIONS
 SPEC NO. 11-4
 INIT. TEMP. = 1200 F INIT. LOAD = 2600 LBS INIT. STRESS RATIO = .1
 FINAL TEMP. = 1200 F FINAL LOAD = 1815 LBS FINAL STRESS RATIO = .1
 NO. OF INCREMENTS 12
 FINAL SIZE LT. SIDE = .125 RT. SIDE = .203

NO. POINTS = 27
 P_{MIN} .182 KIPS P_{MAX} 1.815 KIPS R = .1002755
 TEMP. = 1400 F ENVIRONMENT = AIR
 SPECIMEN: CT B = .4994 IN. W = 1.99

OBS NO. CYCLES A (REAS.) REMARKS

1	0	.720
2	2400	.731
3	4950	.739
4	7350	.754
5	9750	.767
6	12000	.776
7	14700	.800
8	18150	.821
9	20850	.839
10	25050	.871
11	29250	.909
12	33450	.946
13	38250	.997
14	41100	1.040
15	42600	1.073
16	45000	1.108
17	46800	1.118
18	47850	1.174
19	48600	1.195
20	49350	1.224
21	50100	1.251
22	50850	1.281
23	51600	1.342
24	52350	1.391
25	52650	1.440
26	52800	1.535
27	52950	1.608

exceeds ASTM crack length requirement

PRECRACKING CONDITIONS
 SPEC NO. 11-5
 INIT. TEMP. = 1000 F INIT. LOAD = 4000 LBS INIT. STRESS RATIO = .9
 FINAL TEMP. = 1000 F FINAL LOAD = 2100 LBS FINAL STRESS RATIO = .1
 NO. OF INCREMENTS 24
 FINAL SIZE LT. SIDE = .247 RT. SIDE = .2

NO. POINTS = 29
 P_{MIN} .266 KIPS P_{MAX} 2.462 KIPS R = .0999249
 TEMP. = 1200 F ENVIRONMENT = AIR
 SPECIMEN: CT B = .5 IN. W = 1.992

OBS NO. CYCLES A (REAS.) REMARKS

1	0	.899
2	132	.903
3	437	.910
4	593	.912
5	1364	.928
6	1615	.933
7	1873	.938
8	2044	.946
9	2238	.950
10	2318	.952
11	2591	.961
12	2746	.965
13	3508	.984
14	3694	.991
15	3964	.998
16	4132	1.009
17	4387	1.024
18	4481	1.037
19	4782	1.041
20	4873	1.048
21	5000	1.059
22	5500	1.089
23	6000	1.124
24	6500	1.169
25	7000	1.224
26	7250	1.259
27	7500	1.324
28	7750	1.444
29	7837	1.585

exceeds ASTM crack length requirement

APPENDIX C

```

395      REAL MX,MM,N1,M2,MPT9,MPT5
396      REAL MPPT9,N
397      INPUT T,R,TC,LT
398      V025=0.025-1.E-10
399      T999=1000.-1.E-10
400      TPT4=.4-1.E-10
401      RPT9=.9+1.E-10
402      S=-5.3+4.4E-0+T
403      IF(S.LT.0)S=0
404      N=8E-4*T-0.04
405      IF(N.LT.1.0)N=1.0
406      B=(T-1200)*.0019-4.52
407      IF(B.GT.-4.52)B=-4.52
408      Y1=S*(ALOG10(TC/TPT4))**N+R
409      N1=1.+1.16E-02*(T-T999)-2.81E-05*(T-T999)**2
410      S1=4.27E-13*(T-T999)**4-7.8E-12
411      B1=7.607E-13*(1400.-T)**4-605+4.77
412      B1=-B1
413      Y2=S1*(ALOG10(TC/TPT4))**N1+B1
414      S2=2.145E-04*(T-T999)**3-1.14E-05
415      B2=-2.628E-03*(T-T999)**3-0.51+6.70
416      B2=.9953+1.09E-03*(T-T999)-4.7E-04*(T-T999)**2
417      B2=-B2
418      Y3=S2*(ALOG10(TC/TPT4))**N2+B2
419      IF(Y1.LT.Y2.AND.0.LT.Y3)C=Y3
420      IF(Y1.GT.Y2.AND.0.GT.Y3)C=Y3
421      DADN=10.**C
422      V=1/T
423      IF(HT.EQ.0)GO TO 550
424      EFCT=0.
425      IF(T.LE.1200)HTB=0.0045*(T-1200)
426      EFCT=4.75E-03*(ALOG10(V/V025))**2-9879-1.
427      IF(T.GE.1200)EFCT=EFCT*(T-1200)
428      IF(T.LE.1200)HTA=0.
429      IF(T.GE.1200)HTA=0.005*(T-1000)
430      IF(T.GT.1200)HTA=1.
431      IF(T.GT.1200)HTB=5.75E-04*(T-1200)-1.3
432      HTQ=HTB+HTA*(ALOG10(HT/TC))+EFCT
433      IF(HTQ.LT.0)HTQ=0.
434      DADN1=HTQ+Y1
435      HTB=1.454E-04*(T-1000)**2-0.275*(ALOG10(V/V025))**2-1.
436      HTB=HTB*(T-1000.)+.652-1.1)
437      CR5=2.609E-02*(T-1000.)*.5905+ETP
438      EVT=1.55-1.739E-06*(T-1000.)*.998*(ALOG10(V/V025))**2-1.
439      CR5=.55+7.1579E-03*(T-1000.)-1.55E-05*(T-1000.)**2
440      HTQ5=CR5+CR5*(ALOG10(HT/TC))
441      IF(HTQ5.LT.0)HTQ5=0
442      DADN5=HTQ5+Y2
443      EVT2=(0.64-3.147E-05*(T-1000.)*.1513*(ALOG10(V/V025))**2-1.
444      CR9=.64+6.371E-03*(T-1000.)-1.49E-05*(T-1000.)*.7
445      CR9=.15+.3543*(T-1000.)*.1339
446      CR9=.13+4.9E-05*(T-1000.)*.156*(ALOG10(V/V025))**2-1.
447      CR9=CR9*(Z
448      IF(CR9.LT.0)CR9=0.
449      HTQ9=CR9+CR9*(ALOG10(HT/TC))
450      IF(HTQ9.LT.0)HTQ9=0
451      DADN9=HTQ9+Y3
452      DADN=(DADN1+DADN5)/.25377*(ALOG10(1.-R))+DADN9
453      IF(DADN1.LT.DADN5.AND.DADN1.LT.DADN9)DADN=DADN9
454      IF(DADN1.GT.DADN5.AND.DADN1.GT.DADN9)DADN=DADN1
455      DADN=10.**DADN

```

```

664 D2=1.37183-5.83102E-10*(T-T999)**3.34553
665 A=2.081-(D1*(ALOG10(RPT9/(1-R)))*P2)
666 MM=.13
667 IF(R.LE.0.5)GO TO 17
668 MRPT9=9.898E-04*(T-T999)**1.5847
669 SLPM=(.13-MRPT9)/.49897
670 MM=.13-SLPM*(ALOG10(1.5/(1-R)))
671 17 CONTINUE
672 DELK=10.**A*DAPN**MM
673 YKC=122*(1-R)
674 YKS=10.**((1-((.231+3.404E-03*(T-1000)**.729)*(ALOG10(1.9/(1-R))))))
675 VHT=1/(V+HT)
676 IF(R.NE.0.1)GO TO 600
677 TTEMP=T
678 IF(T.GT.1300)TTEMP=1300
679 E=1.55E-02*(TTEMP-1200)*((ALOG10(V/V025))**.0902-1)
680 IF(E.LT.0.)E=0.
681 PRIM=2.7+6.88E-03*(T-1000)-1.94E-05*(T-1300)**7.1-E
682 IF(HT.EQ.0)GO TO 620
683 A25T=2.737E-07*(TTEMP-1000)**2.74
684 AVT=A25T+E
685 DVT=5.346E-03*(TTEMP-1000)**.7331
686 QVHT=AVT+BVT*(ALOG10(HT/20.))
687 PRIM=PRIM-QVHT
688 IF(T.LE.1200)UP=2.7-1.5E-03*(T-1000)
689 IF(T.GT.1200)UP=2.4-1.37E-03*(T-1000)**.5100
690 IF(PRIM.LT.UP)PRIM=UP
691 600 CONTINUE
692 GAMA=1.7-8.25E-10*(T-1000)**3.51
693 E=1.734E-10*(T-1000)**3.547*(ALOG10(1.15/(1.15+V/V025))**.4000-1)
694 PRIM=2.25+6.875E-03*(T-1000)-2.188E-05*(T-1300)**7.1+E
695 IF(HT.EQ.0)GO TO 610
696 A25T=1.352E-02*(T-1000)**.4516
697 ALPHA=.5228+4.23E-03*(1400-T)
698 IF(ALPHA.GT.1.17)ALPHA=1.17
699 BETA=.152+7.165E-03*(1400-T)
700 IF(BETA.GT.1.58)BETA=1.58
701 B25T=.1388*(T-1200)**.11
702 AVT=A25T+3.18E-09*(T-1000)**7.94*(ALOG10(V/V025))**.4194-1)
703 DVT=B25T+4.58E-11*(T-1000)**3.755*(ALOG10(V/V025))**.4194-1)
704 QVHT=AVT+BVT*(ALOG10(HT/20.))
705 PRIM=PRIM-QVHT
706 LE=2.25-2.613E-09*(T-1000)**3.51
707 610 IF(PRIM.LT.UP)PRIM=UP
708 E=4.351E-03*(T-1000)**.7215*(ALOG10(1.15/(1.15+V/V025))**.4194-1)
709 PRIM=1.4+5.425E-03*(T-1000)-1.302E-05*(T-1300)**7.1+E
710 IF(HT.EQ.0)GO TO 620
711 ALPHA=1.775+2.045E-03*(1400-T)
712 A25T=7.17E-06*(T-1000)**.704
713 IF(ALPHA.GT.2.157)ALPHA=2.157
714 AVT=A25T+7.971E-08*(T-1000)**4.71*(ALOG10(V/V025))**.4194-1)
715 B25T=1.575E-03*(T-1000)-2.375E-06*(T-1300)**2.
716 GAMA=.8194-2.48E-03*(1400-T)
717 IF(GAMA.LT.0.1000)GAMA=.1000
718 EVT=B25T*((ALOG10(HT/20.25))**.4194-1)
719 BVT=B25T+EVT
720 QVHT=AVT+BVT*(ALOG10(HT/20.))
721 PRIM=PRIM-QVHT
722 IF(1.5-7.1E-03*(T-1000)
723 IF(T.GT.1200)UP=2.4-1.37E-03*(T-1000)**.5100
724 IF(PRIM.LT.UP)PRIM=UP
725 PRIM=PRIM
726 LE=ALOG10(2.5)+7.404E-17*(T-1000)
727 D=10.**((APE+.57*(ALOG10(1/R))))
728 IF(D.GT.3.)D=3.

```



```

786      SRD=(SORT(Q)*ALOG(XKC)-ALOG(DELK)*SORT(Q))/ (A LOG(DELK)-ALOG(XKC))
787      D=- (SRD**2.)
788      P=DADNP-(Q/(ALOG(DELK)-ALOG(XKS)))+(B/(ALOG(XKC)-ALOG(DELK)))
910      BP=ALOG(DADN)-Q*ALOG(ALOG(DELK)-ALOG(XKS))-D*ALOG(ALOG(XKC)-ALOG(DELK))
920      B=BP-P*(ALOG(DELK)-ALOG(XKS))
930      PRINT 40,B,P,Q,D,XKS,XKC,DADN,DADNP
940      PRINT 41,T,R,V,HT
950 40    FORMAT(6(2X,F8.4),E11.5,2X,F8.4)
960 41    FORMAT(4(F10.4,2X))
9999      STOP;END

```

*

```

100 REAL KS,KC,PYAX,CRACK(200),CYCLES(200)
110 DIMENSION U(5),R(5),DADN(200),DELTAK(200)
115 COMMON/INFO/DELP,THICK,W1,ALPHA,DELK
120 PRINT,"INPUT MAX LOAD , MIN LOAD, KIPS";READ,P,PMIN
130 PRINT,"INPUT SPECIMEN THICKNESS, INCH";READ,THICK
140 PRINT,"INPUT SPECIMEN WIDTH, INCH";READ,W1
150 PRINT,"INPUT INITIAL CRACK LENGTH";READ,A
160 PRINT,"INPUT ULTIMATE STRESS, KSI";READ,OUT
170 PRINT,"INPUT B, P, Q, D, KS, KC";READ,BB,P1,Q1,D1,K1,K2
180 DELP=PMAX-PMIN
190 AF=W1
200 DELA=(AF-A)/200
210 CRACK(1)=A;CYCLES(1)=0
220 ALPHA=A/W1
230 CALL EQ1
240 DELK=DELP
250 IF (DELK.GT. 1E-09) GO TO 10
260 PRINT,"INITIAL CRACK SIZE TOO SMALL GO TO 100"
270 12 CONTINUE
280 U(1)=.0744371695;U(2)=.216697697;U(3)=.39976791
290 U(4)=.432531683;U(5)=.486953264;R(1)=.147762112
300 R(2)=.134633360;R(3)=.109543131;R(4)=.074725766;R(5)=.044325111
310 A1=A
320 DO 50 K=2,200
330 X=ALOG(99)
340 10 X=X
350 ALPHA=A1/W1
360 CALL EQ1
370 DK=DDELK
380 Y=1/(EXP(PB)*(1-B*AS)+P1*(1+Q1*EXP(2/KS))*Q*(1+Q1*EXP(2/KS))+P1)
390 IF (J.EQ.1) GO TO 35
400 IF (J.EQ.2) GO TO 40
410 IF (J.EQ.3) GO TO 40
420 IF (J.EQ.4) GO TO 40
430 B3=B1
440 B4=B1-DELA
450 N0=1
460 IF (A0.EQ.0) GO TO 51
470 IF (N0.LT.100) GO TO 51
480 A=A0
490 IF (A0.EQ.1) GO TO 40
500 B=(B4-A0)/A0
510 B=A
520 20 B=B+B
530 IF (B.LE.P0) GO TO 15
540 IF (B.GT.P0) GO TO 15
550 B=P0
560 15 C=5*(B+A)
570 C2=B-A
580 B=C;I=0
590 30 I=I+1

```

```

580      W=C2*(1/Y)
590      X=C1+4
600      J=1
610      GO TO 12
620 35   S=S+R(I)*Y
630      X=C1-W
640      J=2
650      GO TO 10
660 40   S=S+R(I)*Y
670      IF(I.LT.5)GO TO 30
680      IF(N0.EQ.1)GO TO 45
690      Z0=Z0+S*C2
700      A=B
710      GO TO 20
720 45   Z0=S*C2
730 46   CONTINUE
732      DELTAK(K)=DK3
734      DADN(K)=1./Y
750      CYCLES(K)=CYCLES(K)+1+37
755      A1=A1+D+DN(K)*Z0
756      CRACK(K)=A1
760      DN=2*P1*(2*W1+A1)/(W1-A1)+*2
780      IF(DN.GT.0ULT)GO TO 51
790      KMAX=.96*KC
805      PRINT 900,DELTAK(K),CYCLES(K),A1,DADN(K),CRACK(K)
806 900   FORMAT(5(E16.7,2X))
810      IF(DK3.GT.KMAX)GO TO 51
815      IF(A1.GT.W1)GO TO 51
820 50   CONTINUE
840 51   WRITE (02,08) (CRACK(I),CYCLES(I),DADN(I),DELTAK(I),I=1,N)
850 08   FORMAT(2X,F8.5,F23.3,E15.7,F15.4)
880 999   CONTINUE
890      STOP/END
900      SUBROUTINE EQ1
910      COMMON/INFO/DP,T,W1,A,DK
920      E1=(DP/(T*SQRT(W1)))*((2-A)/(1-A))+*1/F1
930      DK=E1*(2.886+4.64*A-13.27*A**2+A**4,T*W1**2*F1)
940      RETURN/END

```